Internet Appendix

"A Decomposition of Conditional Risk Premia and Implications for Representative Agent Models"

By Fousseni Chabi-Yo and Johnathan Loudis

The Internet Appendix is organized as indicated in the Table of Contents below. All figures and tables can be found at the end of the end of the appendix.

Contents

IA.1 Notation

Symbol	Description
t	Generic current date
T	Generic future date
S_t	Market index value at date t
$R_{M,t\to T}$	Gross market return from date t to T (Note: $R_{M,t\to T} = S_T/S_t$)
$R_{f,t\to T}$	Risk-free rate from date t to T
$C_{t\to T}[K]$	Call price at date t with expiration at date T and strike price K
$P_{t\to T}[K]$	Put price at date t with expiration at date T and strike price K
*	Denotes the risk-neutral measure; for instance, $\mathbb{VAR}^*$ denotes risk-neutral variance.
$\mathbb{E}_t^*[\cdot]$	Expectation at time t under the risk-neutral measure
$\mathbb{E}_t[\cdot]$	Expectation at time t under the physical measure
$\mathbb{P}_t^*[B]$	Risk-neutral probability at time t of event B occurring at time T
$\mathbb{P}_t[B]$	Physical probability at time t of event B occurring at time T
A_s	Set describing regions of the gross market return space with $s \in \{d, c, u\}$ (see Equations 4, 5, and 6); note that $A \equiv A_d \cup A_c \cup A_u$
$\mathbb{I}_{A_s}$	Indicator function for gross market return inclusion in set A_s
$\underline{x}$	Threshold in gross market return space for computing downside truncated moments (see Equation 4); we set $\underline{x} = 0.9$ for all empirical results
$\overline{x}$	Threshold in gross market return space for computing upside truncated moments (see Equation 6); we set $\overline{x} = 1.1$ for all empirical results
x_s	Points in gross market return space around which Taylor expansions are taken and at which preference parameters are estimated; $s \in \{d, c, u\}$ (see Equations 4, 5, and 6); we set $x_d = 0.85$, $x_c = 1$, and $x_u = 1.15$ for all empirical results
$\tau(x_s)$	Risk tolerance evaluated at x_s (see Equation 14)
$\rho(x_s)$	Skewness tolerance evaluated at x_s (see Equation 15)
$\kappa(x_s)$	Kurtosis tolerance evaluated at x_s (see Equation 16)
$\theta_k(x_s)$	Parameters related to utility function derivatives (see Equation 12)
$\lambda_t(x_s, k, j)$	Function of preference parameters defined in Equation 26
$\mathbb{M}_{i,t\to T}^{*(n)}[A_s]$	Shorthand for $\mathbb{E}_t^*[(R_{i,t\to T} - R_{f,t\to T})^n \mathbb{I}_{A_s}]$ (see Equation 20)
$\mathbb{M}_{i,t\to T}^{(n)}[A_s]$	Shorthand for $\mathbb{E}_t[(R_{i,t\to T} - R_{f,t\to T})^n \mathbb{I}_{A_s}]$ (see Equation 21)
$\mathbb{RP}_{t\to T}^{(n)}[A_s]$	Shorthand for the risk premia defined in Equation 29
$U(W_T)$	Generic representative investor utility function evaluated at investor wealth, W_T
$M_{t\to T}$	Stochastic discount factor realization over the time period from t to T
$\beta_{t,s}^*$	Risk quantity associated with $\mathbb{RP}_{t\to T}^{(1)}[A_s]$ (see Proposition 4)
$\sigma_{t,M,s}^{*2}$	Risk price associated with $\mathbb{RP}_{t\to T}^{(1)}[A_s]$ (see Proposition 4)
$\omega_{t,M,s}$	Component of risk price associated with risk premium on $\frac{\mathbb{E}_t[M_{t\to T}]}{M_{t\to T}}\mathbb{I}_{A_s}$ (see Proposition 4)
$\sigma_{t,s}^2$	Component of risk price associated with probability risk (see Proposition 4)

IA.2 Model-Implied Market Risk Premium Decompositions: A More Detailed Summary

In this section, we provide a more in-depth summary of the model-implied market risk premium decompositions by model and compare them to the data-implied decomposition. We relegate these details to the Internet Appendix for the sake of brevity in the main text.

IA.2.1 Long Run Risk Models

In this subsection, we consider the class of models in which the representative agent has recursive preferences as in Epstein and Zin (1989). Specifically, we estimate our decomposition for models in Bansal and Yaron (2004), Bansal, Kiku, and Yaron (2012), and Drechsler and Yaron (2011).[38]

IA.2.1.1 Bansal and Yaron (2004) and Bansal, Kiku, and Yaron (2012)

Bansal and Yaron (2004) propose an economic mechanism that relies on long-run risk to explain key stylized empirical asset pricing facts. Bansal, Kiku, and Yaron (2012) extend the Bansal and Yaron (2004) model by allowing consumption shocks to affect the dividend process.[39] Both models include two state variables (x_t and σ_t^2), so we use $\log(P_t/E_t)$ and $\mathbb{M}_{t\to T}^{*(2)}$ to extract implied state variables at each date for both models (independently) using Result IA.1. We use Results IA.2 and IA.3 to compute the implied physical and risk-neutral moments, respectively. See Internet Appendix IA.8.5.1 for additional details.

Panels (a) and (d) ((b) and (e)) in Figure 3 plot the risk premium decompositions for the Bansal and Yaron (2004) (Bansal, Kiku, and Yaron, 2012) model. Compared to the data-implied 30-day horizon decompositions (Figure 2, Panels (a) and (d)), both the Bansal and Yaron (2004) and Bansal, Kiku, and Yaron (2012) decompositions imply that the central risk premium comprises a larger fraction of the overall risk premium than in the data-implied decomposition. Consequently, the upside and downside risk premia implied by these models comprise a smaller fraction of the overall risk premium than in the data-implied decomposition. The discrepancies are a consequence of the fact that these models are conditionally log-normal and therefore do not often generate realized returns in regions of the return space for which we define downside and upside risk. Interestingly, the unconditional contribution of downside and upside risk is not (effectively) zero, as implied by the unconditional models and documented by Beason and Schreindorfer (2022). This is related to the fact that our state variables are more volatile than those implied by the calibrated state variable processes in each of these models, which occasionally widens the return distribution enough so that the downside and upside risk premia contribute to the overall risk premium in a non-negligible manner.[40]

Table 4 provides summary statistics for these market risk premium decompositions. The average total risk premia implied by the data for Bansal and Yaron (2004) and Bansal, Kiku, and

[38] We also report results for Bollerslev, Tauchen, and Zhou (2009) in Internet Appendix IA.8.5.2, but leave them out of the main text due to the fact that this model is known to generate implausible risk premia (see, for instance, Bekaert, Engstrom, and Ermolov (2023) for further documentation of this fact).

[39] The model in Bansal, Kiku, and Yaron (2012) was designed to highlight important differences in the asset pricing implications of the long run risk model relative to the habit formation model in Campbell and Cochrane (1999).

[40] It is also interesting to note that the upside risk premium is larger in magnitude than the downside risk premium. If we were concerned with the risk premium on log-returns, we would expect the downside and upside risk premia to be symmetric. However, since we use simple returns this induces positive skewness in the simple return distribution relative to the log return distribution, causing the upside risk premium to be larger in magnitude than the downside risk premium in these models. This is counterfactual to what we observe in the data.

Yaron (2012) are 5.66% and 6.75%, respectively, which are similar to model-implied values based on simulation (5.55% and 6.67%, respectively).[41] The conditional means of the risk premium decomposition measures imply that all components of the risk premium are increasing with market volatility, which is what we observe in the data. However, as implied by the risk premium plots, the central risk premium comprises the majority of the total risk premium in both models, which is inconsistent with observations from the data-implied decomposition.

Table 5 provides the average differences between the data-implied market risk premia and those implied by Bansal and Yaron (2004) and Bansal, Kiku, and Yaron (2012). The data-implied total, downside, and upside risk premia are significantly larger than those implied by the models. The data-implied central risk premium is significantly lower than that implied by the models.

IA.2.1.2 Drechsler and Yaron (2011)

Drechsler and Yaron (2011) extend the Bansal and Yaron (2004) model by allowing for jumps in both consumption growth and its volatility. Doing so allows them to better match the mean, volatility, skewness, and kurtosis of consumption growth and stock market returns observed in the data. Their model also generates a variance risk premium that forecasts market excess returns, which is a key stylized fact in the data. The model includes three state variables (x_t, $\overline{\sigma}_t^2$ and σ_t^2), so we use $\log(P_t/E_t)$, $\mathbb{M}_{t\to T}^{*(2)}$, and $\mathbb{M}_{t\to T}^{*(3)}$ to extract implied state variables at each date using Result IA.7. We use Results IA.8 and IA.9 to compute the implied physical and risk-neutral moments, respectively. See Internet Appendix IA.8.5.3 for additional details.

Panels (c), and (f) in Figure 3 plot the market risk premium decompositions. The downside risk premium is typically a large contributor to the total risk premium. However, during periods of low volatility the central risk premium becomes the dominant contributor to the total risk premium.

Table 4 provides summary statistics for the market risk premium decomposition. Conditionally, the average the downside market risk premium increases in magnitude as risk-neutral volatility increases, similar to the data-implied results. Table 5 provides the average difference between the data-implied risk premia and those implied by the Drechsler and Yaron (2011) model, and shows that the contributions of the downside/central/upside market risk premia are significantly lower/higher/higher than those implied by the data.

IA.2.2 Habit Formation Models: Bekaert, Engstrom, and Ermolov (2023)

Bekaert, Engstrom, and Ermolov (2023) and Bekaert and Engstrom (2017) develop a new class of habit formation models that aim to better capture features of macroeconomic variables.[42] The Bekaert and Engstrom (2017) model requires a computationally intensive numerical solution procedure, but Bekaert, Engstrom, and Ermolov (2023) propose a more tractable version of the model that is able to explain key stylized asset pricing facts while retaining the desirable features of the consumption growth distribution featured in Bekaert and Engstrom (2017). We therefore focus on the habit formation model from Bekaert, Engstrom, and Ermolov (2023) in our analysis.

The Bekaert, Engstrom, and Ermolov (2023) model has two variants: one with preference shocks and one without preference shocks. The model without preference shocks has two state variables (q_t and n_t), so we use $\log(P_t/E_t)$ and $\mathbb{M}_{t\to T}^{*(2)}$ to extract implied state variables for this model at

[41] This is true for all models we investigate since we transform the $\log P_t/E_t$ and risk-neutral moments from the data to have the same unconditional means as the $\log P_t/D_t$ and risk-neutral moments implied by each model for the purposes of state variable extraction.

[42] Their models represent an improvement on the habit formation model in Campbell and Cochrane (1999). In particular, their setup allows them to better match observed consumption growth skewness in the data.

each date. The model with preference shocks has three state variables (q_t, n_t, and s_t), so we use $\log(P_t/E_t)$, $\mathbb{M}^{*(2)}_{t\to T}$, and $\mathbb{M}^{*(3)}_{t\to T}$ to extract implied state variables at each date. We can use Result IA.10 for the state variable extraction in both cases. We use Results IA.11 and IA.12 to compute the implied physical and risk-neutral moments, respectively. See Internet Appendix IA.8.6 for additional details.

Panels (a) and (d) ((b) and (e)) in Figure 4 plot the market risk premium decompositions under the model with (without) preference shocks. The models with and without preference shocks yield decompositions with quite different implications regarding which regions of the return space contribute most to the total risk premium. In the case of the model without preference shocks (Panel (d)) it is clear that the downside risk premium is the largest contributor to the the total risk premium, consistently contributing approximately 80%. The central risk premium typically contributes between approximately 15%-20% to the total risk premium. In the case of the model with preference shocks (Panel (c)), the central risk premium is typically the largest contributor ranging between approximately 60-80%. The downside risk premium contribution ranges between approximately 20-60% and occasionally contributes more than the central risk premium. In both cases, the upside risk premium provides only a minor contribution to the total risk premium.

Comparing these results to those implied by the data at the 30-day horizon (Figure 2, Panels (a) and (d)), the model with preference shocks matches many key features of the data. The contribution of the central risk premium is relatively large during low market volatility periods, but is outweighed by the contribution of the downside risk premium during high market volatility periods. The downside and upside risk premia also typically increase in tandem in both the data- and the model-implied decompositions.

Table 4 provides summary statistics for implied market risk premium decomposition. The average total risk premia implied by the data for the models with and without preference shocks are 4.84% and 5.92%, respectively, which are similar to model-implied values based on simulation (4.26% and 5.56%, respectively). The conditional means of the market risk premium decomposition measures imply that all components of the risk premium are increasing with market volatility, which is what we observe in the data. The downside risk premium comprises the majority of the total risk premium in the model without preference shocks, which is inconsistent with observations from the data-implied decomposition. However, the contributions and time series behavior of the downside, upside, and central risk premia in the model with preference shocks are qualitatively more similar to the data-implied decomposition than for other models we study.

Table 5 provides the average difference between the data-implied risk premia and those implied by the models with and without preference shocks. The data-implied total, downside, central, and upside risk premia are significantly larger than those implied by the models in level (Panel A). This holds in all cases except for the downside risk premium in the model without preference shocks, which is significantly lower than what the data implies. In terms of the contribution to total risk premium (Panel B), the data implies a central risk premium contribution that is significantly lower than that implied by model with preference shocks. The data also implies downside risk premium contribution that is significantly lower than that implied by the model with preference shocks. In all other cases, the data implies contributions that are higher than those implied by the models.

IA.2.3 Disaster Risk Models

IA.2.3.1 Gabaix (2012)

Gabaix (2012) develops a time-varying disaster risk model that is able to quantitatively explain many standard asset pricing puzzles. We follow the Dew-Becker et al. (2017) implementation (in-

cluding their parameter choices) in our analysis.[43] In this model, the log price-dividend ratio is non-linear in the model's single state variable, L_t. Therefore, we solve for $\mathbb{M}^{*(2)}_{t\to T}$ as a function of the state variable numerically given the assumed L_t process conditionally as a function of L_t. Given an estimate for the the model-implied $\mathbb{M}^{*(2)}_{t\to T}$ as a function of L_t, we extract the implied L_t at each date by matching the transformed $\mathbb{M}^{*(2)}_{t\to T}$ from the data as usual. Given the extracted state variable, we estimate physical and risk-neutral moments needed for our decomposition at each date via simulation according to expressions for these moments in Internet Appendix IA.8.7.1.

Panels (a) and (c) in Figure 5 plot the market risk premium decomposition. The downside risk premium is consistently the largest contributor to the total risk premium with the upside risk premium contributing essentially nothing. Table 4 provides summary statistics for the implied market risk premium decomposition. Conditionally, the average downside market risk premium increases in magnitude as risk-neutral volatility increases, which is similar to the data-implied results. Table 5 provides the average difference between the data-implied risk premia and those implied by the Gabaix (2012) model. The contributions of the downside/central/upside market risk premia are significantly higher/lower/lower than those implied by the data.

IA.2.3.2 Wachter (2013)

Wachter (2013) develops a time-varying disaster risk model that aims to explain the excess volatility puzzle. We follow the Dew-Becker et al. (2017) discretization of Wachter (2013) (including their parameter choices) since this provides a convenient version of the model that is calibrated at the monthly frequency. The model includes one state variable, λ_t, so we use $\mathbb{M}^{*(2)}_{t\to T}$ to extract the implied state variable at each date using Result IA.15. We then use Results IA.14 and IA.15 to compute the implied physical and risk-neutral moments needed for the risk premium decompositions. See Internet Appendix IA.8.5.2 for additional details.

Panels (b) and (d) in Figure 5 plot the market risk premium decomposition. The central risk premium contributes the majority of the total risk premium. The downside risk premium contributes less than the central risk premium, but more than the upside risk premium. Interestingly, the time variation in these decomposition contributions are similar to those from the data (see Figure 2, Panel (d)). Table 4 provides summary statistics for the implied market risk premium decomposition and Table 5 provides the average difference between the data-implied risk premia and those implied by the Wachter (2013) model. The contributions of the downside/central/upside market risk premia are significantly lower/higher/higher than those implied by the data.

IA.3 Robustness and Additional Results

In this section, we explore the robustness of our results to various modifications and provide some additional results.

IA.3.1 Data-Implied Risk Quantities and Prices by Horizon

In this subsection, we provide a summary of average risk quantity and price levels according to the data-implied decomposition over different horizons (30, 60, 90, 180, and 360 days) in Table IA.4 and risk premium variance decompositions at the same horizons in Table IA.5. Results for the 30-day

[43] This calibration is similar to that in Gabaix (2012) and is also able to match the Sharpe ratio of one-month variance swaps reported in Dew-Becker et al. (2017). We use this version of the model since we are also interested in evaluating the model's ability to match the conditional variance risk premium and its decomposition.

horizon are the same as in Tables 6 and 7. Table IA.4 shows that, on average, risk quantities are generally stable as the horizon increases, but risk prices generally decrease as the horizon increases. The probability-related risk price ($\sigma^2_{t,s}$) is always the main contributor to the total risk price (as opposed to the SDF-related risk price, $\omega_{t,M,s}$) and its importance increases with horizon.

Table IA.5 shows that variation in the total market risk premium (based on the variance risk premium decomposition described in Subsection 6.3) is primarily driven by variation in risk prices at all horizons. Note that the probability-related risk price is zero when the region of interest is A (the total market return space) so that all risk price variation is attributed to the SDF-related risk price, $\omega_{t,M,s}$, in this case. Variation in the risk premia associated with each sub-region of the market return space are primarily driven by the probability-related price of risk at short horizons (30 days). However, as horizon increases, variation in risk quantity typically becomes the primary driver of variation in risk premia associated with these sub-regions.

IA.3.2 Decomposing Truncated Moments into Conditional Moments and Probability Components

In the main draft, we use option prices to estimate conditional truncated risk-neutral moments ($\mathbb{M}^{*(1)}_{t\to T}[A_s] \equiv \mathbb{E}^*_t[(R_{M,t\to T} - R_{f,t\to T})\,\mathbb{I}_{A_s}]$) and then we use Corollary 1 to estimate physical truncated moments ($\mathbb{M}^{*(1)}_{t\to T}[A_s] \equiv \mathbb{E}_t[(R_{M,t\to T} - R_{f,t\to T})\,\mathbb{I}_{A_s}]$) from the risk-neutral moments. By the definition of conditional probability, we can decompose the truncated moments into a component related to conditional moments and the probabilities of ending up in a particular region as

$$\mathbb{E}^*_t[(R_{M,t\to T} - R_{f,t\to T})\,\mathbb{I}_{A_s}] \equiv \mathbb{E}^*_t[(R_{M,t\to T} - R_{f,t\to T})\,|\,\mathbb{I}_{A_s}]\,\mathbb{P}^*_t[A_s] \text{ and} \tag{IA.1}$$

$$\mathbb{E}_t[(R_{M,t\to T} - R_{f,t\to T})\,\mathbb{I}_{A_s}] \equiv \mathbb{E}_t[(R_{M,t\to T} - R_{f,t\to T})\,|\,\mathbb{I}_{A_s}]\,\mathbb{P}_t[A_s], \tag{IA.2}$$

where $\mathbb{P}^*_t[A_s]$ ($\mathbb{P}_t[A_s]$) represents the risk-neutral (physical) probability of ending up in region s at time T. The conditional moments on the right-hand side of the above equations represent how changes in the shapes of the excess market return distribution affect the truncated moments, whereas the probabilities represent how the changing probability associated with ending up in each region affects the related truncated moment. To get an understanding of the time series dynamics of these quantities, we provide plots in Figure IA.1. Time series variation in both the physical and risk-neutral moments in the down and up regions is primarily driven by variation in the probability component. In contrast, variation in the physical and risk-neutral moments in the central region is primarily driven by variation in the conditional moments and not the probabilities. In other words, our results imply that the shapes of the tails of the physical and risk-neutral excess market returns do not change much relative to the probabilities of ending up in the tails, which is what primarily drives variation in truncated first moments associated with the tails of the distribution. The opposite is true for the central region of the distributions.

One might be tempted to use the results above to decompose our market risk premium in each region into components related to the shape of the excess return distribution and probabilities. However, this setup does not allow for a clean distinction between probabilities and other contributors to the risk premia, which is why we implement Proposition 4 using the covariance-based definition of risk premia. To highlight the issue, consider our definition of the market risk premium in region A_s based on Equation 29:

$$\mathbb{RP}^{(1)}[A_s] \equiv \mathbb{E}_t[(R_{M,t\to T} - R_{f,t\to T})\,\mathbb{I}_{A_s}] - \mathbb{E}^*_t[(R_{M,t\to T} - R_{f,t\to T})\,\mathbb{I}_{A_s}].$$

Substituting expression from Equations IA.1 and IA.2 (and with some algebra), this becomes

$$\mathbb{RP}^{(1)}\left[A_s\right] = \left\{\mathbb{E}_t\left[\left(R_{M,t\to T} - R_{f,t\to T}\right) \mid \mathbb{I}_{A_s}\right] - \mathbb{E}_t^*\left[\left(R_{M,t\to T} - R_{f,t\to T}\right) \mid \mathbb{I}_{A_s}\right] \frac{\mathbb{P}_t^*[A_s]}{\mathbb{P}_t[A_s]}\right\} \mathbb{P}_t\left[A_s\right]. \quad \text{(IA.3)}$$

This alternative risk premium expression (compared to that in Proposition 4) breaks the risk premium into a difference between conditional moments under the physical and risk-neutral measures (with the latter being distorted by a probability ratio) and the physical probability of ending up in region A_s. We analyze contributors to risk premia according to Proposition 4 since it decomposes risk premia into more standard objects associated with risk quantities and prices, and since the relationship in Equation IA.3 convolutes probabilities with conditional expectations (and risk quantities and prices). However, all else equal, it is clear that as $\mathbb{P}_t\left[A_s\right]$ increases (which happens in the tails of the market return distribution as horizon increases as we show in the next paragraph), the risk premium also increases. Similarly, as $\mathbb{P}_t\left[A_d\right]$ and $\mathbb{P}_t\left[A_u\right]$ increase relative to $\mathbb{P}_t\left[A_c\right]$ their contributions to the total market risk premium will also increase even if the total risk premium decreases, which is what we observe with increase horizon. It is ultimately an empirical question as to whether the isolated probability term in Equation IA.3 ($\mathbb{P}_t\left[A_s\right]$) varies more with horizon than the first term ($\mathbb{E}_t\left[\left(R_{M,t\to T} - R_{f,t\to T}\right) \mid \mathbb{I}_{A_s}\right] - \mathbb{E}_t^*\left[\left(R_{M,t\to T} - R_{f,t\to T}\right) \mid \mathbb{I}_{A_s}\right] \frac{\mathbb{P}_t^*[A_s]}{\mathbb{P}_t[A_s]}$), which we explore next.

Figure IA.2 provides plots of the time-varying probability ($\mathbb{P}_t\left[A_s\right]$) of entering each region of interest by the end of each horizon we study (30, 60, 90, 180, and 360 days). We compute these physical probability measures using Corollary 1 with preference parameters from Table 1. The average physical probabilities of entering both the downside region ($\mathbb{P}_t\left[A_d\right]$) and the upside region ($\mathbb{P}_t\left[A_u\right]$) increase monotonically in horizon. The average $\mathbb{P}_t\left[A_d\right]$ ranges from 2.9% at the 30-day horizon to 17.2% at the 360-day horizon. The average $\mathbb{P}_t\left[A_c\right]$ ranges from 2.9% at the 30-day horizon to 39.3% at the 360-day horizon. Accordingly, the average physical probabilities of entering the central region ($\mathbb{P}_t\left[A_c\right]$) decrease monotonically in horizon. The average $\mathbb{P}_t\left[A_c\right]$ ranges from 94.2% at the 30-day horizon to 43.5% at the 360-day horizon. Importantly, all time series vary quite a bit over time, implying that the probability-related risk price ($\sigma_{t,s}^2 \equiv \mathbb{VAR}\left(\mathbb{I}_s\right) \equiv \mathbb{P}_t\left[A_s\right]\left(1 - \mathbb{P}_t\left[A_s\right]\right)$) described in Section 6 is also highly time-varying, consistent with our observations there that the probability-related risk price often explains a large fraction of variation in risk premia.

Figure IA.3 provides plots of the first term in Equation IA.3 ($\mathbb{E}_t\left[\left(R_{M,t\to T} - R_{f,t\to T}\right) \mid \mathbb{I}_{A_s}\right] - \mathbb{E}_t^*\left[\left(R_{M,t\to T} - R_{f,t\to T}\right) \mid \mathbb{I}_{A_s}\right] \frac{\mathbb{P}_t^*[A_s]}{\mathbb{P}_t[A_s]}$) for each region of interest and for each horizon we study (30, 60, 90, 180, and 360 days). Importantly, the average values in each region do not change much with horizon relative to how the average values of $\mathbb{P}_t\left[A_s\right]$ change with horizon in Figure IA.2. This result implies that most of the variation we observe in average upside and downside risk premium contributions with horizon is driven by increases in the probability associated with ending up in those regions rather than the terms related to the moment risk premia themselves (which are related to the relative shapes of the excess market return distribution under the physical and risk-neutral measures). This analysis supports our main conclusion from the risk quantity and price analysis in Section 6, which yielded the same conclusion.

IA.3.3 Variance Risk Premium Decomposition Results

In this section, we present results related to the variance risk premium decompositions implied by the data and models.

IA.3.3.1 Data-Implied Variance Risk Premium Decomposition

Figure IA.4 provides plots of the data-implied variance risk premium decomposition (i.e., when $n = 2$ in Equation 29) when preference parameters from Table 1 are used to construct physical moments according to Corollary 1. Panels (a), (b), and (c) plot the risk premium decomposition in levels, and Panels (d), (e), and (f) plot them in terms of the fraction of the overall risk premium for horizons of 30, 90, and 360 days, respectively. The downside risk premium is the main contributor to the total variance risk premium over all horizons and the upside risk premium becomes a larger contributor as the horizon increases.

Table IA.1 provides summary statistics for the data-implied variance risk premium decomposition using preference parameters from Table 1. Panels A and B provide summary statistics for the decomposition in levels and as fractions of the total variance risk premium, respectively. We begin by focusing on the "Unconditional Statistics" in Panel A, which are averaged over our full sample. The average annualized 30-day (360-day) variance risk premium during our sample period is -1.03% (-1.54%). These are similar in magnitude to variance risk premium estimates reported in Carr and Wu (2009),[44] Dew-Becker et al. (2017),[45] and Bekaert, Engstrom, and Ermolov (2023).[46] Conditionally, the variance risk premium increases during periods of high volatility, which implies investors are willing to pay relatively more for insurance against volatility during turbulent times. This finding is consistent with those in Dew-Becker et al. (2017), who use different data (variance swap contracts) to characterize the variance risk premium.

IA.3.3.2 Model-Implied Variance Risk Premium Decompositions

Figure IA.5 and Table IA.2 provide variance risk premium decomposition plots and summary statistics for the representative agent models we study. Table IA.3 provides two different difference measures between the data- and model-implied variance risk premium decompositions: average differences and the corridor measure (both defined as in our market risk premium results from Table 5). We omit decompositions for the Bansal and Yaron (2004) and Bansal, Kiku, and Yaron (2012) since these are log-normal models which imply there is no variance risk premium. Note that, as in the case of the model-implied market risk premium, we need not estimate preference parameters for these models to implement the variance risk premium decomposition. We can simply compute the risk-neutral and physical moments needed to apply Proposition 3 using the conditional extracted state variables.

Panels (a) and (d) in Figure IA.5 show that the downside risk premium effectively constitutes the entire variance risk premium in the Drechsler and Yaron (2011) model, except during periods when the total risk premium is small. Table IA.2 provides summary statistics for the variance risk premium decomposition. Conditionally, the average the downside variance risk premium increases in magnitude as risk-neutral volatility increases, similar to the data-implied results. Table IA.3

[44] The variance risk premium in this case ranged from -0.66% to -2.74% at the one-month horizon for the S&P 500 index based on Table 3 in Carr and Wu (2009).

[45] The variance risk premium in this case was approximately -1.5% at the one-month horizon based on Figure 2 in Dew-Becker et al. (2017). Specifically, one can approximate the implied variance risk premium (annualized and in percent) by taking $100 \times 12 \left(\mathbb{E}\left[F_t^0\right] - \mathbb{E}\left[F_t^1\right]\right)$ using their nomenclature with $100 \times \sqrt{12 \times \mathbb{E}\left[F_t^0\right]} \approx 17.4$ and $100 \times \sqrt{12 \times \mathbb{E}\left[F_t^1\right]} \approx 21.2$ according to the figure.

[46] The variance risk premium in this case was approximately -1.9% at the one-month horizon based on Table 8 in Bekaert, Engstrom, and Ermolov (2023). The annualized value reported herein takes their reported monthly value (0.0016) and multiplies it by -1, 12, and 100. The -1 is to account for the fact that they define the variance risk premium to be the risk-neutral minus physical variance, the 12 is to annualize it, and the 100 is to give it the interpretation of being in percent. Note that they define the variance risk premium using log market returns whereas we use simple market returns, which could lead to some discrepancies between the measures.

provides the average difference between the data-implied risk premia and those implied by the Drechsler and Yaron (2011) model, and shows that the contributions of the downside/central/upside variance risk premia are significantly lower/lower/higher than those implied by the data.

Figure IA.5 Panels (b) and (e) ((c) and (f)) provide plots variance risk premium decomposition plots for the Bekaert, Engstrom, and Ermolov (2023) model with (without) preference shocks. In both cases, the primary contributor is the downside risk premium, although there are periods where the central risk premium becomes a sizable contributor (particularly for the model with preference shocks). Table IA.3 provides the average difference and corridor measures between the data-implied risk premia and those implied by the Bekaert, Engstrom, and Ermolov (2023) models and shows that the contributions of the downside/central/upside variance risk premia are significantly lower/higher/higher (higher/lower/higher) in the model with (without) preference shocks than those implied by the data. Visually comparing the preference-shock-based model results in Figure IA.5 Panels (c) and (f) to the data-implied results in Figure IA.4 Panels (a) and (d) imply that this model fits the data relatively well. The associated aggregated corridor measures for both variance risk premium levels (31.78) and contributions (84.73) in Table IA.3 supports this visual conclusion, as they are the largest aggregated corridor measures among the models in that table.

Figure IA.5 Panels (g) and (i) plot variance risk premium decomposition plots for the Gabaix (2012) model. Table IA.2) provides summary statistics for the implied market (variance) risk premium decomposition. Conditionally, both the average downside market and variance risk premia increase in magnitude as risk-neutral volatility increases, which is similar to the data-implied results. Table IA.3 provides the average difference between the data-implied risk premia and those implied by the Gabaix (2012) model. The contributions of the downside/central/upside market (variance) risk premia are significantly higher/lower/lower (higher/lower/higher) than those implied by the data.

Figure IA.5 Panels (h) and (j) plot the variance risk premium decomposition for the Wachter (2013) model. The downside risk premium effectively constitutes the entire variance risk premium. Table IA.3 provides the average difference between the data-implied risk premia and those implied by the Wachter (2013) model. The contributions of the downside/central/upside variance risk premia are significantly higher/lower/lower than those implied by the data.

Overall, according to our aggregated corridor measures in Table IA.3, the Bekaert, Engstrom, and Ermolov (2023) model without preference shocks provides the best fit of the data. This is consistent with the visual impressions based on comparing the data-implied decomposition results in Figure IA.4 (Panels (a) and (d)) with those from the models in Figure IA.5.

IA.3.4 Data-Implied Decomposition Results Using $\pm 5\%$ Cutoffs

In this subsection, we re-estimate the data-implied decomposition when setting $\underline{x} = 0.95$ and $\overline{x} = 1.05$ with $x_d = 0.92$, $x_c = 1$, and $x_d = 1.08$. Aside from these changes, our decomposition estimation procedure is unchanged from that used to generate our main results with $\underline{x} = 0.9$ and $\overline{x} = 1.1$. We use these decomposition results to forecast realized truncated excess market returns in Table 3. We use $\pm 5\%$ cutoffs for this purpose since there are very few realized excess market return realizations that are less than -10% or greater than $+10\%$. For instance, 1.93% (6.63%, 14.38%) of return realizations are below -10% at 30-day (90-day, 360-day) horizon. 1.56% (9.34%, 51.29%) of return realizations are above 10% at the 30-day (90-day, 360-day) horizon. In comparison, 10.06% (14.68%, 17.86%) of return realizations are below -5% at 30-day (90-day, 360-day) horizon. 12.30% (33.14%, 65.22%) of return realizations are above 5% at the 30-day (90-day, 360-day) horizon. Regression results are similar when using physical moments estimated based on our main decomposition which uses the $\pm 10\%$ cutoffs, but statistical significance is lower likely due

to having fewer observations of realized excess returns in the tails. Results are also similar when we use ±3% cutoffs, but we omit these for brevity.

Table IA.6 provides preference parameter estimates using the ±5% cutoffs. Parameter estimates are similar to our main results in Table 1 that use ±10% cutoffs but with some slight differences. For instance, the downside risk aversion estimates ($1/\tau(x_d)$) in this case tend to be lower than in the main results, implying investors are less risk averse when the downside risk definition is less severe. Similarly, the upside risk aversion estimates ($1/\tau(x_u)$) in this case tend to be higher than in our main results, implying investors are more risk averse when the upside risk definition includes more central region risk. Another way to think about these results is that the downside and upside risk now encompass more of what was formerly designated as central region risk and, as such, the risk aversion parameters estimated for these regions are a combination of either downside and central region risk or upside and central region risk in our main specification. Hence, the downside and upside risk aversion parameters are closer to our central region risk aversion parameters in our main specification.

Figure IA.6 provides market risk premium plots using ±5% cutoffs with preference parameters from Table IA.6. Results are similar to our main results in Figure 2 that use ±10% cutoffs with one notable difference. In this case, the central risk premium is smaller and contributes less to the overall risk premium, which is expected since there is "less" risk in the central region with the lower cutoffs. The correlations between the downside, central, and upside physical moment estimates under the ±10% and ±5% cutoffs are 95%, 13%, and 91% at the 30-day horizon (97%, 79%, and 98% at the 90-day horizon; 97%, 92%, and 99% at the 360-day horizon). For the central physical moment, the low correlation at the 30-day horizon is the result of this moment having relatively low overall variation when the ±5% cutoffs are used relative to the ±10% cutoffs. For instance, if we use ±3% cutoffs, the correlation between the 30-day central physical moment in this case and that from the ±5% case is 72% and in this case the variation is also low relative to the moment from the ±10% cutoff.

Table IA.7 provides summary statistics for the data-implied market risk premium decomposition constructed using ±5% cutoffs with preference parameters from Table IA.6. Results are similar to our main results in Table 2 that use ±10% cutoffs but, as implied by Figure IA.6, the central risk premium levels and contributions are lower. In unreported results, we find similar patterns when using ±3% cutoffs, which we omit for brevity.

IA.3.5 Effects from Modifying $\tau(x_s)$, $\rho(x_s)$, and $\kappa(x_s)$

To provide more intuition for the link between our preference parameters and the resulting decompositions, we perform an exercise where we modify one set of parameters at a time (either $\tau(x_s)$, $\rho(x_s)$, or $\kappa(x_s)$), recompute the decompositions, and compare results to those using the original parameters. In particular, we either increase or decrease all the $\tau(x_s)$'s, $\rho(x_s)$'s, or $\kappa(x_s)$'s from their original values reported in Table 1 by one-half of a standard deviation (based on the bootstrap analysis), which yields six new decompositions.[47] Results are reported in Table IA.8 for the market risk premium at just the 30-day horizon for brevity (results are similar at longer horizons). Decreasing (increasing) τ corresponds with increasing (decreasing) risk aversion (see Equation 14). As expected, increasing (decreasing) risk aversion increases (decreases) the market risk premium. This is true for the total risk premium as well as each of its three components. What may be

[47] We use one-half of a standard deviation (as opposed to one standard deviation) since the property that downside, central, and upside risk premia add to the total risk premium imposes implicit restrictions on the relationships between $\tau(x_s)$, $\rho(x_s)$, and $\kappa(x_s)$. If we modify one parameter by a large amount while holding the others fixed, the property does not hold. As long as we do not modify each parameter too much, the property holds approximately.

less intuitive is that increasing risk aversion results in a lower (higher) contribution from downside (upside) risk. This effect is due to the fact that increasing risk aversion results in a higher probability of bad return outcomes relative to good return outcomes under the risk-neutral measure, so the downside risk premium increases relatively less than the upside risk premium in response to increasing in risk aversion. This behavior is also apparent in result reported in Table IA.17 when we assume the representative investor has specific utility functions and investigate changing risk aversion on decompositions in this context. ρ is directly proportional to investor prudence and the total market risk premium should be decreasing in ρ according to Equations 13 and 27, which is exactly what we find in Table IA.8. κ is directly proportional to investor temperance and the total market risk premium should be increasing in κ according to Equations 13 and 27, which is indeed what we find in Table IA.8. One way to intuitively think about the effect of ρ and κ on the relative contributions of down and upside risk is to recognize that the market return distribution is left skewed. In this case, variations in these parameters will have more of an effect on downside risk premia, so increasing ρ (κ) leads to a relatively smaller (larger) contribution of the downside risk premium to the overall risk premium, which is what we observe in Table IA.8.

IA.3.6 Data-Implied Decomposition Preference Parameter Plots and the Implied SDF

Figure IA.7 plots estimates relative risk aversion and Figure IA.8 plots estimates of τ, ρ, and κ reported in Table 1 for visualization. These estimated preference parameters have implications for the behavior of the SDF in different regions of the return space. Given a set of estimated preference parameters in each region and measures of risk neutral moments at date t for horizon T, we can construct the conditional implied SDF in each region as the inverse of Equation 18. We do this for three different dates in Figure IA.9. The dates are chosen to be on dates with low market volatility (3 January, 2006 and 2 January, 2014) and one date with large market volatility (15 September, 2008). Within a given horizon, the SDF plots are very consistent across dates implying that the SDF does not change much over time.[48] It should also be noted that, although different preference parameters are used to construct the implied SDF in different regions, the SDF does not jump much at the boundaries between different regions relative to the overall range of the SDF across the plotted market return space. The SDF flattens with horizon, implying investor marginal utility increases more for equivalent decreases in market value in the short term than the long term.

IA.3.7 Generating Non-Monotonic SDFs

The preference parameters we estimate in our main decomposition (reported in Table 1) paired with our estimated risk-neutral moments imply the SDF is monotonically decreasing (see Figure IA.9 for examples). This result is inconsistent with a line of literature that documents an "SDF puzzle" - namely, that over some regions of the market return space, the SDF is actually increasing (see Jackwerth and Cuesdeanu (2018) for a review of the SDF puzzle literature).

One point to note is that papers documenting the SDF puzzle typically use disparate information sets to estimate the physical and risk-neutral distributions necessary to construct the SDF. In particular, they rely on past market return data to estimate the physical distribution and forward-looking options data to estimate the risk-neutral distribution. Linn, Shive, and Shumway (2018) and Barone-Adesi et al. (2020) have recently made the point that this inconsistency in information

[48] The only exception is during November, 2008 in the peak of the financial crisis. During this period, the upper limit of the SDF became lower in the down region of the return space. This implies that during the financial crises investor marginal utility was particularly high in states of the world with very low realized market returns.

sets can actually generate the SDF puzzle. Each provide a different methodology for estimating physical and risk-neutral distributions using consistent information sets (i.e., only forward-looking information), and neither generate an SDF puzzle. Our decomposition offers a third approach to estimate the SDF using only forward-looking information. Consistent with the logic in Linn, Shive, and Shumway (2018) and Barone-Adesi et al. (2020), we find our approach does not generate an SDF puzzle.

Regardless, it is interesting to ask the question: Is our approach flexible enough to generate a non-monotonic SDF? To this end, we identify preference parameters that minimize the squared distance between an SDF characterized by our Equation 18 and non-monotonic SDFs from: 1) Figure 6 in Rosenberg and Engle (2002), and 2) Figure 2 in Beason and Schreindorfer (2022). Table IA.9 provides the sets of preference parameters that minimize the squared distance between each of these prototypical non-monotonic SDFs and the SDF implied by our Equation 18. Figure IA.10 plots our optimized SDFs against those originally reported in Rosenberg and Engle (2002) and Beason and Schreindorfer (2022). In both cases, our SDF is also non-monotonic and able to match the target SDFs fairly well. Put simply, if the data were to indicate a non-monotonic SDF, our Equation 18 is sufficiently flexible to capture the non-monotonicity. The fact that our estimated SDFs are monotonically decreasing implies that our approach, like the philosophically similar approaches in Linn, Shive, and Shumway (2018) and Barone-Adesi et al. (2020), does not imply an SDF puzzle.

Some points to note regarding reproducing the SDFs in Rosenberg and Engle (2002) and Beason and Schreindorfer (2022) are as follows. First, these are both unconditional SDFs. Since our SDF implied by Equation 18 is conditional (varying with the conditional risk-neutral moments), when we identify optimal preference parameters to match the target non-monotonic SDFs we use unconditional time series averages for the risk-neutral moments when constructing our mimicking SDF. However, we are able to generate similar non-monotonic SDFs when using randomly-selected dates on which to measure conditional risk-neutral moments for use in the parameter optimization. Second, Table IA.9 implies that some preference parameters are negative, and we find that it is necessary to allow negative preference parameters to generate the SDF puzzle. We originally restricted the search space used to estimate parameters in our Table 1 to include only non-negative preference parameters in order to impose the economically-motivated preference parameter restrictions discussed in footnote 5. However, when we re-estimate the preference parameters in our main data-implied decomposition allowing for negative preference parameters in the search space, the optimal parameters are the same as those reported in Table 1 (up to at least the second decimal place across all regions and horizons). In other words, even if we allow our optimization algorithm to search over negative preference parameters, we still arrive at (effectively) the same optimal (positive) preference parameters which do not generate non-monotonic SDFs. Third, since the SDF reported by Rosenberg and Engle (2002) does not have support for market returns below -10% or above $+10\%$, we use $\pm 5\%$ cutoffs in this case (i.e., $\underline{x} = 0.95$ and $\overline{x} = 1.05$). This is not an issue for the Beason and Schreindorfer (2022) SDF, which has support for market returns well below -10% and above $+10\%$.

IA.3.8 Data-Implied Risk Premium Decomposition (Using Corollary 2)

Our main risk premium decomposition results rely on Corollary 1 to estimate nine region-specific preference parameters ($\tau(x_s)$, $\rho(x_s)$, and $\kappa(x_s)$) according to the methodology described in Internet Appendix IA.6, which are then used to construct physical moments according to Corollary 1. These physical moments are then used as inputs to compute our main decomposition results according to Proposition 3. In this section, we estimate a single set of preference parameters (τ, ρ, and κ)

that apply to all regions. We achieve this using Corollary 2 and the same procedure described in Internet Appendix IA.6 (adapted in the obvious way to apply to Corollary 2). We report these estimated parameters in Table IA.10.[49] Note that these estimated preference parameters are similar to the averages of preference parameters across the three regions from our main decomposition reported in Table 1. We use this single set of estimated preference parameters to construct physical moments according to Corollary 2. These physical moments are then used as inputs to compute a decomposition in the usual way according to Proposition 3. This is effectively the same approach as we use in our restricted decomposition (see Subsection IA.3.9) using the estimated set of preference parameters rather than preference parameters that we fix ex-ante without estimation.

Figure IA.11 plots the resulting market risk premium decompositions at various horizons and Table IA.11 provides related summary statistics. These are analogous to our main decomposition results (that use region-specific preference parameters) reported in Figure 2 and Table 2. The main message is results that rely on a single set of estimated parameters are similar to the more flexible parameterization that uses nine region-specific parameters. One notable difference is that the three-parameter decomposition implies the downside risk premium contribution is slightly higher than in our main nine-parameter data-implied decomposition. This comes at the expense of both the central and upside risk premium contributions (these are both slightly lower than in our main results). We do not report variance risk premium decomposition results under this more parsimonious parameterization for brevity, and since they are also quite similar to our main data-implied decomposition results summarized in Figure IA.4 and Table IA.1. However, in this case, the three-parameter decomposition implies that the downside risk premium contribution is slightly lower than in our main results.

IA.3.9 Data-Implied Decomposition Using Restricted Preference Parameters

One might be concerned that our measures in the previous sub-section are overly-reliant on in-sample estimates of the preference parameters. To mitigate this concern, in this sub-section we impose the same restrictions on our preference parameters as those used by Chabi-Yo and Loudis (2020) to construct a restricted lower bound on the market risk premium. Namely, we set $\tau = 1$, $\rho = 2$, and $\kappa = 4$ across all regions and horizons.[50] We use Corollary 2 to compute the physical moments using risk-neutral moments since we only have one set of preference parameters for the whole return space in this case. The restricted preference parameter values are similar to the values of $\tau(x_s)$, $\rho(x_s)$, and $\kappa(x_s)$ reported in Table 1 averaged over all horizons and regions, which are 0.73, 2.88, and 2.84, respectively. Under standard preference assumptions, the market risk premium is decreasing in τ, increasing in ρ, and decreasing in κ, so we expect the average market risk premium constructed using these restricted parameters to be lower than that constructed using the estimated parameters and reported in Table 2.

Table IA.12 reports summary statistics when the risk premium decomposition is constructed using the restricted preference parameters. Results are generally in line with those reported using estimated preference parameters in Table 2 except for one notable exception: average total risk premia are lower (higher) at short (long) horizons than the related values in Table 2. This is because: 1. The restricted τ is typically higher (lower) than the estimated value at short (long) horizons, 2. The restricted ρ is typically lower (higher) than the estimated value at short (long)

[49] We assume these are constant over time rather than a function of $R_{f,t\to T}$ for parsimony.

[50] See Chabi-Yo and Loudis (2020) for more details on these restrictions. We also note here that Noussair, Trautmann, and VanDeKuilen (2014) provide evidence that $\tau < 1$, $\rho > 1$, and $\kappa > 1$ in a different empirical setting, which imply that our choices for the restricted τ, ρ, and κ yield a lower bound on the market risk premium.

horizons, and 3. The restricted κ is typically higher (lower) than the estimated value at short (long) horizons. We provide the associated risk premium decomposition plots in Figure IA.12, which are visually quite similar to our main decomposition plots in Figure 2.

Table IA.13 provides forecasting regression results of the form in Equation 33 but using the risk premium decomposition constructed using the restricted preference parameters and using ±5% cutoffs (as we do for our main results in Table 3 due to data limitations related to limited observations outside our standard ±10% cutoffs). Results are similar to those from our main decomposition reported in Table 3, although we reject the nulls that $a_T = 0$ and $b_T = 1$. This is as expected since these preference parameters generate a lower bound on the market risk premium rather than a rational forecast, as discussed in Chabi-Yo and Loudis (2020).

IA.3.10 Using Observed Prices Instead of Implied Volatility Fitting

In this subsection, we explore whether constructing risk-neutral moments by numerically integrating over observed options prices rather than using the implied volatility fitting methodology (described in Section 4.1 and footnote 10) alters our main results related to the market risk premium decomposition. Aside from numerically integrating over observed option prices (using the same equations summarized in Internet Appendix IA.5) rather than prices imputed from fitted implied volatility curves, all procedures are the same. This includes re-estimating preference parameters, which are similar to the original estimates so we do not report these. Results for the modified market risk premium decomposition are provided in Figure IA.13 and Table IA.14. These results can be compared with our analogous main results in Figure 2 and Table 2. The modified decomposition produces results that are both qualitatively and quantitatively similar to our main results and we conclude that the choice to compute risk-neutral moments by integrating over options prices implied by fitted implied volatility curves versus integrating over observed prices is innocuous. In unreported results (for brevity), we also find that the variance risk premium decomposition using this methodology is similar to that from our main results.

IA.3.11 Using an SVI Model to Estimate Implied Volatility

Our implied volatility fitting methodology described in footnote 10 implicitly assumes market returns are log-normally distributed above (below) the highest (lowest) observed strikes. One might be concerned that this assumption leads to measurement bias in risk-neutral moments that are sensitive to the tails of the market return distribution, which may consequently lead to bias in our main decomposition results. To address this concern, we model implied volatilities using the Gatheral and Jacquier (2014) SVI model and report results in this subsection.

In particular, we use the Gatheral and Jacquier (2014) SVI model to estimate implied volatilities at each date and observed maturity.[51] We then use these implied volatilities rather than those from the implied volatility fitting methodology described in Section 4.1 and footnote 10 to construct

[51] To fit the model, we minimize the sum-of-squared differences between model-implied implied volatilities and implied volatilities inverted from observed option prices using the Black-Scholes model. To be consistent with the way in which we estimate implied volatilities in our main results, we only use implied volatilities imputed from observed out-of-the-money option prices. We also impose an upper bound of 300% on the SVI-implied volatilities at the lower bound of our numerical integrations (i.e., at a strike-price-to-market-price ratio of 0.01), and an upper bound of 100% on the SVI-implied volatilities at the upper bound of our numerical integrations (i.e., at a strike price-to-market-price ratio of 2). Note that these are annualized values. We find that these upper bounds are rarely binding, and that they prevent unstable SVI parameterizations when a relatively small cross-section of options is available. They also represent upper bounds that are quite high. For reference, the one-month risk-neutral volatility we estimate at the peak of the financial crisis was about 65% (annualized).

the risk-neutral moments used in our analysis. Aside from using a different procedure to estimate implied volatilities, all procedures are the same. This includes re-estimating preference parameters, which are similar to the original estimates (so we do not report these for brevity).

Results for the SVI-based market risk premium decomposition are provided in Figure IA.14 and Table IA.15. These results can be compared with our analogous main results in Figure 2 and Table 2. The modified decomposition produces results that are both qualitatively and quantitatively similar to our main results and we conclude that the choice to compute risk-neutral moments by assuming market returns are log-normally distributed above (below) the highest (lowest) observed strikes is innocuous for our main conclusions. This result may be surprising given that the SVI model allows for fatter tails in the market return distribution than under our main volatility fitting methodology. However, the equations used to compute risk-neutral moments from option prices in Internet Appendix IA.5 put low weights on far out-of-the-money option prices relative to close-to-the-money option prices. Our results in this section imply that these relatively low weights make it so that our decomposition is relatively insensitive to either assuming market returns are log-normally distributed in the tails compared to allowing for stochastic volatility via the Gatheral and Jacquier (2014) SVI model. In unreported results (for brevity), we also find that the variance risk premium decomposition using the SVI methodology is similar to that from our main results.

IA.3.12 Adjusting for Potentially Overpriced Options

There is evidence that the well-known implied volatility smirk displayed by index option prices is at least partially the result of supply/demand imbalances caused by the inability of market makers to perfectly hedge option exposures (Garleanu, Pedersen, and Poteshman, 2009). These imbalances imply that observed option prices are mispriced and do not reflect no-arbitrage prices. Garleanu, Pedersen, and Poteshman (2009) define mispricing in the cross-section of option moneyness as deviations in measured Black-Scholes implied volatility from the physical volatility estimated using Bates (2006). The authors show that this difference is on average decreasing in option moneyness (see Figure 1 in their paper). Importantly, they show that (on average) the implied volatility of OTM calls is approximately the same as the Bates (2006) volatility measure (i.e., these options are "correctly" priced if the Bates (2006) measure is the correct measure of volatility).

If the option prices we observed deviate from their no-arbitrage prices due to demand pressure, this is a problem for the risk-neutral moments we construct and use to perform the empirical implementation of our risk premium decomposition. Although a full estimation of demand-driven option pricing models and their effects on observed option prices is beyond the scope of this paper, we construct a heuristic method for assessing the potential effect of such demand pressure on observed options prices. We do this by modifying our measured implied volatility curves for cross-sections of option prices (in moneyness) at each date and for each maturity. Our main task is to provide a reasonable transformation of observed implied volatility curves to account for potential demand-driven mispricing and effectively correct observed options prices so that they reflect no-arbitrage relationships.

One approach would be to simply use the Bates (2006) volatility measure as the "correct" measure of implied volatility across all strikes for each date/maturity combination. We feel that this is too restrictive since it implies index prices are log-normal (i.e., the standard Black-Scholes assumption). There is significant evidence that this is not the case and that index prices are negatively skewed. To allow for this empirical fact, we consider approaches to shrink observed implied volatility curves towards the constant Black-Scholes benchmark. Two key insights from Garleanu, Pedersen, and Poteshman (2009) are that demand-corrected implied volatility curves should be lower than observed implied volatility curves and that OTM calls are approximately correctly priced. Given

these insights, we assume that the OTM call with the lowest observed implied volatility is approximately correctly priced for sets of options at each date/maturity. We denote the associated implied volatility and strike price as IV_0 and K_0, respectively. We then construct a transformed implied volatility curve for each date/maturity as follows. Let all observed volatilities and strikes be denoted by IV_i and K_i. Let the transformed implied volatilities be denoted by $\tilde{IV}_i$. For any OTM calls with $K_i > K_0$, we set $\tilde{IV}_i = IV_0$. Next, for any options with $IV_i < IV_0$, we set $\tilde{IV}_i = IV_0$. Finally, we select a constant, a, and transform all other implied volatilities according to: $\tilde{IV}_i = IV_i - a\,(IV_i - IV_0)$. As long as $a \in [0, 1]$, this transformation shrinks the observed implied volatilities, IV_i, towards IV_0. When $a = 1$, we have $\tilde{IV}_i = IV_0\ \forall i$ (i.e., the transformed implied volatility curve is flat and takes on a value equal to the implied volatility of the OTM call option with the lowest implied volatility). When $a = 0$, we obtain the original implied volatilities (i.e., $\tilde{IV}_i = IV_i\ \forall i$).

The final ingredient in our heuristic correction is to select a. We do this in a conservative way that sets the risk-neutral market return skewness (approximately) to the physical skewness. Our baseline risk-neutral and physical skewness measures imply that risk-neutral skewness measured from observed options prices is approximately twice that of the physical skewness implied by our estimated preference parameters in Table 1. This holds unconditionally and is approximately true conditionally. As outside validation of this result, results reported in Beason and Schreindorfer (2022) imply that the ratio of unconditional risk-neutral to physical skewness is about 2. As an identifying assumption, we assume that this relationship holds conditionally and identify the a value such that this is true. We find that this holds on average when $a \approx 0.45$ and set a to this value in our analysis.

This implied volatility transformation attempts to match risk-neutral implied volatility and skewness to those from the physical market return distribution by shrinking the implied volatility curve towards IV_0. The idea is that any differences between IV_i and $\tilde{IV}_i$ represent options price premia that are the result of supply/demand imbalances unrelated to risk. To the extent that these price pressures exist, our transformation should produce implied options prices that are closer to their no-arbitrage benchmarks.

Given our estimated value of a, we re-estimate all risk-neutral moments using the transformed implied volatility curves, re-estimate preference parameters, and report the resulting market risk premium decomposition in Figure IA.15 and Table IA.16. These results can be compared with our analogous main results in Figure 2 and Table 2. The modified decomposition produces results that are both qualitatively and quantitatively similar to our main results. The most noticeable difference is that this modification results in the central risk premium becoming a relatively larger component of the total risk premium at the expense of the downside risk premium. This is expected given that we have effectively decreased the implied risk-neutral skewness, making it more similar to the physical distribution skewness. The effect of this is to reduce the importance of the downside risk premium. It should be noted, though, that the downside risk premium still maintains a large contribution to the total risk premium. The upside risk premium contribution is very similar to in our main specification. The implied volatility transformation we impose in this subsection represents a drastic shift of the risk-neutral distribution towards the physical distribution (it effectively cuts the implied volatility smirk slope in half), yet the analysis produces similar results for the risk premium decomposition. We conclude that potential demand-driven options mispricing (or any other mispricing that generates an excessive implied volatility smirk) does not significantly alter our main results and conclusions.

IA.4 Utility Function-Implied Decompositions: Log, CRRA, CARA, and HARA Utilities

This section derives exact closed-form expressions for physical truncated moments in terms of risk neutral quantities when investor utility takes on various commonly specified functional forms. We focus on the log, CRRA, CARA,[52] and HARA utility since these represent the most common forms of time-separable utility functions in extant literature. Given the utility-implied physical moments and corresponding risk-neutral moments, we can estimate risk premium decompositions implied under these various preference assumptions. Analytic expressions for the physical and risk-neutral moments as functions of option prices are provided in Internet Appendix IA.5. Note that, given any utility function, one can compute such closed-form expressions in terms of risk-neutral moments that can be estimated from option prices.

These formulations of our decomposition put slightly more structure on the decomposition than in the data-implied decomposition since they make assumptions about the functional form of representative investor preferences. Hence, they impose restrictions on the preference parameters that we estimate from the data for our data-implied decomposition. They do not, however, impose as much structure as the representative agent models discussed in Section 5, which make assumptions about both the functional forms of preferences and state variable processes that govern the economy. Importantly, to derive results under these specific utility assumptions, we do not make any assumptions about the distribution of market returns or other state variables that govern the economy.

Remark 1. *Assume there exists a representative agent with log utility whose wealth is entirely invested in the market. Given no-arbitrage, the inverse SDF is given by*

$$\frac{\mathbb{E}_t\left[M_{t\to T}\right]}{M_{t\to T}} = \frac{R_{M,t\to T}}{\mathbb{E}_t^*\left[R_{M,t\to T}\right]}$$

and the conditional physical truncated moments are given by

$$\mathbb{M}_{t\to T}^{(n)}\left[A_s\right] = \frac{1}{R_{f,t\to T}}\mathbb{M}_{t\to T}^{*(n+1)}\left[A_s\right] + \mathbb{M}_{t\to T}^{*(n)}\left[A_s\right] \tag{IA.4}$$

for any n and any $A_s \in \{A, A_d, A_c, A_u\}$. Closed form expressions for these risk-neutral moments are provided in Internet Appendix IA.5.

Proof. See Internet Appendix IA.5. ■

Remark 2. *Assume there exists a representative agent with CRRA utility over final wealth given by*

$$U\left(W_T\right) \quad = \quad \frac{W_T^{1-\alpha} - 1}{1-\alpha}$$

[52] Note that fixing $\tau\left(x_s\right)$ to be constant in our main analysis does not imply our representative investor has CRRA utility. CRRA utility implies $-U^{'}\left(W_t R_{M,t\to T}\right)/\left[W_t R_{M,t\to T} U^{''}\left(W_t R_{M,t\to T}\right)\right]$ is constant for all potential realizations of future wealth, $W_T = W_t R_{M,t\to T}$. CRRA utility also imposes restrictions on higher order preference parameters such as ρ and κ given a particular choice for relative risk aversion to achieve constant relative risk aversion regardless of future wealth. For instance, if the representative investor were to have CRRA utility with risk aversion $\gamma = 1/\tau$, this implies the skewness tolerance must be given by $\rho = (1+\gamma)/(2\gamma)$, which we do not impose. Furthermore, we assume $-U^{'}\left(W_t x_s\right)/\left[W_t x_s U^{''}\left(W_t x_s\right)\right]$ is constant in each region given current wealth. By not imposing CRRA parameter restrictions on $\rho\left(x_s\right)$ and $\kappa\left(x_s\right)$ given $\tau\left(x_s\right)$, we do not have a relative risk aversion that is constant for all potential realizations of future wealth, $W_T = W_t R_{M,t\to T}$ as is the case for CRRA utility.

where α is the relative risk aversion, $W_T \equiv W_t R_{M,t\to T}$ is the final wealth, W_t is the initial wealth, and $R_{M,t\to T}$ is the return on the market. Assuming no-arbitrage, the inverse SDF is given by

$$\frac{\mathbb{E}_t\left[M_{t\to T}\right]}{M_{t\to T}} = \frac{R^{\alpha}_{M,t\to T}}{\mathbb{E}^*_t\left[R^{\alpha}_{M,t\to T}\right]}$$

and the conditional physical truncated moments are given by

$$\mathbb{M}^{(n)}_{t\to T}\left[A_s\right] = \frac{\mathbb{E}^*_t\left[R^{\alpha}_{M,t\to T}\left(R_{M,t\to T} - R_{f,t\to T}\right)^n \mathbb{I}_{A_s}\right]}{\mathbb{E}^*_t\left[R^{\alpha}_{M,t\to T}\right]} \tag{IA.5}$$

for any n and any $A_s \in \{A, A_d, A_c, A_u\}$. Closed-form expressions for Equation IA.5 are provided in Internet Appendix IA.5.

Proof. See Internet Appendix IA.5. ■

Remark 3. *Assume there exists a representative agent with CARA utility of the form*

$$U\left(W_T\right) \quad = \quad 1 - e^{-\tilde{\alpha} W_T}$$

where $\tilde{\alpha}$ is the absolute risk aversion, $W_T \equiv W_t R_{M,t\to T}$ is the final wealth, W_t is the initial wealth, and $R_{M,t\to T}$ is the return on the market. Define relative risk aversion as $\alpha \equiv \tilde{\alpha} W_t$. Assuming no-arbitrage, the inverse SDF is given by

$$\frac{\mathbb{E}_t\left[M_{t\to T}\right]}{M_{t\to T}} = \frac{e^{\alpha R_{M,t\to T}}}{\mathbb{E}^*_t\left[e^{\alpha R_{M,t\to T}}\right]}$$

and the conditional physical truncated moments are given by

$$\mathbb{M}^{(n)}_{t\to T}\left[A_s\right] = \frac{\mathbb{E}^*_t\left[e^{\alpha R_{M,t\to T}}\left(R_{M,t\to T} - R_{f,t\to T}\right)^n \mathbb{I}_{A_s}\right]}{\mathbb{E}^*_t\left[e^{\alpha R_{M,t\to T}}\right]} \tag{IA.6}$$

for any n any $A_s \in \{A, A_d, A_c, A_u\}$. Closed-form expressions for Equation IA.6 are provided in Internet Appendix IA.5.

Proof. See Internet Appendix IA.5. ■

Remark 4. *Assume there exists a representative agent with HARA utility of the form*

$$U\left(W_T\right) = \frac{1-\gamma}{\gamma}\left(\frac{a W_T}{1-\gamma} + b\right)^{\gamma} \text{ with } a > 0 \text{ and } \frac{a W_T}{1-\gamma} + b > 0,$$

where $W_T \equiv W_t R_{M,t\to T}$ is the final wealth, W_t is the initial wealth, and $R_{M,t\to T}$ is the return on the market. Assuming no-arbitrage and decreasing relative risk aversion,[53] the inverse SDF is given by

$$\frac{\mathbb{E}_t\left[m_{t\to T}\right]}{m_{t\to T}} = \frac{\left(-a^*\left(R_{M,t\to T}/R_{f,t\to T}\right) - 1\right)^{1-\gamma}}{\mathbb{E}^*_t\left[\left(-a^*\left(R_{M,t\to T}/R_{f,t\to T}\right) - 1\right)^{1-\gamma}\right]}$$

[53] Decreasing relative risk aversion implies $b < 0$. We could also derive a similar expression assuming increasing relative risk aversion ($b > 0$), but choose to omit this less economically relevant case.

where

$$a^* = \left(\frac{1-\gamma}{\mathcal{R}} - 1\right)^{-1}$$

and $\mathcal{R}$ *is the relative risk aversion evaluated at* $W_t R_{f,t\to T}$*. The conditional physical truncated moment is given by*

$$\mathbb{M}^{(n)}_{t\to T}\left[A_s\right] = \frac{\mathbb{E}^*_t\left[\left(-a^*\left(R_{M,t\to T}/R_{f,t\to T}\right)-1\right)^{1-\gamma}\left(R_{M,t\to T}-R_{f,t\to T}\right)^n \mathbb{I}_{A_s}\right]}{\mathbb{E}^*_t\left[\left(-a^*\left(R_{M,t\to T}/R_{f,t\to T}\right)-1\right)^{1-\gamma}\right]} \tag{IA.7}$$

for any n *any* $A_s \in \{A, A_d, A_{c,} A_u\}$*. The closed-form expression for Equation IA.7 is provided in Internet Appendix IA.5.*

Proof. See Internet Appendix IA.5. ■

Given these physical moments and measured risk-neutral moments, we can compute our risk premium decomposition according to Equation 29 under these various preference specifications. Closed-form expressions that allow us to compute these moments directly from option prices are provided in Internet Appendix IA.5. Table IA.17 provides a summary of the average risk premium levels and contributions from each region under each set of preference assumptions. In the case of CRRA and CARA utility, we provide results for levels of relative risk aversion at three, five, and seven. In the case of HARA utility, we are limited to relatively low levels of risk aversion due to the functional form, and set these to 1.0, 1.1, and 1.2. Although the levels of risk premia implied by each specific utility function (Panel A) can be quite different than those from our data-implied decomposition, the contributions (Panel B) are actually more similar to those from the data-implied decomposition relative to those from the representative agent model-implied decompositions. This implies that the additional structure implied by these models can lead to model misspecification that has counterfactual implications for the relative contributions to the total risk premium to which the utility-based decomposition are immune.

IA.5 Expressions for Computing Risk-Neutral Moments

In this section, we use the Carr and Madan (2001) spanning formula to derive expressions for various risk-neutral moments needed for our decomposition as functions of observable options prices. The spanning formula can be written as:

$$h\left(y\right) = h\left(y_0\right) + \left(y-y_0\right)h_y\left(y_0\right) + \int_0^{y_0} h_{yy}\left(K\right)\left(K-y\right)^+ dK + \int_{y_0}^{\infty} h_{yy}\left(K\right)\left(y-K\right)^+ dK \tag{IA.8}$$

where $h\left(y\right)$ represents a generic function of y. We refer to y_0 as the "Carr and Madan expansion point." In our case, we are interested in functions of the future market index at time T, S_T (i.e., we set $y = S_T$). We can think of y_0 as a baseline market index value (e.g., $y_0 = R_{f,t\to T}S_t$, where S_t is the current market price at time t). We switch between using $R_{M,t\to T}$ with the equivalent expression S_T/S_t in this section when appropriate for clarity. We also make use of the following indicator functions when computing truncated moments: $\mathbb{I}_{A_c} \equiv \mathbb{I}_{\{\underline{x}S_t \le S_T \le \overline{x}S_T\}}$, $\mathbb{I}_{A_d} \equiv \mathbb{I}_{\{S_T < \underline{x}S_t\}}$, and $\mathbb{I}_{A_u} \equiv \mathbb{I}_{\{S_T > \overline{x}S_t\}}$.

Expressions in this section require us to compute integrals of functions of option prices with respect to the strike price. Using the Black-Scholes formula, there is a one-to-one mapping between observed prices and implied volatilities. To compute risk-neutral moments we map observed prices

to implied volatilities, fit the implied volatilities according to the procedure described in footnote 10, then invert the fitted volatilities to obtain prices needed for the expressions in this section.

IA.5.1 Risk-Neutral Moments Centered on $R_{f,t\to T}$

In this subsection, we derive expressions for risk-neutral moments of the form $\mathbb{E}^*\left[\left(R_{M,t\to T}-R_{f,t\to T}\right)^n\right]$ and $\mathbb{E}^*\left[\left(R_{M,t\to T}-R_{f,t\to T}\right)^n \mathbb{I}_{A_s}\right]$ where $R_{M,t\to T}$ is the gross market return from time t to T, $R_{f,t\to T}$ is the risk-free rate from time t to T, and $\mathbb{I}_{A_s}$ is an indicator function for realized market returns belonging to sets A_s defined in Equations 4, 5, and 6. Note that we can express the gross market return as $R_{M,t\to T}=S_T/S_t$.

IA.5.1.1 Untruncated Risk-Neutral Moments Centered on $R_{f,t\to T}$: $\mathbb{E}^*\left[\left(R_{M,t\to T}-R_{f,t\to T}\right)^n\right]$

Set the function $h(\cdot)$ in Equation IA.8 to

$$h(S_T) = \left(\frac{S_T}{S_t}-R_{f,t\to T}\right)^n. \tag{IA.9}$$

Derivatives of this function are

$$h_y(S_T) = \frac{n}{S_t}\left(\frac{S_T}{S_t}-R_{f,t\to T}\right)^{n-1} \text{ and} \tag{IA.10}$$

$$h_{yy}(S_T) = \frac{n(n-1)}{S_t^2}\left(\frac{S_T}{S_t}-R_{f,t\to T}\right)^{n-2}. \tag{IA.11}$$

Next, set $y_0=R_{f,t\to T}S_t$. Evaluating the function and its derivatives at values needed for Equation IA.8 yields:

$$h\left(R_{f,t\to T}S_t\right) = 0,$$

$$h_y\left(R_{f,t\to T}S_t\right) = 0, \text{ and}$$

$$h_{yy}(K) = \frac{n(n-1)}{S_t^2}\left(\frac{K}{S_t}-R_{f,t\to T}\right)^{n-2}.$$

Substituting these expressions into Equation IA.8 yields:

$$\begin{aligned}\left(\frac{S_T}{S_t}-R_{f,t\to T}\right)^n = {} & \frac{n(n-1)}{S_t^2}\int_0^{R_{f,t\to T}S_t}\left(\frac{K}{S_t}-R_{f,t\to T}\right)^{n-2}(K-S_T)^+\,dK \\ & +\frac{n(n-1)}{S_t^2}\int_{R_{f,t\to T}S_t}^{\infty}\left(\frac{K}{S_t}-R_{f,t\to T}\right)^{n-2}(S_T-K)^+\,dK.\end{aligned}$$

Taking expectations under the risk-neutral measure at time t yields:

$$\begin{aligned}&\mathbb{E}_t^*\left[\left(R_{M,t\to T}-R_{f,t\to T}\right)^n\right] \\ = {} & \frac{n(n-1)R_{f,t\to T}}{S_t^2}\int_0^{R_{f,t\to T}S_t}\left(\frac{K}{S_t}-R_{f,t\to T}\right)^{n-2}P_{t\to T}[K]\,dK \\ & +\frac{n(n-1)R_{f,t\to T}}{S_t^2}\int_{R_{f,t\to T}S_t}^{\infty}\left(\frac{K}{S_t}-R_{f,t\to T}\right)^{n-2}C_{t\to T}[K]\,dK\end{aligned} \tag{IA.12}$$

where $P_{t\to T}[K]$ and $C_{t\to T}[K]$ are the put and call prices with strike prices K at time t and expiration date T. Note that when $n=1$ the expression yields $\mathbb{E}_t^*\left[\left(R_{M,t\to T}-R_{f,t\to T}\right)\right]=0$ as expected (i.e., because the risk-neutral expected market return is the risk-free rate).

IA.5.1.2 Downside Risk-Neutral Moments Centered on $R_{f,t\to T}$: $\mathbb{E}^*\left[\left(R_{M,t\to T}-R_{f,t\to T}\right)^n \mathbb{I}_{A_d}\right]$

Set the function $h(\cdot)$ in Equation IA.8 to that in Equation IA.9. Next, set $y_0 = \underline{x}S_t$. Evaluating the function and its first derivative at values needed for Equation IA.8 yields:

$$\begin{aligned} h\left(\underline{x}S_t\right) &= \left(\underline{x}-R_{f,t\to T}\right)^n \text{ and} \\ h_y\left(\underline{x}S_t\right) &= \frac{n}{S_t}\left(\underline{x}-R_{f,t\to T}\right)^{n-1}. \end{aligned}$$

Substituting these expressions into Equation IA.8 yields:

$$\begin{aligned} \left(\frac{S_T}{S_t}-R_{f,t\to T}\right)^n &= \left(\underline{x}-R_{f,t\to T}\right)^n + n\left(\underline{x}-R_{f,t\to T}\right)^{n-1}\left(\frac{S_T}{S_t}-\underline{x}\right) \\ &+\frac{n(n-1)}{S_t^2}\int_0^{\underline{x}S_t}\left(\frac{K}{S_t}-R_{f,t\to T}\right)^{n-2}(K-S_T)^+\,dK \\ &+\frac{n(n-1)}{S_t^2}\int_{\underline{x}S_t}^{\infty}\left(\frac{K}{S_t}-R_{f,t\to T}\right)^{n-2}(S_T-K)^+\,dK. \end{aligned}$$

Multiplying by $\mathbb{I}_{\{S_T<\underline{x}S_t\}}$ yields:

$$\begin{aligned} \left(\frac{S_T}{S_t}-R_{f,t\to T}\right)^n \mathbb{I}_{\{S_T<\underline{x}S_t\}} &= \left(\underline{x}-R_{f,t\to T}\right)^n \mathbb{I}_{\{S_T<\underline{x}S_t\}} + n\left(\underline{x}-R_{f,t\to T}\right)^{n-1}\left(\frac{S_T}{S_t}-\underline{x}\right)\mathbb{I}_{\{S_T<\underline{x}S_t\}} \\ &+\frac{n(n-1)}{S_t^2}\int_0^{\underline{x}S_t}\left(\frac{K}{S_t}-R_{f,t\to T}\right)^{n-2}(K-S_T)^+\,\mathbb{I}_{\{S_T<\underline{x}S_t\}}dK \\ &+\frac{n(n-1)}{S_t^2}\int_{\underline{x}S_t}^{\infty}\left(\frac{K}{S_t}-R_{f,t\to T}\right)^{n-2}(S_T-K)^+\,\mathbb{I}_{\{S_T<\underline{x}S_t\}}dK. \end{aligned}$$

Simplifying this expression yields:

$$\begin{aligned} \left(\frac{S_T}{S_t}-R_{f,t\to T}\right)^n \mathbb{I}_{\{S_T<\underline{x}S_t\}} &= \left(\underline{x}-R_{f,t\to T}\right)^n \mathbb{I}_{\{S_T<\underline{x}S_t\}} - n\left(\underline{x}-R_{f,t\to T}\right)^{n-1}\frac{1}{S_t}\left(\underline{x}S_t-S_T\right)\mathbb{I}_{\{S_T<\underline{x}S_t\}} \\ &+\frac{n(n-1)}{S_t^2}\int_0^{\underline{x}S_t}\left(\frac{K}{S_t}-R_{f,t\to T}\right)^{n-2}(K-S_T)^+\,dK. \end{aligned}$$

Taking expectations under the risk-neutral measure at time t yields:

$$\begin{aligned} &\mathbb{E}^*\left[\left(R_{M,t\to T}-R_{f,t\to T}\right)^n \mathbb{I}_{A_d}\right] \\ =\ &\left(\underline{x}-R_{f,t\to T}\right)^n Prob_t^*\left[R_{M,t\to T}<\underline{x}\right] - n\left(\underline{x}-R_{f,t\to T}\right)^{n-1}\frac{R_{f,t\to T}}{S_t}P_{t\to T}\left[\underline{x}S_t\right] \\ &+\frac{n(n-1)R_{f,t\to T}}{S_t^2}\int_0^{\underline{x}S_t}\left(\frac{K}{S_t}-R_{f,t\to T}\right)^{n-2}P_{t\to T}[K]\,dK \end{aligned} \tag{IA.13}$$

where $Prob_t^*\left[R_{M,t\to T}<\underline{x}\right]$ is the risk-neutral probability at time t that $R_{M,t\to T}<\underline{x}$ and can be computed as:

$$Prob_t^*\left[R_{M,t\to T}<\underline{x}\right] = R_{f,t\to T}\left.\frac{\partial P_{t\to T}[K]}{\partial K}\right|_{K=\underline{x}S_t} \tag{IA.14}$$

where $\left.\frac{\partial P_{t\to T}[K]}{\partial K}\right|_{K=\underline{x}S_t}$ is the partial derivative of the put price with respect to K evaluated at $K=\underline{x}S_t$. We also make use of the definitions $\mathbb{I}_{A_d}\equiv\mathbb{I}_{\{S_T<\underline{x}S_t\}}$ and $R_{M,t\to T}\equiv S_T/S_t$. We compute $\left.\frac{\partial P_{t\to T}[K]}{\partial K}\right|_{K=\underline{x}S_t}$ by computing the slope between put prices with strikes that span $\underline{x}S_t$.

IA.5.1.3 Upside Risk-Neutral Moments Centered on $R_{f,t\to T}$: $\mathbb{E}^*\left[\left(R_{M,t\to T}-R_{f,t\to T}\right)^n \mathbb{I}_{A_u}\right]$

Set the function $h(\cdot)$ in Equation IA.8 to that in Equation IA.9. Next, set $y_0 = \overline{x}S_t$. Evaluating the function and its first derivative at values needed for Equation IA.8 yields:

$$\begin{aligned} h\left(\overline{x}S_t\right) &= \left(\overline{x}-R_{f,t\to T}\right)^n \text{ and} \\ h_y\left(\overline{x}S_t\right) &= \frac{n}{S_t}\left(\overline{x}-R_{f,t\to T}\right)^{n-1}. \end{aligned}$$

Substituting these expressions into Equation IA.8 yields:

$$\begin{aligned} \left(\frac{S_T}{S_t}-R_{f,t\to T}\right)^n &= \left(\overline{x}-R_{f,t\to T}\right)^n + n\left(\overline{x}-R_{f,t\to T}\right)^{n-1}\left(\frac{S_T}{S_t}-\overline{x}\right) \\ &+\frac{n(n-1)}{S_t^2}\int_0^{\overline{x}S_t}\left(\frac{K}{S_t}-R_{f,t\to T}\right)^{n-2}\left(K-S_T\right)^+ dK \\ &+\frac{n(n-1)}{S_t^2}\int_{\overline{x}S_t}^{\infty}\left(\frac{K}{S_t}-R_{f,t\to T}\right)^{n-2}\left(S_T-K\right)^+ dK. \end{aligned}$$

Multiplying by $\mathbb{I}_{\{S_T>\overline{x}S_t\}}$ yields:

$$\begin{aligned} \left(\frac{S_T}{S_t}-R_{f,t\to T}\right)^n \mathbb{I}_{\{S_T>\overline{x}S_t\}} &= \left(\overline{x}-R_{f,t\to T}\right)^n \mathbb{I}_{\{S_T>\overline{x}S_t\}} + n\left(\overline{x}-R_{f,t\to T}\right)^{n-1}\left(\frac{S_T}{S_t}-\overline{x}\right)\mathbb{I}_{\{S_T>\overline{x}S_t\}} \\ &+\frac{n(n-1)}{S_t^2}\int_0^{\overline{x}S_t}\left(\frac{K}{S_t}-R_{f,t\to T}\right)^{n-2}\left(K-S_T\right)^+ \mathbb{I}_{\{S_T>\overline{x}S_t\}}dK \\ &+\frac{n(n-1)}{S_t^2}\int_{\overline{x}S_t}^{\infty}\left(\frac{K}{S_t}-R_{f,t\to T}\right)^{n-2}\left(S_T-K\right)^+ \mathbb{I}_{\{S_T>\overline{x}S_t\}}dK. \end{aligned}$$

Simplifying this expression yields:

$$\begin{aligned} \left(\frac{S_T}{S_t}-R_{f,t\to T}\right)^n \mathbb{I}_{\{S_T>\overline{x}S_t\}} &= \left(\overline{x}-R_{f,t\to T}\right)^n \mathbb{I}_{\{S_T>\overline{x}S_t\}} + n\left(\overline{x}-R_{f,t\to T}\right)^{n-1}\frac{1}{S_t}\left(S_T-\overline{x}S_t\right)^+ \\ &+\frac{n(n-1)}{S_t^2}\int_{\overline{x}S_t}^{\infty}\left(\frac{K}{S_t}-R_{f,t\to T}\right)^{n-2}\left(S_T-K\right)^+ dK. \end{aligned}$$

Taking expectations under the risk-neutral measure at time t yields:

$$\begin{aligned} &\mathbb{E}^*\left[\left(R_{M,t\to T}-R_{f,t\to T}\right)^n \mathbb{I}_{A_u}\right] \\ =\ &\left(\overline{x}-R_{f,t\to T}\right)^n Prob_t^*\left[R_{M,t\to T}>\overline{x}\right] + n\left(\overline{x}-R_{f,t\to T}\right)^{n-1}\frac{R_{f,t\to T}}{S_t}C_{t\to T}\left[\overline{x}S_t\right] \\ &+\frac{n(n-1)R_{f,t\to T}}{S_t^2}\int_{\overline{x}S_t}^{\infty}\left(\frac{K}{S_t}-R_{f,t\to T}\right)^{n-2}C_{t\to T}\left[K\right]dK \end{aligned} \tag{IA.15}$$

where $Prob_t^*\left[R_{M,t\to T}>\overline{x}\right]$ is the risk-neutral probability at time t that $R_{M,t\to T}>\overline{x}$ and can be computed as:

$$Prob_t^*\left[R_{M,t\to T}>\overline{x}\right] = -R_{f,t\to T}\left.\frac{\partial C_{t\to T}\left[K\right]}{\partial K}\right|_{K=\overline{x}S_t} \tag{IA.16}$$

where $\left.\frac{\partial C_{t\to T}[K]}{\partial K}\right|_{K=\overline{x}S_t}$ is the partial derivative of the call price with respect to K evaluated at $K=\overline{x}S_t$. We also make use of the definitions $\mathbb{I}_{A_u}\equiv\mathbb{I}_{\{S_T>\overline{x}S_t\}}$ and $R_{M,t\to T}\equiv S_T/S_t$. We compute $\left.\frac{\partial C_{t\to T}[K]}{\partial K}\right|_{K=\overline{x}S_t}$ by computing the slope between call prices with strikes that span $\overline{x}S_t$.

IA.5.1.4 Central Risk-Neutral Moments Centered on $R_{f,t\to T}$: $\mathbb{E}^*\left[\left(R_{M,t\to T}-R_{f,t\to T}\right)^n \mathbb{I}_{A_c}\right]$

Observe the following identity:

$$\mathbb{I}_{\{\underline{x}S_t\leq S_T\leq \overline{x}S_T\}} \equiv 1-\mathbb{I}_{\{S_T<\underline{x}S_t\}}-\mathbb{I}_{\{S_T>\overline{x}S_t\}}. \tag{IA.17}$$

This identity implies the following identity relating the risk-neutral moments:

$$\begin{aligned}\mathbb{E}^*\left[\left(R_{M,t\to T}-R_{f,t\to T}\right)^n \mathbb{I}_{A_c}\right] \equiv\ & \mathbb{E}_t^*\left[\left(R_{M,t\to T}-R_{f,t\to T}\right)^n\right]\\ & -\mathbb{E}^*\left[\left(R_{M,t\to T}-R_{f,t\to T}\right)^n \mathbb{I}_{A_d}\right]\\ & -\mathbb{E}^*\left[\left(R_{M,t\to T}-R_{f,t\to T}\right)^n \mathbb{I}_{A_u}\right]\end{aligned}$$

where we have made use of the definitions $\mathbb{I}_{A_c}\equiv\mathbb{I}_{\{\underline{x}S_t\leq S_T\leq\overline{x}S_T\}}$, $\mathbb{I}_{A_d}\equiv\mathbb{I}_{\{S_T<\underline{x}S_t\}}$, and $\mathbb{I}_{A_u}\equiv\mathbb{I}_{\{S_T>\overline{x}S_t\}}$. Substituting in expressions from Equations IA.12, IA.13, and IA.15 and simplifying yields:

$$\begin{aligned}&\mathbb{E}^*\left[\left(R_{M,t\to T}-R_{f,t\to T}\right)^n \mathbb{I}_{A_c}\right]\\ =\ & -\left(\underline{x}-R_{f,t\to T}\right)^n Prob_t^*\left[S_T<\underline{x}S_t\right]-\left(\overline{x}-R_{f,t\to T}\right)^n Prob_t^*\left[S_T>\overline{x}S_t\right]\\ & +n\left(\underline{x}-R_{f,t\to T}\right)^{n-1}\frac{R_{f,t\to T}}{S_t}P_{t\to T}\left[\underline{x}S_t\right]-n\left(\overline{x}-R_{f,t\to T}\right)^{n-1}\frac{R_{f,t\to T}}{S_t}C_{t\to T}\left[\overline{x}S_t\right]\\ & +\frac{n\left(n-1\right)R_{f,t\to T}}{S_t^2}\left[\int_{\underline{x}S_t}^{R_{f,t\to T}S_t}\left(\frac{K}{S_t}-R_{f,t\to T}\right)^{n-2}P_{t\to T}\left[K\right]dK\right]\\ & +\frac{n\left(n-1\right)R_{f,t\to T}}{S_t^2}\left[\int_{R_{f,t\to T}S_t}^{\overline{x}S_t}\left(\frac{K}{S_t}-R_{f,t\to T}\right)^{n-2}C_{t\to T}\left[K\right]dK\right].\end{aligned} \tag{IA.18}$$

IA.5.2 Risk-Neutral Moments for log Utility-Based Physical Moments

Proof. Proof of Remark 1. Assuming no-arbitrage conditions, we can show

$$\begin{aligned}\mathbb{M}_{t\to T}^{(n)}\left[A_s\right] &\equiv \mathbb{E}_t\left[\frac{M_{t\to T}}{\mathbb{E}_t\left[M_{t\to T}\right]}\frac{\mathbb{E}_t\left[M_{t\to T}\right]}{M_{t\to T}}\left(R_{M,t\to T}-R_{f,t\to T}\right)^n\mathbb{I}_{A_s}\right]\\ &= \mathbb{E}_t^*\left[\frac{\mathbb{E}_t\left[M_{t\to T}\right]}{M_{t\to T}}\left(R_{M,t\to T}-R_{f,t\to T}\right)^n\mathbb{I}_{A_s}\right]\\ &= \frac{\mathbb{E}_t^*\left[R_{M,t\to T}\left(R_{M,t\to T}-R_{f,t\to T}\right)^n\mathbb{I}_{A_s}\right]}{\mathbb{E}_t^*\left[R_{M,t\to T}\right]}\\ &= \frac{\mathbb{E}_t^*\left[\left(R_{M,t\to T}-R_{f,t\to T}+R_{f,t\to T}\right)\left(R_{M,t\to T}-R_{f,t\to T}\right)^n\mathbb{I}_{A_s}\right]}{\mathbb{E}_t^*\left[R_{M,t\to T}\right]}\\ &= \frac{\mathbb{M}_{t\to T}^{*(n+1)}\left[A_s\right]}{R_{f,t\to T}}+\mathbb{M}_{t\to T}^{*(n)}\left[A_s\right].\end{aligned} \tag{IA.19}$$

■

IA.5.3 Risk-Neutral Moments for CRRA Utility-Based Physical Moments

Proof. Proof of Remark 2. Assuming no-arbitrage conditions, we can show

$$\begin{aligned}\mathbb{M}_{t\to T}^{(n)}\left[A_s\right] &\equiv \mathbb{E}_t\left[\frac{M_{t\to T}}{\mathbb{E}_t\left[M_{t\to T}\right]}\frac{\mathbb{E}_t\left[m_{t\to T}\right]}{m_{t\to T}}\left(R_{M,t\to T}-R_{f,t\to T}\right)^n\mathbb{I}_{A_s}\right]\\ &= \mathbb{E}_t^*\left[\frac{\mathbb{E}_t\left[m_{t\to T}\right]}{m_{t\to T}}\left(R_{M,t\to T}-R_{f,t\to T}\right)^n\mathbb{I}_{A_s}\right]\\ &= \frac{\mathbb{E}_t^*\left[R_{M,t\to T}^{\alpha}\left(R_{M,t\to T}-R_{f,t\to T}\right)^n\mathbb{I}_{A_s}\right]}{\mathbb{E}_t^*\left[R_{M,t\to T}^{\alpha}\right]}.\end{aligned} \tag{IA.20}$$

The second expression is obtained by replacing the inverse of the SDF by its expression. This ends the proof.

■

We then show how to compute risk-neutral moments in Remark 2 (Equation IA.5). Specifically, we would like to compute moments of the form $\mathbb{E}_t^*\left[(R_{M,t\to T})^\alpha\left(\frac{S_T}{S_t}-R_{f,t\to T}\right)^n\mathbb{I}_{A_s}\right]$. We first apply the binomial theorem to show:

$$\begin{aligned}&\mathbb{E}_t^*\left[(R_{M,t\to T})^\alpha\left(R_{M,t\to T}-R_{f,t\to T}\right)^n\mathbb{I}_{A_s}\right]\\ =&\sum_{k=0}^{n}(-1)^{n-k}\frac{n!}{k!\,(n-k)!}\left(R_{f,t\to T}\right)^{n-k}\mathbb{E}_t^*\left[(R_{M,t\to T})^{k+\alpha}\,\mathbb{I}_{A_s}\right].\end{aligned}\tag{IA.21}$$

So we need only compute moments of $(R_{M,t\to T})^{k+\alpha}\,\mathbb{I}_{A_s}$ in order to construct moments of $(R_{M,t\to T})^\alpha\left(R_{M,t\to T}-R_{f,t\to T}\right)^n\mathbb{I}_{A_s}$. We again make use of the Carr and Madan (2001) spanning formula (Equation IA.8) to compute these moments as functions of options prices.

IA.5.3.1 CRRA: Untruncated Risk-Neutral Moments: $\mathbb{E}_t^*\left[(R_{M,t\to T})^{k+\alpha}\right]$

Set the function $h(\cdot)$ in Equation IA.8 to

$$h^{CRRA}(S_T) = \left(\frac{S_T}{S_t}\right)^{k+\alpha}.\tag{IA.22}$$

Derivatives of this function are

$$h_y^{CRRA}(S_T) = \frac{k+\alpha}{S_t}\left(\frac{S_T}{S_t}\right)^{k+\alpha-1}\text{ and}\tag{IA.23}$$

$$h_{yy}^{CRRA}(S_T) = \frac{(k+\alpha)(k+\alpha-1)}{S_t^2}\left(\frac{S_T}{S_t}\right)^{k+\alpha-2}.\tag{IA.24}$$

Next, set $y_0=R_{f,t\to T}S_t$. Evaluating the function and its derivatives at values needed for Equation IA.8 yields:

$$\begin{aligned}h^{CRRA}(R_{f,t\to T}S_t) &= (R_{f,t\to T})^{k+\alpha},\\ h_y^{CRRA}(R_{f,t\to T}S_t) &= \frac{k+\alpha}{S_t}(R_{f,t\to T})^{k+\alpha-1},\text{ and}\\ h_{yy}^{CRRA}(K) &= \frac{(k+\alpha)(k+\alpha-1)}{S_t^2}\left(\frac{K}{S_t}\right)^{k+\alpha-2}.\end{aligned}$$

Substituting these expressions into Equation IA.8 yields:

$$\begin{aligned}\left(\frac{S_T}{S_t}\right)^{k+\alpha} =&\ (R_{f,t\to T})^{k+\alpha}+(k+\alpha)\left(\frac{S_T}{S_t}-R_{f,t\to T}\right)(R_{f,t\to T})^{k+\alpha-1}\\ &+\frac{(k+\alpha)(k+\alpha-1)}{S_t^2}\int_0^{R_{f,t\to T}S_t}\left(\frac{K}{S_t}\right)^{k+\alpha-2}(K-S_T)^+\,dK\\ &+\frac{(k+\alpha)(k+\alpha-1)}{S_t^2}\int_{R_{f,t\to T}S_t}^{\infty}\left(\frac{K}{S_t}\right)^{k+\alpha-2}(S_T-K)^+\,dK.\end{aligned}$$

Taking expectations under the risk-neutral measure at time t yields:

$$\begin{aligned}
&\mathbb{E}_t^*\left[\left(R_{M,t\to T}\right)^{k+\alpha}\right] \\
= \;& \left(R_{f,t\to T}\right)^{k+\alpha} \\
&+\frac{(k+\alpha)(k+\alpha-1)R_{f,t\to T}}{S_t^2}\int_0^{R_{f,t\to T}S_t}\left(\frac{K}{S_t}\right)^{k+\alpha-2}P_{t\to T}[K]\,dK \\
&+\frac{(k+\alpha)(k+\alpha-1)R_{f,t\to T}}{S_t^2}\int_{R_{f,t\to T}S_t}^{\infty}\left(\frac{K}{S_t}\right)^{k+\alpha-2}C_{t\to T}[K]\,dK. \qquad \text{(IA.25)}
\end{aligned}$$

Equation IA.25 can be combined with Equation IA.21 to compute the risk-neutral moments required for Equation IA.5 in Remark 2 when $\mathbb{I}_{A_s}=1$ (i.e., the untruncated moment case).

IA.5.3.2 CRRA: Downside Risk-Neutral Moments: $\mathbb{E}_t^*\left[\left(R_{M,t\to T}\right)^{k+\alpha}\mathbb{I}_{A_d}\right]$

Set the function $h(\cdot)$ in Equation IA.8 to that in Equation IA.22. Next, set $y_0=\underline{x}S_t$. Evaluating the function and its first derivative at values needed for Equation IA.8 yields:

$$h^{CRRA}(\underline{x}S_t) = (\underline{x})^{k+\alpha} \text{ and}$$

$$h_y^{CRRA}(\underline{x}S_t) = \frac{k+\alpha}{S_t}(\underline{x})^{k+\alpha-1}.$$

Note that $h_{yy}^{CRRA}(K)$ based on Equation IA.24 is unchanged. We can substitute these into the Carr and Madan (2001) spanning formula (Equation IA.8) and multiply the whole equation by $\mathbb{I}_{\{S_T<\underline{x}S_t\}}$ to obtain:

$$\begin{aligned}
\left(\frac{S_T}{S_t}\right)^{k+\alpha}\mathbb{I}_{\{S_T<\underline{x}S_t\}} = \;& (\underline{x})^{k+\alpha}\mathbb{I}_{\{S_T<\underline{x}S_t\}} + (S_T-\underline{x}S_t)\frac{k+\alpha}{S_t}(\underline{x})^{k+\alpha-1}\mathbb{I}_{\{S_T<\underline{x}S_t\}} \\
&+\frac{(k+\alpha)(k+\alpha-1)}{S_t^2}\int_0^{\underline{x}S_t}\left(\frac{K}{S_t}\right)^{k+\alpha-2}(K-S_T)^+\mathbb{I}_{\{S_T<\underline{x}S_t\}}dK \\
&+\frac{(k+\alpha)(k+\alpha-1)}{S_t^2}\int_{\underline{x}S_t}^{\infty}\left(\frac{K}{S_t}\right)^{k+\alpha-2}(S_T-K)^+\mathbb{I}_{\{S_T<\underline{x}S_t\}}dK.
\end{aligned}$$

Rearranging and simplifying (noting that the second integral is zero) yields:

$$\begin{aligned}
\left(\frac{S_T}{S_t}\right)^{k+\alpha}\mathbb{I}_{\{S_T<\underline{x}S_t\}} = \;& (\underline{x})^{k+\alpha}\mathbb{I}_{\{S_T<\underline{x}S_t\}} - (k+\alpha)(\underline{x})^{k+\alpha-1}\frac{1}{S_t}(\underline{x}S_t-S_T)^+ \\
&+\frac{(k+\alpha)(k+\alpha-1)}{S_t^2}\int_0^{\underline{x}S_t}\left(\frac{K}{S_t}\right)^{k+\alpha-2}(K-S_T)^+\,dK.
\end{aligned}$$

Taking expectations under the risk-neutral measure yields:

$$\begin{aligned}
&\mathbb{E}_t^*\left[\left(R_{M,t\to T}\right)^{k+\alpha}\mathbb{I}_{A_d}\right] \\
= \;& (\underline{x})^{k+\alpha}\,Prob_t^*\left[S_T<\underline{x}S_t\right] - (k+\alpha)(\underline{x})^{k+\alpha-1}\frac{R_{f,t\to T}}{S_t}P_{t\to T}[\underline{x}S_t] \\
&+\frac{(k+\alpha)(k+\alpha-1)R_{f,t\to T}}{S_t^2}\int_0^{\underline{x}S_t}\left(\frac{K}{S_t}\right)^{k+\alpha-2}P_{t\to T}[K]\,dK. \qquad \text{(IA.26)}
\end{aligned}$$

Equation IA.26 can be combined with Equation IA.21 to compute the risk-neutral moments required for Equation IA.5 in Remark 2 with $\mathbb{I}_{A_s}=\mathbb{I}_{A_d}$.

IA.5.3.3 CRRA: Upside Risk-Neutral Moments: $\mathbb{E}_t^* \left[\left(R_{M,t\to T} \right)^{k+\alpha} \mathbb{I}_{A_u} \right]$

Set the function $h(\cdot)$ in Equation IA.8 to that in Equation IA.22. Next, set $y_0 = \overline{x} S_t$. Evaluating the function and its first derivative at values needed for Equation IA.8 yields:

$$h^{CRRA}(\overline{x} S_t) = (\overline{x})^{k+\alpha} \text{ and}$$

$$h_y^{CRRA}(\overline{x} S_t) = \frac{k+\alpha}{S_t} (\overline{x})^{k+\alpha-1}.$$

Note that $h_{yy}^{CRRA}(K)$ based on Equation IA.24 is unchanged. We can substitute these into the Carr and Madan (2001) spanning formula (Equation IA.8) and multiply the whole equation by $\mathbb{I}_{\{S_T > \overline{x} S_t\}}$ to obtain:

$$\begin{aligned}\left(\frac{S_T}{S_t}\right)^{k+\alpha} \mathbb{I}_{\{S_T>\overline{x}S_t\}} &= (\overline{x})^{k+\alpha} \mathbb{I}_{\{S_T>\overline{x}S_t\}} + (S_T - \overline{x} S_t) \frac{k+\alpha}{S_t} (\overline{x})^{k+\alpha-1} \mathbb{I}_{\{S_T>\overline{x}S_t\}} \\ &+ \frac{(k+\alpha)(k+\alpha-1)}{S_t^2} \int_0^{\overline{x}S_t} \left(\frac{K}{S_t}\right)^{k+\alpha-2} (K - S_T)^+ \mathbb{I}_{\{S_T>\overline{x}S_t\}} dK \\ &+ \frac{(k+\alpha)(k+\alpha-1)}{S_t^2} \int_{\overline{x}S_t}^{\infty} \left(\frac{K}{S_t}\right)^{k+\alpha-2} (S_T - K)^+ \mathbb{I}_{\{S_T>\overline{x}S_t\}} dK.\end{aligned}$$

Rearranging and simplifying (noting that the first integral is zero) yields:

$$\begin{aligned}\left(\frac{S_T}{S_t}\right)^{k+\alpha} \mathbb{I}_{\{S_T>\overline{x}S_t\}} &= (\overline{x})^{k+\alpha} \mathbb{I}_{\{S_T>\overline{x}S_t\}} + \frac{k+\alpha}{S_t} (\overline{x})^{k+\alpha-1} (S_T - \overline{x} S_t)^+ \\ &+ \frac{(k+\alpha)(k+\alpha-1)}{S_t^2} \int_{\overline{x}S_t}^{\infty} \left(\frac{K}{S_t}\right)^{k+\alpha-2} (S_T - K)^+ dK.\end{aligned}$$

Taking expectations under the risk-neutral measure yields:

$$\begin{aligned}&\mathbb{E}_t^* \left[\left(R_{M,t\to T} \right)^{k+\alpha} \mathbb{I}_{A_u} \right] \\ = \; &(\overline{x})^{k+\alpha} Prob_t^* \left[S_T > \overline{x} S_t \right] + (k+\alpha) (\overline{x})^{k+\alpha-1} \frac{R_{f,t\to T}}{S_t} C_{t\to T} \left[\overline{x} S_t \right] \\ &+ \frac{(k+\alpha)(k+\alpha-1) R_{f,t\to T}}{S_t^2} \int_{\overline{x}S_t}^{\infty} \left(\frac{K}{S_t}\right)^{k+\alpha-2} C_{t\to T}[K] \, dK. \qquad \text{(IA.27)}\end{aligned}$$

Equation IA.27 can be combined with Equation IA.21 to compute the risk-neutral moments required for Equation IA.5 in Remark 2 with $\mathbb{I}_{A_s} = \mathbb{I}_{A_u}$.

IA.5.3.4 CRRA: Central Risk-Neutral Moments: $\mathbb{E}_t^* \left[\left(R_{M,t\to T} \right)^{k+\alpha} \mathbb{I}_{A_c} \right]$

The identity in Equation IA.17 implies the following identity relating the risk-neutral moments:

$$\begin{aligned}\mathbb{E}^* \left[\left(R_{M,t\to T} \right)^{k+\alpha} \mathbb{I}_{A_c} \right] \equiv \; &\mathbb{E}_t^* \left[\left(R_{M,t\to T} \right)^{k+\alpha} \right] \\ &- \mathbb{E}^* \left[\left(R_{M,t\to T} \right)^{k+\alpha} \mathbb{I}_{A_d} \right] \\ &- \mathbb{E}^* \left[\left(R_{M,t\to T} \right)^{k+\alpha} \mathbb{I}_{A_u} \right]\end{aligned}$$

where we have made use of the definitions $\mathbb{I}_{A_c} \equiv \mathbb{I}_{\{\underline{x} S_t \le S_T \le \overline{x} S_T\}}$, $\mathbb{I}_{A_d} \equiv \mathbb{I}_{\{S_T < \underline{x} S_t\}}$, and $\mathbb{I}_{A_u} \equiv \mathbb{I}_{\{S_T > \overline{x} S_t\}}$. Substituting in expressions from Equations IA.25, IA.26, and IA.27 and simplifying

yields:

$$\begin{aligned}
&\mathbb{E}^*\left[\left(R_{M,t\to T}\right)^{k+\alpha}\mathbb{I}_{A_c}\right]\\
=\;&\left(R_{f,t\to T}\right)^{k+\alpha}-\left(\underline{x}\right)^{k+\alpha}Prob_t^*\left[S_T<\underline{x}S_t\right]-\left(\overline{x}\right)^{k+\alpha}Prob_t^*\left[S_T>\overline{x}S_t\right]\\
&+\left(k+\alpha\right)\left(\underline{x}\right)^{k+\alpha-1}\frac{R_{f,t\to T}}{S_t}P_{t\to T}\left[\underline{x}S_t\right]-\left(k+\alpha\right)\left(\overline{x}\right)^{k+\alpha-1}\frac{R_{f,t\to T}}{S_t}C_{t\to T}\left[\overline{x}S_t\right]\\
&+\frac{\left(k+\alpha\right)\left(k+\alpha-1\right)R_{f,t\to T}}{S_t^2}\int_{\underline{x}S_t}^{R_{f,t\to T}S_t}\left(\frac{K}{S_t}\right)^{k+\alpha-2}P_{t\to T}\left[K\right]dK\\
&+\frac{\left(k+\alpha\right)\left(k+\alpha-1\right)R_{f,t\to T}}{S_t^2}\int_{R_{f,t\to T}S_t}^{\overline{x}S_t}\left(\frac{K}{S_t}\right)^{k+\alpha-2}C_{t\to T}\left[K\right]dK.
\end{aligned}\tag{IA.28}$$

Equation IA.28 can be combined with Equation IA.21 to compute the risk-neutral moments required for Equation IA.5 in Remark 2 with $\mathbb{I}_{A_s}=\mathbb{I}_{A_c}$.

IA.5.4 Risk-Neutral Moments for CARA Utility-Based Physical Moments

Proof. Proof of Remark 3. The conditional truncated moment is

$$\begin{aligned}
\mathbb{M}_{t\to T}^{(n)}\left[A_s\right]&=\mathbb{E}_t^*\left[\frac{\mathbb{E}_t\left[m_{t\to T}\right]}{m_{t\to T}}\left(R_{M,t\to T}-R_{f,t\to T}\right)^n\mathbb{I}_{A_s}\right]\\
&=\mathbb{E}_t^*\left[\frac{e^{\alpha R_{M,t\to T}}}{\mathbb{E}_t^*\left[e^{\alpha R_{M,t\to T}}\right]}\left(R_{M,t\to T}-R_{f,t\to T}\right)^n\mathbb{I}_{A_s}\right]\\
&=\frac{\mathbb{E}_t^*\left[e^{\alpha R_{M,t\to T}}\left(R_{M,t\to T}-R_{f,t\to T}\right)^n\mathbb{I}_{A_s}\right]}{\mathbb{E}_t^*\left[e^{\alpha R_{M,t\to T}}\right]}.
\end{aligned}\tag{IA.29}$$

This ends the proof. ■

The last expression is obtained by replacing the inverse of the SDF by its expression. In this sub-section, we show how to compute risk-neutral moments in Remark 3 (Equation IA.6). Specifically, we would like to compute moments of the form $\mathbb{E}_t^*\left[e^{\alpha R_{M,t\to T}}\left(R_{M,t\to T}-R_{f,t\to T}\right)^n\mathbb{I}_{A_s}\right]$. We first apply the binomial theorem to show:

$$\begin{aligned}
&\mathbb{E}_t^*\left[e^{\alpha R_{M,t\to T}}\left(R_{M,t\to T}-R_{f,t\to T}\right)^n\mathbb{I}_{A_s}\right]\\
=\;&\sum_{k=0}^{n}\left(-1\right)^{n-k}\frac{n!}{k!\left(n-k\right)!}\left(R_{f,t\to T}\right)^{n-k}\mathbb{E}_t^*\left[e^{\alpha R_{M,t\to T}}\left(R_{M,t\to T}\right)^k\mathbb{I}_{A_s}\right].
\end{aligned}\tag{IA.30}$$

So we need only compute moments of $e^{\alpha R_{M,t\to T}}\left(R_{M,t\to T}\right)^k\mathbb{I}_{A_s}$ in order to construct moments of $e^{\alpha R_{M,t\to T}}\left(R_{M,t\to T}-R_{f,t\to T}\right)^n\mathbb{I}_{A_s}$. We again make use of the Carr and Madan (2001) spanning formula (Equation IA.8) to compute these moments as functions of options prices.

IA.5.4.1 CARA: Untruncated Risk-Neutral Moments: $\mathbb{E}_t^*\left[e^{\alpha R_{M,t\to T}}\left(R_{M,t\to T}\right)^k\right]$

Set the function $h\left(\cdot\right)$ in Equation IA.8 to

$$h^{CARA}\left(S_T\right)=e^{\alpha\frac{S_T}{S_t}}\left(\frac{S_T}{S_t}\right)^k.\tag{IA.31}$$

Derivatives of this function are

$$h_y^{CARA}\left(S_T\right)=\frac{\alpha}{S_t}e^{\alpha\frac{S_T}{S_t}}\left(\frac{S_T}{S_t}\right)^k+\frac{k}{S_t}e^{\alpha\frac{S_T}{S_t}}\left(\frac{S_T}{S_t}\right)^{k-1}\text{ and}\tag{IA.32}$$

$$h_{yy}^{CARA}(S_T) = \frac{\alpha^2}{S_t^2}e^{\alpha\frac{S_T}{S_t}}\left(\frac{S_T}{S_t}\right)^k + 2\frac{\alpha k}{S_t^2}e^{\alpha\frac{S_T}{S_t}}\left(\frac{S_T}{S_t}\right)^{k-1} + \frac{k(k-1)}{S_t^2}e^{\alpha\frac{S_T}{S_t}}\left(\frac{S_T}{S_t}\right)^{k-2}. \quad \text{(IA.33)}$$

Next, set $y_0 = R_{f,t\to T}S_t$. Evaluating the function and its derivatives at values needed for Equation IA.8 yields:

$$h^{CARA}(R_{f,t\to T}S_t) = e^{\alpha R_{f,t\to T}}(R_{f,t\to T})^k,$$

$$h_y^{CARA}(R_{f,t\to T}S_t) = \frac{\alpha}{S_t}e^{\alpha R_{f,t\to T}}(R_{f,t\to T})^k + \frac{k}{S_t}e^{\alpha R_{f,t\to T}}(R_{f,t\to T})^{k-1}, \text{ and}$$

$$h_{yy}^{CARA}(K) = \frac{\alpha^2}{S_t^2}e^{\alpha\frac{K}{S_t}}\left(\frac{K}{S_t}\right)^k + 2\frac{\alpha k}{S_t^2}e^{\alpha\frac{K}{S_t}}\left(\frac{K}{S_t}\right)^{k-1} + \frac{k(k-1)}{S_t^2}e^{\alpha\frac{K}{S_t}}\left(\frac{K}{S_t}\right)^{k-2}.$$

Substituting these expressions into Equation IA.8 yields:

$$\begin{aligned}
& e^{\alpha\frac{S_T}{S_t}}\left(\frac{S_T}{S_t}\right)^k \\
= \; & e^{\alpha R_{f,t\to T}}(R_{f,t\to T})^k + (S_T - R_{f,t\to T}S_t)\left[\frac{\alpha}{S_t}e^{\alpha R_{f,t\to T}}(R_{f,t\to T})^k + \frac{k}{S_t}e^{\alpha R_{f,t\to T}}(R_{f,t\to T})^{k-1}\right] \\
& + \int_0^{R_{f,t\to T}S_t}\left[\frac{\alpha^2}{S_t^2}e^{\alpha\frac{K}{S_t}}\left(\frac{K}{S_t}\right)^k + 2\frac{\alpha k}{S_t^2}e^{\alpha\frac{K}{S_t}}\left(\frac{K}{S_t}\right)^{k-1} + \frac{k(k-1)}{S_t^2}e^{\alpha\frac{K}{S_t}}\left(\frac{K}{S_t}\right)^{k-2}\right](K - S_T)^+ dK \\
& + \int_{R_{f,t\to T}S_t}^{\infty}\left[\frac{\alpha^2}{S_t^2}e^{\alpha\frac{K}{S_t}}\left(\frac{K}{S_t}\right)^k + 2\frac{\alpha k}{S_t^2}e^{\alpha\frac{K}{S_t}}\left(\frac{K}{S_t}\right)^{k-1} + \frac{k(k-1)}{S_t^2}e^{\alpha\frac{K}{S_t}}\left(\frac{K}{S_t}\right)^{k-2}\right](S_T - K)^+ dK.
\end{aligned}$$

Taking expectations under the risk-neutral measure at time t yields:

$$\begin{aligned}
& \mathbb{E}_t^*\left[e^{\alpha R_{M,t\to T}}(R_{M,t\to T})^k\right] \\
= \; & e^{\alpha R_{f,t\to T}}(R_{f,t\to T})^k \\
& + \frac{R_{f,t\to T}}{S_t^2}\int_0^{R_{f,t\to T}S_t} e^{\alpha\frac{K}{S_t}}\left[\alpha^2\left(\frac{K}{S_t}\right)^k + 2\alpha k\left(\frac{K}{S_t}\right)^{k-1} + k(k-1)\left(\frac{K}{S_t}\right)^{k-2}\right]P_{t\to T}[K]\,dK \\
& + \frac{R_{f,t\to T}}{S_t^2}\int_{R_{f,t\to T}S_t}^{\infty} e^{\alpha\frac{K}{S_t}}\left[\alpha^2\left(\frac{K}{S_t}\right)^k + 2\alpha k\left(\frac{K}{S_t}\right)^{k-1} + k(k-1)\left(\frac{K}{S_t}\right)^{k-2}\right]C_{t\to T}[K]\,dK. \quad \text{(IA.34)}
\end{aligned}$$

Equation IA.34 can be combined with Equation IA.30 to compute the risk-neutral moments required for Equation IA.6 in Remark 3 when $\mathbb{I}_{A_s} = 1$ (i.e., the untruncated moment case).

IA.5.4.2 CARA: Downside Risk-Neutral Moments: $\mathbb{E}_t^*\left[e^{\alpha R_{M,t\to T}}(R_{M,t\to T})^k \mathbb{I}_{A_d}\right]$

Set the function $h(\cdot)$ in Equation IA.8 to that in Equation IA.31. Next, set $y_0 = \underline{x}S_t$. Evaluating the function and its first derivative at values needed for Equation IA.8 yields:

$$h^{CARA}(\underline{x}S_t) = e^{\alpha\underline{x}}(\underline{x})^k \text{ and}$$

$$h_y^{CARA}(\underline{x}S_t) = \frac{\alpha}{S_t}e^{\alpha\underline{x}}(\underline{x})^k + \frac{k}{S_t}e^{\alpha\underline{x}}(\underline{x})^{k-1}.$$

Note that $h_{yy}^{CARA}(K)$ based on Equation IA.33 is unchanged. We can substitute these into the Carr and Madan (2001) spanning formula (Equation IA.8) and multiply the whole equation by $\mathbb{I}_{\{S_T<\underline{x}S_t\}}$

to obtain:

$$
\begin{aligned}
& e^{\alpha \frac{S_T}{S_t}} \left(\frac{S_T}{S_t}\right)^k \mathbb{I}_{\{S_T<\underline{x}S_t\}} \\
= \; & e^{\alpha \underline{x}} (\underline{x})^k \mathbb{I}_{\{S_T<\underline{x}S_t\}} + (S_T - \underline{x}S_t)\left[\frac{\alpha}{S_t} e^{\alpha \underline{x}} (\underline{x})^k + \frac{k}{S_t} e^{\alpha \underline{x}} (\underline{x})^{k-1}\right] \mathbb{I}_{\{S_T<\underline{x}S_t\}} \\
& + \int_0^{\underline{x}S_t} \left[\frac{\alpha^2}{S_t^2} e^{\alpha \frac{K}{S_t}} \left(\frac{K}{S_t}\right)^k + 2\frac{\alpha k}{S_t^2} e^{\alpha \frac{K}{S_t}} \left(\frac{K}{S_t}\right)^{k-1} + \frac{k(k-1)}{S_t^2} e^{\alpha \frac{K}{S_t}} \left(\frac{K}{S_t}\right)^{k-2}\right] (K - S_T)^+ \mathbb{I}_{\{S_T<\underline{x}S_t\}} dK \\
& + \int_{\underline{x}S_t}^{\infty} \left[\frac{\alpha^2}{S_t^2} e^{\alpha \frac{K}{S_t}} \left(\frac{K}{S_t}\right)^k + 2\frac{\alpha k}{S_t^2} e^{\alpha \frac{K}{S_t}} \left(\frac{K}{S_t}\right)^{k-1} + \frac{k(k-1)}{S_t^2} e^{\alpha \frac{K}{S_t}} \left(\frac{K}{S_t}\right)^{k-2}\right] (S_T - K)^+ \mathbb{I}_{\{S_T<\underline{x}S_t\}} dK.
\end{aligned}
$$

Rearranging and simplifying (noting that the second integral is zero) yields:

$$
\begin{aligned}
& e^{\alpha \frac{S_T}{S_t}} \left(\frac{S_T}{S_t}\right)^k \mathbb{I}_{\{S_T<\underline{x}S_t\}} \\
= \; & e^{\alpha \underline{x}} (\underline{x})^k \mathbb{I}_{\{S_T<\underline{x}S_t\}} - \left[\alpha e^{\alpha \underline{x}} (\underline{x})^k + k e^{\alpha \underline{x}} (\underline{x})^{k-1}\right] \frac{1}{S_t} (\underline{x}S_t - S_T)^+ \\
& + \int_0^{\underline{x}S_t} \left[\frac{\alpha^2}{S_t^2} e^{\alpha \frac{K}{S_t}} \left(\frac{K}{S_t}\right)^k + 2\frac{\alpha k}{S_t^2} e^{\alpha \frac{K}{S_t}} \left(\frac{K}{S_t}\right)^{k-1} + \frac{k(k-1)}{S_t^2} e^{\alpha \frac{K}{S_t}} \left(\frac{K}{S_t}\right)^{k-2}\right] (K - S_T)^+ dK.
\end{aligned}
$$

Taking expectations under the risk-neutral measure yields:

$$
\begin{aligned}
& \mathbb{E}_t^* \left[e^{\alpha R_{M,t\to T}} (R_{M,t\to T})^k \mathbb{I}_{A_d}\right] \\
= \; & e^{\alpha \underline{x}} (\underline{x})^k \, Prob_t^* \left[S_T < \underline{x}S_t\right] - \left[\alpha e^{\alpha \underline{x}} (\underline{x})^k + k e^{\alpha \underline{x}} (\underline{x})^{k-1}\right] \frac{R_{f,t\to T}}{S_t} P_{t\to T} \left[\underline{x}S_t\right] \\
& + \frac{R_{f,t\to T}}{S_t^2} \int_0^{\underline{x}S_t} e^{\alpha \frac{K}{S_t}} \left[\alpha^2 \left(\frac{K}{S_t}\right)^k + 2\alpha k \left(\frac{K}{S_t}\right)^{k-1} + k(k-1) \left(\frac{K}{S_t}\right)^{k-2}\right] P_{t\to T}[K] \, dK. \qquad \text{(IA.35)}
\end{aligned}
$$

Equation IA.35 can be combined with Equation IA.30 to compute the risk-neutral moments required for Equation IA.6 in Remark 3 with $\mathbb{I}_{A_s} = \mathbb{I}_{A_d}$.

IA.5.4.3 CARA: Upside Risk-Neutral Moments: $\mathbb{E}_t^* \left[e^{\alpha R_{M,t\to T}} (R_{M,t\to T})^k \mathbb{I}_{A_u}\right]$

Set the function $h(\cdot)$ in Equation IA.8 to that in Equation IA.31. Next, set $y_0 = \overline{x}S_t$. Evaluating the function and its first derivative at values needed for Equation IA.8 yields:

$$
\begin{aligned}
h^{CARA}(\overline{x}S_t) &= e^{\alpha \overline{x}} (\overline{x})^k \text{ and} \\
h_y^{CARA}(\overline{x}S_t) &= \frac{\alpha}{S_t} e^{\alpha \overline{x}} (\overline{x})^k + \frac{k}{S_t} e^{\alpha \overline{x}} (\overline{x})^{k-1}.
\end{aligned}
$$

Note that $h_{yy}^{CARA}(K)$ based on Equation IA.33 is unchanged. We can substitute these into the Carr and Madan (2001) spanning formula (Equation IA.8) and multiply the whole equation by $\mathbb{I}_{\{S_T>\overline{x}S_t\}}$ to obtain:

$$
\begin{aligned}
& e^{\alpha \frac{S_T}{S_t}} \left(\frac{S_T}{S_t}\right)^k \mathbb{I}_{\{S_T>\overline{x}S_t\}} \\
= \; & e^{\alpha \overline{x}} (\overline{x})^k \mathbb{I}_{\{S_T>\overline{x}S_t\}} + (S_T - \overline{x}S_t)\left[\frac{\alpha}{S_t} e^{\alpha \overline{x}} (\overline{x})^k + \frac{k}{S_t} e^{\alpha \overline{x}} (\overline{x})^{k-1}\right] \mathbb{I}_{\{S_T>\overline{x}S_t\}} \\
& + \int_0^{\overline{x}S_t} \left[\frac{\alpha^2}{S_t^2} e^{\alpha \frac{K}{S_t}} \left(\frac{K}{S_t}\right)^k + 2\frac{\alpha k}{S_t^2} e^{\alpha \frac{K}{S_t}} \left(\frac{K}{S_t}\right)^{k-1} + \frac{k(k-1)}{S_t^2} e^{\alpha \frac{K}{S_t}} \left(\frac{K}{S_t}\right)^{k-2}\right] (K - S_T)^+ \mathbb{I}_{\{S_T>\overline{x}S_t\}} dK \\
& + \int_{\overline{x}S_t}^{\infty} \left[\frac{\alpha^2}{S_t^2} e^{\alpha \frac{K}{S_t}} \left(\frac{K}{S_t}\right)^k + 2\frac{\alpha k}{S_t^2} e^{\alpha \frac{K}{S_t}} \left(\frac{K}{S_t}\right)^{k-1} + \frac{k(k-1)}{S_t^2} e^{\alpha \frac{K}{S_t}} \left(\frac{K}{S_t}\right)^{k-2}\right] (S_T - K)^+ \mathbb{I}_{\{S_T>\overline{x}S_t\}} dK.
\end{aligned}
$$

Rearranging and simplifying (noting that the first integral is zero) yields:

$$\begin{aligned}
& e^{\alpha\frac{S_T}{S_t}}\left(\frac{S_T}{S_t}\right)^k \mathbb{I}_{\{S_T>\overline{x}S_t\}} \\
= \; & e^{\alpha\overline{x}}(\overline{x})^k \mathbb{I}_{\{S_T>\overline{x}S_t\}} + \left[\alpha e^{\alpha\overline{x}}(\overline{x})^k + k e^{\alpha\overline{x}}(\overline{x})^{k-1}\right]\frac{1}{S_t}(S_T-\overline{x}S_t)^+ \\
& + \frac{1}{S_t^2}\int_{\overline{x}S_t}^{\infty}\left[\alpha^2 e^{\alpha\frac{K}{S_t}}\left(\frac{K}{S_t}\right)^k + 2\alpha k e^{\alpha\frac{K}{S_t}}\left(\frac{K}{S_t}\right)^{k-1} + k(k-1)e^{\alpha\frac{K}{S_t}}\left(\frac{K}{S_t}\right)^{k-2}\right](S_T-K)^+ dK.
\end{aligned}$$

Taking expectations under the risk-neutral measure yields:

$$\begin{aligned}
& \mathbb{E}_t^*\left[e^{\alpha R_{M,t\to T}}(R_{M,t\to T})^k \mathbb{I}_{A_u}\right] \\
= \; & e^{\alpha\overline{x}}(\overline{x})^k Prob_t^*\left[S_T>\overline{x}S_t\right] + \left[\alpha e^{\alpha\overline{x}}(\overline{x})^k + k e^{\alpha\overline{x}}(\overline{x})^{k-1}\right]\frac{R_{f,t\to T}}{S_t}C_{t\to T}\left[\overline{x}S_t\right] \\
& + \frac{R_{f,t\to T}}{S_t^2}\int_{\overline{x}S_t}^{\infty} e^{\alpha\frac{K}{S_t}}\left[\alpha^2\left(\frac{K}{S_t}\right)^k + 2\alpha k\left(\frac{K}{S_t}\right)^{k-1} + k(k-1)\left(\frac{K}{S_t}\right)^{k-2}\right]C_{t\to T}[K]\,dK. \qquad \text{(IA.36)}
\end{aligned}$$

Equation IA.36 can be combined with Equation IA.30 to compute the risk-neutral moments required for Equation IA.6 in Remark 3 with $\mathbb{I}_{A_s} = \mathbb{I}_{A_u}$.

IA.5.4.4 CARA: Central Risk-Neutral Moments: $\mathbb{E}_t^*\left[e^{\alpha R_{M,t\to T}}(R_{M,t\to T})^k \mathbb{I}_{A_c}\right]$

The identity in Equation IA.17 implies the following identity relating the risk-neutral moments:

$$\begin{aligned}
\mathbb{E}^*\left[e^{\alpha R_{M,t\to T}}(R_{M,t\to T})^k \mathbb{I}_{A_c}\right] \equiv \; & \mathbb{E}_t^*\left[e^{\alpha R_{M,t\to T}}(R_{M,t\to T})^k\right] \\
& -\mathbb{E}^*\left[e^{\alpha R_{M,t\to T}}(R_{M,t\to T})^k \mathbb{I}_{A_d}\right] \\
& -\mathbb{E}^*\left[e^{\alpha R_{M,t\to T}}(R_{M,t\to T})^k \mathbb{I}_{A_u}\right]
\end{aligned}$$

where we have made use of the definitions $\mathbb{I}_{A_c} \equiv \mathbb{I}_{\{\underline{x}S_t\le S_T\le\overline{x}S_T\}}$, $\mathbb{I}_{A_d} \equiv \mathbb{I}_{\{S_T<\underline{x}S_t\}}$, and $\mathbb{I}_{A_u} \equiv \mathbb{I}_{\{S_T>\overline{x}S_t\}}$. Substituting in expressions from Equations IA.34, IA.35, and IA.36 and simplifying yields:

$$\begin{aligned}
& \mathbb{E}^*\left[e^{\alpha R_{M,t\to T}}(R_{M,t\to T})^k \mathbb{I}_{A_c}\right] \\
= \; & e^{\alpha R_{f,t\to T}}(R_{f,t\to T})^k - e^{\alpha\underline{x}}(\underline{x})^k Prob_t^*\left[S_T<\underline{x}S_t\right] - e^{\alpha\overline{x}}(\overline{x})^k Prob_t^*\left[S_T>\overline{x}S_t\right] \\
& + \left[\alpha e^{\alpha\underline{x}}(\underline{x})^k + k e^{\alpha\underline{x}}(\underline{x})^{k-1}\right]\frac{R_{f,t\to T}}{S_t}P_{t\to T}\left[\underline{x}S_t\right] - \left[\alpha e^{\alpha\overline{x}}(\overline{x})^k + k e^{\alpha\overline{x}}(\overline{x})^{k-1}\right]\frac{R_{f,t\to T}}{S_t}C_{t\to T}\left[\overline{x}S_t\right] \\
& + \frac{R_{f,t\to T}}{S_t^2}\int_{\underline{x}S_t}^{R_{f,t\to T}S_t} e^{\alpha\frac{K}{S_t}}\left[\alpha^2\left(\frac{K}{S_t}\right)^k + 2\alpha k\left(\frac{K}{S_t}\right)^{k-1} + k(k-1)\left(\frac{K}{S_t}\right)^{k-2}\right]P_{t\to T}[K]\,dK \\
& + \frac{R_{f,t\to T}}{S_t^2}\int_{R_{f,t\to T}S_t}^{\overline{x}S_t} e^{\alpha\frac{K}{S_t}}\left[\alpha^2\left(\frac{K}{S_t}\right)^k + 2\alpha k\left(\frac{K}{S_t}\right)^{k-1} + k(k-1)\left(\frac{K}{S_t}\right)^{k-2}\right]C_{t\to T}[K]\,dK. \qquad \text{(IA.37)}
\end{aligned}$$

Equation IA.37 can be combined with Equation IA.30 to compute the risk-neutral moments required for Equation IA.6 in Remark 3 with $\mathbb{I}_{A_s} = \mathbb{I}_{A_c}$.

IA.5.5 Risk-Neutral Moments for HARA Utility-Based Physical Moments

Proof. Proof of Remark 4. The conditional truncated moment is

$$\begin{aligned}\mathbb{M}_{t\to T}^{(n)}\left[A_s\right] &= \mathbb{E}_t^*\left[\frac{\mathbb{E}_t\left[m_{t\to T}\right]}{m_{t\to T}}\left(R_{M,t\to T}-R_{f,t\to T}\right)^n\mathbb{I}_{A_s}\right]\\ &= \frac{\mathbb{E}_t^*\left[\left(-a^*\left(R_{M,t\to T}/R_{f,t\to T}\right)-1\right)^{1-\gamma}\left(R_{M,t\to T}-R_{f,t\to T}\right)^n\mathbb{I}_{A_s}\right]}{\mathbb{E}_t^*\left[\left(-a^*\left(R_{M,t\to T}/R_{f,t\to T}\right)-1\right)^{1-\gamma}\right]}.\end{aligned} \tag{IA.38}$$

■

Next, we show how to compute risk-neutral moments in Remark 4 (Equation IA.7). Specifically, we would like to compute moments of the form $\mathbb{E}_t^*\left[\left(-\frac{a^*}{R_{f,t\to T}}R_{M,t\to T}-1\right)^{1-\gamma}\left(R_{M,t\to T}-R_{f,t\to T}\right)^n\mathbb{I}_{A_s}\right]$. We first apply the binomial theorem to show:

$$\begin{aligned}&\mathbb{E}_t^*\left[\left(-\frac{a^*}{R_{f,t\to T}}R_{M,t\to T}-1\right)^{1-\gamma}\left(R_{M,t\to T}-R_{f,t\to T}\right)^n\mathbb{I}_{A_s}\right]\\ =\ &\sum_{k=0}^{n}\frac{(-1)^{n-k}\,n!}{k!\,(n-k)!}\left(R_{f,t\to T}\right)^{n-k}\mathbb{E}_t^*\left[\left(-\frac{a^*}{R_{f,t\to T}}R_{M,t\to T}-1\right)^{1-\gamma}\left(R_{M,t\to T}\right)^k\mathbb{I}_{A_s}\right].\end{aligned} \tag{IA.39}$$

So we need only compute moments of $\left(-\frac{a^*}{R_{f,t\to T}}R_{M,t\to T}-1\right)^{1-\gamma}\left(R_{M,t\to T}\right)^k\mathbb{I}_{A_s}$ in order to construct moments of $\left(-\frac{a^*}{R_{f,t\to T}}R_{M,t\to T}-1\right)^{1-\gamma}\left(R_{M,t\to T}-R_{f,t\to T}\right)^n\mathbb{I}_{A_s}$. We again make use of the Carr and Madan (2001) spanning formula (Equation IA.8) to compute these moments as functions of options prices.

IA.5.5.1 HARA: Untruncated Risk-Neutral Moments:

Our goal is to compute:

$$\mathbb{E}_t^*\left[\left(-\frac{a^*}{R_{f,t\to T}}R_{M,t\to T}-1\right)^{1-\gamma}\left(R_{M,t\to T}\right)^k\right]$$

Set the function $h\left(\cdot\right)$ in Equation IA.8 to

$$h^{HARA}\left(S_T\right) = \left(-\frac{a^*}{R_{f,t\to T}}\left(\frac{S_T}{S_t}\right)-1\right)^{1-\gamma}\left(\frac{S_T}{S_t}\right)^k. \tag{IA.40}$$

Derivatives of this function are

$$\begin{aligned}h_y^{HARA}\left(S_T\right) &= -\left(1-\gamma\right)\frac{a^*}{R_{f,t\to T}S_t}\left(-\frac{a^*}{R_{f,t\to T}}\left(\frac{S_T}{S_t}\right)-1\right)^{-\gamma}\left(\frac{S_T}{S_t}\right)^k\\ &\quad+\frac{k}{S_t}\left(-\frac{a^*}{R_{f,t\to T}}\left(\frac{S_T}{S_t}\right)-1\right)^{1-\gamma}\left(\frac{S_T}{S_t}\right)^{k-1}\ \text{and}\end{aligned} \tag{IA.41}$$

$$\begin{aligned}h_{yy}^{HARA}\left(S_T\right) &= -\gamma\left(1-\gamma\right)\left(\frac{a^*}{R_{f,t\to T}S_t}\right)^2\left(-\frac{a^*}{R_{f,t\to T}}\left(\frac{S_T}{S_t}\right)-1\right)^{-\gamma-1}\left(\frac{S_T}{S_t}\right)^k\\ &\quad-2\frac{k\left(1-\gamma\right)a^*}{R_{f,t\to T}S_t^2}\left(-\frac{a^*}{R_{f,t\to T}}\left(\frac{S_T}{S_t}\right)-1\right)^{-\gamma}\left(\frac{S_T}{S_t}\right)^{k-1}\\ &\quad+\frac{k\left(k-1\right)}{S_t^2}\left(-\frac{a^*}{R_{f,t\to T}}\left(\frac{S_T}{S_t}\right)-1\right)^{1-\gamma}\left(\frac{S_T}{S_t}\right)^{k-2}.\end{aligned} \tag{IA.42}$$

Next, set $y_0 = R_{f,t\to T}S_t$. Evaluating the function and its derivatives at values needed for Equation IA.8 yields:

$$h^{HARA}\left(R_{f,t\to T}S_t\right) = \left(-a^*-1\right)^{1-\gamma}\left(R_{f,t\to T}\right)^k,$$

$$\begin{aligned} h_y^{HARA}\left(R_{f,t\to T}S_t\right) &= -\left(1-\gamma\right)\frac{a^*}{R_{f,t\to T}S_t}\left(-a^*-1\right)^{-\gamma}\left(R_{f,t\to T}\right)^k \\ &\quad +\frac{k}{S_t}\left(-a^*-1\right)^{1-\gamma}\left(R_{f,t\to T}\right)^{k-1}, \text{ and} \end{aligned}$$

$$\begin{aligned} h_{yy}^{HARA}\left(K\right) &= -\gamma\left(1-\gamma\right)\left(\frac{a^*}{R_{f,t\to T}S_t}\right)^2\left(-\frac{a^*}{R_{f,t\to T}}\left(\frac{K}{S_t}\right)-1\right)^{-\gamma-1}\left(\frac{K}{S_t}\right)^k \\ &\quad -2\frac{k\left(1-\gamma\right)a^*}{R_{f,t\to T}S_t^2}\left(-\frac{a^*}{R_{f,t\to T}}\left(\frac{K}{S_t}\right)-1\right)^{-\gamma}\left(\frac{K}{S_t}\right)^{k-1} \\ &\quad +\frac{k\left(k-1\right)}{S_t^2}\left(-\frac{a^*}{R_{f,t\to T}}\left(\frac{K}{S_t}\right)-1\right)^{1-\gamma}\left(\frac{K}{S_t}\right)^{k-2}. \end{aligned}$$

Substituting these expressions into Equation IA.8 yields:

$$\begin{aligned} &\left(-\frac{a^*}{R_{f,t\to T}}\left(\frac{S_T}{S_t}\right)-1\right)^{1-\gamma}\left(\frac{S_T}{S_t}\right)^k \\ &= \left(-a^*-1\right)^{1-\gamma}\left(R_{f,t\to T}\right)^k \\ &\quad +\left(S_T-R_{f,t\to T}S_t\right)h_y^{HARA}\left[R_{f,t\to T}S_t\right] \\ &\quad +\int_0^{R_{f,t\to T}S_t} h_{yy}^{HARA}\left(K\right)\left(K-S_T\right)^+ dK \\ &\quad +\int_{R_{f,t\to T}S_t}^{\infty} h_{yy}^{HARA}\left(K\right)\left(S_T-K\right)^+ dK. \end{aligned}$$

Taking expectations under the risk-neutral measure at time t yields:

$$\begin{aligned} &\mathbb{E}_t^*\left[\left(-\frac{a^*}{R_{f,t\to T}}R_{M,t\to T}-1\right)^{1-\gamma}\left(R_{M,t\to T}\right)^k\right] \\ &= \left(-a^*-1\right)^{1-\gamma}\left(R_{f,t\to T}\right)^k \\ &\quad +R_{f,t\to T}\int_0^{R_{f,t\to T}S_t} h_{yy}^{HARA}\left(K\right)P_{t\to T}\left[K\right]dK \\ &\quad +R_{f,t\to T}\int_{R_{f,t\to T}S_t}^{\infty} h_{yy}^{HARA}\left(K\right)C_{t\to T}\left[K\right]dK. \end{aligned} \tag{IA.43}$$

Equation IA.43 can be combined with Equation IA.39 to compute the risk-neutral moments required for Equation IA.7 in Remark 4 when $\mathbb{I}_{A_s} = 1$ (i.e., the untruncated moment case).

IA.5.5.2 HARA: Downside Risk-Neutral Moments: $\mathbb{E}_t^*\left[\left(-\frac{a^*}{R_{f,t\to T}}R_{M,t\to T}-1\right)^{1-\gamma}\left(R_{M,t\to T}\right)^k\mathbb{I}_{A_d}\right]$

Set the function $h\left(\cdot\right)$ in Equation IA.8 to that in Equation IA.40. Next, set $y_0 = \underline{x}S_t$. Evaluating the function and its first derivative at values needed for Equation IA.8 yields:

$$h^{HARA}\left(\underline{x}S_t\right) = \left(-\frac{a^*}{R_{f,t\to T}}\underline{x}-1\right)^{1-\gamma}\left(\underline{x}\right)^k \text{ and}$$

$$
\begin{aligned}
h_{y}^{HARA}\left(\underline{x}S_t\right) &= -\left(1-\gamma\right)\frac{a^*}{R_{f,t\to T}S_t}\left(-\frac{a^*}{R_{f,t\to T}}\underline{x}-1\right)^{-\gamma}\left(\underline{x}\right)^k \\
&\quad +\frac{k}{S_t}\left(-\frac{a^*}{R_{f,t\to T}}\underline{x}-1\right)^{1-\gamma}\left(\underline{x}\right)^{k-1}.
\end{aligned}
$$

Note that $h_{yy}^{HARA}\left(K\right)$ based on Equation IA.42 is unchanged. We can substitute these into the Carr and Madan (2001) spanning formula (Equation IA.8) and multiply the whole equation by $\mathbb{I}_{\{S_T<\underline{x}S_t\}}$ to obtain:

$$
\begin{aligned}
&\left(-\frac{a^*}{R_{f,t\to T}}\left(\frac{S_T}{S_t}\right)-1\right)^{1-\gamma}\left(\frac{S_T}{S_t}\right)^k\mathbb{I}_{\{S_T<\underline{x}S_t\}} \\
=\;&\left(-\frac{a^*}{R_{f,t\to T}}\underline{x}-1\right)^{1-\gamma}\left(\underline{x}\right)^k\mathbb{I}_{\{S_T<\underline{x}S_t\}} \\
&+\left(S_T-\underline{x}S_t\right)h_{y}^{HARA}\left(\underline{x}S_t\right)\mathbb{I}_{\{S_T<\underline{x}S_t\}} \\
&+\int_0^{\underline{x}S_t}h_{yy}^{HARA}\left(K\right)\left(K-S_T\right)^+\mathbb{I}_{\{S_T<\underline{x}S_t\}}dK \\
&+\int_{\underline{x}S_t}^{\infty}h_{yy}^{HARA}\left(K\right)\left(S_T-K\right)^+\mathbb{I}_{\{S_T<\underline{x}S_t\}}dK.
\end{aligned}
$$

Rearranging and simplifying (noting that the second integral is zero) yields:

$$
\begin{aligned}
&\left(-\frac{a^*}{R_{f,t\to T}}\left(\frac{S_T}{S_t}\right)-1\right)^{1-\gamma}\left(\frac{S_T}{S_t}\right)^k\mathbb{I}_{\{S_T<\underline{x}S_t\}} \\
=\;&\left(-\frac{a^*}{R_{f,t\to T}}\underline{x}-1\right)^{1-\gamma}\left(\underline{x}\right)^k\mathbb{I}_{\{S_T<\underline{x}S_t\}} \\
&-h_{y}^{HARA}\left(\underline{x}S_t\right)\left(\underline{x}S_t-S_T\right)^+ \\
&+\int_0^{\underline{x}S_t}h_{yy}^{HARA}\left(K\right)\left(K-S_T\right)^+dK.
\end{aligned}
$$

Taking expectations under the risk-neutral measure yields:

$$
\begin{aligned}
&\mathbb{E}_t^*\left[\left(-\frac{a^*}{R_{f,t\to T}}R_{M,t\to T}-1\right)^{1-\gamma}\left(R_{M,t\to T}\right)^k\mathbb{I}_{A_d}\right] \\
=\;&\left(-\frac{a^*}{R_{f,t\to T}}\underline{x}-1\right)^{1-\gamma}\left(\underline{x}\right)^k Prob_t^*\left[S_T<\underline{x}S_t\right] \\
&-R_{f,t\to T}h_{y}^{HARA}\left(\underline{x}S_t\right)P_{t\to T}\left[\underline{x}S_t\right] \\
&+R_{f,t\to T}\int_0^{\underline{x}S_t}h_{yy}^{HARA}\left(K\right)P_{t\to T}\left[K\right]dK. \qquad \text{(IA.44)}
\end{aligned}
$$

Equation IA.44 can be combined with Equation IA.39 to compute the risk-neutral moments required for Equation IA.7 in Remark 4 with $\mathbb{I}_{A_s}=\mathbb{I}_{A_d}$.

IA.5.5.3 HARA: Upside Risk-Neutral Moments: $\mathbb{E}_t^*\left[\left(-\frac{a^*}{R_{f,t\to T}}R_{M,t\to T}-1\right)^{1-\gamma}\left(R_{M,t\to T}\right)^k\mathbb{I}_{A_u}\right]$

Set the function $h\left(\cdot\right)$ in Equation IA.8 to that in Equation IA.40. Next, set $y_0=\overline{x}S_t$. Evaluating the function and its first derivative at values needed for Equation IA.8 yields:

$$
h^{HARA}\left(\overline{x}S_t\right) = \left(-\frac{a^*}{R_{f,t\to T}}\overline{x}-1\right)^{1-\gamma}\left(\overline{x}\right)^k \text{ and}
$$

$$
\begin{aligned}
h_{y}^{HARA}\left(\overline{x}S_t\right) &= -\left(1-\gamma\right)\frac{a^*}{R_{f,t\to T}S_t}\left(-\frac{a^*}{R_{f,t\to T}}\overline{x}-1\right)^{-\gamma}\left(\overline{x}\right)^k \\
&\quad +\frac{k}{S_t}\left(-\frac{a^*}{R_{f,t\to T}}\overline{x}-1\right)^{1-\gamma}\left(\overline{x}\right)^{k-1}.
\end{aligned}
$$

Note that $h_{yy}^{HARA}\left(K\right)$ based on Equation IA.42 is unchanged. We can substitute these into the Carr and Madan (2001) spanning formula (Equation IA.8) and multiply the whole equation by $\mathbb{I}_{\{S_T>\overline{x}S_t\}}$ to obtain:

$$
\begin{aligned}
&\left(-\frac{a^*}{R_{f,t\to T}}\left(\frac{S_T}{S_t}\right)-1\right)^{1-\gamma}\left(\frac{S_T}{S_t}\right)^k\mathbb{I}_{\{S_T>\overline{x}S_t\}} \\
=\;&\left(-\frac{a^*}{R_{f,t\to T}}\overline{x}-1\right)^{1-\gamma}\left(\overline{x}\right)^k\mathbb{I}_{\{S_T>\overline{x}S_t\}} \\
&+\left(S_T-\overline{x}S_t\right)h_{y}^{HARA}\left(\overline{x}S_t\right)\mathbb{I}_{\{S_T>\overline{x}S_t\}} \\
&+\int_0^{\overline{x}S_t}h_{yy}^{HARA}\left(K\right)\left(K-S_T\right)^+\mathbb{I}_{\{S_T>\overline{x}S_t\}}dK \\
&+\int_{\overline{x}S_t}^{\infty}h_{yy}^{HARA}\left(K\right)\left(S_T-K\right)^+\mathbb{I}_{\{S_T>\overline{x}S_t\}}dK.
\end{aligned}
$$

Rearranging and simplifying (noting that the first integral is zero) yields:

$$
\begin{aligned}
&\left(-\frac{a^*}{R_{f,t\to T}}\left(\frac{S_T}{S_t}\right)-1\right)^{1-\gamma}\left(\frac{S_T}{S_t}\right)^k\mathbb{I}_{\{S_T>\overline{x}S_t\}} \\
=\;&\left(-\frac{a^*}{R_{f,t\to T}}\overline{x}-1\right)^{1-\gamma}\left(\overline{x}\right)^k\mathbb{I}_{\{S_T>\overline{x}S_t\}} \\
&+h_{y}^{HARA}\left(\overline{x}S_t\right)\left(S_T-\overline{x}S_t\right)^+ \\
&+\int_{\overline{x}S_t}^{\infty}h_{yy}^{HARA}\left(K\right)\left(S_T-K\right)^+dK.
\end{aligned}
$$

Taking expectations under the risk-neutral measure yields:

$$
\begin{aligned}
&\mathbb{E}_t^*\left[\left(-\frac{a^*}{R_{f,t\to T}}R_{M,t\to T}-1\right)^{1-\gamma}\left(R_{M,t\to T}\right)^k\mathbb{I}_{\{S_T>\overline{x}S_t\}}\right] \\
=\;&\left(-\frac{a^*}{R_{f,t\to T}}\overline{x}-1\right)^{1-\gamma}\left(\overline{x}\right)^k Prob_t^*\left[S_T>\overline{x}S_t\right] \\
&+R_{f,t\to T}h_{y}^{HARA}\left(\overline{x}S_t\right)C_{t\to T}\left[\overline{x}S_t\right] \\
&+R_{f,t\to T}\int_{\overline{x}S_t}^{\infty}h_{yy}^{HARA}\left(K\right)C_{t\to T}\left[K\right]dK. \qquad \text{(IA.45)}
\end{aligned}
$$

Equation IA.45 can be combined with Equation IA.39 to compute the risk-neutral moments required for Equation IA.7 in Remark 4 with $\mathbb{I}_{A_s}=\mathbb{I}_{A_u}$.

IA.5.5.4 HARA: Central Risk-Neutral Moments: $\mathbb{E}_t^*\left[\left(-\frac{a^*}{R_{f,t\to T}}R_{M,t\to T}-1\right)^{1-\gamma}\left(R_{M,t\to T}\right)^k\mathbb{I}_{A_c}\right]$

The identity in Equation IA.17 implies the following identity relating the risk-neutral moments:

$$\begin{aligned}
&\mathbb{E}^*\left[\left(-\frac{a^*}{R_{f,t\to T}}R_{M,t\to T}-1\right)^{1-\gamma}\left(R_{M,t\to T}\right)^k\mathbb{I}_{A_c}\right]\\
\equiv\ &\mathbb{E}_t^*\left[\left(-\frac{a^*}{R_{f,t\to T}}R_{M,t\to T}-1\right)^{1-\gamma}\left(R_{M,t\to T}\right)^k\right]\\
&-\mathbb{E}^*\left[\left(-\frac{a^*}{R_{f,t\to T}}R_{M,t\to T}-1\right)^{1-\gamma}\left(R_{M,t\to T}\right)^k\mathbb{I}_{A_d}\right]\\
&-\mathbb{E}^*\left[\left(-\frac{a^*}{R_{f,t\to T}}R_{M,t\to T}-1\right)^{1-\gamma}\left(R_{M,t\to T}\right)^k\mathbb{I}_{A_u}\right]
\end{aligned}$$

where we have made use of the definitions $\mathbb{I}_{A_c}\equiv\mathbb{I}_{\{\underline{x}S_t\leq S_T\leq\overline{x}S_T\}}$, $\mathbb{I}_{A_d}\equiv\mathbb{I}_{\{S_T<\underline{x}S_t\}}$, and $\mathbb{I}_{A_u}\equiv\mathbb{I}_{\{S_T>\overline{x}S_t\}}$. Substituting in expressions from Equations IA.43, IA.44, and IA.45 and simplifying yields:

$$\begin{aligned}
&\mathbb{E}^*\left[\left(-\frac{a^*}{R_{f,t\to T}}R_{M,t\to T}-1\right)^{1-\gamma}\left(R_{M,t\to T}\right)^k\mathbb{I}_{A_c}\right]\\
=\ &\left(-a^*-1\right)^{1-\gamma}\left(R_{f,t\to T}\right)^k\\
&-\left(-\frac{a^*}{R_{f,t\to T}}\underline{x}-1\right)^{1-\gamma}\left(\underline{x}\right)^k Prob_t^*\left[S_T<\underline{x}S_t\right]-\left(-\frac{a^*}{R_{f,t\to T}}\overline{x}-1\right)^{1-\gamma}\left(\overline{x}\right)^k Prob_t^*\left[S_T>\overline{x}S_t\right]\\
&+R_{f,t\to T}\left(h_y^{HARA}\left(\underline{x}S_t\right)P_{t\to T}\left[\underline{x}S_t\right]-h_y^{HARA}\left(\overline{x}S_t\right)C_{t\to T}\left[\overline{x}S_t\right]\right)\\
&+R_{f,t\to T}\left(\int_{\underline{x}S_t}^{R_{f,t\to T}S_t}h_{yy}^{HARA}\left(K\right)P_{t\to T}\left[K\right]dK+\int_{R_{f,t\to T}S_t}^{\overline{x}S_t}h_{yy}^{HARA}\left(K\right)C_{t\to T}\left[K\right]dK\right).
\end{aligned}\tag{IA.46}$$

Equation IA.46 can be combined with Equation IA.39 to compute the risk-neutral moments required for Equation IA.7 in Remark 4 with $\mathbb{I}_{A_s}=\mathbb{I}_{A_c}$.

IA.6 Nonlinear Least Squares Estimation of Preference Parameters

IA.6.1 Data-Implied Decomposition Estimation Procedure

We would like to estimate the preference parameters $\tau\left(x_s\right)$, $\rho\left(x_s\right)$, and $\kappa\left(x_s\right)$ at three points in the market return space corresponding to $s\in\{d,\,c,\,u\}$. These preference parameters are required to compute the physical moments (via Corollary 1)[54] needed to implement the risk premium decomposition in Proposition 3. We use the relationship between physical and risk-neutral moments from Corollary 1 to estimate preference parameters. Start by writing powers of realized excess market returns as:

$$\left(R_{M,t\to T}-R_{f,t\to T}\right)^n\ =\ \mathbb{E}_t\left[\left(R_{M,t\to T}-R_{f,t\to T}\right)^n\right]+\varepsilon_{t\to T,s}^{(n)}$$

[54] Recall that this relationship is based on Corollary1, $\mathbb{M}_{t\to T}^{*(n)}$ are untruncated risk-neutral moments, and $\lambda_t\left(x_s,k,j\right)$ is a function of the preference parameters $\tau\left(x_s\right)$, $\rho\left(x_s\right)$, and $\kappa\left(x_s\right)$ according to Equations 26 and 12.

Applying Corollary 1, we can replace $\mathbb{E}_t\left[\left(R_{M,t\to T}-R_{f,t\to T}\right)^n\right]$ to obtain:

$$\left(R_{M,t\to T}-R_{f,t\to T}\right)^n = \mathbb{M}_{t\to T}^{*(n)}+\frac{\sum_{k=1}^{\infty}\sum_{j=0}^{k}\lambda_t\left(x_s,k,j\right)\left(\mathbb{M}_{t\to T}^{*(n+k-j)}-\mathbb{M}_{t\to T}^{*(k-j)}\mathbb{M}_{t\to T}^{*(n)}\right)}{1+\sum_{k=1}^{\infty}\sum_{j=0}^{k}\lambda_t\left(x_s,k,j\right)\mathbb{M}_{t\to T}^{*(k-j)}}+\varepsilon_{t\to T,s}^{(n)}.$$

We truncate this summation at $k=3$ for tractability. This balances truncation error induced by choosing lower k with the fact that estimated higher-order risk-neutral moments (needed for higher k) can be inaccurate.[55] Assuming the truncation error is time invariant, we can write:

$$\left(R_{M,t\to T}-R_{f,t\to T}\right)^n = a_{T,s}^{(n)}+\mathbb{M}_{t\to T}^{*(n)}+\frac{\sum_{k=1}^{3}\sum_{j=0}^{k}\lambda_t\left(x_s,k,j\right)\left(\mathbb{M}_{t\to T}^{*(n+k-j)}-\mathbb{M}_{t\to T}^{*(k-j)}\mathbb{M}_{t\to T}^{*(n)}\right)}{1+\sum_{k=1}^{3}\sum_{j=0}^{k}\lambda_t\left(x_s,k,j\right)\mathbb{M}_{t\to T}^{*(k-j)}}+\varepsilon_{t\to T,s}^{(n)} \tag{IA.47}$$

where we include the constant $a_{T,s}^{(n)}$ to account for the truncation error induced by limiting the upper limit on the sum over k to be 3.[56] To the extent that this error may be time varying, it will be relegated to the error term, $\varepsilon_{t\to T,\,s}^{(n)}$. Note that this can be applied to moments of any order (n), any time horizon (T). Recall that $\lambda_t\left(x_s,k,j\right)$ is a function of the preference parameters $\tau\left(x_s\right)$, $\rho\left(x_s\right)$, and $\kappa\left(x_s\right)$ according to Equations 26 and 12. We set $\underline{x}=0.9$ and $\overline{x}=1.1$ with $x_d=0.85$, $x_c=1$, and $x_d=1.15$ in all reported results. That is, we are interested in studying risk premia associated with down market returns less than -10%, central market returns between -10% and +10%, and up market returns greater than +10%.

Note that we must estimate nine total preference parameters for each horizon of interest: three parameters ($\tau\left(x_s\right)$, $\rho\left(x_s\right)$, and $\kappa\left(x_s\right)$) for each of the three regions of interest ($s\in\{d,c,u\}$) in the return space. Given realized excess market returns and measured risk-neutral moments, we estimate the preference parameters $\tau\left(x_s\right)$, $\rho\left(x_s\right)$, and $\kappa\left(x_s\right)$ using non-linear weighted least squares to minimize the squared error using three versions of Equation IA.47: $n=1$, 2, and 3. Each value of n brings with it three equations: one for each set of preference parameters in each of our three regions of interest. Therefore, we have nine total equations and sets of error terms that are generated using Equation IA.47 in our estimation.

Since we are also interested in estimating truncated risk premia, we need to ensure that the preference parameters satisfy the restriction that the sum of truncated physical moments equals the untruncated physical moment (at least on average across time). This restriction can be introduced to the nonlinear least squares estimation by considering relationships of the form

$$\begin{aligned}&\left(R_{M,t\to T}-R_{f,t\to T}\right)^n\\ =\;& a_T^{(n)}+\\ &\sum_{s\in\{d,c,u\}}\left[\mathbb{M}_{t\to T}^{*(n)}\left[A_s\right]+\frac{\sum_{k=1}^{3}\sum_{j=0}^{k}\lambda_t\left(x_s,k,j\right)\left(\mathbb{M}_{t\to T}^{*(n+k-j)}\left[A_s\right]-\mathbb{M}_{t\to T}^{*(k-j)}\left[A\right]\mathbb{M}_{t\to T}^{*(n)}\left[A_s\right]\right)}{1+\sum_{k=1}^{3}\sum_{j=0}^{k}\lambda_t\left(x_s,k,j\right)\mathbb{M}_{t\to T}^{*(k-j)}\left[A\right]}\right]+\varepsilon_{t\to T}^{(n)}.\end{aligned} \tag{IA.48}$$

This relationship follows from Corollary 1 and the identity in Equation 28. We allow for the

[55] For example, see Rompolis and Tzavalis (2017), who investigate the accuracy of higher-order risk-neutral moments computed from options when the cross-section of options is limited.

[56] Note that all moments in Equation IA.47 are untruncated moments (i.e., $\mathbb{M}_{t\to T}^{*(n)}\left[A\right]$). We suppress the $[A]$ dependence here for simplicity.

relationship to not hold exactly both conditionally (through inclusion of $\varepsilon_{t\to T}^{(n)}$) and on average across time (through the inclusion of $a_T^{(n)}$). We do not require the relationship to hold exactly conditionally due to the use of slightly different data from options prices when computing truncated moments relative to untruncated moments (see Internet Appendix IA.5.1.1 for a description of how these moments are computed using option price data). With $n = 1$, 2, and 3, Equation IA.48 adds three additional equations and sets of error terms to include in the estimation.[57]

When minimizing the sum of squared errors implied by Equations IA.47 and IA.48, we weight the error terms by the inverse standard deviation of the left-hand-side time series associated with each equation (i.e. the inverse of the standard deviation of $(R_{M,t\to T} - R_{f,t\to T})^n$). We do this because the volatilities of each left-hand-side variable are naturally of a different magnitude for different n values. We would like the error terms associated with equations having different n values to have approximately the same weight in the least squares minimization, which is effectively achieved using this weighting scheme.

The final ingredient in our estimation comes in the form of a Ridge-type penalty on the estimated preference parameters. That is, in addition to the sum of squared error terms from the twelve sets of restrictions discussed above, we add an additional term of the form

$$\tilde{\varepsilon}_T^2 \quad = \quad \phi_T \sum_{s\in\{d,c,u\}} \left[\tau_T \left(x_s\right)^2 + \rho_T \left(x_s\right)^2 + \kappa_T \left(x_s\right)^2\right] \tag{IA.49}$$

where ϕ_T is a tuning parameter. We add this penalty to the squared error objective function for estimations at each horizon, T. We include the parameter horizon dependence here explicitly for clarity. We include the penalty term since the right-hand-side risk-neutral moments are highly correlated. This can induce excessive noise in the preference parameter estimates (see Hastie, Tibshirani, and Friedman, 2009, pp. 63-64). Adding a small penalty of this form can help reduce variance in the estimated parameters without increasing estimation bias much. We select the tuning parameter, ϕ_T, using a standard approach. We apply a 10-fold cross validation to the estimation and find that the test error is approximately flat for tuning parameter values below 10^{-3}. We select a moderate value of $\phi_T = 2 \times 10^{-5}$ across all horizons to mitigate estimation bias induced by the penalty.

Given these ingredients, we estimate preference parameters separately at each horizon of interest (30, 60, 90, 180, and 360 days) by minimizing an objective function that sums squared errors from the 12 sets of equations described above (Equations IA.47 and IA.48) and the penalty term in Equation IA.49 using daily data from January 1996 through June 2019. We then use these preference parameters to compute risk premia according to Proposition 3 (and using Corollary 1 to estimate physical moments).

IA.6.2 Possible Estimation Bias in Estimated Parameters is Likely Small

Our NLS estimation strategy described above uses powers of realized excess market returns to the power n as proxies for physical moments, expressed as

$$\left(R_{M,t\to T} - R_{f,t\to T}\right)^n \quad = \quad \mathbb{E}_t\left[\left(R_{M,t\to T} - R_{f,t\to T}\right)^n\right] + \varepsilon_{t\to T}^{(n)} \text{ with } n = 1, 2, 3$$

[57] We could also include equation restrictions related to individual truncated moments (i.e., expressions for $\mathbb{M}_{t\to T}^{(n)}[A_s]$ according to Corollary 1 and using $\left(R_{M,t\to T} - R_{f,t\to T}\right)^n \mathbb{I}_{A_s}$ as realizations in the left hand side of Equation IA.48 (without the summation). We choose not to use these since there are not many instances where $\mathbb{I}_{A_d} = 1$ nor are there many instances of $\mathbb{I}_{A_u} = 1$ in the data (i.e., the extreme market events for which we are interested in estimating risk premia) are not often realized in the data.

where $R_{M,t\to T}$ is the market return from time t to T, $R_{f,t\to T}$ is the prevailing risk-free rate observable at time t, $\mathbb{E}_t\left[(R_{M,t\to T}-R_{f,t\to T})^n\right]$ is the physical moment of interest, and $\varepsilon^{(n)}_{t\to T}$ is unforecastable noise given information at time t. A concern with $(R_{M,t\to T}-R_{f,t\to T})^n$ as a proxy for $\mathbb{E}_t\left[(R_{M,t\to T}-R_{f,t\to T})^n\right]$ is that it may introduce bias to our estimated preference parameters $\tau(x_s)$, $\rho(x_s)$, and $\kappa(x_s)$ due to the noise, $\varepsilon^{(n)}_{t\to T}$.

To address this concern, we implement the following simulation procedure to help understand whether our estimation strategy introduces bias in our parameter estimates. There will be some bias induced by the ridge-type penalty function, so we set the tuning parameter, ϕ_T, to zero in this case so that known bias induced by this technique does not affect results in our analysis. On a side note, recall that we follow standard methods for identifying an optimal tuning parameter to balance the standard variance-bias tradeoff in our main estimation (see, e.g., Hastie, Tibshirani, and Friedman (2009, pp. 63-64)). Given this slight modification from our main estimation procedure, the simulation procedure described below will capture potential bias induced by using noisy proxies for the physical moments in which we are interested as left-hand-side variables.

The simulation procedure is as follows:

1. Assume that Corollary 1 describes the true data-generating process for physical moments. Choose preference parameters for this data-generating process. For this step, we assume that the preference parameters are given by our estimated values reported in Table 1. This is innocuous to your concern, since your concern is that given this expression for physical moments, using noisy proxies to estimate the preference parameters leads to biased estimates of the parameters.

2. Given observed risk-neutral moments (computed from option prices) and the assumed parameters from Step 1, construct the implied conditional physical moment time series according to Corollary 1 needed for our NLS estimation procedure. Note that for each simulation described below, we use the same risk-neutral and physical moments, which is different from in our main bootstrap procedure used to estimate confidence intervals on our estimated preference parameters. This is since, in the current exercise, we are interested in how random noise in the LHS variables might affect preference parameter estimates rather than time series sampling, as in our main bootstrap procedure.

3. Randomly sample error terms from the empirical error distribution given the computed physical moments and the observed powers of realized excess market returns to the power n (i.e., the $\varepsilon^{(n)}_{t\to T}$ from our main parameter estimation described in Internet Appendix IA.6.1) and add the randomly sampled errors to our computed physical moments from Step 2. At each date we sample a new error term from the empirical distribution and add it to the conditional moment. This provides a simulated proxy for our LHS variable, which is the sum of the true physical moment plus noise sampled from the empirical (ex-post) noise distribution. We could have also solely used random noise sampled from normal distributions, for instance, but we wanted to use noise from the empirical distributions in case any non-normalities affect the potential estimation bias. In unreported results, we find that using noise sampled from normal distributions yields similar results to those we report herein when sampling from the empirical error distribution.

4. Use our NLS procedure to estimate the associated set of preference parameters given the moments plus noise sampled from the empirical distribution. Importantly, we verified that this procedure reproduces the original preference parameter estimate when no noise is added, as expected.

5. Repeat Steps 3 and 4 10,000 times to construct parameter distributions, and compare these to the true (assumed) parameters.

Results are provided in Figure IA.16, which plots the parameter distributions (blue histograms) along with the true parameter values (red vertical lines) when assuming that the true parameters are given by our estimates from Table 1. In almost all cases, results indicate no appreciable bias in our estimated parameters due to noise in the left-hand-side variable that we use for estimation. See reported simulated parameter means and medians reported in the figure legends. There are a few cases in the restricted parameter-based simulation (Figure IA.17) that appear to have some bias (see the κ-related simulations in Panels (c), (f), and (i)). However, this is likely due to the highly skewed nature of the parameter distributions and the fact that we may not be accurately capturing this skewness. Even with 10,000 simulations, the right tails of these distributions appear sparse. Even if there is some small bias in our parameter estimates, results in Internet Appendix IA.3.5 ("Effects from Modifying $\tau(x_s)$, $\rho(x_s)$, and $\kappa(x_s)$") indicate that our main conclusions would be unchanged due to changes in the parameter values even larger than the potentially small bias in some parameter estimates indicated by the analysis in this section.

Figure IA.17 provides results when we repeat this simulation procedure assuming that preference parameters are the same as those in our restricted decomposition from Internet Appendix IA.3.9 ("Data-Implied Decomposition Using Restricted Preference Parameters"), which are consistent with economic theory (i.e., $\tau(x_s) = 1$, $\rho(x_s) = 2$, and $\kappa(x_s) = 4$ $\forall s \in \{d, c, u\}$. Conclusions are similar to those when using our estimated preference parameters from Table 1.

In summary, this analysis indicates that there is likely very little bias in our parameter estimates induced by noise in the left-hand-side variables that we use in our estimation strategy. Furthermore, to the extent that there is some small bias, it is unlikely to affect our results in a meaningful way.

IA.6.3 Modifications for Applying the Estimation Procedure to Representative Agent Models

In this subsection, we describe the slight modifications to the estimation procedure described in the previous subsection that we use to apply it to representative agent models as described in subsection 5.3. First, in our data-implied decomposition estimation, we use realized market return moments as proxies for the ex-ante physical moments. This introduces a significant amount of noise in the data. Since we observe these exact physical moments (i.e., the first, second, and third moments of excess market returns) in the models, we use these as left-hand variables in the NLS estimation. Second, since this eliminates noise in our left-hand side variables, we no longer use the Ridge-type shrinkage penalty in the estimation.

IA.7 Projection of Generic SDF onto Aggregate Wealth

In this section, we show how the SDF in any representative agent model can be approximated as a function projected onto investor wealth. Such a projected SDF can be used to price any payoff related to functions of returns on wealth (i.e., the decomposition components in which we are interested). This justifies applying our data decomposition methodology (i.e., Corollary 1) directly to representative agent models in Subsection 5.3. Note that our main model decomposition results in Section 5 only relied on our Proposition 3, which is independent of the assumption that the SDF can be approximated using a projection onto investor wealth (whether in the actual economy or in the context of a representative agent model).

Without loss of generality, we set $T = t + 1$ to be consistent with the notation in the representative agent models. Let $M_{t\to t+1}$ denote the projection of the representative agent SDF on a set spanned by aggregate wealth $\{1, W_{t+1}, .W_{t+1}^2, .W_{t+1}^3 ...\}$. The projected SDF, which can be written as $M_{t\to t+1} = h(W_{t+1})$, can alternatively be expressed as

$$M_{t\to t+1} = h(W_{ct} R_{M,t\to t+1}),$$

where $W_{ct} = W_t - C_t$ and $R_{M,t\to t+1}$ is the market return, which we use as a proxy for the return on wealth.[58] This projected SDF can alternatively be written as

$$M_{t\to t+1} = \mu_t g(W_{ct} R_{M,t\to t+1}),$$

where μ_t is a (potentially) time-varying variable known at time t. The function $g(.)$ is defined as $g(x) = (\mu_t)^{-1} h(x)$. The constant μ_t can be written as

$$\mu_t = M_{t\to t+1} (g(W_{ct} R_{M,t\to t+1}))^{-1}.$$

This enables us to write

$$\begin{aligned}
\mu_t &= (\mathbb{E}_t[M_{t\to t+1}]) \mathbb{E}_t \left[\frac{M_{t\to t+1}}{\mathbb{E}_t[M_{t\to t+1}]} (g(W_{ct} R_{M,t\to t+1}))^{-1} \right] \\
&= (\mathbb{E}_t[M_{t\to t+1}]) \mathbb{E}_t^* \left[(g(W_{ct} R_{M,t\to t+1}))^{-1} \right].
\end{aligned}$$

Thus,

$$\frac{\mathbb{E}_t[M_{t\to t+1}]}{M_{t\to t+1}} = \frac{\frac{1}{g(W_{ct} R_{M,t\to t+1})}}{\mathbb{E}_t^* \left[\frac{1}{g(W_{ct} R_{M,t\to t+1})} \right]}. \tag{IA.50}$$

The inverse SDF in Equation IA.50 has a similar functional form compared to that in Equation 3. The only difference is that $g(.)$ is a generic function that describes the projection of a representative agent model's SDF onto returns on investor wealth. The inverse SDF in Equation 3 is stated in terms of the investor utility function, $U(.)$, since we assumed the representative investor has utility over final period wealth. When we relax this assumption, $U(.)$ takes on the same interpretation as $g(.)$ in Equation IA.50. So, given the assumption that the market return is a proxy for returns on investor wealth in a given representative agent model, we can apply our data-implied decomposition methodology to the model. In other words, we can use Corollary 1 to estimate physical moments in the model and use these to construct our decomposition according to Proposition 3 (as opposed to using the exact physical moments implied by the model). The fact that we find these data-methodology–applied-to-models decompositions match the exact model-implied decompositions relatively well (Table IA.20), this assumption appears innocuous.

[58] As in our data-implied decompositions, when we apply the data methodology to representative agent models we make the assumption that market returns proxy for returns on wealth in the models. Although we have not verified the correlation among market and wealth returns in each model, this can be done. This is certainly the case in models with only one shock (such as the Gabaix (2012) and Wachter (2013) models). This is likely a good approximation in other models as well since we find good agreement between the exact model-implied decompositions and the data-methodology-applied-to-models decompositions (see Table IA.20).

IA.8 Results and Proofs Related to Representative Agent Models

Our goal in this section is to derive relationships between state variables and asset pricing moments in each model to allow us to extract state variables at each date, and to compute the model-implied risk premia implied by each model given state variables. The state variable extraction procedure is done as described in the paper with related results necessary for the extraction below. Summary statistics for extracted state variables are provided in Table IA.18.

We also evaluate model-implied decompositions at each model's unconditional state variable values and compare results to our main model-implied decompositions in Table IA.19. Average risk premium levels and contributions from our main model-implied decompositions (that use our extracted state variables) are similar to those using unconditional average state variable values from each model (which are independent of our state variable extraction method). In other words, even though our extracted state variables have implied processes that are slightly inconsistent with assumed processes in each model's original calibration, our decompositions have similar unconditional implications whether we use our extracted state variables or unconditional state variables from each model.

The risk premia are the same as we have defined in our main draft, $\mathbb{RP}^{(n)}_{t\to T}[A_s]$ (see Equation 29). We therefore need to compute the model-implied physical and risk-neutral moments as defined in our main draft, $\mathbb{M}^{(n)}_{t\to T}[A_s]$ and $\mathbb{M}^{*(n)}_{t\to T}[A_s]$ (see Equations 20 and 21). Note that in many cases it will be easier to compute non-central market return moments rather than excess market return moments as required in our definition of $\mathbb{RP}^{(n)}_{t\to T}[A_s]$. In these cases, we can use the binomial theorem to transform non-centered moments of the market return to excess return moments according to

$$\begin{aligned}
\mathbb{E}_t\left[(R_{M,t\to t+1}-R_{f,t\to t+1})^n\right] &= \sum_{k=0}^{n}\frac{n!}{(n-k)!k!}\left(\mathbb{E}_t\left[R^k_{M,t\to t+1}\right]\right)(-1)^{n-k}R^{n-k}_{f,t\to t+1},\\
\mathbb{E}_t\left[(R_{M,t\to t+1}-R_{f,t\to t+1})^n\mathbb{I}_{\{R_{M,t\to t+1}>a\}}\right] &= \sum_{k=0}^{n}\frac{n!}{(n-k)!k!}\left(\mathbb{E}_t\left[R^k_{M,t\to t+1}\mathbb{I}_{\{R_{M,t\to t+1}>a\}}\right]\right)(-1)^{Rn-k}R^{n-k}_{f,t\to t+1}
\end{aligned}$$

and

$$\begin{aligned}
\mathbb{E}^*_t\left[(R_{M,t\to t+1}-R_{f,t\to t+1})^n\right] &= \sum_{k=0}^{n}\frac{n!}{(n-k)!k!}\left(\mathbb{E}^*_t\left[R^k_{M,t\to t+1}\right]\right)(-1)^{n-k}R^{n-k}_{f,t\to t+1},\\
\mathbb{E}^*_t\left[(R_{M,t\to t+1}-R_{f,t\to t+1})^n\mathbb{I}_{\{R_{M,t\to t+1}>a\}}\right] &= \sum_{k=0}^{n}\frac{n!}{(n-k)!k!}\left(\mathbb{E}^*_t\left[R^k_{M,t\to t+1}\mathbb{I}_{\{R_{M,t\to t+1}>a\}}\right]\right)(-1)^{n-k}R^{n-k}_{f,t\to t+1}.
\end{aligned}$$

Results needed to compute these moments given model state variables are provided below.

IA.8.1 Applying the Data-Implied Decomposition Methodology to Models

We present results for our data-methodology-applied-to-models (DMAM) market risk premium decompositions in this subsection. See Subsection 5.3 for more details on this procedure. We limit our study to those models with significant downside risk premia in the original model-implied decompositions including the models from Drechsler and Yaron (2011), Bekaert, Engstrom, and Ermolov (2023), Gabaix (2012), and Wachter (2013). These are likely a better approximation of the true economy, which also features significant downside risk premia, thereby giving a better sense of our data-implied decomposition's ability to capture the dynamic risk premium behavior in such economies.

Results are presented in Figure IA.18 and Table IA.20. In all cases, the DMAM risk premium levels and contributions are highly correlated with the original model-implied decomposition time

series.[59] Furthermore, the DMAM time series averages and standard deviations typically match the corresponding original model-implied values well. This is true in all cases except for the DMAM risk premium average level values from the Drechsler and Yaron (2011) model, which are a bit too high. Regardless, in this case the time series are still highly correlated and match the average contributions from the original model-implied decomposition well. Furthermore, the DMAM values do not match the Gabaix (2012) model-implied decomposition values well, but this is the model whose model-implied decomposition typically performed the worst at matching empirical risk premium patterns among all models we investigate. In other words, this is not a case that would invalidate our assertion that the evidence from this exercise implies that our data-implied decomposition is likely to accurately reflect the true risk premium decomposition in the data given that it is able to match the model-implied decompositions well.

IA.8.2 Linking State Variable Shocks to Risk-Neutral Moment Shocks

For illustration purposes, in this subsection we show how shocks to state variables in representative agent models are related to the model-implied shocks to asset pricing variables of interest up to a first-order approximation. Examples of such asset pricing variables include the log-price-dividend ratio ($\log(P_t/D_t)$), risk-neutral moments ($\mathbb{M}_{t\to T}^{*(n)}$), physical moments ($\mathbb{M}_{t\to T}^{(n)}$), and so forth. Let $\boldsymbol{x_t}$ denote the vector of n state variables in a given model and assume the state variables follow the VAR(1) process

$$\boldsymbol{x_{t+1}} = \boldsymbol{\mu} + \boldsymbol{B}\boldsymbol{x_t} + \boldsymbol{C_t}\boldsymbol{\varepsilon_{t+1}}, \tag{IA.51}$$

where $\boldsymbol{\mu}$ is a vector of constants, $\boldsymbol{B}$ is a time-invariant invertible matrix, $\boldsymbol{C_t}$ is a (potentially) time-varying invertible matrix, and $\boldsymbol{\varepsilon_{t+1}}$ is a vector of state variable shocks having generic distributions with mean zero. Note that all representative agent models we investigate have state variable processes that can be mapped into this framework.

In all models we investigate, model-implied asset pricing variables such as the log-price-dividend ratio and risk-neutral moments are functions of the state variables. Let $\boldsymbol{Y_{t+1}}$ be a vector of asset pricing variables of interest and $F(\boldsymbol{x_{t+1}})$ be a vector-valued function that maps the state variables, $\boldsymbol{x_{t+1}}$, into the conditional variables of interest, $\boldsymbol{Y_{t+1}}$, as

$$\boldsymbol{Y_{t+1}} = F(\boldsymbol{x_{t+1}}). \tag{IA.52}$$

A first-order Taylor expansion around the unconditional average state variable values, $\overline{\boldsymbol{x}}$, implies

$$\begin{aligned} \boldsymbol{Y_{t+1}} &\approx \tilde{\boldsymbol{a}} + \boldsymbol{J}(\boldsymbol{x_{t+1}} - \overline{\boldsymbol{x}}) \\ &= \boldsymbol{a} + \boldsymbol{J}\boldsymbol{x_{t+1}} \\ &\quad \boldsymbol{a} + \boldsymbol{J}\boldsymbol{\mu} + \boldsymbol{J}\boldsymbol{B}\boldsymbol{x_t} + \boldsymbol{J}\boldsymbol{C_t}\boldsymbol{\varepsilon_{t+1}}, \end{aligned} \tag{IA.53}$$

where $\tilde{\boldsymbol{a}}$ is a vector of constants, $\boldsymbol{a} \equiv \tilde{\boldsymbol{a}} + \boldsymbol{J}\overline{\boldsymbol{x}}$, $\boldsymbol{J}$ is the Jacobian of $F(\overline{\boldsymbol{x}})$ (i.e., $J \equiv \nabla F(x)|_{x=\overline{x}}$), and the last line makes use of Equation IA.51. The time-t expectation of this first-order approximation

[59] This is true for all cases except the central risk premium level under the Gabaix (2012) model, which has a large negative correlation with the original model-implied time series. This is likely because the original time series has a small standard deviation, such that small deviations implied by the DMAM decomposition do not contribute much to the overall sum of squared errors in the NLS estimation used to pin down preference parameters (see Internet Appendix IA.6).

of $\boldsymbol{Y_{t+1}}$ is

$$\begin{aligned} \mathbb{E}_t\left[\boldsymbol{Y_{t+1}}\right] &\approx \boldsymbol{a} + \boldsymbol{J}\mathbb{E}_t\left[\boldsymbol{x_{t+1}}\right] \\ &= \boldsymbol{a} + \boldsymbol{J\mu} + \boldsymbol{JBx_t}. \end{aligned} \tag{IA.54}$$

Combining Equations IA.53 and IA.54, the shocks to the asset pricing variables of interest are approximately

$$\boldsymbol{Y_{t+1}} - \mathbb{E}_t\left[\boldsymbol{Y_{t+1}}\right] \approx \boldsymbol{JC_t\varepsilon_{t+1}}. \tag{IA.55}$$

Therefore, to a first-order approximation, shocks to asset pricing variables of interest are linearly related to the state variable shocks themselves.

If we specialize $\boldsymbol{Y_{t+1}}$ to be the variables we use to extract state variables from models (the log-price-dividend ratio, risk-neutral variance, and risk-neutral skewness), this implies shocks to these variables are approximately

$$\begin{bmatrix} \log\left(P_{t+1}/D_{t+1}\right) - \mathbb{E}_t\left[\log\left(P_{t+1}/D_{t+1}\right)\right] \\ \mathbb{M}^{*(2)}_{t\to T} - \mathbb{E}_t\left[\mathbb{M}^{*(2)}_{t\to T}\right] \\ \mathbb{M}^{*(3)}_{t\to T} - \mathbb{E}_t\left[\mathbb{M}^{*(3)}_{t\to T}\right] \end{bmatrix} \approx \boldsymbol{J_{PD,M2,M3}C_t\varepsilon_{t+1}} \tag{IA.56}$$

where $\boldsymbol{J_{PD,M2,M3}}$ is the Jacobian of a vector-valued function that maps state variables to these asset pricing variables/moments of interest. In unreported results, we find that modeling risk-neutral moments as AR(p) processes yields implied shock distributions that are non-normally distributed. Therefore, for a model to match the conditional shock distribution of these asset pricing variables, the state variable shocks must themselves be non-normally distributed. A symptom of the disconnect between model-implied shocks to these variables of interest and those implied by the data is the fact that the state variable processes we extract from models are often slightly inconsistent with the originally-assumed processes in the models (see Table IA.18). Our analysis indicates that this disconnect is potentially worse for models whose state variable shocks are normally distributed.

These results have two direct implications for building representative agent models that better fit the data (in particular, that better fit our risk premium decomposition and risk-neutral moment processes implied by the data). First, state variables must have non-normally distributed shocks whose distributions are chosen to be consistent with the risk-neutral moment shock distributions implied by the data. Second, using our conditional risk premia as moment targets when calibrating future asset pricing models can help pin down the preference parameters (which determine $\boldsymbol{J}$) and parameters associated with these non-normally distributed shocks.

IA.8.3 Risk-Neutral Moments when the SDF and Returns are Log-Normally Distributed

The following analysis will be useful for deriving some results related to representative agent models. Without loss of generality, set $T = t + 1$. Note that

$$\begin{aligned}
\log\left(\mathbb{E}_t^*\left(R_{t\to t+1}^n\right)\right) &= \log\left(\mathbb{E}_t\left(\tfrac{M_{t\to t+1}}{\mathbb{E}_t M_{t\to t+1}} R_{t\to t+1}^n\right)\right) \\
&= \log R_{f,t\to t+1} + \log\left(\mathbb{E}_t M_{t\to t+1} R_{t\to t+1}^n\right) \\
&= \log R_{f,t\to t+1} + \mathbb{E}_t \log\left(M_{t\to t+1}\right) + n\mathbb{E}_t \log\left(R_{t\to t+1}\right) + \tfrac{1}{2}\mathbb{VAR}_t\left(\log M_{t\to t+1}\right) \\
&\quad + \tfrac{n^2}{2} VAR_t \log R_{t\to t+1} + n\mathbb{COV}_t\left(\log M_{t\to t+1}, \log R_{t\to t+1}\right)
\end{aligned}$$

which simplifies to

$$\begin{aligned}
\log\left(\mathbb{E}_t^*\left(R_{t\to t+1}^n\right)\right) &= \log R_{f,t\to t+1} + \mathbb{E}_t \log\left(M_{t\to t+1}\right) + \tfrac{1}{2}\mathbb{VAR}_t\left(\log M_{t\to t+1}\right) + \tfrac{n^2}{2}\mathbb{VAR}_t \log R_{t\to t+1} \\
&\quad + n(\mathbb{E}_t \log\left(R_{t\to t+1}\right) + \mathbb{COV}_t\left(\log M_{t\to t+1}, \log R_{t\to t+1}\right)).
\end{aligned}$$

The Euler equation $\mathbb{E}_t M_{t\to t+1} = \frac{1}{R_{f,t\to t+1}}$ allows us to write

$$-\log R_{f,t\to t+1} = \mathbb{E}_t \log\left(M_{t\to t+1}\right) + \frac{1}{2}\mathbb{VAR}_t\left(\log M_{t\to t+1}\right)$$

Thus,

$$\log\left(\mathbb{E}_t^*\left(R_{t\to t+1}^n\right)\right) = n(\mathbb{E}_t \log\left(R_{t\to t+1}\right) + \mathbb{COV}_t\left(\log M_{t\to t+1}, \log R_{t\to t+1}\right)) + \tfrac{n^2}{2}\mathbb{VAR}_t \log R_{t\to t+1} \ .$$

Under the log-normality assumption, the Euler equation $\mathbb{E}_t M_{t\to t+1} R_{t\to t+1} = 1$ can be expressed as

$$\begin{aligned}
&\mathbb{E}_t \log\left(M_{t\to t+1}\right) + \mathbb{E}_t \log\left(R_{t\to t+1}\right) + \tfrac{1}{2}\mathbb{VAR}_t \log R_{t\to t+1} \\
&+\tfrac{1}{2}\mathbb{VAR}_t\left(\log M_{t\to t+1}\right) + \mathbb{COV}_t\left(\log M_{t\to t+1}, \log R_{t\to t+1}\right) = 0.
\end{aligned}$$

The above expression is equivalent to

$$-\log R_{f,t\to t+1} + \mathbb{E}_t \log\left(R_{t\to t+1}\right) + \tfrac{1}{2}\mathbb{VAR}_t \log R_{t\to t+1} + \mathbb{COV}_t\left(\log M_{t\to t+1}, \log R_{t\to t+1}\right) = 0$$

which simplifies to

$$\mathbb{E}_t \log\left(R_{t\to t+1}\right) + \mathbb{COV}_t\left(\log M_{t\to t+1}, \log R_{t\to t+1}\right) = \log R_{f,t\to t+1} - \tfrac{1}{2}\mathbb{VAR}_t \log R_{t\to t+1}.$$

Finally

$$\log\left(\mathbb{E}_t^*\left(R_{t\to t+1}^n\right)\right) = n \log R_{f,t\to t+1} + \tfrac{n(n-1)}{2}\mathbb{VAR}_t \log R_{t\to t+1} \ . \tag{IA.57}$$

IA.8.4 Truncated Moments of a Log Normal Distribution

The following lemma will be useful for deriving some results related to representative agent models.

Lemma IA.1. *Assume that a random variable* $\log X$ *follows a normal distribution, from Lien (1985), it follows that*

$$\mathbb{E}[X\mathbb{I}_{X>a}] = \left(\mathcal{N}\left[d_1\right]\right) \exp\left(\mathbb{E}\left(\log X\right) + \frac{1}{2}\mathbb{VAR}\left(\log X\right)\right)$$

with

$$d_1 = \frac{\mathbb{VAR}\left(\log X\right) + \mathbb{E}\left(\log X\right) - \log a}{\sqrt{\mathbb{VAR}\left(\log X\right)}}.$$

and

$$\overline{d}_2 = \overline{d}_1 - \sqrt{\mathbb{VAR}_t\left[\log X\right]}.$$

IA.8.5 Long-Run Risk Models

Solving the representative agent problem via indirect utility, Epstein and Zin (1989) show that the SDF has the form

$$M_{t\to t+1} = \delta^{\theta}\left(\frac{C_{t+1}}{C_t}\right)^{-\frac{\theta}{\psi}} R_{a,t\to t+1}^{-(1-\theta)}, \tag{IA.58}$$

where C_{t+1} is the consumption level, δ is the time discount rate, and $R_{a,t\to t+1}$ is the gross return on aggregate consumption. The parameter $\theta = (1-\gamma)/\left(1-\frac{1}{\psi}\right)$ where γ is the risk aversion parameter and ψ is the intertemporal elasticity of substitution (IES). This is the utility specification used by all models in this subsection.

IA.8.5.1 Bansal and Yaron (2004) and Bansal, Kiku, and Yaron (2012)

The economies in both Bansal and Yaron (2004) and Bansal, Kiku, and Yaron (2012) can be described by the following time series

$$\begin{aligned}
\Delta c_{t+1} &= \mu_c + x_t + \phi_c\sigma_t\eta_{c,t+1},\\
x_{t+1} &= \rho x_t + \phi_x\sigma_t\eta_{x,t+1},\\
\sigma_{t+1}^2 &= \overline{\sigma}^2\left(1-\nu\right) + \nu\sigma_t^2 + \phi_\sigma\omega_{t+1},\\
\Delta d_{t+1} &= \mu_d + \phi x_t + \phi_d\sigma_t\eta_{d,t+1} + \phi_{d,c}\sigma_t\eta_{c,t+1},
\end{aligned} \tag{IA.59}$$

where $\eta_{c,t+1}$, $\eta_{x,t+1}$, $\eta_{d,t+1}$, and ω_{t+1} are i.i.d, $\Delta c_{t+1} = \log\frac{C_{t+1}}{C_t}$ is the log consumption growth, and $\Delta d_{t+1} = \log\frac{D_{t+1}}{D_t}$ is the log dividend growth. The Bansal and Yaron (2004) model obtains when $\phi_{d,c} = 0$. In both models, σ_t^2 drives uncertainty in the economies. There are two state variables in each model: x_t and σ_t^2. Given this setup, we show the following results.

Main Results

Result IA.1. *Given the state variables x_t and σ_t^2, the Bansal and Yaron (2004) and Bansal, Kiku, and Yaron (2012) model-implied log price-dividend ratio is given by*

$$\log\frac{P_t}{D_t} = A_{0,m} + A_{1,m}x_t + A_{2,m}\sigma_t^2, \tag{IA.60}$$

and the risk-neutral market return variance is given by

$$\mathbb{M}_{t\to t+1}^{*(2)}\left[A\right] = \exp\left(\mathbb{A}_0^{sq} + \mathbb{A}_1^{sq}x_t + \mathbb{A}_2^{sq}\sigma_t^2\right) - \exp\left(2\mathbb{A}_0^{rf} + 2\mathbb{A}_1^{rf}x_t + 2\mathbb{A}_2^{rf}\sigma_t^2\right). \tag{IA.61}$$

The coefficients $A_{0,m}$, $A_{1,m}$, $A_{2,m}$, $\mathbb{A}_0^{sq}$, $\mathbb{A}_1^{sq}$, and $\mathbb{A}_2^{sq}$ are defined below.

Proof. See below. ■

Result IA.2. *The conditional non-central physical moment and non-central truncated physical moments of the market return are*

$$\begin{aligned}\mathbb{E}_t\left[R^n_{M,t\to t+1}\right] &= \exp\left\{n\mathbb{E}_t\left[\log R_{M,t\to t+1}\right]+\frac{n^2}{2}\mathbb{VAR}_t\left[\log R_{M,t\to t+1}\right]\right\},\\ \mathbb{E}_t\left[R^n_{M,t\to t+1}\mathbb{I}_{\left\{R_{M,t+1}>a\right\}}\right] &= \mathcal{N}\left[\overline{d}_{1,n}\right]\exp\left\{n\left(\mathbb{E}_t\left[\log R_{M,t\to t+1}\right]\right)+\frac{n^2}{2}\left(\mathbb{VAR}_t\left[\log R_{M,t\to t+1}\right]\right)\right\},\end{aligned}$$

and

$$\overline{d}_{1,n}=\frac{n^2\left(\mathbb{VAR}_t\left[\log R_{M,t\to t+1}\right]\right)+n\mathbb{E}_t\left[\log R_{M,t\to t+1}\right]-n\log a}{n\sqrt{\mathbb{VAR}_t\left[\log R_{M,t\to t+1}\right]}},$$

where

$$\mathbb{E}_t\left[\log R_{M,t\to t+1}\right]=\mathbb{A}_0^{er}+\mathbb{A}_1^{er}x_t+\mathbb{A}_2^{er}\sigma_t^2 \text{ and } \mathbb{VAR}_t\left[\log R_{M,t\to t+1}\right]=\mathbb{A}_0^{vr}+\mathbb{A}_1^{vr}\sigma_t^2$$

Further

$$\mathcal{N}\left[\overline{d}_{2,n}\right]=\mathbb{P}_t\left[n\log R_{M,t\to t+1}>n\log a\right]$$

where

$$\overline{d}_{2,n}=\overline{d}_{1,n}-n\sqrt{\mathbb{VAR}_t\left[\log R_{M,t\to t+1}\right]}.$$

All parameters are defined below.

Proof. See below. ■

Result IA.3. *The conditional non-central moment and truncated non-central moment of the market return under the risk neutral measure are*

$$\mathbb{E}^*_t\left[R^n_{M,t\to t+1}\right]=\exp\left(n\log R_{f,t\to t+1}+\frac{n\left(n-1\right)}{2}\mathbb{VAR}_t\left[\log R_{M,t\to t+1}\right]\right).$$

$$\mathbb{E}^*_t\left[R^n_{M,t\to t+1}\mathbb{I}_{\left\{R_{M,t\to t+1}>a\right\}}\right] = \mathcal{N}\left[\overline{d}^*_{1,n}\right]\mathbb{E}^*_t\left[R^n_{M,t\to t+1}\right],$$

where

$$\overline{d}^*_{1,n}=\frac{\mathbb{A}^{'}_{n,t}\mathbb{A}_{n,t}-\log a^*_n}{\sqrt{\mathbb{A}^{'}_{n,t}\mathbb{A}_{n,t}}},$$

and

$$\log a^*_n=\mathbb{A}^{'}_{n,t}\mathbb{A}^R_{n,t}\left(\mathbb{A}^{R'}_{n,t}\mathbb{A}^R_{n,t}\right)^{-1}\left(n\log a-\mu^R_{n,t}\right)$$

with

$$\begin{aligned}\mu^{x,\sigma}_{n,t} &= \mathbb{A}_{0,n}+\mathbb{A}_{1,n}x_t+\mathbb{A}_{2,n}\sigma_t^2,\\ \mathbb{A}^{'}_{n,t} &= \left[\mathbb{A}_{3,n}\sigma_t,\ \mathbb{A}_{4,n}\sigma_t,\ \mathbb{A}_{5,n},\ \mathbb{A}_{6,n}\sigma_t\right],\\ \mu^R_{n,t} &= n\mathbb{A}_0^{er}+n\mathbb{A}_1^{er}x_t+n\mathbb{A}_2^{er}\sigma_t^2,\\ \mathbb{A}^{R'}_{n,t} &= \left[n\kappa_{1,m}A_{1,m}\phi_x\sigma_t,\ n\phi_{d,c}\sigma_t,\ n\kappa_{1,m}A_{2,m}\phi_\sigma,\ n\phi_d\sigma_t\right].\end{aligned}$$

Further,

$$\overline{d}^*_{2,n}=\overline{d}^*_{1,n}-\sqrt{\mathbb{A}^{'}_{n,t}\mathbb{A}_{n,t}}$$

and

$$\mathbb{E}^*_t\left[\mathbb{I}_{\left\{R_{M,t\to t+1}>a\right\}}\right]=N\left[\overline{d}^*_{2,n}\right].$$

All parameters are defined below.

Proof. See below. ■

Derivations and Proofs We can use the Campbell and Shiller (1988) approximation to write the log gross return as

$$\log R_{a,t\to t+1} = \kappa_0 + \kappa_1 z_{t+1} - z_t + \Delta c_{t+1},$$

where z is the log price-consumption ratio and

$$\kappa_0 = \log\left(1+e^{\overline{z}}\right) - \kappa_1 \overline{z} \text{ and } \kappa_1 = \frac{e^{\overline{z}}}{1+e^{\overline{z}}}.$$

The log price consumption ratio follows

$$z_t = A_0 + A_1 x_t + A_2 \sigma_t^2,$$

where

$$A_0 = \frac{\left(\log\delta + \left(1-\frac{1}{\psi}\right)\mu_c + \kappa_0 + \kappa_1 A_2 \overline{\sigma}^2 (1-\nu) + \frac{1}{2}\theta\left(\kappa_1 A_2 \phi_\sigma\right)^2\right)}{(1-\kappa_1)}, \tag{IA.62}$$

$$A_1 = \frac{1-\frac{1}{\psi}}{1-\kappa_1\rho}, \tag{IA.63}$$

$$A_2 = \frac{1}{2}\frac{\theta\left(1-\frac{1}{\psi}\right)^2\phi_c^2 + \theta\left(\kappa_1 A_1 \phi_x\right)^2}{1-\kappa_1\nu}. \tag{IA.64}$$

The proof of these coefficients A_0, A_1, and A_2 are given below. Using the Campbell and Shiller (1988) approximation, the log market return can be written as

$$\log R_{M,t\to t+1} = \kappa_{0,m} + \kappa_{1,m} z_{m,t+1} - z_{m,t} + \Delta d_{t+1}, \tag{IA.65}$$

where $r_{t+1} = \log R_{M,t\to t+1}$, $z_{m,t} = \log\left(S_t/D_t\right)$ is the log price-dividend ratio and d_{t+1} is the dividend growth. The price dividend ratio is

$$z_{m,t} = A_{0,m} + A_{1,m} x_t + A_{2,m}\sigma_t^2. \tag{IA.66}$$

where

$$A_{0,m} = \frac{1}{(1-\kappa_{1,m})}\left\{\begin{array}{c} \mu_d + \theta\log\delta - (1-\theta)\kappa_0 + \kappa_{0,m} + (1-\theta)A_0(1-\kappa_1) + \left(-\frac{\theta}{\psi} - (1-\theta)\right)\mu_c \\ + \left\{-(1-\theta)\kappa_1 A_2 + \kappa_{1,m}A_{2,m}\right\}\overline{\sigma}^2(1-\nu) + \frac{1}{2}\left(-(1-\theta)\kappa_1 A_2 + \kappa_{1,m}A_{2,m}\right)^2\phi_\sigma^2 \end{array}\right\} \tag{IA.67}$$

$$A_{1,m} = \frac{\phi - \frac{1}{\psi}}{1-\kappa_{1,m}\rho}, \tag{IA.68}$$

$$A_{2,m} = \frac{1}{(1-\kappa_{1,m}\nu)}\left\{\begin{array}{c} \frac{1}{2}\left(\phi_{d,c} - \frac{\theta}{\psi}\phi_c - (1-\theta)\phi_c\right)^2 + \frac{1}{2}\left(\kappa_{1,m}A_{1,m} - (1-\theta)\kappa_1 A_1\right)^2\phi_x^2 \\ + (1-\theta)A_2(1-\kappa_1\nu) + \frac{1}{2}\phi_d^2 \end{array}\right\}. \tag{IA.69}$$

We also show that the log risk-free return is

$$\log R_{f,t} = \mathbb{A}_0^{\text{rf}} + \mathbb{A}_1^{\text{rf}} x_t + \mathbb{A}_2^{\text{rf}}\sigma_t^2 \text{ with }, \tag{IA.70}$$

$$\mathbb{A}_0^{\text{rf}} = -\left\{\begin{array}{c} \theta\log\delta - \gamma\mu_c - (1-\theta)\kappa_0 + (1-\kappa_1)(1-\theta)A_0 \\ -(1-\theta)\kappa_1 A_2\overline{\sigma}^2(1-\nu) + \frac{1}{2}(1-\theta)^2\kappa_1^2 A_2^2\phi_\sigma^2 \end{array}\right\}, \tag{IA.71}$$

$$\mathbb{A}_1^{\text{rf}} = -\left\{-\gamma + (1-\kappa_1\rho)(1-\theta)A_1\right\}, \tag{IA.72}$$

$$\mathbb{A}_2^{\text{rf}} = -\left\{(1-\kappa_1\nu)(1-\theta)A_2 + \frac{1}{2}\gamma^2\phi_c^2 + \frac{1}{2}(1-\theta)^2\kappa_1^2 A_1^2\phi_x^2\right\}. \tag{IA.73}$$

where the proof of $\mathbb{A}_0^{\text{rf}}$, $\mathbb{A}_1^{\text{rf}}$, and $\mathbb{A}_2^{\text{rf}}$ are is given below:

Proof of the A Coefficients. Observe that

$$\begin{aligned}
&\log M_{t+1} + \log R_{a,t+1} \\
= \;& \left(\theta \log \delta - \frac{\theta}{\psi}\Delta c_{t+1} - (1-\theta)\log R_{a,t+1}\right) + \log R_{a,t+1} \\
= \;& \theta \log \delta + \left(\theta - \frac{\theta}{\psi}\right)\Delta c_{t+1} + (\theta\kappa_0 + \theta\kappa_1 z_{t+1} - \theta z_t) \\
= \;& \left\{\theta \log \delta + \left(\theta - \frac{\theta}{\psi}\right)\mu_c + \theta\kappa_0 + \theta\kappa_1 A_0 + \theta\kappa_1 A_2 \overline{\sigma}^2 (1-\nu) - \theta A_0\right\} \\
& + \left\{\left(\theta - \frac{\theta}{\psi}\right) + \theta\kappa_1 A_1 \rho - \theta A_1\right\} x_t + \left(\theta - \frac{\theta}{\psi}\right)\phi_c \sigma_t \eta_{c,t+1} \\
& + \theta\kappa_1 A_1 \phi_x \sigma_t \eta_{x,t+1} + \left\{\theta\kappa_1 A_2 \nu - \theta A_2\right\}\sigma_t^2 + \theta\kappa_1 A_2 \phi_\sigma \omega_{t+1}.
\end{aligned}$$

Therefore, the log of the expected value of $M_{t\to t+1}R_{a,t\to t+1}$ is

$$\begin{aligned}
\log\left(\mathbb{E}\left[M_{t\to t+1}R_{a,t\to t+1}\right]\right) = \;& \left\{\; \theta \log \delta + \left(\theta - \tfrac{\theta}{\psi}\right)\mu_c + \theta\kappa_0 + \theta\kappa_1 A_0 + \theta\kappa_1 A_2 \overline{\sigma}^2 (1-\nu) - \theta A_0 + \tfrac{1}{2}\left(\theta\kappa_1 A_2 \phi_\sigma\right)^2 \;\right\} \\
& + \left\{\left(\theta - \frac{\theta}{\psi}\right) + \theta\kappa_1 A_1 \rho - \theta A_1\right\} x_t. \\
& + \left\{\; \tfrac{1}{2}\left(\theta - \tfrac{\theta}{\psi}\right)^2 \phi_c^2 + \tfrac{1}{2}\left(\theta\kappa_1 A_1 \phi_x\right)^2 + \left(\theta\kappa_1 A_2 \nu - \theta A_2\right) \;\right\}\sigma_t^2
\end{aligned}$$

Thus, the Euler equation $\mathbb{E}_t M_{t\to t+1}R_{a,t\to t+1}$=1 implies

$$\begin{aligned}
\left\{\; \theta \log \delta + \left(\theta - \tfrac{\theta}{\psi}\right)\mu_c + \theta\kappa_0 + (\kappa_1 - 1)\theta A_0 + \theta\kappa_1 A_2 \overline{\sigma}^2 (1-\nu) + \tfrac{1}{2}\left(\theta\kappa_1 A_2 \phi_\sigma\right)^2 \;\right\} &= 0 \\
\theta - \frac{\theta}{\psi} + \theta\kappa_1 A_1 \rho - \theta A_1 &= 0 \\
\left\{\; \theta\kappa_1 A_2 \nu - \theta A_2 + \tfrac{1}{2}\left(\theta - \tfrac{\theta}{\psi}\right)^2 \phi_c^2 + \tfrac{1}{2}\left(\theta\kappa_1 A_1 \phi_x\right)^2 \;\right\} &= 0
\end{aligned}$$

which implies

$$\begin{aligned}
A_0 &= \frac{\left\{\; \log \delta + \left(1 - \tfrac{1}{\psi}\right)\mu_c + \kappa_0 + \kappa_1 A_2 \overline{\sigma}^2 (1-\nu) + \tfrac{1}{2}\theta\left(\kappa_1 A_2 \phi_\sigma\right)^2 \;\right\}}{(1-\kappa_1)}, \\
A_1 &= \frac{1 - \frac{1}{\psi}}{1 - \kappa_1 \rho}, \\
A_2 &= \frac{1}{2}\frac{\theta\left(1 - \frac{1}{\psi}\right)^2 \phi_c^2 + \theta\left(\kappa_1 A_1 \phi_x\right)^2}{1 - \kappa_1 \rho}.
\end{aligned}$$

Next, note that

$$\log M_{t\to t+1} + \log R_{M,t\to t+1} = \theta \log \delta - \frac{\theta}{\psi}\Delta c_{t+1} - (1-\theta)\left(\kappa_0 + \kappa_1 z_{t+1} - z_t + \Delta c_{t+1}\right) + \kappa_{0,m} + \kappa_{1,m} z_{m,t+1} - z_{m,t} + \Delta d_{t+1}$$

which simplifies to

$$
\begin{aligned}
&\log M_{t\to t+1}+\log R_{M,t\to t+1}\\
=&\left\{\begin{array}{c}\theta\log\delta-(1-\theta)\kappa_0-(1-\theta)\kappa_1A_0+\left(-\frac{\theta}{\psi}-(1-\theta)\right)\mu_c+(1-\theta)A_0+\kappa_{0,m}+\kappa_{1,m}A_{0,m}-A_{0,m}+\mu_d\\ +\left\{-(1-\theta)\kappa_1A_2+\kappa_{1,m}A_{2,m}\right\}\left\{\overline{\sigma}^2(1-\nu)\right\}\end{array}\right\}\\
&+\left\{\begin{array}{c}-\frac{\theta}{\psi}-(1-\theta)+(1-\theta)A_1+\phi-A_{1,m}+(\kappa_{1,m}A_{1,m}-(1-\theta)\kappa_1A_1)\rho\end{array}\right\}x_t\\
&+\left\{\left(-\frac{\theta}{\psi}-(1-\theta)\right)\phi_c\sigma_t+\phi_{d,c}\sigma_t\right\}\eta_{c,t+1}+\left\{\begin{array}{c}(-(1-\theta)\kappa_1A_2+\kappa_{1,m}A_{2,m})\nu+(1-\theta)A_2-A_{2,m}\end{array}\right\}\sigma_t^2\\
&+\left\{\kappa_{1,m}A_{1,m}-(1-\theta)\kappa_1A_1\right\}\phi_x\sigma_t\eta_{x,t+1}+\left\{-(1-\theta)\kappa_1A_2+\kappa_{1,m}A_{2,m}\right\}\phi_\sigma\omega_{t+1}+\phi_d\sigma_t\eta_{d,t+1}.
\end{aligned}
$$

Thus the quantity below

$$
\begin{aligned}
&\left\{\begin{array}{c}\theta\log\delta-(1-\theta)\kappa_0-(1-\theta)\kappa_1A_0+\left(-\frac{\theta}{\psi}-(1-\theta)\right)\mu_c+(1-\theta)A_0+\kappa_{0,m}+\kappa_{1,m}A_{0,m}-A_{0,m}+\mu_d\\ +\left\{-(1-\theta)\kappa_1A_2+\kappa_{1,m}A_{2,m}\right\}\left\{\overline{\sigma}^2(1-\nu)\right\}+\frac{1}{2}\left(-(1-\theta)\kappa_1A_2+\kappa_{1,m}A_{2,m}\right)^2\phi_\sigma^2\end{array}\right\}\\
&+\left\{\begin{array}{c}-\frac{\theta}{\psi}-(1-\theta)+(1-\theta)A_1-A_{1,m}+\left\{-(1-\theta)\kappa_1A_1+\kappa_{1,m}A_{1,m}\right\}\rho+\phi\end{array}\right\}x_t\\
&+\left\{\begin{array}{c}\frac{1}{2}\left(-\frac{\theta}{\psi}\phi_c+\phi_{d,c}-(1-\theta)\phi_c\right)^2+\frac{1}{2}\left(\kappa_{1,m}A_{1,m}-(1-\theta)\kappa_1A_1\right)^2\phi_x^2\\ +(1-\theta)A_2-A_{2,m}+(\kappa_{1,m}A_{2,m}-(1-\theta)\kappa_1A_2)\nu+\frac{1}{2}\phi_d^2\end{array}\right\}\sigma_t^2.
\end{aligned}
$$

is equal to zero. This implies that

$$
\begin{aligned}
A_{0,m} &= \frac{1}{(1-\kappa_{1,m})}\left\{\begin{array}{c}\mu_d+\theta\log\delta-(1-\theta)\kappa_0+\kappa_{0,m}+(1-\theta)A_0(1-\kappa_1)+\left(-\frac{\theta}{\psi}-(1-\theta)\right)\mu_c\\ +\left\{-(1-\theta)\kappa_1A_2+\kappa_{1,m}A_{2,m}\right\}\overline{\sigma}^2(1-\nu)+\frac{1}{2}\left(-(1-\theta)\kappa_1A_2+\kappa_{1,m}A_{2,m}\right)^2\phi_\sigma^2\end{array}\right\}\\
A_{1,m} &= \frac{\phi-\frac{1}{\psi}}{1-\kappa_{1,m}\rho}\\
A_{2,m} &= \frac{1}{(1-\kappa_{1,m}\nu)}\left\{\begin{array}{c}\frac{1}{2}\left(\phi_{d,c}-\frac{\theta}{\psi}\phi_c-(1-\theta)\phi_c\right)^2+\frac{1}{2}\left(\kappa_{1,m}A_{1,m}-(1-\theta)\kappa_1A_1\right)^2\phi_x^2+(1-\theta)A_2(1-\kappa_1\nu)+\frac{1}{2}\phi_d^2\end{array}\right\}.
\end{aligned}
$$

Now, observe that:

$$
\begin{aligned}
\log R_{M,t\to t+1} &= \kappa_{0,m}+\kappa_{1,m}z_{m,t+1}-z_{m,t}+\Delta d_{t+1}\\
&= \mathbb{A}_0^{\text{er}}+\mathbb{A}_1^{\text{er}}x_t+\mathbb{A}_2^{\text{er}}\sigma_t^2+\kappa_{1,m}A_{1,m}\phi_x\sigma_t\eta_{x,t+1}+\kappa_{1,m}A_{2,m}\phi_\sigma\omega_{t+1}+\phi_d\sigma_t\eta_{d,t+1}+\phi_{d,c}\sigma_t\eta_{c,t+1}
\end{aligned}
$$

with

$$
\begin{aligned}
\mathbb{A}_0^{\text{er}} &= \kappa_{0,m}+(\kappa_{1,m}-1)A_{0,m}+\mu_d+\kappa_{1,m}A_{2,m}\overline{\sigma}^2(1-\nu),\\
\mathbb{A}_1^{\text{er}} &= (\kappa_{1,m}\rho-1)A_{1,m}+\phi,\\
\mathbb{A}_2^{\text{er}} &= (\kappa_{1,m}\nu-1)A_{2,m}.
\end{aligned}
$$

Therefore,

$$
\mathbb{E}_t\left[\log R_{M,t\to t+1}\right]=\mathbb{A}_0^{\text{er}}+\mathbb{A}_1^{\text{er}}x_t+\mathbb{A}_2^{\text{er}}\sigma_t^2
$$

and

$$
\mathbb{VAR}_t\left[\log R_{M,t\to t+1}\right]=\mathbb{A}_0^{\text{vr}}+\mathbb{A}_1^{\text{vr}}\sigma_t^2
$$

with

$$
\begin{aligned}
\mathbb{A}_0^{\text{vr}} &= \kappa_{1,m}^2A_{2,m}^2\phi_\sigma^2\\
\mathbb{A}_1^{\text{vr}} &= \kappa_{1,m}^2A_{1,m}^2\phi_x^2+\phi_d^2+\phi_{d,c}^2.
\end{aligned}
$$

Thus,

$$\mathbb{E}_t\left[R^n_{M,t\to t+1}\right]=\exp\left(n\left(\mathbb{A}_0^{\text{er}}+\mathbb{A}_1^{\text{er}}x_t+\mathbb{A}_2^{\text{er}}\sigma_t^2\right)+\frac{n^2}{2}\left(\mathbb{A}_0^{\text{vr}}+\mathbb{A}_1^{\text{vr}}\sigma_t^2\right)\right)$$

Now, let us find the risk free rate.

$$\begin{aligned}
\log M_{t\to t+1} &= \theta\log\delta-\frac{\theta}{\psi}\Delta c_{t+1}-(1-\theta)\log R_{a,t\to t+1}\\
&= \theta\log\delta+\left\{-\frac{\theta}{\psi}-(1-\theta)\right\}\mu_c-(1-\theta)\kappa_0-(1-\theta)\kappa_1A_0-(1-\theta)\kappa_1A_2\overline{\sigma}^2(1-\nu)+(1-\theta)A_0\\
&\quad+\left\{-\frac{\theta}{\psi}-(1-\theta)-(1-\theta)\kappa_1A_1\rho+(1-\theta)A_1\right\}x_t+(1-\kappa_1\nu)(1-\theta)A_2\sigma_t^2\\
&\quad+\left\{-\frac{\theta}{\psi}-(1-\theta)\right\}\phi_c\sigma_t\eta_{c,t+1}-(1-\theta)\kappa_1A_1\phi_x\sigma_t\eta_{x,t+1}-(1-\theta)\kappa_1A_2\phi_\sigma\omega_{t+1}.
\end{aligned}$$

Thus

$$\begin{aligned}
-\log R_{f,t\to t+1} &= \theta\log\delta+\left\{-\frac{\theta}{\psi}-(1-\theta)\right\}\mu_c-(1-\theta)\kappa_0-(1-\theta)\kappa_1A_0-(1-\theta)\kappa_1A_2\overline{\sigma}^2(1-\nu)+(1-\theta)A_0\\
&\quad+\left\{-\frac{\theta}{\psi}-(1-\theta)-(1-\theta)\kappa_1A_1\rho+(1-\theta)A_1\right\}x_t+\frac{1}{2}(1-\theta)^2\kappa_1^2A_2^2\phi_\sigma^2\\
&\quad+\left\{\ (1-\kappa_1\nu)(1-\theta)A_2\sigma_t^2+\tfrac{1}{2}\left(-\tfrac{\theta}{\psi}-(1-\theta)\right)^2\phi_c^2\sigma_t^2+\tfrac{1}{2}(1-\theta)^2\kappa_1^2A_1^2\phi_x^2\sigma_t^2\ \right\}.
\end{aligned}$$

This simplifies to

$$\log R_{f,t\to t+1}=\mathbb{A}_0^{\text{rf}}+\mathbb{A}_1^{\text{rf}}x_t+\mathbb{A}_2^{\text{rf}}\sigma_t^2$$

with

$$\begin{aligned}
\mathbb{A}_0^{\text{rf}} &= -\left\{\begin{array}{c}\theta\log\delta+\left\{-\frac{\theta}{\psi}-(1-\theta)\right\}\mu_c-(1-\theta)\kappa_0-(1-\theta)\kappa_1A_0\\-(1-\theta)\kappa_1A_2\overline{\sigma}^2(1-\nu)+(1-\theta)A_0+\frac{1}{2}(1-\theta)^2\kappa_1^2A_2^2\phi_\sigma^2\end{array}\right\},\\
\mathbb{A}_1^{\text{rf}} &= -\left\{-\frac{\theta}{\psi}-(1-\theta)-(1-\theta)\kappa_1A_1\rho+(1-\theta)A_1\right\},\\
\mathbb{A}_2^{\text{rf}} &= -\left\{(1-\kappa_1\nu)(1-\theta)A_2+\frac{1}{2}\left(-\frac{\theta}{\psi}-(1-\theta)\right)^2\phi_c^2+\frac{1}{2}(1-\theta)^2\kappa_1^2A_1^2\phi_x^2\right\}.
\end{aligned}$$

■

We now provide a proof of Result IA.1.

Proof. Proof of Result IA.1. From Equation IA.57, it follows that

$$\log\left(\mathbb{E}_t^*\left(R^2_{M,t\to t+1}\right)\right)=2\log R_{f,t\to t+1}+\mathbb{VAR}_t\log R_{M,t\to t+1}$$

which simplifies to

$$\log\left(\mathbb{E}_t^*\left(R^2_{M,t\to t+1}\right)\right)=\left(2\mathbb{A}_0^{\text{rf}}+\mathbb{A}_0^{\text{vr}}\right)+2\mathbb{A}_1^{\text{rf}}x_t+\left(2\mathbb{A}_2^{\text{rf}}+\mathbb{A}_1^{\text{vr}}\right)\sigma_t^2$$

since

$$\log R_{f,t\to t+1}=\mathbb{A}_0^{\text{rf}}+\mathbb{A}_1^{\text{rf}}x_t+\mathbb{A}_2^{\text{rf}}\sigma_t^2$$

and

$$\mathbb{VAR}_t\left[\log R_{M,t\to t+1}\right]=\mathbb{A}_0^{\text{vr}}+\mathbb{A}_1^{\text{vr}}\sigma_t^2.$$

Thus,

$$\mathbb{VAR}_t^*\left[R_{M,t\to t+1}\right]=\exp\left(\mathbb{A}_0^{sq}+\mathbb{A}_1^{sq}x_t+\mathbb{A}_2^{sq}\sigma_t^2\right)-\exp\left(2\mathbb{A}_0^{\text{rf}}+2\mathbb{A}_1^{\text{rf}}x_t+2\mathbb{A}_2^{\text{rf}}\sigma_t^2\right).\tag{IA.74}$$

with

$$\mathbb{A}_0^{sq}=2\mathbb{A}_0^{\text{rf}}+\mathbb{A}_0^{\text{vr}},\ \mathbb{A}_1^{sq}=2\mathbb{A}_1^{\text{rf}}.\ \mathbb{A}_2^{sq}=2\mathbb{A}_2^{\text{rf}}+\mathbb{A}_1^{\text{vr}}.$$

Next, from Equation IA.66, the price-dividend ratio is of the form

$$\log \frac{P_t}{D_t} = A_{0,m} + A_{1,m} x_t + A_{2,m} \sigma_t^2. \tag{IA.75}$$

Combining Equations IA.74 and IA.75 ends the proof.

■

Next, denote

$$\begin{aligned}
\mathbb{A}_{0,n} &= \left\{ \begin{array}{c} \log R_{f,t\to t+1} + \theta \log \delta - \gamma \mu_c - (1-\theta)\kappa_0 + n\kappa_{0,m} + n\mu_d + (\kappa_{1,m}-1) n A_{0,m} \\ + (1-\kappa_1)(1-\theta) A_0 + (n\kappa_{1,m} A_{2,m} - (1-\theta)\kappa_1 A_2)\overline{\sigma}^2 (1-\nu) \end{array} \right\} \\
\mathbb{A}_{1,n} &= \{-\gamma + n\phi + (1-\theta) A_1 (1-\kappa_1 \rho) + (\kappa_{1,m}\rho - 1) n A_{1,m}\} \\
\mathbb{A}_{2,n} &= \{(1-\kappa_1 \nu)(1-\theta) A_2 + n(\kappa_{1,m}\nu - 1) A_{2,m}\} \\
\mathbb{A}_{3,n} &= (n\kappa_{1,m} A_{1,m} \phi_x - (1-\theta)\kappa_1 A_1 \phi_x) \\
\mathbb{A}_{4,n} &= (n\phi_{d,c} - \gamma \phi_c) \\
\mathbb{A}_{5,n} &= (n\kappa_{1,m} A_{2,m} \phi_\sigma - (1-\theta)\kappa_1 A_2 \phi_\sigma) \\
\mathbb{A}_{6,n} &= n\phi_d
\end{aligned}$$

and

$$\begin{aligned}
\mathbb{A}_0^{\text{er}} &= \kappa_{0,m} + (\kappa_{1,m}-1) A_{0,m} + \mu_d + \kappa_{1,m} A_{2,m} \overline{\sigma}^2 (1-\nu), \\
\mathbb{A}_1^{\text{er}} &= (\kappa_{1,m}\rho - 1) A_{1,m} + \phi, \\
\mathbb{A}_2^{\text{er}} &= (\kappa_{1,m}\nu - 1) A_{2,m}, \\
\mathbb{A}_0^{\text{vr}} &= \kappa_1^2 A_{2,m}^2 \phi_\sigma^2, \\
\mathbb{A}_1^{\text{vr}} &= \kappa_1^2 A_{1,m}^2 \phi_x^2 + \phi_d^2 + \phi_{d,c}^2.
\end{aligned}$$

We now provide a proof for Result IA.2.

Proof. Proof of Result IA.2. Observe that

$$\mathbb{E}_t \left[R_{M,t\to t+1}^n \right] = \exp\left(n\mathbb{E}_t \left[\log R_{M,t\to t+1} \right] + \frac{n^2}{2} \mathbb{VAR}_t \left[\log R_{M,t\to t+1} \right] \right)$$

with

$$\mathbb{E}_t \left[\log R_{M,t\to t+1} \right] = \mathbb{A}_0^{\text{er}} + \mathbb{A}_1^{\text{er}} x_t + \mathbb{A}_2^{\text{er}} \sigma_t^2 \text{ and } \mathbb{VAR}_t \left[\log R_{M,t\to t+1} \right] = \mathbb{A}_0^{\text{vr}} + \mathbb{A}_1^{\text{vr}} \sigma_t^2. \tag{IA.76}$$

Now we will provide the formula for

$$\begin{aligned}
\mathbb{E}_t \left[R_{M,t\to t+1}^n \mathbb{I}_{\{R_{M,t\to t+1} > a\}} \right] &= \mathbb{E}_t \left[\exp\left(n \log R_{M,t\to t+1} \right) \mathbb{I}_{\log R_{M,t\to t+1} > \log a} \right] \\
&= \mathbb{E}_t \left[\exp\left(n \log R_{M,t\to t+1} \right) | \log R_{M,t\to t+1} > \log a \right] \mathbb{P}_t \left[\log R_{M,t\to t+1} > \log a \right]
\end{aligned}$$

We then exploit Lemma IA.1 and show

$$\begin{aligned}
\mathbb{E}_t \left[\exp\left(n \log R_{M,t\to t+1} \right) | \log R_{M,t\to t+1} > \log a \right] &= \mathbb{E}_t \left[\exp\left(n \log R_{M,t\to t+1} \right) | n \log R_{M,t\to t+1} > n \log a \right] \\
&= \frac{\exp\left[n\mathbb{E}_t \left[\log R_{M,t\to t+1} \right] + \frac{n^2}{2} \mathbb{VAR}_t \left[\log R_{M,t\to t+1} \right] \right] \mathcal{N}\left[\overline{d}_{1,n} \right]}{\mathcal{N}\left[\overline{d}_{2,n} \right]}
\end{aligned}$$

where $\mathcal{N}\left[\overline{d}_{2,n} \right] = \mathbb{P}_t \left[n \log R_{M,t\to t+1} > n \log a \right]$ and

$$\begin{aligned}
\overline{d}_{1,n} &= \frac{n^2 \mathbb{VAR}_t \left[\log R_{M,t\to t+1} \right] + n\mathbb{E}_t \left[\log R_{M,t\to t+1} \right] - n \log a}{n\sqrt{\mathbb{VAR}_t \left[\log R_{M,t\to t+1} \right]}} \\
\overline{d}_{2,n} &= \overline{d}_{1,n} - n\sqrt{\mathbb{VAR}_t \left[\log R_{M,t\to t+1} \right]}
\end{aligned}$$

and $\mathcal{N}$ represents the CDF function for the standard normal distribution. Thus,

$$\mathbb{E}_t\left[R^n_{M,t\to t+1}\mathbb{I}_{\{R_{M,t\to t+1}>a\}}\right]=\left\{\frac{\exp\left[n\left(\mathbb{A}^{\text{er}}_0+\mathbb{A}^{\text{er}}_1x_t+\mathbb{A}^{\text{er}}_2\sigma^2_t\right)+\frac{n^2}{2}\left(\mathbb{A}^{\text{vr}}_0+\mathbb{A}^{\text{vr}}_1\sigma^2_t\right)\right]N\left[\overline{d}_{1,n}\right]}{\mathcal{N}\left[\overline{d}_{2,n}\right]}\right\}\mathcal{N}\left[\overline{d}_{2,n}\right]$$

where

$$\begin{aligned}\overline{d}_{1,n}&=\frac{n^2\left(\mathbb{A}^{\text{vr}}_0+\mathbb{A}^{\text{vr}}_1\sigma^2_t\right)+n\left(\mathbb{A}^{\text{er}}_0+\mathbb{A}^{\text{er}}_1x_t+\mathbb{A}^{\text{er}}_2\sigma^2_t\right)-n\log a}{n\sqrt{\mathbb{A}^{\text{vr}}_0+\mathbb{A}^{\text{vr}}_1\sigma^2_t}}\\ \overline{d}_{2,n}&=\overline{d}_{1,n}-n\sqrt{\mathbb{A}^{\text{vr}}_0+\mathbb{A}^{\text{vr}}_1\sigma^2_t}.\end{aligned}$$

■

We now provide a proof of Result IA.3.

Proof. Proof of Result IA.3. Observe that

$$\mathbb{E}^*_t\left[R^n_{M,t\to t+1}\right]=\mathbb{E}_t\left[\frac{M_{t\to t+1}}{\mathbb{E}_t\left[M_{t\to t+1}\right]}R^n_{M,t\to t+1}\right].$$

We then show:

$$\begin{aligned}\log\left(\frac{M_{t\to t+1}}{\mathbb{E}_t\left[M_{t\to t+1}\right]}R^n_{M,t\to t+1}\right)&=\log R_{f,t\to t+1}+\theta\log\delta+\left\{-\frac{\theta}{\psi}-(1-\theta)\right\}\Delta c_{t+1}-(1-\theta)\kappa_0\\&\quad-(1-\theta)\kappa_1z_{t+1}+(1-\theta)z_t+n\kappa_{0,m}+n\kappa_{1,m}z_{m,t+1}-nz_{m,t}+n\Delta d_{t+1}\end{aligned}$$

and

$$\log\left(\frac{M_{t\to t+1}}{\mathbb{E}_t\left[M_{t\to t+1}\right]}R^n_{M,t\to t+1}\right)=\mathbb{A}_{0,n}+\mathbb{A}_{1,n}x_t+\mathbb{A}_{2,n}\sigma^2_t+\mathbb{A}_{3,n}\sigma_t\eta_{x,t+1}+\mathbb{A}_{4,n}\sigma_t\eta_{c,t+1}+\mathbb{A}_{5,n}\omega_{t+1}+\mathbb{A}_{6,n}\sigma_t\eta_{d,t+1}$$

with

$$\begin{aligned}\mathbb{A}_{0,n}&=\left\{\begin{array}{l}\log R_{f,t\to t+1}+\theta\log\delta-\gamma\mu_c-(1-\theta)\kappa_0+n\kappa_{0,m}+n\mu_d+n\kappa_{1,m}A_{0,m}-nA_{0,m}\\-(1-\theta)\kappa_1A_0+(1-\theta)A_0-(1-\theta)\kappa_1A_2\overline{\sigma}^2(1-\nu)+n\kappa_{1,m}A_{2,m}\overline{\sigma}^2(1-\nu)\end{array}\right\}\\\mathbb{A}_{1,n}&=\left\{-\gamma+n\phi-nA_{1,m}+(1-\theta)A_1-(1-\theta)\kappa_1A_1\rho+n\kappa_{1,m}A_{1,m}\rho\right\}\\\mathbb{A}_{2,n}&=\left\{-(1-\theta)\kappa_1A_2\nu+(1-\theta)A_2-nA_{2,m}+n\kappa_{1,m}A_{2,m}\nu\right\}\\\mathbb{A}_{3,n}&=n\kappa_{1,m}A_{1,m}\phi_x-(1-\theta)\kappa_1A_1\phi_x\\\mathbb{A}_{4,n}&=n\phi_{d,c}-\gamma\phi_c\\\mathbb{A}_{5,n}&=-(1-\theta)\kappa_1A_2\phi_\sigma+n\kappa_{1,m}A_{2,m}\phi_\sigma\\\mathbb{A}_{6,n}&=n\phi_d.\end{aligned}$$

Thus

$$\log\mathbb{E}^*_t\left[R^n_{M,t\to t+1}\right]=\log\left(\frac{M_{t\to t+1}}{\mathbb{E}_t\left[M_{t\to t+1}\right]}R^n_{M,t\to t+1}\right)=\mu^{x,\sigma}_{n,t}+\mathbb{A}^{'}_{n,t}\eta_{x,c,\omega,d}$$

where

$$\begin{aligned}\mu^{x,\sigma}_{n,t}&=\mathbb{A}_{0,n}+\mathbb{A}_{1,n}x_t+\mathbb{A}_{2,n}\sigma^2_t\\\mathbb{A}^{'}_{n,t}&=\left[\mathbb{A}_{3,n}\sigma_t,\mathbb{A}_{4,n}\sigma_t,\mathbb{A}_{5,n},\mathbb{A}_{6,n}\sigma_t\right]\\\eta^{'}_{x,c,\omega,d}&=\left[\eta_{x,t+1},\eta_{c,t+1},\omega_{t+1},\eta_{d,t+1}\right].\end{aligned}$$

Further, from Equation IA.57, we can also infer that

$$\mathbb{E}_t^*\left[R_{M,t\to t+1}^n\right]=\exp\left(n\log R_{f,t\to t+1}+\frac{n\left(n-1\right)}{2}\mathbb{VAR}_t\left[\log R_{M,t\to t+1}\right]\right).$$

Next, recall that

$$\log R_{M,t\to t+1} \quad = \quad \mathbb{A}_0^{\text{er}}+\mathbb{A}_1^{\text{er}}x_t+\mathbb{A}_2^{\text{er}}\sigma_t^2+\kappa_{1,m}A_{1,m}\phi_x\sigma_t\eta_{x,t+1}+\kappa_{1,m}A_{2,m}\phi_\sigma\omega_{t+1}+\phi_d\sigma_t\eta_{d,t+1}+\phi_{d,c}\sigma_t\eta_{c,t+1}$$

which simplifies to $n\log R_{M,t\to t+1}=\mu_{n,t}^{\text{R}}+\mathbb{A}_{n,t}^{\text{R}'}\eta_{x,c,\omega,d}$ with

$$\begin{aligned}\mu_{n,t}^{\text{R}} &= n\mathbb{A}_0^{\text{er}}+n\mathbb{A}_1^{\text{er}}x_t+n\mathbb{A}_2^{\text{er}}\sigma_t^2\\ \mathbb{A}_{n,t}^{\text{R}'} &= \left[n\kappa_{1,m}A_{1,m}\phi_x\sigma_t,n\phi_{d,c}\sigma_t,n\kappa_{1,m}A_{2,m}\phi_\sigma,n\phi_d\sigma_t\right]\end{aligned}$$

Then

$$\mathbb{E}_t^*\left[R_{M,t\to t+1}^n\right]=\exp\left(n\log R_{f,t\to t+1}+\frac{n\left(n-1\right)}{2}\mathbb{VAR}_t\left[\log R_{M,t\to t+1}\right]\right).$$

Now let us compute

$$\begin{aligned}\mathbb{E}_t^*\left[R_{M,t\to t+1}^n\mathbb{I}_{\left\{R_{M,t\to t+1}>a\right\}}\right] &= \mathbb{E}_t\left[\frac{M_{t\to t+1}}{\mathbb{E}_t\left[M_{t\to t+1}\right]}R_{M,t\to t+1}^n\mathbb{I}_{\left\{R_{M,t\to t+1}>a\right\}}\right]\\ &= \exp\left(\mu_{n,t}^{x,\sigma}\right)\mathbb{E}_t\left[\left(\exp\left(\mathbb{A}_{n,t}^{'}\eta_{x,c,\omega,d}\right)\right)\mathbb{I}_{\left\{\mu_{n,t}^{\text{R}}+\mathbb{A}_{n,t}^{\text{R}'}\eta_{x,c,\omega,d}>n\log a\right\}}\right]\\ &= \exp\left(\mu_{n,t}^{x,\sigma}\right)\mathbb{E}_t\left[\left(\exp\left(\mathbb{A}_{n,t}^{'}\eta_{x,c,\omega,d}\right)\right)\mathbb{I}_{\left\{\mathbb{A}_{n,t}^{\text{R}'}\eta_{x,c,\omega,d}>\left(n\log a\right)-\mu_{n,t}^{\text{R}}\right\}}\right].\end{aligned}$$

Now observe that

$$\begin{aligned}\mathbb{I}_{\left\{\mathbb{A}_n^{\text{R}'}\eta_{x,c,\omega,d}>\left(\log a\right)-\mu_{n,t}^{\text{R}}\right\}} &= \mathbb{I}_{\left\{\mathbb{A}_{n,t}^{'}\mathbb{A}_n^{\text{R}}\left(\mathbb{A}_n^{\text{R}'}\mathbb{A}_n^{\text{R}}\right)^{-1}\mathbb{A}_n^{\text{R}'}\eta_{x,c,\omega,d}>\mathbb{A}_{n,t}^{'}\mathbb{A}_n^{\text{R}}\left(\mathbb{A}_n^{\text{R}'}\mathbb{A}_n^{\text{R}}\right)^{-1}\left(\left(n\log a\right)-\mu_{n,t}^{\text{R}}\right)\right\}}\\ &= \mathbb{I}_{\left\{\mathbb{A}_{n,t}^{'}\eta_{x,c,\omega,d}>\log a_n^*\right\}}.\end{aligned}$$

with $\log a_n^*=\mathbb{A}_{n,t}^{'}\mathbb{A}_{n,t}^{\text{R}}\left(\mathbb{A}_{n,t}^{\text{R}'}\mathbb{A}_{n,t}^{\text{R}}\right)^{-1}\left(n\log a-\mu_{n,t}^{\text{R}}\right)$. We then exploit Lemma IA.1 to show

$$\mathbb{E}_t^*\left[R_{M,t\to t+1}^n\mathbb{I}_{\left\{R_{M,t\to t+1}>a\right\}}\right]=\exp\left(\mu_{n,t}^{x,\sigma}\right)\mathbb{E}_t\left[\exp\left(\mathbb{A}_{n,t}^{'}\eta_{x,c,\omega,d}\right)\mathbb{I}_{\left\{\exp\left(\mathbb{A}_{n,t}^{'}\eta_{x,c,\omega,d}\right)>a_n^*\right\}}\right].$$

Thus

$$\mathbb{E}_t^*\left[R_{M,t\to t+1}^n\mathbb{I}_{\left\{R_{M,t\to t+1}>a\right\}}\right]=\exp\left(\mu_{n,t}^{x,\sigma}\right)\mathcal{N}\left[\overline{d}_{1,n}^*\right]\exp\left(\frac{1}{2}\mathbb{A}_{n,t}^{'}\mathbb{A}_{n,t}\right)$$

where $\overline{d}_{1,n}^*=\frac{\mathbb{A}_{n,t}^{'}\mathbb{A}_{n,t}-\log a_n^*}{\sqrt{\mathbb{A}_{n,t}^{'}\mathbb{A}_{n,t}}}$ and $\overline{d}_{2,n}^*=\overline{d}_{1,n}^*-\sqrt{\mathbb{A}_{n,t}^{'}\mathbb{A}_{n,t}}$ and $\mathbb{E}_t^*\left[\mathbb{I}_{\left\{R_{M,t\to t+1}>a\right\}}\right]=N\left[\overline{d}_{2,n}^*\right]$. ■

IA.8.5.2 Bollerslev, Tauchen, and Zhou (2009)

Bollerslev, Tauchen, and Zhou (2009) use the Epstein and Zin (1989) SDF and approximate $R_{a,t\to t+1}$ in Equation IA.58 by the market return$R_{M,t\to t+1}$. They set up an economy governed by the following time series

$$\begin{aligned}g_{t+1} &= d_{t+1}=\mu_g+\sigma_{g,t}z_{g,t+1},\\ \sigma_{g,t+1}^2 &= a_\sigma+\rho_\sigma\sigma_{g,t}^2+\sqrt{q_t}z_{\sigma,t+1},\\ q_{t+1} &= a_q+\rho_q q_t+\phi_q\sqrt{q_t}z_{q,t+1}\end{aligned}\tag{IA.77}$$

where g_{t+1} represents consumption growth. There are two state variables in their framework, $\sigma_{g,t}^2$ and q_t.

Bollerslev, Tauchen, and Zhou (2009) build a model that combines stochastic volatility with Epstein and Zin (1989) preferences to provide a theoretical foundation for the empirical fact that

the variance risk premium can be used to forecast market returns at short horizons. Their model includes two state variables ($\sigma_{g,t}^2$ and q_t), so we use $\log(P_t/E_t)$ and $\mathbb{M}_{t\to T}^{*(2)}$ to extract implied state variables at each date using Result IA.4.

Summary statistics for the extracted state variables can be found in Table IA.18. Average state variable values are similar in magnitude to and fall within the confidence intervals implied by the calibrated model. Data-implied $\sigma_{g,t}^2$ and q_t standard deviations are higher than those implied by the models and fall outside the model-implied confidence intervals. The data-implied $\sigma_{g,t}^2$ (g_t) autocorrelation is lower (higher) than the model-implied value.

Given values for the data-implied state variables, we can compute the physical and risk-neutral moments necessary for the risk premium decomposition using model-implied moments from Results IA.5 and IA.6, which can be found below. Table IA.21 provides summary statistics for the market risk premium decomposition and Table IA.22 provides the average difference between the data-implied risk premia and those implied by the Bollerslev, Tauchen, and Zhou (2009) model. The risk premia implied by Bollerslev, Tauchen, and Zhou (2009) are quite surprising. For instance, the total risk premium is often negative. We confirm that this also happens in the simulated model in approximately 44% of the simulated values.[60] We also find that the data-implied risk premium standard deviation is quite high at about 145% (annualized), which is higher than the model-implied value of 19% and is likely caused by the relatively high data-implied state variable volatility compared to the model-implied values. Despite the high fraction of negative values, the unconditional risk premium implied by the simulated model is more reasonable at 8.67%. This is slightly lower than the average risk premium implied using extracted state variables (10.71%),[61] although the discrepancy is small relative to the risk premium volatility based on our extracted state variables. Unconditionally, the central risk premium contributes about 80% of the total risk premium, although the contribution varies significantly over time. For instance, during the 2008 Financial Crisis, the upside risk premium actually contributed up to almost 90% of the total risk premium. During the Dot-com bust, the total risk premium implied by the model actually becomes negative, and the downside risk premium actually comprised approximately 90% of this premium. That is, the model implies that during this period investors were willing to accept negative expected returns for exposure to downside risk.

Main Results Given this setup, we show the following results.

Result IA.4. *Given the state variables $\sigma_{g,t}^2$ and q_t, the Bollerslev, Tauchen, and Zhou (2009) model-implied log price-dividend ratio is given by*

$$\log \frac{P_t}{D_t} = A_0 + A_\sigma \sigma_{g,t}^2 + A_q q_t, \tag{IA.78}$$

and the risk-neutral market return variance is given by

$$\mathbb{M}_{t\to t+1}^{*(2)}[A] = \exp\left(\mathbb{B}_0^{sq} + \mathbb{B}_1^{sq}\sigma_{g,t}^2 + \mathbb{B}_2^{sq} q_t\right) - \exp\left(\mathbb{A}_0^{rf} + \mathbb{A}_1^{rf}\sigma_{g,t}^2 + \mathbb{A}_2^{rf} q_t\right). \tag{IA.79}$$

The coefficients A_0, A_σ, A_q, $\mathbb{B}_0^{sq}$, $\mathbb{B}_1^{sq}$, and $\mathbb{B}_2^{sq}$ are defined below.

[60] This finding is consistent with related issues documented by Bekaert, Engstrom, and Ermolov (2023) with respect to the Bollerslev, Tauchen, and Zhou (2009) model.

[61] This discrepancy is primarily caused by the fact that the extracted state variables are more volatile than the model-implied state variables. Since the risk premium is related to exponentials of functions that are affine in state variables, Jensen's inequality effects cause the risk premium based on our extracted state variables to be higher than that implied by the simulated model using the state variable processes from the original calibrated model.

Proof. See below. ■

Result IA.5. *The conditional non-central physical moment of the market return is*

$$\mathbb{E}_t\left[R_{M,t\to t+1}^n\right] = \exp\left(n\mathbb{E}_t\left[\log R_{M,t\to t+1}\right] + \frac{n^2}{2}\mathbb{VAR}_t\left[\log R_{M,t\to t+1}\right]\right).$$

where

$$\begin{aligned}\mathbb{E}_t\left[\log R_{M,t\to t+1}\right] &= \kappa_0 + \kappa_1 A_0 - A_0 + \kappa_1 A_\sigma a_\sigma + \kappa_1 A_q a_q + \mu_g \\ &\quad + \left(\kappa_1\rho_\sigma - 1\right) A_\sigma \sigma_{g,t}^2 + \left(\kappa_1\rho_q - 1\right) A_q q_t\end{aligned}$$

and

$$\mathbb{VAR}_t\left[\log R_{M,t\to t+1}\right] = \left(\kappa_1 A_\sigma\right)^2 q_t + \left(\kappa_1 A_q \phi_q\right)^2 q_t + \sigma_{g,t}^2.$$

Using Lemma IA.1, the conditional non-central truncated physical moment of the market return is

$$\begin{aligned}\mathbb{E}_t\left[R_{M,t\to t+1}^n \mathbb{I}_{\left\{R_{M,t\to t+1}>a\right\}}\right] &= \mathbb{E}_t\left[e^{n\log R_{M,t\to t+1}}\mathbb{I}_{\left\{n\log R_{M,t\to t+1}>n\log a\right\}}\right] \\ &= \left(\exp\left\{n\mathbb{E}_t\left[\log R_{M,t\to t+1}\right] + \frac{n^2}{2}\mathbb{VAR}_t\left[\log R_{M,t\to t+1}\right]\right\}\right)\mathcal{N}\left[\overline{d}_1\right]\end{aligned}$$

where

$$\overline{d}_1 = \frac{n\mathbb{E}_t\left[\log R_{M,t\to t+1}\right] + n^2\mathbb{VAR}_t\left[\log R_{M,t\to t+1}\right] - n\log a}{n\sqrt{\mathbb{VAR}_t\left[\log R_{M,t\to t+1}\right]}}$$

with $\overline{d}_2 = \overline{d}_1 - n\sqrt{\mathbb{VAR}_t\left[\log R_{t+1}\right]}$. *All parameters are defined below.*

Proof. See below. ■

Result IA.6. *The conditional non-central risk neutral moment of the market return is*

$$\mathbb{E}_t^*\left[R_{M,t\to t+1}^n\right] = \exp\left\{n\log R_{f,t\to t+1} + \frac{n\left(n-1\right)}{2}\mathbb{VAR}_t\left[\log R_{M,t\to t+1}\right]\right\}$$

The conditional non-central truncated risk neutral moment of the market return is

$$\mathbb{E}_t^*\left[R_{M,t\to t+1}^n \mathbb{I}_{\left\{R_{M,t\to t+1}>a\right\}}\right] = e^{A_0^{mr}}\mathcal{N}\left[\overline{d}_1\right]\exp\left\{\frac{1}{2}\lambda_t^{m'}\lambda_t^m\right\}$$

where

$$\overline{d}_1 = \frac{\lambda_t^{m'}\lambda_t^m - \lambda\left(n\log a - \mathbb{A}_{0,t}^r\right)}{\sqrt{\lambda_t^{m'}\lambda_t^m}}$$

and $\overline{d}_2 = \overline{d}_1 - \sqrt{\lambda_t^{m'}\lambda_t^m}$. *All parameters are defined below.*

Proof. See below. ■

Derivations and Proofs

We can use the Campbell and Shiller (1988) approximation to write the log gross return as

$$\log R_{a,t\to t+1} = \kappa_0 + \kappa_1 z_{t+1} - z_t + g_{t+1}.$$

In this model, there is no distinction between the aggregate and market returns, so we denote $r_{t+1} = \log R_{M,t\to t+1} = \log R_{a,t\to t+1}$. The log price-consumption ratio is given by

$$z_t = A_0 + A_\sigma\sigma_{g,t}^2 + A_q q_t.$$

The representative agent's first-order conditions imply

$$\log\left(\mathbb{E}_t\exp\left\{m_{t+1} + r_{t+1}\right\}\right) = 0.$$

Under this model, we can write

$$\begin{aligned}
m_{t+1}+r_{t+1} &= \theta\log\delta-\frac{\theta}{\psi}g_{t+1}+\theta r_{t+1}\\
&= \theta\log\delta-\frac{\theta}{\psi}\mu_g-\frac{\theta}{\psi}\sigma_{g,t}z_{g,t+1}+\theta\kappa_0+\theta\kappa_1 z_{t+1}-\theta z_t+\theta g_{t+1}\\
&= \theta\log\delta-\frac{\theta}{\psi}\mu_g-\frac{\theta}{\psi}\sigma_{g,t}z_{g,t+1}\\
&\quad +\theta\kappa_0+\theta\kappa_1A_0+\theta\kappa_1A_\sigma a_\sigma+\theta\kappa_1A_\sigma\rho_\sigma\sigma_{g,t}^2+\theta\kappa_1A_\sigma\sqrt{q_t}z_{\sigma,t+1}\\
&\quad +\theta\kappa_1A_qa_q+\theta\kappa_1A_q\rho_qq_t+\theta\kappa_1A_q\phi_q\sqrt{q_t}z_{q,t+1}\\
&\quad -\theta A_0-\theta A_\sigma\sigma_{g,t}^2-\theta A_qq_t+\theta\mu_g+\theta\sigma_{g,t}z_{g,t+1}
\end{aligned}$$

which simplifies to

$$\begin{aligned}
m_{t+1}+r_{t+1} &= \left\{\theta\log\delta-\frac{\theta}{\psi}\mu_g+\theta\kappa_0+\theta\kappa_1A_0+\theta\kappa_1A_\sigma a_\sigma+\theta\kappa_1A_qa_q+\theta\mu_g-\theta A_0\right\}\\
&\quad +\left\{\theta\sigma_{g,t}-\frac{\theta}{\psi}\sigma_{g,t}\right\}z_{g,t+1}+\left\{\theta\kappa_1A_\sigma\rho_\sigma-\theta A_\sigma\right\}\sigma_{g,t}^2+\theta\kappa_1A_\sigma\sqrt{q_t}z_{\sigma,t+1}\\
&\quad +\left\{\theta\kappa_1A_q\rho_q-\theta A_q\right\}q_t+\theta\kappa_1A_q\phi_q\sqrt{q_t}z_{q,t+1}.
\end{aligned}$$

Therefore,

$$\begin{aligned}
&\left\{\ \theta\log\delta-\tfrac{\theta}{\psi}\mu_g+\theta\kappa_0+\theta\kappa_1A_0+\theta\kappa_1A_\sigma a_\sigma+\theta\kappa_1A_qa_q+\theta\mu_g-\theta A_0\ \right\}\\
&+\left\{\theta\kappa_1A_\sigma\rho_\sigma-\theta A_\sigma+\frac{1}{2}\left\{\theta-\frac{\theta}{\psi}\right\}^2\right\}\sigma_{g,t}^2\\
&+\left\{\frac{1}{2}\left(\theta\kappa_1A_\sigma\right)^2+\left(\theta\kappa_1\rho_q-\theta\right)A_q+\frac{1}{2}\left(\theta\kappa_1\phi_q\right)^2A_q^2\right\}q_t\\
=\ & 0
\end{aligned}$$

which implies that

$$\begin{aligned}
A_0 &= \frac{\theta\log\delta-\frac{\theta}{\psi}\mu_g+\theta\kappa_0+\theta\kappa_1A_\sigma a_\sigma+\theta\kappa_1A_qa_q+\theta\mu_g}{\left(1-\kappa_1\right)\theta},\\
A_\sigma &= \frac{1}{2}\frac{\left(1-\gamma\right)^2}{\left(1-\kappa_1\rho_\sigma\right)\theta},
\end{aligned}$$

and

$$\left(\kappa_1\rho_q-1\right)A_q+\theta\left(\kappa_1A_\sigma\right)^2+\theta\left(\kappa_1\phi_q\right)^2A_q^2=0.$$

Consequently,

$$A_q=\frac{\left(1-\kappa_1\rho_q\right)\pm\sqrt{\left(1-\kappa_1\rho_q\right)^2-\theta^2\kappa_1^4A_\sigma^2\phi_q^2}}{\theta\left(\kappa_1\phi_q\right)^2}.$$

Now, let us find the risk-free rate. Notice that

$$\begin{aligned}
m_{t+1} &= \theta\log\delta-\frac{\theta}{\psi}g_{t+1}-\left(1-\theta\right)r_{t+1}\\
&= \left\{\begin{array}{c}\theta\log\delta-\frac{\theta}{\psi}\mu_g-\left(1-\theta\right)\kappa_0-\left(1-\theta\right)\mu_g-\kappa_1\left(1-\theta\right)A_0\\ -A_\sigma\kappa_1\left(1-\theta\right)a_\sigma-A_q\kappa_1\left(1-\theta\right)a_q+\left(1-\theta\right)A_0\end{array}\right\}\\
&\quad -\gamma\sigma_{g,t}z_{g,t+1}+\left\{\left(1-\theta\right)A_\sigma-A_\sigma\kappa_1\left(1-\theta\right)\rho_\sigma\right\}\sigma_{g,t}^2\\
&\quad -A_\sigma\kappa_1\left(1-\theta\right)\sqrt{q_t}z_{\sigma,t+1}\\
&\quad +\left\{\left(1-\theta\right)A_q-A_q\kappa_1\left(1-\theta\right)\rho_q\right\}q_t-A_q\kappa_1\left(1-\theta\right)\phi_q\sqrt{q_t}z_{q,t+1}.
\end{aligned}$$

Hence

$$\begin{aligned}\log R_{f,t\to t+1} &= -\left\{\begin{array}{c}\theta\log\delta-\frac{\theta}{\psi}\mu_g-(1-\theta)\kappa_0-(1-\theta)\mu_g\\+(1-\theta)A_0(1-\kappa_1)-A_\sigma\kappa_1(1-\theta)a_\sigma\\-A_q\kappa_1(1-\theta)a_q\end{array}\right\}\\&\quad-\left\{\frac{1}{2}\gamma^2+(1-\theta)A_\sigma(1-\kappa_1\rho_\sigma)\right\}\sigma_{g,t}^2\\&\quad-\left\{\begin{array}{c}\frac{1}{2}\left(A_\sigma\kappa_1(1-\theta)\right)^2+(1-\theta)A_q(1-\kappa_1\rho_q)\\+\frac{1}{2}\left(A_q\kappa_1(1-\theta)\phi_q\right)^2\end{array}\right\}q_t.\end{aligned}$$

Hence

$$\log R_{f,t\to t+1}=\mathbb{A}_0^{\text{rf}}+\mathbb{A}_1^{\text{rf}}\sigma_{g,t}^2+\mathbb{A}_2^{\text{rf}}q_t \tag{IA.80}$$

with

$$\begin{aligned}\mathbb{A}_0^{\text{rf}} &= -\left\{\begin{array}{c}\theta\log\delta-\frac{\theta}{\psi}\mu_g-(1-\theta)\kappa_0-(1-\theta)\mu_g\\+(1-\theta)A_0(1-\kappa_1)-A_\sigma\kappa_1(1-\theta)a_\sigma\\-A_q\kappa_1(1-\theta)a_q\end{array}\right\},\\\mathbb{A}_1^{\text{rf}} &= -\left\{\frac{1}{2}\gamma^2+(1-\theta)A_\sigma(1-\kappa_1\rho_\sigma)\right\},\\\mathbb{A}_2^{\text{rf}} &= -\left\{\begin{array}{c}\frac{1}{2}\left(A_\sigma\kappa_1(1-\theta)\right)^2+(1-\theta)A_q(1-\kappa_1\rho_q)\\+\frac{1}{2}\left(A_q\kappa_1(1-\theta)\phi_q\right)^2\end{array}\right\}.\end{aligned}$$

Next, note that

$$\begin{aligned}\log R_{M,t\to t+1} &= \kappa_0+\kappa_1 z_{t+1}-z_t+g_{t+1}\\&= \kappa_0+\kappa_1A_0-A_0+\kappa_1A_\sigma a_\sigma+\kappa_1A_q a_q+\mu_g\\&\quad+(\kappa_1\rho_\sigma-1)A_\sigma\sigma_{g,t}^2+\kappa_1A_\sigma\sqrt{q_t}z_{\sigma,t+1}\\&\quad+(\kappa_1\rho_q-1)A_q q_t+\kappa_1A_q\phi_q\sqrt{q_t}z_{q,t+1}\\&\quad+\sigma_{g,t}z_{g,t+1}.\end{aligned}$$

Hence

$$\begin{aligned}\mathbb{E}_t\left[\log R_{M,t\to t+1}\right] &= \kappa_0+\kappa_1A_0-A_0+\kappa_1A_\sigma a_\sigma+\kappa_1A_q a_q+\mu_g\\&\quad+(\kappa_1\rho_\sigma-1)A_\sigma\sigma_{g,t}^2+(\kappa_1\rho_q-1)A_q q_t\end{aligned}$$

and

$$\mathbb{VAR}_t\left[\log R_{M,t\to t+1}\right]=(\kappa_1A_\sigma)^2q_t+(\kappa_1A_q\phi_q)^2q_t+\sigma_{g,t}^2.$$

We now provide a proof of Result IA.4.

Proof. Proof of Result IA.4. From Equation IA.57, it follows that

$$\log\left(\mathbb{E}_t^*\left(R_{M,t\to t+1}^2\right)\right)=2\log R_{f,t\to t+1}+\mathbb{VAR}_t\log R_{M,t\to t+1}$$

Thus,

$$\log\left(\mathbb{E}_t^*\left(R_{M,t\to t+1}^2\right)\right)=2\mathbb{A}_0^{\text{rf}}+2\mathbb{A}_1^{\text{rf}}\sigma_{g,t}^2+2\mathbb{A}_2^{\text{rf}}q_t+(\kappa_1A_\sigma)^2q_t+(\kappa_1A_q\phi_q)^2q_t+\sigma_{g,t}^2.$$

Hence,

$$\log\left(\mathbb{E}_t^*\left(R_{M,t\to t+1}^2\right)\right)=2\mathbb{A}_0^{\text{rf}}+\left(2\mathbb{A}_2^{\text{rf}}+(\kappa_1A_\sigma)^2+(\kappa_1A_q\phi_q)^2\right)q_t+\left(1+2\mathbb{A}_1^{\text{rf}}\right)\sigma_{g,t}^2$$

which simplifies to

$$\log\left(\mathbb{E}_t^*\left[R_{M,t\to t+1}^2\right]\right) = \mathbb{B}_0^{sq} + \mathbb{B}_1^{sq}\sigma_{g,t}^2 + \mathbb{B}_2^{sq}q_t,$$

where

$$\begin{aligned}
\mathbb{B}_0^{sq} &= 2\mathbb{A}_0^{\text{rf}}, \\
\mathbb{B}_1^{sq} &= 1 + 2\mathbb{A}_1^{\text{rf}}, \\
\mathbb{B}_2^{sq} &= 2\mathbb{A}_2^{\text{rf}} + (\kappa_1 A_\sigma)^2 + (\kappa_1 A_q \phi_q)^2.
\end{aligned}$$

The variance of the market return under the risk neutral measure is

$$\mathbb{VAR}_t^*\left[R_{M,t\to t+1}\right] = \exp\left\{\mathbb{B}_0^{sq} + \mathbb{B}_1^{sq}\sigma_{g,t}^2 + \mathbb{B}_2^{sq}q_t\right\} - \exp\left\{2\mathbb{A}_0^{\text{rf}} + 2\mathbb{A}_1^{\text{rf}}\sigma_{g,t}^2 + 2\mathbb{A}_2^{\text{rf}}q_t\right\}. \tag{IA.81}$$

Recall that the log price consumption ratio follows

$$\log\frac{P_t}{D_t} = A_0 + A_\sigma\sigma_{g,t}^2 + A_q q_t. \tag{IA.82}$$

This ends the proof.

■

We now provide a proof of Result IA.5.

Proof. Proof of Result IA.5. Note that the log return, which is given by expression

$$\begin{aligned}
\log R_{M,t\to t+1} &= \kappa_0 + \kappa_1 A_0 - A_0 + \kappa_1 A_\sigma a_\sigma + \kappa_1 A_q a_q + \mu_g \\
&\quad + (\kappa_1\rho_\sigma - 1) A_\sigma\sigma_{g,t}^2 + \kappa_1 A_\sigma\sqrt{q_t}z_{\sigma,t+1} \\
&\quad + (\kappa_1\rho_q - 1) A_q q_t + \kappa_1 A_q\phi_q\sqrt{q_t}z_{q,t+1} \\
&\quad + \sigma_{g,t}z_{g,t+1},
\end{aligned}$$

is normally distributed. Thus,

$$\mathbb{E}_t\left[R_{M,t\to t+1}^n\right] = \exp\left(n\mathbb{E}_t\left[\log R_{M,t\to t+1}\right] + \frac{n^2}{2}\mathbb{VAR}_t\left[\log R_{M,t\to t+1}\right]\right) \tag{IA.83}$$

with

$$\begin{aligned}
\mathbb{E}_t\left[\log R_{M,t\to t+1}\right] &= \kappa_0 + \kappa_1 A_0 - A_0 + \kappa_1 A_\sigma a_\sigma + \kappa_1 A_q a_q + \mu_g \\
&\quad + (\kappa_1\rho_\sigma - 1) A_\sigma\sigma_{g,t}^2 + (\kappa_1\rho_q - 1) A_q q_t
\end{aligned}$$

and

$$\mathbb{VAR}_t\left[\log R_{M,t\to t+1}\right] = (\kappa_1 A_\sigma)^2 q_t + (\kappa_1 A_q\phi_q)^2 q_t + \sigma_{g,t}^2.$$

Using Lemma IA.1, the conditional truncated physical moment of the market return is

$$\begin{aligned}
\mathbb{E}_t\left[R_{M,t\to t+1}^n\mathbb{I}_{\{R_{M,t\to t+1}>a\}}\right] &= \mathbb{E}_t\left[e^{n\log R_{M,t\to t+1}}\mathbb{I}_{\{n\log R_{M,t\to t+1}>n\log a\}}\right] \\
&= \left(\exp\left\{\mathbb{E}_t\left[\log R_{M,t\to t+1}\right] + \frac{1}{2}\mathbb{VAR}_t\left[\log R_{M,t\to t+1}\right]\right\}\right)\mathcal{N}\left[\overline{d}_1\right]
\end{aligned}$$

where

$$\overline{d}_1 = \frac{\mathbb{E}_t\left[\log R_{M,t\to t+1}\right] + \mathbb{VAR}_t\left[\log R_{M,t\to t+1}\right] - n\log a}{\sqrt{\mathbb{VAR}_t\left[\log R_{M,t\to t+1}\right]}}$$

with $\overline{d}_2 = \overline{d}_1 - \sqrt{\mathbb{VAR}_t\left[\log R_{M,t\to t+1}\right]}$.

■

We now provide a proof of Result IA.6.

Proof. Proof of Result IA.6. Recall that

$$\log\left(\mathbb{E}_t^*\left[R_{M,t\to t+1}^n\right]\right) = n\log R_{f,t\to T} + \frac{n\left(n-1\right)}{2}\mathbb{VAR}_t\left[\log R_{M,t\to t+1}\right].$$

To derive expressions for the truncated physical and risk-neutral moments, observe that

$$\mathbb{E}_t^*\left[R_{M,t\to t+1}^n \mathbb{I}_{\left\{R_{M,t\to t+1}>a\right\}}\right] = \mathbb{E}_t\left[e^{\left(m_{t+1}+n\log R_{M,t\to t+1}\right)}\mathbb{I}_{\left\{n\log R_{M,t\to t+1}>n\log a\right\}}\right].$$

Thus,

$$\begin{aligned}
& m_{t+1} + n\log R_{M,t\to t+1} \\
= \;& \theta\log\delta - \frac{\theta}{\psi}g_{t+1} - \left(1-\theta\right)r_{t+1} + nr_{t+1} \\
= \;& \theta\log\delta - \frac{\theta}{\psi}g_{t+1} + \left(n+\theta-1\right)r_{t+1} \\
= \;& \left\{\begin{array}{c} \theta\log\delta + \left(n+\theta-1\right)\kappa_0 + \left(\left(n+\theta-1\right) - \frac{\theta}{\psi}\right)\mu_g + \left(n+\theta-1\right)\kappa_1 A_0 \\ -\left(n+\theta-1\right)A_0 + \left(n+\theta-1\right)\kappa_1 A_\sigma a_\sigma + \left(n+\theta-1\right)\kappa_1 A_q a_q \end{array}\right\} \\
& + \left\{\begin{array}{c} \left(n+\theta-1\right)\kappa_1 A_q\rho_q - \left(n+\theta-1\right)A_q \end{array}\right\} q_t + \left\{\begin{array}{c} \left(n+\theta-1\right)\kappa_1 A_\sigma\rho_\sigma - \left(n+\theta-1\right)A_\sigma\sigma_{g,t}^2 \end{array}\right\}\sigma_{g,t}^2 \\
& + \left(n+\theta-1\right)\kappa_1 A_\sigma\sqrt{q_t}z_{\sigma,t+1} + \left(\left(n+\theta-1\right) - \frac{\theta}{\psi}\right)\sigma_{g,t}z_{g,t+1} + \left(n+\theta-1\right)\kappa_1 A_q\phi_q\sqrt{q_t}z_{q,t+1}.
\end{aligned}$$

Hence

$$m_{t+1} + n\log R_{M,t\to t+1} = A_0^{mr} + \lambda_t^{m'}\mathbf{z}_t^{mr},$$

where

$$\begin{aligned}
\mathbb{A}_0^{mr} \;=\; & \left\{\begin{array}{c} \theta\log\delta + \left(n+\theta-1\right)\kappa_0 + \left(\left(n+\theta-1\right) - \frac{\theta}{\psi}\right)\mu_g + \left(n+\theta-1\right)\kappa_1 A_0 \\ -\left(n+\theta-1\right)A_0 + \left(n+\theta-1\right)\kappa_1 A_\sigma a_\sigma + \left(n+\theta-1\right)\kappa_1 A_q a_q \end{array}\right\} \\
& \left\{\begin{array}{c} \left(n+\theta-1\right)\kappa_1 A_q\rho_q - \left(n+\theta-1\right)A_q \end{array}\right\} q_t + \left\{\begin{array}{c} \left(n+\theta-1\right)\kappa_1 A_\sigma\rho_\sigma - \left(n+\theta-1\right)A_\sigma\sigma_{g,t}^2 \end{array}\right\}\sigma_{g,t}^2
\end{aligned}$$

and

$$\lambda_t^m = \left[\begin{array}{c} \left(n+\theta-1\right)\kappa_1 A_\sigma\sqrt{q_t} \\ \left(\left(n+\theta-1\right) - \frac{\theta}{\psi}\right)\sigma_{g,t} \\ \left(n+\theta-1\right)\kappa_1 A_q\phi_q\sqrt{q_t} \end{array}\right] \text{ and } \mathbf{z}_t^{mr} = \left[\begin{array}{c} z_{\sigma,t+1} \\ z_{g,t+1} \\ z_{q,t+1} \end{array}\right].$$

Next,

$$\log R_{M,t\to t+1} = \mathbb{A}_{0,t}^r + \lambda_t^{r'}\mathbf{z}_t^{mr}$$

where

$$\mathbb{A}_{0,t}^r \;=\; \kappa_0 + \kappa_1 A_0 - A_0 + \kappa_1 A_\sigma a_\sigma + \kappa_1 A_q a_q + \mu_g + \left(\kappa_1\rho_\sigma - 1\right)A_\sigma\sigma_{g,t}^2 + \left(\kappa_1\rho_q - 1\right)A_q q_t$$

and

$$\lambda_t^{r'} = \left[\begin{array}{c} \kappa_1 A_\sigma\sqrt{q_t} \\ \sigma_{g,t} \\ \kappa_1 A_q\phi_q\sqrt{q_t} \end{array}\right].$$

Finally

$$\begin{aligned}\mathbb{E}_t^*\left[R_{M,t\to t+1}^n \mathbb{I}_{\{R_{M,t\to t+1}>a\}}\right] &= \mathbb{E}_t\left[e^{A_0^{mr}+\lambda_t^{m'}\mathbf{z}_t^{mr}}\mathbb{I}_{\left\{\mathbb{A}_{0,t}^r+\lambda_t^{r'}\mathbf{z}_t^{mr}>n\log a\right\}}\right] \\ &= e^{A_0^{mr}}\mathbb{E}_t\left[e^{\lambda_t^{m'}\mathbf{z}_t^{mr}}\mathbb{I}_{\left\{\lambda_t^{m'}\mathbf{z}_t^{mr}>\lambda\left(n\log a-\mathbb{A}_{0,t}^r\right)\right\}}\right]\end{aligned}$$

where

$$\lambda_t^{m'} = \lambda\lambda_t^{r'}.$$

Hence,

$$\lambda = \left(\lambda_t^{m'}\lambda_t^r\right)\left(\lambda_t^{r'}\lambda_t^r\right)^{-1}.$$

We then exploit Lemma IA.1 to show

$$\mathbb{E}_t\left[e^{\lambda_t^{m'}\mathbf{z}_t^{mr}}\mathbb{I}_{\left\{\lambda_t^{m'}\mathbf{z}_t^{mr}>\lambda\left(n\log a-\mathbb{A}_{0,t}^r\right)\right\}}\right] = \left(\exp\left\{\frac{1}{2}\lambda_t^{m'}\lambda_t^m\right\}\right)\mathcal{N}\left[\overline{d}_1\right]$$

with

$$\overline{d}_1 = \frac{\lambda_t^{m'}\lambda_t^m - \lambda\left(n\log a - \mathbb{A}_{0,t}^r\right)}{\sqrt{\lambda_t^{m'}\lambda_t^m}}$$

and

$$\overline{d}_2 = \overline{d}_1 - \sqrt{\lambda_t^{m'}\lambda_t^m}.$$

■

IA.8.5.3 Drechsler and Yaron (2011)

The key variables that drive the economy in Drechsler and Yaron (2011) are summarized by

$$Y_{t+1} = \mu + FY_t + G_t z_{t+1} + J_{t+1}$$

where $Y_t^{'} = \left(\Delta c_t, x_t, \overline{\sigma}_t^2, \sigma_t^2, \Delta d_t\right)$, z_{t+1} is a vector of standard normal shocks, and J_{t+1} is a compound Poisson process.

Main Results

Result IA.7. *Given the vector Y_t, the Drechsler and Yaron (2011) model-implied log price-dividend ratio is*

$$\log\frac{P_t}{D_t} = A_{0,m} + A_m^{'}Y_t, \tag{IA.84}$$

and the non-central risk-neutral market return moments are

$$\mathbb{E}_t^*\left[R_{M,t\to t+1}^n\right] = R_{f,t\to t+1}\exp\left\{\begin{array}{c}\theta\log\delta - (1-\theta)\left(\kappa_0 + A_0\left(\kappa_1 - 1\right)\right) + \mathbf{f}\left(\Lambda^*\right) \\ + \left(n\kappa_{0,m} + n\kappa_{1,m}A_{0,m} - nA_{0,m}\right) \\ + \left(-\left(\theta-1\right)A - nA_m + \mathbf{g}\left(\Lambda^*\right)\right)Y_t\end{array}\right\}$$

with

$$R_{f,t\to t+1} = \exp\left\{\begin{array}{c}-\left(\theta\log\delta + \mathbf{f}\left(-\Lambda\right) - (1-\theta)\left(\kappa_0 + A_0\left(\kappa_1 - 1\right)\right)\right) \\ -\left(\left(1-\theta\right)A + \mathbf{g}\left(-\Lambda\right)\right)^{'}Y_t\end{array}\right\}$$

and

$$\Lambda = \gamma e_c + (1-\theta)\,\kappa_1 A \text{ and } \Lambda^* + \Lambda = n\kappa_{1,m}A_m + ne_d.$$

The coefficients, A_0, A, $A_{0,m}$ and A_m are given below. e_c and e_d are column vectors that select log consumption growth and log dividend growth in Y_{t+1}. $R_{f,t\to t+1}$ is the model-implied risk-free rate. Given $\mathbb{E}_t^*\left[R_{M,t\to t+1}^k\right]$, $\mathbb{M}_{t\to t+1}^{*(n)}$ can be computed using Equation 17 by setting $x = R_{M,t\to t+1}$ and $x_s = R_{f,t\to t+1}$, then taking expectations under the risk-neutral measure:

$$\mathbb{M}_{t\to t+1}^{*(n)} = \sum_{k=0}^{n} \frac{n!\,(-1)^{n-k}}{(n-k)!k!} \left(\mathbb{E}_t^*\left[R_{M,t\to t+1}\right]\right)^{n-k} \left(\mathbb{E}_t^*\left[R_{M,t\to t+1}^k\right]\right). \tag{IA.85}$$

Proof. See below. ■

Result IA.8. *The non-central physical moment of the market return is*

$$\mathbb{E}_t R_{M,t+1}^n = \exp\left\{\begin{array}{c}(n\kappa_{0,m} + n\kappa_{1,m}A_{0,m} - nA_{0,m}) + \mathbf{f}\left(n\kappa_{1,m}A_m + ne_d\right) \\ + \left\{\mathbf{g}\left(n\kappa_{1,m}A_m + ne_d\right) - nA_m\right\}' Y_t\end{array}\right\}$$

and the truncated moment is

$$\mathbb{E}_t\left[R_{M,t+1}^n 1_{R_{M,t+1}>a}\right] = \mathbb{E}_t\left\{\left(\exp\left\{\mathcal{A}_{y,t} + \left(\Lambda^* + \Lambda\right)' Y_{t+1}\right\}\right)\mathbb{I}_{\left\{\mathcal{A}_{y,t} + \left(\Lambda^*+\Lambda\right)' Y_{t+1} > n\log a\right\}}\right\}$$

with

$$\mathcal{A}_{y,t} = (n\kappa_{0,m} + n\kappa_{1,m}A_{0,m} - nA_{0,m}) - nA_m' Y_t$$

where

$$\Lambda = \gamma e_c + (1-\theta)\,\kappa_1 A \text{ and } \Lambda^* + \Lambda = n\kappa_{1,m}A_m + ne_d.$$

All parameters are defined below.

Proof. See below. ■

Result IA.9. *The non-central risk-neutral moment of the market return is*

$$\mathbb{E}_t^* R_{M,t\to t+1}^n = R_{f,t+1}\exp\left\{\begin{array}{c}\theta\log\delta - (1-\theta)\left[\kappa_0 + A_0\left(\kappa_1 - 1\right)\right] \\ + (n\kappa_{0,m} + n\kappa_{1,m}A_{0,m} - nA_{0,m}) + \mathbf{f}\left(\Lambda^*\right) \\ + \left\{-\left(\theta-1\right)A - nA_m + \mathbf{g}\left(\Lambda^*\right)\right\} Y_t\end{array}\right\}$$

and the truncated risk-neutral moment is

$$\mathbb{E}_t^*\left[R_{M,t+1}^n 1_{R_{M,t+1}>a}\right] = R_{f,t+1}\mathbb{E}_t^*\left[e^{\mathcal{A}_{y,t}^* + \Lambda^{*\prime} Y_{t+1}} 1_{\mathcal{A}_{y,t} + \left(\Lambda^*+\Lambda\right)' Y_{t+1} > n\log a}\right]$$

with

$$\mathcal{A}_{y,t} = (n\kappa_{0,m} + n\kappa_{1,m}A_{0,m} - nA_{0,m}) - nA_m' Y_t$$

and

$$\mathcal{A}_{y,t}^{*}=\left\{\begin{array}{c}\theta\log\delta-(1-\theta)\left[\kappa_{0}+A_{0}\left(\kappa_{1}-1\right)\right]\\+\left(n\kappa_{0,m}+n\kappa_{1,m}A_{0,m}-nA_{0,m}\right)\\-\left(\theta-1\right)A^{'}Y_{t}-nA_{m}^{'}Y_{t}\end{array}\right\}$$

where

$$\Lambda=\gamma e_{c}+\left(1-\theta\right)\kappa_{1}A\ \textit{and}\ \Lambda^{*}+\Lambda=n\kappa_{1,m}A_{m}+ne_{d}.$$

All parameters are defined below.

Proof. See below. ■

Derivations and Proofs The Y_t process in Drechsler and Yaron (2011) is

$$\begin{pmatrix}\Delta c_{t+1}\\x_{t+1}\\\overline{\sigma}_{t+1}^{2}\\\sigma_{t+1}^{2}\\\Delta d_{t+1}\end{pmatrix}=\mu+F\begin{pmatrix}\Delta c_{t}\\x_{t}\\\overline{\sigma}_{t}^{2}\\\sigma_{t}^{2}\\\Delta d_{t}\end{pmatrix}+G_{t}\begin{pmatrix}z_{c,t+1}\\z_{x,t+1}\\z_{\overline{\sigma},t+1}\\z_{\sigma,t+1}\\z_{d,t+1}\end{pmatrix}+\begin{pmatrix}0\\J_{x,t+1}\\0\\J_{\sigma,t+1}\\0\end{pmatrix},$$

where the $z_{i,t+1}$ shocks are normally distributed, and

$$F=\begin{pmatrix}0&1&0&0&0\\0&\rho_{x}&0&0&0\\0&0&\rho_{\overline{\sigma}}&0&0\\0&0&(1-\widetilde{\rho}_{\sigma})&\rho_{\sigma}&0\\0&\phi&0&0&0\end{pmatrix}.$$

Drechsler and Yaron (2011) define G as

$$G_{t}G_{t}^{'}=h+H_{\sigma}\sigma_{t}^{2},$$

with

$$h = \begin{pmatrix} h_c & 0 & 0 & 0 & \varphi_c\varphi_d\sqrt{1-\omega_c}\sqrt{1-\omega_d}\Omega_{cd} \\ 0 & h_x & 0 & 0 & 0 \\ 0 & 0 & h_{\overline{\sigma}} & 0 & 0 \\ 0 & 0 & 0 & h_\sigma & 0 \\ \varphi_c\varphi_d\sqrt{1-\omega_c}\sqrt{1-\omega_d}\Omega_{cd} & 0 & 0 & 0 & h_d \end{pmatrix}$$

and

$$H_\sigma = \begin{pmatrix} \overline{H}_c & 0 & 0 & 0 & \varphi_c\varphi_d\sqrt{\omega_c}\sqrt{\omega_d}\Omega_{cd} \\ 0 & \overline{H}_x & 0 & 0 & 0 \\ 0 & 0 & \overline{H}_{\overline{\sigma}} & 0 & 0 \\ 0 & 0 & 0 & \overline{H}_\sigma & 0 \\ \varphi_c\varphi_d\sqrt{\omega_c}\sqrt{\omega_d}\Omega_{cd} & 0 & 0 & 0 & \overline{H}_d \end{pmatrix}$$

with

$$h_i = \varphi_i^2\left(1-\omega_i\right)\mathbb{E}\left[\sigma_t^2\right], \overline{H}_i = \varphi_i^2\omega_i,$$

$J_{x,t}$ and $J_{\sigma,t}$ are compound Poisson processes defined as

$$J_{x,t+1} = \sum_{j=1}^{N_{t+1}^x} \xi_{j,t+1}^x \text{ where } N_{t+1}^x \sim \text{Poisson}\left(\lambda_t^x\right) \text{ and } \xi_{j,t+1}^x \sim -\Gamma\left(\nu_x, \frac{\mu_x}{\nu_x}\right) + \mu_x$$

and

$$J_{\sigma,t+1} = \sum_{j=1}^{N_{t+1}^\sigma} \xi_{j,t+1}^\sigma \text{ where } N_{t+1}^\sigma \sim \text{Poisson}\left(\lambda_t^\sigma\right) \text{ and } \xi_{j,t+1}^\sigma \sim \Gamma\left(\nu_\sigma, \frac{\mu_\sigma}{\nu_\sigma}\right)$$

where $\Gamma\left(x,y\right)$ represents a gamma distribution with shape parameter x and scale parameter y.[62] The jump intensities are

$$\lambda_t^x = l_0^x + l_{1,\sigma}^x\sigma_t^2 \text{ and } \lambda_t^\sigma = l_0^\sigma + l_{1,\sigma}^\sigma\sigma_t^2$$

where $l_0^\sigma = l_0^x = 0$. Note that in this model,

$$\rho_\sigma = \widetilde{\rho}_\sigma - l_{1,\sigma}^\sigma\mu_\sigma$$

[62] Drechsler and Yaron (2011) also explore using $\xi_{j,t+1}^x \sim N\left(0,\sigma_x^2\right)$ and $\xi_{j,t+1}^\sigma \sim N\left(0,\sigma_\sigma^2\right)$ as alternatives, which we omit here.

and:

$$\begin{aligned}\mathbb{E}x_{t+1} &= \frac{\widetilde{\mu}_x}{1-\rho_x} \\ \mathbb{E}\overline{\sigma}^2_{t+1} &= \frac{\widetilde{\mu}_{\overline{\sigma}}}{1-\rho_{\overline{\sigma}}} \\ \mathbb{E}\sigma^2_{t+1} &= \frac{\widetilde{\mu}_\sigma}{(1-\widetilde{\rho}_\sigma)} + \frac{\widetilde{\mu}_{\overline{\sigma}}}{(1-\rho_{\overline{\sigma}})}\end{aligned}$$

with

$$\widetilde{\mu}_x = 0,\ \widetilde{\mu}_{\overline{\sigma}} = 1-\rho_{\overline{\sigma}},\ \widetilde{\mu}_\sigma = 0.$$

We now provide a proof of Result IA.7.

Proof. Proof of Result IA.7.Consider a jump in the state variable x :

$$J_{x,t+1} = \sum_{j=1}^{N^x_{t+1}} \left(-\xi^{x*}_{j,t+1} + \mu_x\right) = N^x_{t+1}\mu_x - \sum_{j=1}^{N^x_{t+1}} \xi^{x*}_{j,t+1}$$

where

$$\xi^{x*}_{j,t+1} \sim \Gamma\left(\nu_x, \frac{\mu_x}{\nu_x}\right).$$

Thus

$$\begin{aligned}\mathbb{E}_t\left[\exp\left\{u_k J_{x,t+1}\right\}\right] &= \mathbb{E}_t\left\{\mathbb{E}_t\left[\exp\left\{u_k J_{x,t+1}\right\}|N^x_{t+1}\right]\right\} \\ &= \mathbb{E}_t\left\{\mathbb{E}_t\left[\exp\left\{u_k N^x_{t+1}\mu_x - u_k\sum_{j=1}^{N^x_{t+1}}\xi^{x*}_{j,t+1}\right\}|N^x_{t+1}\right]\right\} \\ &= \mathbb{E}_t\left\{\exp\left(u_k N^x_{t+1}\mu_x\right)\mathbb{E}_t\left[\exp\left\{-u_k X\right\}\right]\right\},\end{aligned}$$

where

$$X = \sum_{j=1}^{N^x_{t+1}} \xi^{x*}_{j,t+1} | N^x_{t+1} \sim \Gamma\left(N^x_{t+1}\nu_x, \frac{\mu_x}{\nu_x}\right).$$

Note

$$\mathbb{E}_t\left[\exp\left\{-u_k X\right\}\right] = \exp\left\{-N^x_{t+1}\nu_x \ln\left(1+u_k\frac{\mu_x}{\nu_x}\right)\right\}.$$

Hence

$$\begin{aligned}\mathbb{E}_t\left[\exp\left\{u_k J_{x,t+1}\right\}\right] &= \mathbb{E}_t\left\{\exp\left(u_k N^x_{t+1}\mu_x - N^x_{t+1}\nu_x\ln\left(1+u_k\frac{\mu_x}{\nu_x}\right)\right)\right\} \\ &= \mathbb{E}_t\left\{\exp\left(N^x_{t+1}\Delta_k\right)\right\}\end{aligned}$$

with

$$\Delta_k = u_k\mu_x - \nu_x\ln\left(1+u_k\frac{\mu_x}{\nu_x}\right).$$

Thus,

$$\begin{aligned}\mathbb{E}_t\left[\exp\left\{u_k J_{x,t+1}\right\}\right] &= \mathbb{E}_t\left\{\exp\left(N^x_{t+1}\Delta_k\right)\right\} \\ &= \exp\left(\lambda^x_t\left(e^{\Delta_k}-1\right)\right) \\ &= \exp\left(\lambda^x_t\left(\psi\left[u_k\right]-1\right)\right)\end{aligned}$$

with

$$\psi\left[u_k\right] = \exp\left\{u_k\mu_x - \nu_x \ln\left(1+u_k\frac{\mu_x}{\nu_x}\right)\right\}$$

Next, consider a jump in σ^2:

$$\begin{aligned}\mathbb{E}_t\left[\exp\left\{u_k J_{\sigma,t+1}\right\}\right] &= \mathbb{E}_t\left\{\mathbb{E}_t\left[\exp\left\{u_k J_{\sigma,t+1}\right\}|N^\sigma_{t+1}\right]\right\} \\ &= \mathbb{E}_t\left\{\mathbb{E}_t\left[\exp\left\{u_k\sum_{j=1}^{N^\sigma_{t+1}}\xi^\sigma_{j,t+1}\right\}|N^\sigma_{t+1}\right]\right\} \\ &= \mathbb{E}_t\left\{\mathbb{E}_t\left[\exp\left\{u_k X\right\}\right]\right\}\end{aligned}$$

where

$$X = \sum_{j=1}^{N^\sigma_{t+1}}\xi^\sigma_{j,t+1}|N^\sigma_{t+1} \sim \Gamma\left(N^\sigma_{t+1}\nu_\sigma, \frac{\mu_\sigma}{\nu_\sigma}\right)$$

Note

$$\mathbb{E}_t\left[\exp\left\{u_k X\right\}\right] = \exp\left\{-N^\sigma_{t+1}\nu_\sigma \ln\left(1-u_k\frac{\mu_\sigma}{\nu_\sigma}\right)\right\}.$$

Hence

$$\mathbb{E}_t\left[\exp\left\{u_k J_{\sigma,t+1}\right\}\right] = \mathbb{E}_t\left\{\exp\left(N^\sigma_{t+1}\Delta_k\right)\right\}$$

with

$$\Delta_k = -\nu_\sigma \ln\left(1-u_k\frac{\mu_\sigma}{\nu_\sigma}\right).$$

Thus,

$$\mathbb{E}_t\left[\exp\left\{u_k J_{\sigma,t+1}\right\}\right] = \exp\left(\lambda^\sigma_t\left(\psi\left[u_k\right]-1\right)\right)$$

with

$$\psi\left[u_k\right] = \exp\left\{-\nu_\sigma \ln\left(1-u_k\frac{\mu_\sigma}{\nu_\sigma}\right)\right\}.$$

In this model, the log-SDF is

$$m_{t+1} = \theta\log\delta - \frac{\theta}{\psi}\Delta c_{t+1} + (\theta-1)\, r_{c,t+1},$$

where

$$r_{c,t+1} = \kappa_0 + \kappa_1\upsilon_{t+1} - \upsilon_t + \Delta c_{t+1}$$

with

$$\upsilon_t = A_0 + A^{'}Y_t,$$

where $A^{'} = (A_c, A_x, A_{\overline{\sigma}}, A_\sigma, A_d)$ and the market return is

$$r_{m,t+1} = \kappa_{0,m} + \kappa_{1,m}\upsilon_{m,t+1} - \upsilon_{m,t} + \Delta d_{t+1}$$

with

$$\upsilon_{m,t} = A_{0,m} + A_m^{'} Y_t$$

where $A_m = (A_{c,m}, A_{x,m}, A_{\overline{\sigma},m}, A_{\sigma,m}, A_{d,m})$.

Finding A_0, A, κ_0, and κ_1: In this model, we have

$$\begin{aligned} m_{t+1} + r_{c,t+1} &= \theta \log \delta - \frac{\theta}{\psi} \Delta c_{t+1} + \theta r_{c,t+1} \\ &= \theta \log \delta - \frac{\theta}{\psi} \Delta c_{t+1} + \theta \left(\kappa_0 + \kappa_1 \upsilon_{t+1} - \upsilon_t + \Delta c_{t+1} \right). \end{aligned}$$

Denote e_c the vector that selects consumption in Y_{t+1}, we have $\Delta c_{t+1} = e_c^{'} Y_{t+1}$. Thus,

$$\begin{aligned} m_{t+1} + r_{c,t+1} &= \theta \log \delta + \theta \kappa_0 + (\kappa_1 - 1) \theta A_0 - \theta A^{'} Y_t \\ &\quad + \left(\left(\theta - \frac{\theta}{\psi} \right) e_c^{'} + \theta \kappa_1 A^{'} \right) Y_{t+1} \end{aligned}$$

Denote

$$u^{'} = \left(\theta - \frac{\theta}{\psi} \right) e_c^{'} + \theta \kappa_1 A^{'}.$$

Then

$$\mathbb{E}_t e^{(m_{t+1} + r_{c,t+1})} = \left\{ \exp \left(\theta \log \delta + \theta \kappa_0 + (\kappa_1 - 1) \theta A_0 - \theta A^{'} Y_t \right) \right\} \times \left\{ \mathbb{E}_t \exp \left(u^{'} Y_{t+1} \right) \right\}$$

From Equation A.1.2 in Drechsler and Yaron (2011), we have

$$\mathbb{E}_t \left\{ \exp \left(u^{'} Y_{t+1} \right) | Y_t \right\} = \exp \left(\mathbf{f}(u) + \mathbf{g}(u)^{'} Y_t \right)$$

with

$$\begin{aligned} \mathbf{f}(u) &= \mu^{'} u + \frac{1}{2} u^{'} h u + l_0^{'} \left(\psi(u) - 1 \right), \\ \mathbf{g}(u) &= F^{'} u + \frac{1}{2} \left[u^{'} H_i u \right]_{i \in \{1, \ldots, n\}} + l_1^{'} \left(\psi(u) - 1 \right), \end{aligned}$$

where $\left[u^{'} H_i u \right]_{i \in \{1, \ldots, n\}}$ is the $n \times 1$ vector with i component equal to $u^{'} H_i u$. Thus,

$$\mathbb{E}_t e^{(m_{t+1} + r_{c,t+1})} = \exp \left(\begin{array}{c} \theta \log \delta + \theta \kappa_0 + (\kappa_1 - 1) \theta A_0 + \mathbf{f}(u) \\ + \left(\mathbf{g}(u)^{'} - \theta A^{'} \right) Y_t \end{array} \right).$$

The representative agent's first-order conditions imply

$$\log \mathbb{E}_t e^{(m_{t+1} + r_{c,t+1})} = 0$$

which implies

$$\theta \log \delta + \theta \kappa_0 + (\kappa_1 - 1) \theta A_0 + \mathbf{f}(u) + \left(\mathbf{g}(u)^{'} - \theta A^{'} \right) Y_t = 0$$

This implies that

$$\begin{cases} \mathbf{g}(u)' - \theta A' = 0 \\ \theta \log \delta + \theta \kappa_0 + (\kappa_1 - 1)\theta A_0 + \mathbf{f}(u) = 0 \end{cases}$$

This system of equations is a function of κ_0 and κ_1. These two coefficients are solved using

$$\begin{aligned} \kappa_0 &= -\kappa_1 \log \kappa_1 - (1-\kappa_1)\log(1-\kappa_1) \\ \kappa_0 + (\kappa_1 - 1) A_0 &= -\log \kappa_1 + (1-\kappa_1) A' \mathbb{E}[Y_t] \end{aligned}$$

Together A_0, A, κ_0, κ_1 can be solved by using the system of equations

$$\begin{cases} \mathbf{g}(u)' - \theta A' = 0, \\ \theta \log \delta + \theta \kappa_0 + (\kappa_1 - 1)\theta A_0 + \mathbf{f}(u) = 0, \\ -\kappa_0 - \kappa_1 \log \kappa_1 - (1-\kappa_1)\log(1-\kappa_1) = 0, \\ \kappa_0 + (\kappa_1 - 1) A_0 + \log \kappa_1 - (1-\kappa_1) A' \mathbb{E}[Y_t] = 0. \end{cases}$$

Finding $A_{0,m}$, A_m, $\kappa_{0,m}$, and $\kappa_{1,m}$: Recall that

$$\begin{aligned} m_{t+1} + r_{m,t+1} &= \theta \log \delta - \frac{\theta}{\psi} \Delta c_{t+1} + (\theta - 1) r_{c,t+1} \\ &\quad + \kappa_{0,m} + \kappa_{1,m} \upsilon_{m,t+1} - \upsilon_{m,t} + \Delta d_{t+1}. \end{aligned}$$

Note that

$$\begin{aligned} m_{t+1} + r_{m,t+1} &= \theta \log \delta - \frac{\theta}{\psi} \Delta c_{t+1} + (\theta - 1) r_{c,t+1} + r_{m,t+1} \\ &= \mathbb{B}_0 + \mathbb{B}_2' Y_{t+1} + \mathbb{B}_1' Y_t \end{aligned}$$

where

$$\begin{aligned} \mathbb{B}_0 &= \theta \log \delta + (\kappa_1 - 1)(\theta - 1) A_0 + (\theta - 1)\kappa_0 + \kappa_{0,m} + (\kappa_{1,m} - 1) A_{0,m}, \\ \mathbb{B}_1 &= (1-\theta) A - A_m, \\ \mathbb{B}_2 &= -\Lambda + e_d + \kappa_{1,m} A_m, \end{aligned}$$

and

$$\Lambda = \gamma e_c + (1-\theta)\kappa_1 A.$$

Thus, $\log \mathbb{E}_t e^{(m_{t+1} + r_{m,t+1})} = 0$ implies

$$\mathbb{B}_0 + \mathbb{B}_1' Y_t + \mathbf{f}(\mathbb{B}_2) + \mathbf{g}(\mathbb{B}_2)' Y_t = 0,$$

which implies that

$$\begin{cases} \mathbb{B}_0 + \mathbf{f}(\mathbb{B}_2) = 0, \\ \\ \mathbb{B}_1 + \mathbf{g}(\mathbb{B}_2) = 0. \end{cases}$$

These two equations depend on $\kappa_{0,m}$ and $\kappa_{1,m}$, which can be obtained from the two equations below

$$-\kappa_{0,m} - \kappa_{1,m}\log\kappa_{1,m} - (1-\kappa_{1,m})\log(1-\kappa_{1,m}) = 0,$$

$$\kappa_{0,m} + (\kappa_{1,m}-1)A_{0,m} + \log\kappa_{1,m} - (1-\kappa_{1,m})A_m^{'}\mathbb{E}[Y_t] = 0.$$

Finally $A_{0,m}$, A_m, $\kappa_{0,m}$, $\kappa_{1,m}$ can be obtained by simultaneously solving the four equations below:

$$\begin{cases} \left\{ \begin{array}{c} \theta\log\delta + (\kappa_1 - 1)(\theta-1)A_0 + (\theta-1)\kappa_0 + \kappa_{0,m} \\ \\ + (\kappa_{1,m}-1)A_{0,m} + \mathbf{f}(-\Lambda + e_d + \kappa_{1,m}A_m) \end{array} \right\} = 0, \\ (1-\theta)A - A_m + \mathbf{g}(-\Lambda + e_d + \kappa_{1,m}A_m) = 0, \\ -\kappa_{0,m} - \kappa_{1,m}\log\kappa_{1,m} - (1-\kappa_{1,m})\log(1-\kappa_{1,m}) = 0, \\ \kappa_{0,m} + (\kappa_{1,m}-1)A_{0,m} + \log\kappa_{1,m} - (1-\kappa_{1,m})A_m^{'}\mathbb{E}[Y_t] = 0. \end{cases}$$

Now let us find the risk-free rate

$$\log R_{f,t\to t+1} = -\log\left(\mathbb{E}_t e^{m_{t+1}}\right).$$

Note that

$$\begin{aligned} m_{t+1} &= \theta\log\delta - \frac{\theta}{\psi}e_c^{'}Y_{t+1} + (\theta-1)\left(\kappa_0 + \kappa_1\upsilon_{t+1} - \upsilon_t + e_c^{'}Y_{t+1}\right) \\ &= \theta\log\delta - \frac{\theta}{\psi}e_c^{'}Y_{t+1} + (\theta-1)\kappa_0 + (\theta-1)\kappa_1\left(A_0 + A^{'}Y_{t+1}\right) \\ &\quad - (\theta-1)\left(A_0 + A^{'}Y_t\right) + (\theta-1)e_c^{'}Y_{t+1} \end{aligned}$$

which simplifies to

$$\begin{aligned} m_{t+1} &= \{\theta\log\delta + (\theta-1)\kappa_0 + (\theta-1)\kappa_1 A_0 - (\theta-1)A_0\} \\ &\quad + \left\{\left(-\frac{\theta}{\psi} + (\theta-1)\right)e_c^{'} + (\theta-1)\kappa_1 A^{'}\right\}Y_{t+1} \\ &\quad - (\theta-1)A^{'}Y_t \end{aligned}$$

and

$$m_{t+1} = \left\{\theta\log\delta - (1-\theta)[\kappa_0 + A_0(\kappa_1 - 1)] - (\theta-1)A^{'}Y_t\right\} - \Lambda^{'}Y_{t+1}.$$

Thus,

$$\begin{aligned} -\log R_{f,t\to t+1} &= \theta\log\delta-(1-\theta)\left[\kappa_0+A_0\left(\kappa_1-1\right)\right]-\left(\theta-1\right)A^{'}Y_t \\ &\quad +\mathbf{f}\left(-\Lambda\right)+\mathbf{g}\left(-\Lambda\right)^{'}Y_t \end{aligned}$$

which simplifies to:

$$\log R_{f,t\to t+1}=-\left\{\begin{array}{c}\theta\log\delta+\mathbf{f}\left(-\Lambda\right)\\ -\left(1-\theta\right)\left[\kappa_0+A_0\left(\kappa_1-1\right)\right]\end{array}\right\}-\left(\left(1-\theta\right)A+\mathbf{g}\left(-\Lambda\right)\right)^{'}Y_t.$$

■

We now provide a proof of Result IA.8.

Proof. Proof of Result IA.8.

Expression for $\mathbb{E}_t\left[\boldsymbol{R^n_{M,t\to t+1}}\right]$:

$$\mathbb{E}_t R^n_{M,t\to t+1}=\mathbb{E}_t e^{nr_{m,t+1}}$$

Observe that

$$\begin{aligned} nr_{m,t+1} &= n\kappa_{0,m}+n\kappa_{1,m}\upsilon_{m,t+1}-n\upsilon_{m,t}+ne_d^{'}Y_{t+1} \\ &= \left(n\kappa_{0,m}+n\kappa_{1,m}A_{0,m}-nA_{0,m}\right)-nA_m^{'}Y_t \\ &\quad +\left(n\kappa_{1,m}A_m+ne_d\right)^{'}Y_{t+1}. \end{aligned}$$

Thus

$$\begin{aligned} \mathbb{E}_t R^n_{M,t\to t+1} &= \exp\left\{\left(n\kappa_{0,m}+n\kappa_{1,m}A_{0,m}-nA_{0,m}\right)-nA_m^{'}Y_t\right\} \\ &\quad \times\mathbb{E}_t\exp\left\{\left(n\kappa_{1,m}A_m+ne_d\right)^{'}Y_{t+1}\right\} \end{aligned}$$

and

$$\mathbb{E}_t R^n_{M,t\to t+1}=\exp\left\{\begin{array}{c}\left(n\kappa_{0,m}+n\kappa_{1,m}A_{0,m}-nA_{0,m}\right)+\mathbf{f}\left(n\kappa_{1,m}A_m+ne_d\right)\\ +\left\{\mathbf{g}\left(n\kappa_{1,m}A_m+ne_d\right)-nA_m\right\}^{'}Y_t\end{array}\right\}.$$

The truncated physical moment is

$$\mathbb{E}_t\left[R^n_{M,t+1}1_{R_{M,t+1}>a}\right]=\mathbb{E}_t\left\{\left(\exp\left\{\mathcal{A}_{y,t}+\left(\Lambda^*+\Lambda\right)^{'}Y_{t+1}\right\}\right)\mathbb{I}_{\left\{\mathcal{A}_{y,t}+\left(\Lambda^*+\Lambda\right)^{'}Y_{t+1}>n\log a\right\}}\right\}$$

where

$$\mathcal{A}_{y,t}=\left(n\kappa_{0,m}+n\kappa_{1,m}A_{0,m}-nA_{0,m}\right)-nA_m^{'}Y_t.$$

■

We now provide a proof of Result IA.9.

Proof. Proof of Result IA.9.

Expression for $\mathbb{E}_t^*\left[\boldsymbol{R}_{\boldsymbol{M,t\to t+1}}^{\boldsymbol{n}}\right]$:

$$\mathbb{E}_t^* R_{M,t\to t+1}^n = R_{f,t+1}\mathbb{E}_t e^{m_{t+1}+nr_{m,t+1}}.$$

Observe that

$$\begin{aligned} m_{t+1}+nr_{m,t+1} &= \left\{\theta\log\delta-(1-\theta)\left[\kappa_0+A_0\left(\kappa_1-1\right)\right]-\left(\theta-1\right)A^{'}Y_t\right\}-\Lambda^{'}Y_{t+1} \\ &\quad+\left(n\kappa_{0,m}+n\kappa_{1,m}A_{0,m}-nA_{0,m}\right)-nA_m^{'}Y_t+\left(n\kappa_{1,m}A_m+ne_d\right)^{'}Y_{t+1} \end{aligned}$$

which simplifies to

$$\begin{aligned} m_{t+1}+nr_{m,t+1} &= \left\{\begin{array}{c}\theta\log\delta-(1-\theta)\left[\kappa_0+A_0\left(\kappa_1-1\right)\right] \\ +\left(n\kappa_{0,m}+n\kappa_{1,m}A_{0,m}-nA_{0,m}\right) \\ -\left(\theta-1\right)A^{'}Y_t-nA_m^{'}Y_t\end{array}\right\} \\ &\quad+\left\{n\kappa_{1,m}A_m+ne_d-\Lambda\right\}^{'}Y_{t+1}. \end{aligned}$$

Denote

$$\Lambda^* = n\kappa_{1,m}A_m+ne_d-\Lambda.$$

Thus

$$m_{t+1}+nr_{m,t+1} = \left\{\begin{array}{c}\theta\log\delta-(1-\theta)\left[\kappa_0+A_0\left(\kappa_1-1\right)\right] \\ +\left(n\kappa_{0,m}+n\kappa_{1,m}A_{0,m}-nA_{0,m}\right) \\ -\left(\theta-1\right)A^{'}Y_t-nA_m^{'}Y_t\end{array}\right\}+\Lambda^{*'}Y_{t+1}.$$

Therefore,

$$\mathbb{E}_t^* R_{M,t\to t+1}^n = R_{f,t+1}\exp\left\{\begin{array}{c}\theta\log\delta-(1-\theta)\left[\kappa_0+A_0\left(\kappa_1-1\right)\right] \\ +\left(n\kappa_{0,m}+n\kappa_{1,m}A_{0,m}-nA_{0,m}\right)+\mathbf{f}\left(\Lambda^*\right) \\ \left\{-\left(\theta-1\right)A-nA_m+\mathbf{g}\left(\Lambda^*\right)\right\}Y_t\end{array}\right\}.$$

The truncated risk neutral moment is

$$\mathbb{E}_t^*\left[R_{M,t+1}^n 1_{R_{M,t+1}>a}\right] = R_{f,t+1}\mathbb{E}_t^*\left[e^{m_{t+1}+nr_{m,t+1}}1_{R_{M,t+1}>a}\right]$$

Note that

$$m_{t+1}+nr_{m,t+1} = \mathcal{A}_{y,t}^* + \Lambda^{*'}Y_{t+1}$$

where

$$\mathcal{A}_{y,t}^{*}=\left\{\begin{array}{c}\theta\log\delta-(1-\theta)\left[\kappa_{0}+A_{0}\left(\kappa_{1}-1\right)\right]\\+\left(n\kappa_{0,m}+n\kappa_{1,m}A_{0,m}-nA_{0,m}\right)\\-\left(\theta-1\right)A^{'}Y_{t}-nA_{m}^{'}Y_{t}\end{array}\right\}.$$

Therefore,

$$\mathbb{E}_{t}^{*}\left[R_{M,t+1}^{n}1_{R_{M,t+1}>a}\right]=R_{f,t+1}\mathbb{E}_{t}^{*}\left[e^{\mathcal{A}_{y,t}^{*}+\Lambda^{*'}Y_{t+1}}1_{\mathcal{A}_{y,t}+(\Lambda^{*}+\Lambda)'Y_{t+1}>n\log a}\right].$$

■

IA.8.6 Habit Formation Models: Bekaert, Engstrom, and Ermolov (2023)

Bekaert, Engstrom, and Ermolov (2023) consider an expected utility function of the form

$$\mathbb{E}_{t}\left[\sum_{j=t}^{\infty}\beta^{j-t}\frac{\left(C_{j}-H_{j}\right)^{1-\gamma}-1}{1-\gamma}\right],$$

where β is the time discount rate, C_j is consumption and H_j is the habit stock with the restriction $C_j > H_j$. In this framework, the log-SDF is given by

$$m_{t\to t+1}=\log\beta-\gamma g_{t+1}+\gamma\Delta q_{t+1},$$

where $g_{t+1}\equiv\log\left(C_{t+1}/C_{t}\right)$ is the log of consumption growth, and $q_t = \log Q_t$ with $Q_t \equiv C_t/\left(C_t - H_t\right)$. We consider the two models studied in Bekaert, Engstrom, and Ermolov (2023): (i) their model without preference shocks,[63] and (ii) their model with preference shocks. While the model without preference shocks is able to explain many standard stylized facts in the data, it falls short of explaining the low variance risk premium persistence. The model with preference shocks is designed to simultaneously explain the low variance risk premium persistence and the average variance risk premium itself. We present here a general specification that allows for preference shocks then later specialize it by setting some coefficients to zero to obtain the model without preference shocks.

Bekaert, Engstrom, and Ermolov (2023) consider an economy having the following time series dynamics:

$$\begin{aligned}g_{t+1}&=\overline{g}+\phi_{g}\left(n_{t}-\overline{n}\right)+\sigma_{cp}\omega_{p,t+1}-\sigma_{cn}\omega_{n,t+1},\\d_{t+1}&=\overline{g}+\phi_{d}\left(n_{t}-\overline{n}\right)+\gamma_{g}\left(\sigma_{cp}\omega_{p,t+1}-\sigma_{cn}\omega_{n,t+1}\right)+\gamma_{n}\left(-\sigma_{cn}\omega_{n,t+1}\right),\\q_{t+1}&=\overline{q}+\rho_{q}\left(q_{t}-\overline{q}\right)+\sigma_{qp}\omega_{p,t+1}+\sigma_{qn}\omega_{n,t+1}+\sigma_{qq}\omega_{q,t+1}.\end{aligned}$$

where

$$\begin{aligned}p_{t+1}&=\overline{p}+\rho_{p}\left(p_{t}-\overline{p}\right)+\sigma_{pp}\omega_{p,t+1},\\n_{t+1}&=\overline{n}+\rho_{n}\left(n_{t}-\overline{n}\right)+\sigma_{nn}\omega_{n,t+1},\\s_{t+1}&=\overline{s}+\rho_{s}\left(s_{t}-\overline{s}\right)+\sigma_{sq}\omega_{q,t+1},\end{aligned}$$

[63] We use their "Full" model specification in this case, as opposed to their "Baseline" specification.

and where $\omega_{p,t+1}$, $\omega_{n,t+1}$, $\omega_{q,t+1}$ follow demeaned gamma distributions defined by

$$\begin{aligned}\omega_{p,t+1} &\sim \Gamma(p_t, 1) - p_t,\\ \omega_{n,t+1} &\sim \Gamma(n_t, 1) - n_t,\\ \omega_{q,t+1} &\sim \Gamma(s_t, 1) - s_t.\end{aligned}$$

Here, $\Gamma(x, y)$ is a gamma distribution with shape parameter x and scale parameter y. $\omega_{p,t+1}$, $\omega_{n,t+1}$, and $\omega_{q,t+1}$ are independent and have zero mean. The log-SDF has the form

$$m_{t\to t+1} = m_0 + m_q q_t + m_n n_t + m_{\omega,p}\omega_{p,t+1} + m_{\omega,n}\omega_{n,t+1} + m_{\omega,q}\omega_{q,t+1},$$

See below for more details on parameters in the log-SDF. There are, in general, three state variables in this framework: q_t, n_t, and s_t. The model without preference shocks obtains when the state variable s_t is set to zero and certain parameter restrictions are imposed (see below for more details). Given this setup, we show the following results.

Main Results

Result IA.10. *Given $p_t = \overline{p}$ and the state variables q_t, n_t, and s_t, the Bekaert, Engstrom, and Ermolov (2023) model-implied log price-dividend ratio is given by*

$$\log\frac{P_t}{D_t} = K_0^1 + K_p^1 p_t + K_n^1 n_t + K_q^1 q_t + K_s^1 s_t \tag{IA.86}$$

and the non-central risk-neutral market return moments are given by

$$\mathbb{E}_t^*\left[R_{M,t\to t+1}^n\right] = R_{f,t\to t+1}\exp\left(\begin{array}{c} nr_0 + m_0 + \{nr_p - g(nr_{\omega p} + m_{\omega,p})\}p_t \\ + \{nr_n + m_n - g(m_{\omega,n} + nr_{\omega n})\}n_t \\ + (nr_q + m_q)q_t + (nr_s - g(nr_{\omega q} + m_{\omega,q}))s_t \end{array}\right) \tag{IA.87}$$

with

$$R_{f,t\to t+1} = \exp(f_0 + f_q q_t + f_n n_t + f_p p_t + f_s s_t).$$

All parameters are described in more detail below. The function $g(\cdot)$ is defined as $g(x) = x + \log(1-x)$. $R_{f,t\to t+1}$ is the model-implied risk-free rate. Given $\mathbb{E}_t^*\left[R_{M,t\to t+1}^k\right]$, $\mathbb{M}_{t\to t+1}^{*(n)}$ can be computed using Equation 17 by setting $x = R_{M,t\to t+1}$ and $x_s = R_{f,t\to t+1}$, then taking expectations under the risk-neutral measure. The resulting expression can be found in Equation IA.85.

Proof. See below. ■

Result IA.11. *The conditional non-central physical moment of the market return is*

$$\mathbb{E}_t\left[R_{M,t\to t+1}^k\right] = \exp\left\{\begin{array}{c} kr_0 + kr_p p_t + kr_n n_t + kr_q q_t + kr_s s_t \\ -p_t g(kr_{\omega p}) - n_t g(kr_{\omega n}) - s_t g(kr_{\omega q}) \end{array}\right\}.$$

The truncated non-central physical moment is

$$\mathbb{E}_t\left[R_{M,t\to t+1}^k \mathbb{I}_{\{R_{M,t\to t+1}>a\}}\right] = e^{\xi_{r,t}}\mathbb{E}_t\left[e^{Z_{t+1,r}}\mathbb{I}_{\{Z_{t+1,r}>k\ln a - \xi_{r,t}\}}\right]$$

with

$$\begin{aligned} \xi_{r,t} &= kr_0 + (kr_p - kr_{\omega p})\, p_t + (kr_n - kr_{\omega n})\, n_t + kr_q q_t + (kr_s - kr_{\omega q})\, s_t \\ Z_{t+1,r} &= kr_{\omega p}\,(\omega_{p,t+1} + p_t) + kr_{\omega n}\,(\omega_{n,t+1} + n_t) + kr_{\omega q}\,(\omega_{q,t+1} + s_t)\,. \end{aligned}$$

with $p_t = \overline{p}$ *and*

$$\begin{aligned} \omega_{p,t+1} + p_t &\sim \Gamma\,(p_t, 1)\,, \\ \omega_{n,t+1} + n_t &\sim \Gamma\,(n_t, 1)\,, \\ \omega_{q,t+1} + s_t &\sim \Gamma\,(s_t, 1)\,, \end{aligned}$$

Given the state variables, the truncated moment $\mathbb{E}_t\left[R_{M,t\to t+1}^k \mathbb{I}_{\{R_{M,t\to t+1}>a\}}\right]$ *can be computed by simulation at each time* t*. All parameters are defined below.*

Proof. See below. ■

Result IA.12. *The conditional non-central risk neutral moment of the market return is*

$$\mathbb{E}_t^*\left[R_{M,t\to t+1}^k\right] = R_{f,t\to t+1} \exp\left(\begin{array}{c} kr_0 + m_0 + \{kr_p - g\,(kr_{\omega p} + m_{\omega,p})\}\, p_t \\ + \{kr_n + m_n - g\,(m_{\omega,n} + kr_{\omega n})\}\, n_t \\ + (kr_q + m_q)\, q_t + (kr_s - g\,(kr_{\omega q} + m_{\omega,q}))\, s_t \end{array}\right).$$

The truncated non-central risk neutral moment is

$$\mathbb{E}_t^*\left[R_{M,t\to t+1}^k \mathbb{I}_{\{R_{M,t\to t+1}>a\}}\right] = R_{f,t+1}\mathbb{E}_t\left[e^{\zeta_r + Z_{t+1,m}} 1_{Z_{t+1,r} > k\log a - \xi_{r,t}}\right].$$

where

$$\begin{aligned} \zeta_r &= m_0 + kr_0 + (kr_p - kr_{\omega p} - m_{\omega,p})\, p_t + (kr_n - kr_{\omega n} + m_n - m_{\omega,n})\, n_t \\ &\quad + (kr_s - kr_{\omega q} - m_{\omega,q})\, s_t + (kr_q + m_q)\, q_t, \\ Z_{t+1,m} &= (m_{\omega,p} + kr_{\omega p})\,(\omega_{p,t+1} + p_t) + (m_{\omega,n} + kr_{\omega n})\,(\omega_{n,t+1} + n_t) \\ &\quad + (kr_{\omega q} + m_{\omega,q})\,(\omega_{q,t+1} + s_t)\,, \\ \xi_{r,t} &= kr_0 + (kr_p - kr_{\omega p})\, p_t + (kr_n - kr_{\omega n})\, n_t + kr_q q_t + (kr_s - kr_{\omega q})\, s_t \\ Z_{t+1,r} &= kr_{\omega p}\,(\omega_{p,t+1} + p_t) + kr_{\omega n}\,(\omega_{n,t+1} + n_t) + kr_{\omega q}\,(\omega_{q,t+1} + s_t)\,, \end{aligned}$$

$$\omega_{p,t+1} + p_t \sim \Gamma\,(p_t, 1)\,,\ \omega_{n,t+1} + n_t \sim \Gamma\,(n_t, 1)\,,\ \textit{and}\ \omega_{q,t+1} + s_t \sim \Gamma\,(s_t, 1)\,.$$

Given the state variables, $\mathbb{E}_t\left[e^{\zeta_r + Z_{t+1,m}} 1_{Z_{t+1,r} > k\log a - \xi_{r,t}}\right]$ *can be computed by simulation at each time* t*. All parameters are defined below.*

Proof. See below. ■

Derivations and Proofs We provide proofs of Results IA.10, IA.11, and IA.12 below.

Proof. Proofs of Results IA.10, IA.11, and IA.12.

Let us denote $r_{t+1} = \log R_{M,t\to t+1}$. The log-SDF with preference shocks

$$m_{t+1} = \log\beta - \gamma g_{t+1} + \gamma \Delta q_{t+1}$$

can be written as

$$\begin{aligned} m_{t+1} &= \log\beta - \gamma q_t - \gamma g_{t+1} + \gamma q_{t+1} \\ &= \{\log\beta - \gamma\overline{g} + \gamma\phi_g\overline{n} + \gamma\overline{q}\,(1-\rho_q)\} + (\rho_q - 1)\,\gamma q_t - \gamma\phi_g n_t \\ &\quad + (\gamma\sigma_{qp} - \gamma\sigma_{cp})\,\omega_{p,t+1} + (\gamma\sigma_{cn} + \gamma\sigma_{qn})\,\omega_{n,t+1} + \gamma\sigma_{qq}\omega_{q,t+1} \end{aligned}$$

This log-SDF simplifies to

$$\begin{aligned} m_{t+1} &= \log\beta - \gamma q_t - \gamma g_{t+1} + \gamma q_{t+1} \\ &= m_0 + m_q q_t + m_n n_t + m_{\omega,p}\omega_{p,t+1} + m_{\omega,n}\omega_{n,t+1} + m_{\omega,q}\omega_{q,t+1} \end{aligned}$$

with

$$\begin{aligned} m_0 &= \log\beta + \gamma\left(\phi_g\overline{n} - \overline{g}\right) - \overline{q}m_q, & m_n &= -\gamma\phi_g, \\ m_q &= -\left(1-\rho_q\right)\gamma, & m_{\omega,q} &= \gamma\sigma_{qq}, \\ m_{\omega,p} &= \gamma\left(\sigma_{qp} - \sigma_{cp}\right), & m_{\omega,n} &= \gamma\left(\sigma_{cn} + \sigma_{qn}\right). \end{aligned}$$

The log risk-free rate is

$$\log R_{f,t\to t+1} = f_0 + f_q q_t + f_n n_t + f_p p_t + f_s s_t \tag{IA.88}$$

with

$$f_0 = -m_0,\ f_q = -m_q,\ f_n = -\left(m_n - g\left(m_{\omega,n}\right)\right),\ f_p = g\left(m_{\omega,p}\right),\ f_s = g\left(m_{\omega,q}\right).$$

Now the price-dividend ratio is

$$\begin{aligned} \frac{P_t}{D_t} &= \mathbb{E}_t\left[e^{m_{t+1}+d_{t+1}}\right] + \mathbb{E}_t\left[e^{\sum_{j=1}^{2}\left(m_{t+j}+d_{t+j}\right)}\right] + \mathbb{E}_t\left[e^{\sum_{j=1}^{3}\left(m_{t+j}+d_{t+j}\right)}\right] + ... \\ &= \mathbb{E}_t\left[e^{m_{t+1}+d_{t+1}}\right] + \mathbb{E}_t\left[e^{m_{t+1}+d_{t+1}}e^{\left(m_{t+2}+d_{t+2}\right)}\right] + \mathbb{E}_t\left[e^{\sum_{j=1}^{3}\left(m_{t+j}+d_{t+j}\right)}\right] + ... \end{aligned}$$

Observe that

$$\begin{aligned} & m_{t+1} + d_{t+1} \\ = \ & \left\{m_0 + \overline{g} - \phi_d\overline{n}\right\} + m_q q_t + \left\{m_n + \phi_d\right\} n_t \\ & + \left\{m_{\omega,p} + \gamma_g\sigma_{cp}\right\}\omega_{p,t+1} + \left\{m_{\omega,n} - \left(\gamma_n + \gamma_g\right)\sigma_{cn}\right\}\omega_{n,t+1} + m_{\omega,q}\omega_{q,t+1}. \end{aligned}$$

Thus

$$\begin{aligned} & \mathbb{E}_t\left[e^{m_{t+1}+d_{t+1}}\right] \\ = \ & e^{\left\{\left\{m_0+\overline{g}-\phi_d\overline{n}\right\}+m_q q_t+\left\{m_n+\phi_d\right\}n_t\right\}} \\ & \times\mathbb{E}_t\left[e^{\left(m_{\omega,p}+\gamma_g\sigma_{cp}\right)\omega_{p,t+1}}\right]\mathbb{E}_t\left[e^{\left(m_{\omega,n}-\left(\gamma_n+\gamma_g\right)\sigma_{cn}\right)\omega_{n,t+1}}\right]\mathbb{E}_t\left[e^{m_{\omega,q}\omega_{q,t+1}}\right] \end{aligned}$$

Notice that

$$\begin{aligned} \mathbb{E}_t\left[e^{\left(m_{\omega,p}+\gamma_g\sigma_{cp}\right)\omega_{p,t+1}}\right] &= \exp\left\{-p_t g\left(m_{\omega,p} + \gamma_g\sigma_{cp}\right)\right\}, \\ \mathbb{E}_t\left[e^{\left(m_{\omega,n}-\gamma_g\sigma_{cn}-\gamma_n\sigma_{cn}\right)\omega_{n,t+1}}\right] &= \exp\left\{-n_t g\left(m_{\omega,n} - \left(\gamma_g + \gamma_n\right)\sigma_{cn}\right)\right\}, \\ \mathbb{E}_t\left[e^{m_{\omega,q}\omega_{q,t+1}}\right] &= \exp\left\{-s_t g\left(m_{\omega,q}\right)\right\}. \end{aligned}$$

Finally,

$$\begin{aligned} \mathbb{E}_t\left[e^{m_{t+1}+d_{t+1}}\right] &= \exp\left\{\begin{array}{c} \left\{m_0 + \overline{g} - \phi_d\overline{n}\right\} + m_q q_t + \left\{m_n + \phi_d\right\} n_t - p_t g\left(m_{\omega,p} + \gamma_g\sigma_{cp}\right) \\ -n_t g\left(m_{\omega,n} - \left(\gamma_g + \gamma_n\right)\sigma_{cn}\right) - s_t g\left(m_{\omega,q}\right) \end{array}\right\} \\ &= \exp\left\{A_1 + B_1 p_t + C_1 n_t + D_1 q_t + G_1 s_t\right\} \end{aligned}$$

where

$$\begin{aligned}
A_1 &= \overline{g} + m_0 - \phi_d \overline{n}, \\
B_1 &= -g\left(m_{\omega,p} + \gamma_g \sigma_{cp}\right), \\
C_1 &= m_n + \phi_d - g\left(m_{\omega,n} - \left(\gamma_g + \gamma_n\right)\sigma_{cn}\right), \\
D_1 &= m_q, \\
G_1 &= -g\left(m_{\omega,q}\right).
\end{aligned}$$

Now, observe that

$$\mathbb{E}_{t+1}\left[e^{m_{t+2}+d_{t+2}}\right] = \exp\left\{A_1 + B_1 p_{t+1} + C_1 n_{t+1} + D_1 q_{t+1} + G_1 s_{t+1}\right\},$$

and

$$\mathbb{E}_t\left[e^{m_{t+2}+d_{t+2}}\right] = \mathbb{E}_t\left[\exp\left\{A_1 + B_1 p_{t+1} + C_1 n_{t+1} + D_1 q_{t+1} + G_1 s_{t+1}\right\}\right].$$

Recall that

$$\begin{aligned}
q_{t+1} &= \overline{q} + \rho_q\left(q_t - \overline{q}\right) + \sigma_{qp}\omega_{p,t+1} + \sigma_{qn}\omega_{n,t+1} + \sigma_{qq}\omega_{q,t+1}, \\
p_{t+1} &= \overline{p} + \rho_p\left(p_t - \overline{p}\right) + \sigma_{pp}\omega_{p,t+1}, \\
n_{t+1} &= \overline{n} + \rho_n\left(n_t - \overline{n}\right) + \sigma_{nn}\omega_{n,t+1}.
\end{aligned}$$

Thus:

$$\mathbb{E}_t\left[e^{m_{t+1}+d_{t+1}}\right]\mathbb{E}_{t+1}\left[e^{m_{t+2}+d_{t+2}}\right] = \mathbb{E}_t\left[e^{m_{t+1}+d_{t+1}}\right]\exp\left\{A_1 + B_1 p_{t+1} + C_1 n_{t+1} + D_1 q_{t+1} + G_1 s_{t+1}\right\}.$$

However, observe that

$$e^{m_{t+1}+d_{t+1}} = e^{\left\{\{m_0+\overline{g}-\phi_d\overline{n}\}+m_q q_t+\{m_n+\phi_d\}n_t\right\}} \times e^{(m_{\omega,p}+\gamma_g\sigma_{cp})\omega_{p,t+1}} e^{(m_{\omega,n}-(\gamma_n+\gamma_g)\sigma_{cn})\omega_{n,t+1}} e^{m_{\omega,q}\omega_{q,t+1}}.$$

Thus:

$$\mathbb{E}_t\left[e^{m_{t+1}+d_{t+1}}\right]\mathbb{E}_{t+1}\left[e^{m_{t+2}+d_{t+2}}\right] = \mathbb{E}_t\left[\exp\left\{\begin{array}{c}
\left(m_0 + \overline{g} - \phi_d\overline{n}\right) + m_q q_t + \left(m_n + \phi_d\right) n_t \\
A_1 + B_1 p_{t+1} + C_1 n_{t+1} + D_1 q_{t+1} + G_1 s_{t+1} \\
+\left(m_{\omega,p} + \gamma_g\sigma_{cp}\right)\omega_{p,t+1} + \left(m_{\omega,n} - \left(\gamma_n + \gamma_g\right)\sigma_{cn}\right)\omega_{n,t+1} + m_{\omega,q}\omega_{q,t+1}
\end{array}\right\}\right]$$

which simplifies to

$$\begin{aligned}
&\mathbb{E}_t\left[e^{m_{t+1}+d_{t+1}}\right]\mathbb{E}_{t+1}\left[e^{m_{t+2}+d_{t+2}}\right] \\
&= \mathbb{E}_t\left[\exp\left\{\begin{array}{c}
A_2 \\
+\left(D_1\rho_q + m_q\right) q_t + \left(m_n + \phi_d + C_1\rho_n\right) n_t \\
+\left\{\begin{array}{c} B_1\sigma_{pp} + D_1\sigma_{qp} + \left(m_{\omega,p} + \gamma_g\sigma_{cp}\right) \end{array}\right\}\omega_{p,t+1} + B_1\rho_p p_t \\
+\left\{\begin{array}{c} C_1\sigma_{nn} + D_1\sigma_{qn} + \left(m_{\omega,n} - \left(\gamma_n + \gamma_g\right)\sigma_{cn}\right) \end{array}\right\}\omega_{n,t+1} \\
+\left\{D_1\sigma_{qq} + G_1\sigma_{sq} + m_{\omega,q}\right\}\omega_{q,t+1} + G_1\rho_s s_t
\end{array}\right\}\right]
\end{aligned}$$

$$
\begin{aligned}
A_2 &= m_0 + \overline{g} - \phi_d \overline{n} + A_1 + B_1 \overline{p}\,(1-\rho_p) + C_1 \overline{n}\,(1-\rho_n) \\
&\quad + D_1 \overline{q}\,(1-\rho_q) + G_1 \overline{s}\,(1-\rho_s)\,, \\
B_2 &= B_1 \rho_p - g\,(B_1 \sigma_{pp} + D_1 \sigma_{qp} + (m_{\omega,p} + \gamma_g \sigma_{cp}))\,, \\
C_2 &= m_n + \phi_d + C_1 \rho_n - g\,[C_1 \sigma_{nn} + D_1 \sigma_{qn} + (m_{\omega,n} - (\gamma_n + \gamma_g)\,\sigma_{cn})]\,, \\
D_2 &= D_1 \rho_q + m_q, \\
G_2 &= G_1 \rho_s - g\,(D_1 \sigma_{qq} + G_1 \sigma_{sq} + m_{\omega,q})\,.
\end{aligned}
$$

More generally,

$$
\begin{aligned}
A_n &= A_{n-1} + m_0 + \overline{g} - \phi_d \overline{n} + B_{n-1} \overline{p}\,(1-\rho_p) + C_{n-1} \overline{n}\,(1-\rho_n) \\
&\quad + D_{n-1} \overline{q}\,(1-\rho_q) + G_{n-1} \overline{s}\,(1-\rho_s)\,, \\
B_n &= B_{n-1} \rho_p - g\,(D_{n-1} \sigma_{qp} + B_{n-1} \sigma_{pp} + (m_{\omega,p} + \gamma_g \sigma_{cp}))\,, \\
C_n &= C_{n-1} \rho_n + m_n + \phi_d - g\,(C_{n-1} \sigma_{nn} + D_{n-1} \sigma_{qn} + (m_{\omega,n} - (\gamma_g + \gamma_n)\,\sigma_{cn}))\,, \\
D_n &= D_{n-1} \rho_q + m_q, \\
G_n &= G_{n-1} \rho_s - g\,(D_{n-1} \sigma_{qq} + G_{n-1} \sigma_{sq} + m_{\omega,q})\,.
\end{aligned}
$$

The price-dividend ratio can be expressed as

$$
\frac{P_t}{D_t} = \sum_{i=1}^{\infty} e^{A_i + B_i p_t + C_i n_t + D_i q_t + G_i s_t}.
$$

The first-order approximation of the log price-dividend ratio is

$$
pd_t = K_0^1 + K_p^1 p_t + K_n^1 n_t + K_q^1 q_t + K_s^1 s_t
$$

where

$$
\begin{aligned}
K_p^1 &= \frac{\sum_{i=1}^{\infty} B_i \exp\left(A_i + B_i \overline{p} + C_i \overline{n} + D_i \overline{q} + G_i \overline{s}\right)}{\sum_{i=1}^{\infty} \exp\left(A_i + B_i \overline{p} + C_i \overline{n} + D_i \overline{q} + G_i \overline{s}\right)}, \\
K_n^1 &= \frac{\sum_{i=1}^{\infty} C_i \exp\left(A_i + B_i \overline{p} + C_i \overline{n} + D_i \overline{q} + G_i \overline{s}\right)}{\sum_{i=1}^{\infty} \exp\left(A_i + B_i \overline{p} + C_i \overline{n} + D_i \overline{q} + G_i \overline{s}\right)}, \\
K_q^1 &= \frac{\sum_{i=1}^{\infty} D_i \exp\left(A_i + B_i \overline{p} + C_i \overline{n} + D_i \overline{q} + G_i \overline{s}\right)}{\sum_{i=1}^{\infty} \exp\left(A_i + B_i \overline{p} + C_i \overline{n} + D_i \overline{q} + G_i \overline{s}\right)}, \\
K_s^1 &= \frac{\sum_{i=1}^{\infty} G_i \exp\left(A_i + B_i \overline{p} + C_i \overline{n} + D_i \overline{q} + G_i \overline{s}\right)}{\sum_{i=1}^{\infty} \exp\left(A_i + B_i \overline{p} + C_i \overline{n} + D_i \overline{q} + G_i \overline{s}\right)},
\end{aligned}
$$

and

$$
K_0^1 = \ln\left(\sum_{i=1}^{\infty} \exp\left(A_i + B_i \overline{p} + C_i \overline{n} + D_i \overline{q} + G_i \overline{s}\right)\right) - K_p^1 \overline{p} - K_n^1 \overline{n} - K_q^1 \overline{q} - K_s^1 \overline{s}.
$$

The first-order approximation of $\ln\left(1 + \frac{P_{t+1}}{D_{t+1}}\right)$ is

$$
\ln\left(1 + \frac{P_{t+1}}{D_{t+1}}\right) = K_0^2 + K_p^2 p_{t+1} + K_n^2 n_{t+1} + K_q^2 q_{t+1} + K_s^2 s_{t+1},
$$

where

$$\begin{aligned}
K_p^2 &= \frac{\sum_{i=1}^{\infty} B_i \exp\left(A_i + B_i\overline{p} + C_i\overline{n} + D_i\overline{q} + G_i\overline{s}\right)}{1 + \sum_{i=1}^{\infty} \exp\left(A_i + B_i\overline{p} + C_i\overline{n} + D_i\overline{q} + G_i\overline{s}\right)}, \\
K_n^2 &= \frac{\sum_{i=1}^{\infty} C_i \exp\left(A_i + B_i\overline{p} + C_i\overline{n} + D_i\overline{q} + G_i\overline{s}\right)}{1 + \sum_{i=1}^{\infty} \exp\left(A_i + B_i\overline{p} + C_i\overline{n} + D_i\overline{q} + G_i\overline{s}\right)}, \\
K_q^2 &= \frac{\sum_{i=1}^{\infty} D_i \exp\left(A_i + B_i\overline{p} + C_i\overline{n} + D_i\overline{q} + G_i\overline{s}\right)}{1 + \sum_{i=1}^{\infty} \exp\left(A_i + B_i\overline{p} + C_i\overline{n} + D_i\overline{q} + G_i\overline{s}\right)}, \\
K_s^2 &= \frac{\sum_{i=1}^{\infty} G_i \exp\left(A_i + B_i\overline{p} + C_i\overline{n} + D_i\overline{q} + G_i\overline{s}\right)}{1 + \sum_{i=1}^{\infty} \exp\left(A_i + B_i\overline{p} + C_i\overline{n} + D_i\overline{q} + G_i\overline{s}\right)},
\end{aligned}$$

and

$$K_0^2 = \ln\left(1 + \sum_{i=1}^{\infty} \exp\left(A_i + B_i\overline{p} + C_i\overline{n} + D_i\overline{q} + G_i\overline{s}\right)\right) - K_p^2\overline{p} - K_n^2\overline{n} - K_q^2\overline{q} - K_s^2\overline{s}.$$

The expression for the log market return is therefore

$$\begin{aligned}
r_{t+1} &= d_{t+1} + \ln\left(1 + \frac{P_{t+1}}{D_{t+1}}\right) - pd_t \\
&= \overline{g} + \phi_d\left(n_t - \overline{n}\right) + \gamma_g\left(\sigma_{cp}\omega_{p,t+1} - \sigma_{cn}\omega_{n,t+1}\right) + \gamma_n\left(-\sigma_{cn}\omega_{n,t+1}\right) \\
&\quad + K_0^2 + K_p^2 p_{t+1} + K_n^2 n_{t+1} + K_q^2 q_{t+1} + K_s^2 s_{t+1} \\
&\quad - K_0^1 - K_p^1 p_t - K_n^1 n_t - K_q^1 q_t - K_s^1 s_t.
\end{aligned}$$

which simplifies to

$$\begin{aligned}
r_{t+1} &= \left\{ \begin{array}{c} \overline{g} - \phi_d\overline{n} + K_0^2 - K_0^1 + K_p^2\overline{p} - K_p^2\rho_p\overline{p} + K_n^2\overline{n} \\ -K_n^2\rho_n\overline{n} + K_q^2\overline{q} - K_q^2\rho_q\overline{q} + K_s^2\overline{s} - K_s^2\rho_s\overline{s} \end{array} \right\} \\
&\quad + \left\{\gamma_g\sigma_{cp} + K_p^2\sigma_{pp} + K_q^2\sigma_{qp}\right\}\omega_{p,t+1} \\
&\quad + \left\{K_q^2\sigma_{qn} - \left(\gamma_g + \gamma_n\right)\sigma_{cn} + K_n^2\sigma_{nn}\right\}\omega_{n,t+1} \\
&\quad + \left\{K_p^2\rho_p - K_p^1\right\}p_t + \left\{K_n^2\rho_n - K_n^1 + \phi_d\right\}n_t + \left\{K_s^2\rho_s - K_s^1\right\}s_t \\
&\quad + \left\{K_q^2\rho_q - K_q^1\right\}q_t + \left\{K_q^2\sigma_{qq} + K_s^2\sigma_{sq}\right\}\omega_{q,t+1}.
\end{aligned}$$

This can be further simplified as

$$r_{t+1} = r_0 + r_p p_t + r_n n_t + r_q q_t + r_s s_t + r_{\omega p}\omega_{p,t+1} + r_{\omega n}\omega_{n,t+1} + r_{\omega q}\omega_{q,t+1},$$

where

$$\begin{aligned}
r_0 &= \overline{g} - K_0^1 - \phi_d \overline{n} + K_0^2 + K_p^2 \overline{p}\,(1-\rho_p) + K_n^2 \overline{n}\,(1-\rho_n) \\
&\quad + K_q^2 \overline{q}\,(1-\rho_q) + K_s^2 \overline{s}\,(1-\rho_s)\,, \\
r_p &= K_p^2 \rho_p - K_p^1, \\
r_n &= K_n^2 \rho_n - K_n^1 + \phi_d, \\
r_q &= K_q^2 \rho_q - K_q^1, \\
r_s &= K_s^2 \rho_s - K_s^1, \\
r_{\omega p} &= \gamma_g \sigma_{cp} + K_p^2 \sigma_{pp} + K_q^2 \sigma_{qp}, \\
r_{\omega n} &= K_q^2 \sigma_{qn} - (\gamma_g + \gamma_n)\,\sigma_{cn} + K_n^2 \sigma_{nn}, \\
r_{\omega q} &= K_q^2 \sigma_{qq} + K_s^2 \sigma_{sq}.
\end{aligned}$$

Our goal now is to derive

$$\begin{aligned}
\mathbb{E}_t\left[(R_{M,t\to t+1} - R_{f,t\to t+1})^j\right] &= \sum_{k=0}^{j} \frac{j!\,(-1)^{j-k}}{(j-k)!k!} R_{f,t\to t+1}^{j-k} \mathbb{E}_t\left[R_{M,t\to t+1}^k\right], \\
\mathbb{E}_t\left[(R_{M,t\to t+1} - R_{f,t\to t+1})^j \mathbb{I}_{\left\{R_{M,t\to t+1}>a\right\}}\right] &= \sum_{k=0}^{j} \frac{j!\,(-1)^{j-k}}{(j-k)!k!} R_{f,t\to t+1}^{j-k} \mathbb{E}_t\left[R_{M,t\to t+1}^k \mathbb{I}_{\left\{R_{M,t\to t+1}>a\right\}}\right], \\
\mathbb{E}_t^*\left[(R_{M,t\to t+1} - R_{f,t\to t+1})^j\right] &= \sum_{k=0}^{j} \frac{j!\,(-1)^{j-k}}{(j-k)!k!} R_{f,t\to t+1}^{j-k} \mathbb{E}_t^*\left[R_{M,t\to t+1}^k\right], \\
\mathbb{E}_t^*\left[(R_{M,t\to t+1} - R_{f,t\to t+1})^j \mathbb{I}_{\left\{R_{M,t\to t+1}>a\right\}}\right] &= \sum_{k=0}^{j} \frac{j!\,(-1)^{j-k}}{(j-k)!k!} R_{f,t\to t+1}^{j-k} \mathbb{E}_t^*\left[R_{M,t\to t+1}^k \mathbb{I}_{\left\{R_{M,t\to t+1}>a\right\}}\right].
\end{aligned}$$

We need to find

$$\mathbb{E}_t\left[R_{M,t\to t+1}^k\right], \mathbb{E}_t\left[R_{M,t\to t+1}^k \mathbb{I}_{\left\{R_{M,t\to t+1}>a\right\}}\right], \mathbb{E}_t^*\left[R_{M,t\to t+1}^k\right], \text{ and } \mathbb{E}_t^*\left[R_{M,t\to t+1}^k \mathbb{I}_{\left\{R_{M,t\to t+1}>a\right\}}\right].$$

Note that

$$\begin{aligned}
\mathbb{E}_t\left[R_{M,t\to t+1}^k\right] &= \mathbb{E}_t\left[e^{kr_{t+1}}\right] \\
&= \mathbb{E}_t\left[e^{kr_0 + kr_p p_t + kr_n n_t + kr_q q_t + kr_s s_t + kr_{\omega p}\omega_{p,t+1} + kr_{\omega n}\omega_{n,t+1} + kr_{\omega q}\omega_{q,t+1}}\right] \\
&= e^{kr_0 + kr_p p_t + kr_n n_t + kr_q q_t + kr_s s_t}\,\mathbb{E}_t\left[e^{kr_{\omega p}\omega_{p,t+1} + kr_{\omega n}\omega_{n,t+1} + kr_{\omega q}\omega_{q,t+1}}\right] \\
&= \exp\left\{\begin{array}{l} kr_0 + kr_p p_t + kr_n n_t + kr_q q_t + kr_s s_t \\ -p_t g\,(kr_{\omega p}) - n_t g\,(kr_{\omega n}) - s_t g\,(kr_{\omega q}) \end{array}\right\}.
\end{aligned}$$

Next,

$$\mathbb{E}_t^*\left[R_{M,t\to t+1}^k\right] = R_{f,t+1}\mathbb{E}_t\left[M_{t\to t+1} R_{M,t\to t+1}^k\right] = R_{f,t+1}\mathbb{E}_t\left[e^{kr_{t+1}+m_{t+1}}\right].$$

Observe that

$$\begin{aligned} & kr_{t+1}+m_{t+1} \\ = & \left(\begin{array}{c} kr_0+kr_pp_t+kr_nn_t+kr_qq_t+kr_ss_t \\ +kr_{\omega p}\omega_{p,t+1}+kr_{\omega n}\omega_{n,t+1}+kr_{\omega q}\omega_{q,t+1} \\ +m_0+m_qq_t+m_nn_t+m_{\omega,p}\omega_{p,t+1}+m_{\omega,n}\omega_{n,t+1}+m_{\omega,q}\omega_{q,t+1} \end{array}\right) \\ = & \left(\begin{array}{c} kr_0+m_0+kr_pp_t+\left(kr_n+m_n\right)n_t \\ +\left(kr_q+m_q\right)q_t+kr_ss_t+\left(kr_{\omega p}+m_{\omega,p}\right)\omega_{p,t+1} \\ +\left(m_{\omega,n}+kr_{\omega n}\right)\omega_{n,t+1}+\left(kr_{\omega q}+m_{\omega,q}\right)\omega_{q,t+1} \end{array}\right). \end{aligned}$$

Thus

$$\begin{aligned} & R_{f,t\to t+1}\mathbb{E}_t\left[e^{kr_{t+1}+m_{t+1}}\right] \\ = & R_{f,t\to t+1}\mathbb{E}_t\left[\exp\left(\begin{array}{c} kr_0+m_0+kr_pp_t+\left(kr_n+m_n\right)n_t \\ +\left(kr_q+m_qq_t\right)q_t+kr_ss_t+\left(kr_{\omega p}+m_{\omega,p}\right)\omega_{p,t+1} \\ +\left(m_{\omega,n}+kr_{\omega n}\right)\omega_{n,t+1}+\left(kr_{\omega q}+m_{\omega,q}\right)\omega_{q,t+1} \end{array}\right)\right]. \end{aligned}$$

Hence

$$\mathbb{E}_t^*\left[R_{M,t\to t+1}^k\right]=R_{f,t\to t+1}\exp\left(\begin{array}{c} kr_0+m_0+\left\{kr_p-g\left(kr_{\omega p}+m_{\omega,p}\right)\right\}p_t \\ +\left\{kr_n+m_n-g\left(m_{\omega,n}+kr_{\omega n}\right)\right\}n_t \\ +\left(kr_q+m_q\right)q_t+\left(kr_s-g\left(kr_{\omega q}+m_{\omega,q}\right)\right)s_t \end{array}\right). \tag{IA.89}$$

Now, let us find the truncated moments. Observe that

$$\begin{aligned} kr_{t+1} &= kr_0+kr_pp_t+kr_nn_t+kr_qq_t+kr_ss_t \\ &\quad +kr_{\omega p}\omega_{p,t+1}+kr_{\omega n}\omega_{n,t+1}+kr_{\omega q}\omega_{q,t+1} \\ &= kr_0+\left(kr_p-kr_{\omega p}\right)p_t+\left(kr_n-kr_{\omega n}\right)n_t \\ &\quad +kr_qq_t+\left(kr_s-kr_{\omega q}\right)s_t \\ &\quad +kr_{\omega p}\left(\omega_{p,t+1}+p_t\right)+kr_{\omega n}\left(\omega_{n,t+1}+n_t\right) \\ &\quad +kr_{\omega q}\left(\omega_{q,t+1}+s_t\right) \\ &= \xi_{r,t}+Z_{t+1,r} \end{aligned}$$

where

$$\begin{aligned} \xi_{r,t} &= kr_0+\left(kr_p-kr_{\omega p}\right)p_t+\left(kr_n-kr_{\omega n}\right)n_t+kr_qq_t+\left(kr_s-kr_{\omega q}\right)s_t \\ Z_{t+1,r} &= kr_{\omega p}\left(\omega_{p,t+1}+p_t\right)+kr_{\omega n}\left(\omega_{n,t+1}+n_t\right)+kr_{\omega q}\left(\omega_{q,t+1}+s_t\right). \end{aligned}$$

Hence

$$\mathbb{E}_t\left[R_{M,t\to t+1}^k\mathbb{I}_{\left\{R_{M,t\to t+1}>a\right\}}\right]=e^{\xi_{r,t}}\mathbb{E}_t\left[e^{Z_{t+1,r}}\mathbb{I}_{\left\{Z_{t+1,r}>k\ln a-\xi_{r,t}\right\}}\right]$$

Next, let us find $\mathbb{E}_t^*\left[R_{M,t\to t+1}^k\mathbb{I}_{\left\{R_{M,t\to t+1}>a\right\}}\right]$. Observe that

$$\mathbb{E}_t^*\left[R_{M,t\to t+1}^k\mathbb{I}_{\left\{R_{M,t\to t+1}>a\right\}}\right]=R_{f,t\to t+1}\mathbb{E}_t\left[e^{m_{t+1}+\xi_{r,t}+Z_{t+1,r}}\mathbb{I}_{\left\{Z_{t+1,r}>k\log a-\xi_{r,t}\right\}}\right].$$

Now, observe that

$$\begin{aligned} & m_{t+1} + \xi_{r,t} + Z_{t+1,r} \\ = \; & m_0 + m_q q_t + m_n n_t + m_{\omega,p}\omega_{p,t+1} + m_{\omega,n}\omega_{n,t+1} + m_{\omega,q}\omega_{q,t+1} \\ & + kr_0 + (kr_p - kr_{\omega p})\, p_t + (kr_n - kr_{\omega n})\, n_t + kr_q q_t + (kr_s - kr_{\omega q})\, s_t \\ & + kr_{\omega p}\,(\omega_{p,t+1} + p_t) + kr_{\omega n}\,(\omega_{n,t+1} + n_t) + kr_{\omega q}\,(\omega_{q,t+1} + s_t) \end{aligned}$$

which simplifies to

$$\begin{aligned} & m_{t+1} + \xi_{r,t} + Z_{t+1,r} \\ = \; & m_0 + kr_0 \\ & + (kr_p - kr_{\omega p} - m_{\omega,p})\, p_t + (kr_n - kr_{\omega n} + m_n - m_{\omega,n})\, n_t \\ & + (kr_s - kr_{\omega q} - m_{\omega,q})\, s_t + (kr_q + m_q)\, q_t \\ & + (m_{\omega,p} + kr_{\omega p})\,(\omega_{p,t+1} + p_t) + (m_{\omega,n} + kr_{\omega n})\,(\omega_{n,t+1} + n_t) \\ & + (kr_{\omega q} + m_{\omega,q})\,(\omega_{q,t+1} + s_t) \\ = \; & \zeta_r + Z_{t+1,m} \end{aligned}$$

with

$$\begin{aligned} \zeta_r \;=\; & m_0 + kr_0 + (kr_p - kr_{\omega p} - m_{\omega,p})\, p_t + (kr_n - kr_{\omega n} + m_n - m_{\omega,n})\, n_t \\ & + (kr_s - kr_{\omega q} - m_{\omega,q})\, s_t + (kr_q + m_q)\, q_t \end{aligned}$$

and

$$\begin{aligned} Z_{t+1,m} \;=\; & (m_{\omega,p} + kr_{\omega p})\,(\omega_{p,t+1} + p_t) + (m_{\omega,n} + kr_{\omega n})\,(\omega_{n,t+1} + n_t) \\ & + (kr_{\omega q} + m_{\omega,q})\,(\omega_{q,t+1} + s_t) \end{aligned}$$

The model without preference shocks obtains when the state variable s_t is set to zero and the following parameter restrictions are imposed:[64]

$$\overline{s} = \rho_s = \sigma_{qq} = \phi_d = \phi_g = \gamma_n = m_n = m_{\omega q} = 0. \tag{IA.90}$$

■

IA.8.7 Disaster Risk Models

IA.8.7.1 Gabaix (2012)

We follow the Dew-Becker et al. (2017) implementation of Gabaix (2012) (including their parameter choices). The key processes that drive the economy are

$$\begin{aligned} \Delta c_{t+1} &= \mu_c + \sigma_c \varepsilon_{c,t+1} + J_{c,t+1}, \\ L_{t+1} &= (1 - \rho_L)\,\overline{L} + \rho_L L_t + \sigma_L \varepsilon_{L,t+1}, \\ \Delta d_{t+1} &= \eta \sigma_c \varepsilon_{c,t+1} - L_t \mathbb{I}_{J_{c_{t+1}} \neq 0}, \end{aligned}$$

where L_t represents the recovery rate of stocks in a disaster. $J_{c,t+1}$ is a disaster shock that affects the consumption and dividend processes, and follows a compound Poisson process given by

$$J_{c,t} = \sum_{i=1}^{N_t} \xi_{i,t} \text{ where } N_t \sim \text{Poisson}\,(\lambda) \text{ and } \xi_{i,t} \sim N\,(\mu_d, \sigma_d)\,.$$

[64] Note that $\rho_p = \sigma_{pp} = 0$ in both the model with and that without preference shocks.

The number of disasters, N_t, that occur each period follow a Poisson process with intensity λ. $\mathbb{I}$ is an indicator function. $J_{c,t+1}$, $\varepsilon_{L,t+1}$ and $\varepsilon_{c,t+1}$ are independent. In Gabaix (2012), the representative agent has power utility with risk aversion parameter γ. In this setting the SDF takes the form:

$$M_{t\to t+1} = \delta \left(\frac{C_{t+1}}{C_t}\right)^{-\gamma}$$

where δ is the time discount rate. The log-SDF is

$$m_{t+1} = \log \delta - \gamma \Delta c_{t+1}.$$

Thus, the log of the return on the risk-free asset is

$$\begin{aligned}
\log R_{f,t+1} &= -\log\left(\mathbb{E}_t e^{m_{t+1}}\right) \\
&= -\log\left(\mathbb{E}_t e^{(\log\delta - \gamma\Delta c_{t+1})}\right) \\
&= -\log\left(\mathbb{E}_t \exp\left\{\log\delta - \gamma\mu_c - \gamma\sigma_c\varepsilon_{c,t+1} - \gamma J_{c,t+1}\right\}\right) \\
&= -\log\delta + \gamma\mu_c - \log\mathbb{E}_t \exp\left\{-\gamma\sigma_c\varepsilon_{c,t+1} - \gamma J_{c,t+1}\right\}.
\end{aligned}$$

Note that

$$\mathbb{E}_t \exp\left\{-\gamma\sigma_c\varepsilon_{c,t+1} - \gamma J_{c,t+1}\right\} = \left(\mathbb{E}_t \exp\left\{-\gamma\sigma_c\varepsilon_{c,t+1}\right\}\right)\left(\mathbb{E}_t \exp\left\{-\gamma J_{c,t+1}\right\}\right).$$

Since

$$\mathbb{E}_t \exp\left\{-\gamma J_{c,t+1}\right\} = \exp\left(\lambda\left(e^{\varphi_G} - 1\right)\right)$$

with

$$\varphi_G = -\gamma\mu_d + \frac{1}{2}\gamma^2\sigma_d^2.$$

Hence

$$\mathbb{E}_t \exp\left\{-\gamma\sigma_c\varepsilon_{c,t+1} - \gamma J_{c,t+1}\right\} = \exp\left\{\frac{1}{2}\gamma^2\sigma_c^2 + \lambda\left(e^{\varphi_G} - 1\right)\right\}.$$

Thus

$$\log R_{f,t+1} = -\log\delta + \gamma\mu_c - \frac{1}{2}\gamma^2\sigma_c^2 - \lambda\left(e^{\varphi_G} - 1\right).$$

Now, let us compute the physical and risk neutral moments. We use the Campbell and Shiller (1988) to approximate multiples of the log market return as

$$nr_{m,t+1} \approx n\kappa_0 + n\kappa_1 pd_{t+1} - npd_t + n\Delta d_{t+1}$$

Next, we project the log price-dividend ratio (pd_t) on the stock recovery rate, L_t, at each date. In this model, the log price-dividend ratio is not linear in the state variable, L_t. To approximate pd_t as a function of L_t, we project it onto basis functions and impose that the Euler equation holds (approximately) at each point in L_t. Denote the projected price-dividend ratio using

$$pd_t = f\left[L_t\right].$$

The physical non-central moment of the market return is

$$\mathbb{E}_t\left[R_{M,t\to t+1}^n\right] = \mathbb{E}_t\left[e^{nr_{m,t+1}}\right]$$

Similarly, the non-central truncated moment

$$\mathbb{E}_t\left[R^n_{M,t\to t+1}\mathbb{I}_{R_{M,t\to t+1}>a}\right]=\mathbb{E}_t\left[e^{nr_{m,t+1}}\mathbb{I}_{R_{M,t\to t+1}>a}\right]$$

Expressions for the non-central risk neutral and truncated non-central risk neutral moments are

$$\mathbb{E}^*_t\left[R^n_{M,t\to t+1}\right]=R_{f,t\to t+1}\mathbb{E}_t\left[e^{nr_{m,t+1}+m_{t+1}}\right],$$

and

$$\mathbb{E}^*_t\left[R^n_{M,t\to t+1}\mathbb{I}_{R_{M,t\to t+1}>a}\right]=R_{f,t\to t+1}\mathbb{E}_t\left[e^{nr_{m,t+1}+m_{t+1}}\mathbb{I}_{R_{M,t\to t+1}>a}\right].$$

Multiples of the log market return are given by

$$nr_{m,t+1}\approx n\kappa_0+n\kappa_1 f\left[L_{t+1}\right]-nf\left[L_t\right]+n\Delta d_{t+1}.$$

Given the state variable, L_t, we can use this expression to compute the physical and risk-neutral moments above.

IA.8.7.2 Wachter (2013)

We follow the Dew-Becker et al. (2017) discretization of Wachter (2013) (including their parameter choices) so that we can evaluate a monthly-frequency version of this model. The key processes that drive the economy are given by

$$\begin{aligned}\Delta c_{t+1}&=\mu_c+\sigma_c z_{c,t+1}+J_{t+1},\\ \lambda_{t+1}&=(1-\rho_\lambda)\mu_\lambda+\rho_\lambda\lambda_t+\sigma_\lambda\sqrt{\lambda_t}z_{\lambda,t+1},\\ \Delta d_{t+1}&=\phi\mu_c+\phi\sigma_c z_{c,t+1}+\phi J_{t+1},\end{aligned}$$

where the shocks $z_{c,t+1}$ and $z_{\lambda,t+1}$ are uncorrelated and follow standard normal distributions. J_{t+1} follows a compound Poisson process given by

$$J_{t+1}=\sum_{i=1}^{N_{t+1}}\xi_{i,t+1}\text{ where }N_{t+1}\sim\text{Poisson}\left(\lambda_t\right)\text{ and }\xi_{i,t+1}\sim N\left(\mu_d,\sigma_d\right).$$

The number of disasters, N_t, that occur each period follow a Poisson process with intensity λ_t. The variables $z_{c,t+1}$, $z_{\lambda,t+1}$, and J_{t+1} are assumed to be independent. Following Dew-Becker et al. (2017), the household utility is

$$\upsilon_t=(1-\beta)\log C_t+\frac{\beta}{1-\alpha}\log\mathbb{E}_t\left(e^{((1-\alpha)\upsilon_{t+1})}\right),\tag{IA.91}$$

and the log-SDF takes the form

$$m_{t+1}=\log\beta-\Delta c_{t+1}+(1-\alpha)\upsilon_{t+1}-\log\left(\mathbb{E}_t\exp\left\{(1-\alpha)\upsilon_{t+1}\right\}\right).$$

Main Results

Result IA.13. *Given the state variable, λ_t, the model-implied log price-dividend ratio is given by*

$$\log\frac{P_t}{D_t}=A_{0,m}+A_{1,m}\lambda_t,$$

where $A_{0,m}$ and $A_{1,m}$ are given below.

Proof. See below. ■

Result IA.14. *For any $n > 0$, the non-central physical moment of the market return is*

$$\mathbb{E}_t\left(R_{M,t+1}^n\right) = \exp\left\{\begin{array}{c} n\kappa_0 + n\left(\kappa_1 - 1\right)A_{0,m} + n\kappa_1 A_{1,m}\left(1-\rho_\lambda\right)\mu_\lambda \\ +n\phi\mu_c + \frac{1}{2}\left(n\phi\sigma_c\right)^2 \\ +\left\{n\left(\kappa_1\rho_\lambda - 1\right)A_{1,m} + \frac{1}{2}\left(n\kappa_1 A_{1,m}\sigma_\lambda\right)^2 + \left(e^{\varphi_\phi} - 1\right)\right\}\lambda_t \end{array}\right\}$$

with

$$\varphi_\phi = \left(n\phi\right)\mu_d + \frac{1}{2}\left(n\phi\right)^2\sigma_d^2.$$

The truncated non-central physical moment is

$$\mathbb{E}_t\left(R_{M,t\to t+1}^n 1_{R_{M,t\to t+1}>a}\right) = \mathbb{E}_t\left(e^{\mathcal{A}_t + Z_{t+1}} 1_{\mathcal{A}_t + Z_{t+1} > n\log a}\right),$$

where

$$\begin{array}{rcl} \mathcal{A}_t & = & n\kappa_0 + n\left(\kappa_1 - 1\right)A_{0,m} + n\kappa_1 A_{1,m}\left(1-\rho_\lambda\right)\mu_\lambda \\ & & +n\left(\kappa_1\rho_\lambda - 1\right)A_{1,m}\lambda_t + n\phi\mu_c \\ Z_{t+1} & = & n\kappa_1 A_{1,m}\sigma_\lambda\sqrt{\lambda_t}z_{\lambda,t+1} + n\phi\sigma_c z_{c,t+1} + n\phi J_{t+1}. \end{array}$$

All parameters are defined below.

Proof. See below. ■

Result IA.15. *The non-central risk neutral-moments of the market return are*

$$\mathbb{E}_t^*\left[R_{M,t\to t+1}^n\right] = R_{f,t\to t+1}\exp\left(\mathbb{A}_0^* + \mathbb{A}_1^*\lambda_t\right)$$

where

$$\mathbb{A}_0^* = \left\{\begin{array}{c} n\kappa_0 + n\left(\kappa_1 - 1\right)A_{0,m} + n\kappa_1 A_{1,m}\left(1-\rho_\lambda\right)\mu_\lambda \\ +A_0^s + A_2^s\left(1-\rho_\lambda\right)\mu_\lambda + n\phi\mu_c + A_3^s\mu_c \\ +\frac{1}{2}\left(n\phi + A_3^s\right)^2\sigma_c^2 \end{array}\right\}$$

and

$$\mathbb{A}_1^* = \left\{\begin{array}{c} n\left(\kappa_1\rho_\lambda - 1\right)A_{1,m} + A_1^s + A_2^s\rho_\lambda \\ +\frac{1}{2}\left(n\kappa_1 A_{1,m} + A_2^s\right)^2\sigma_\lambda^2 + \left(e^{\varphi_{\phi,s}^*} - 1\right) \end{array}\right\}$$

with

$$\varphi_{\phi,s}^* = \left(n\phi + A_3^s\right)\mu_d + \frac{1}{2}\left(n\phi + A_3^s\right)^2\sigma_d^2.$$

The truncated non-central risk-neutral moments of the market return are

$$\mathbb{E}_t^*\left(R_{M,t+1}^n 1_{R_{M,t+1}>a}\right) = R_{f,t+1}\mathbb{E}_t\left\{\mathcal{N}\left[d_{1,t+1}^*\right]\left(\exp\left\{\mathcal{A}_t^*\right\}\right)\exp\left\{\mu_{z,t+1}^* + \frac{1}{2}\sigma_{z,t+1}^{*2}\right\}\right\}$$

where

$$\mathbb{E}_t^*\left(R_{M,t+1}^n 1_{R_{M,t+1}>a}\right) = R_{f,t+1}\mathbb{E}_t\left(e^{m_{t+1}+nr_{m,t+1}}1_{R_{M,t+1}>a}\right)$$

Note that

$$m_{t+1} + nr_{m,t+1} = Z_{t+1}^* + \mathcal{A}_t^*$$

where

$$Z_{t+1}^* = \left\{n\kappa_1 A_{1,m} + A_2^s\right\}\sigma_\lambda\sqrt{\lambda_t}z_{\lambda,t+1} + \left(n\phi + A_3^s\right)\sigma_c z_{c,t+1} + \left(n\phi + A_3^s\right)J_{t+1}$$

and

$$\begin{aligned}\mathcal{A}_t^* &= \left\{\begin{array}{c} n\kappa_0 + n\left(\kappa_1 - 1\right)A_{0,m} + n.\kappa_1 A_{1,m}\left(1-\rho_\lambda\right)\mu_\lambda \\ \\ +A_0^s + A_2^s\left(1-\rho_\lambda\right)\mu_\lambda + n\phi\mu_c + A_3^s\mu_c \end{array}\right\} \\ &\quad + \left\{n\left(\kappa_1\rho_\lambda - 1\right)A_{1,m} + A_1^s + A_2^s\rho_\lambda\right\}\lambda_t.\end{aligned}$$

All parameters are defined below.

Proof. See below. ■

Derivations and Proofs We start with a conjecture that the log utility-consumption ratio is a linear function of the intensity λ_t

$$\upsilon_t - \log C_t = A_0 + A_1\lambda_t. \tag{IA.92}$$

This allows us to express $(1-\alpha)\upsilon_{t+1}$ as

$$\begin{aligned}(1-\alpha)\upsilon_{t+1} &= (1-\alpha)\log C_t + (1-\alpha)\left(\log C_{t+1} - \log C_t\right) \\ &\quad + (1-\alpha)A_0 + A_1(1-\alpha)\lambda_{t+1}.\end{aligned}$$

Hence

$$\begin{aligned}\mathbb{E}_t \exp\left\{(1-\alpha)\, v_{t+1}\right\} &= \left(\exp\left\{(1-\alpha)\log C_t\right\}\right)\mathbb{E}_t\left(\exp\left\{\begin{array}{c}(1-\alpha)\,\Delta c_{t+1}+(1-\alpha)\,A_0\\ +A_1\,(1-\alpha)\,\lambda_{t+1}\end{array}\right\}\right)\\ &= \left(\exp\left\{\begin{array}{c}(1-\alpha)\log C_t + A_1\,(1-\alpha)\,\rho_\lambda\lambda_t\\ (1-\alpha)\,\mu_c+(1-\alpha)\,A_0\\ +A_1\,(1-\alpha)\,(1-\rho_\lambda)\,\mu_\lambda\end{array}\right\}\right)\\ &\quad\times\mathbb{E}_t\left(\exp\left\{\begin{array}{c}(1-\alpha)\,\sigma_c z_{c,t+1}+(1-\alpha)\,J_{t+1}\\ +A_1\,(1-\alpha)\,\sigma_\lambda\sqrt{\lambda_t}z_{\lambda,t+1}\end{array}\right\}\right)\end{aligned}$$

which simplifies to

$$\begin{aligned}\mathbb{E}_t \exp\left\{(1-\alpha)\, v_{t+1}\right\} &= \left(\exp\left\{\begin{array}{c}(1-\alpha)\log C_t + A_1\,(1-\alpha)\,\rho_\lambda\lambda_t\\ (1-\alpha)\,\mu_c+(1-\alpha)\,A_0\\ +A_1\,(1-\alpha)\,(1-\rho_\lambda)\,\mu_\lambda\\ +\frac{1}{2}\,(1-\alpha)^2\,\sigma_c^2+\frac{1}{2}A_1^2\,(1-\alpha)^2\,\sigma_\lambda^2\lambda_t\end{array}\right\}\right)\\ &\quad\times\mathbb{E}_t\left(\exp\left\{(1-\alpha)\, J_{t+1}\right\}\right).\end{aligned}$$

Note that

$$\mathbb{E}_t\left(\exp\left\{(1-\alpha)\, J_{t+1}\right\}\right)=\mathbb{E}_t\left(\mathbb{E}_t\left(\exp\left\{(1-\alpha)\, J_{t+1}\right\}|N_{t+1}\right)\right).$$

Thus

$$\begin{aligned}\mathbb{E}_t\left(\exp\left\{(1-\alpha)\, J_{t+1}\right\}|N_{t+1}\right) &= \exp\left\{(1-\alpha)\,\mu_d N_{t+1}+\frac{N_{t+1}}{2}\,(1-\alpha)^2\,\sigma_d^2\right\}\\ &= \exp\left\{\varphi_\alpha N_{t+1}\right\},\end{aligned}$$

where

$$\varphi_\alpha=(1-\alpha)\,\mu_d+\frac{1}{2}\,(1-\alpha)^2\,\sigma_d^2.$$

Therefore,

$$\mathbb{E}_t\left(\exp\left\{(1-\alpha)\, J_{t+1}\right\}\right)=\mathbb{E}_t\left(\exp\left\{\varphi_\alpha N_{t+1}\right\}\right)=\exp\left(\lambda_t\left(e^{\varphi_\alpha}-1\right)\right).$$

Consequently,

$$\mathbb{E}_t \exp\left\{(1-\alpha)\, v_{t+1}\right\} = \exp\left\{\begin{array}{c} (1-\alpha)\log C_t + A_1 (1-\alpha)\rho_\lambda \lambda_t \\ (1-\alpha)\mu_c + (1-\alpha) A_0 \\ +A_1 (1-\alpha)(1-\rho_\lambda)\mu_\lambda \\ +\frac{1}{2}(1-\alpha)^2 \sigma_c^2 + \frac{1}{2} A_1^2 (1-\alpha)^2 \sigma_\lambda^2 \lambda_t \\ +\lambda_t (e^{\varphi_\alpha} - 1) \end{array}\right\}.$$

Note that:

$$v_t = (1-\beta)\log C_t + \frac{\beta}{1-\alpha}\log \mathbb{E}_t\left(e^{((1-\alpha)v_{t+1})}\right).$$

We then replace this expression in Equation IA.91 and show:

$$v_t = (1-\beta)\log C_t + \left(\frac{\beta}{1-\alpha}\right)\left\{\begin{array}{c} (1-\alpha)\log C_t + A_1 (1-\alpha)\rho_\lambda \lambda_t \\ (1-\alpha)\mu_c + (1-\alpha) A_0 \\ +A_1 (1-\alpha)(1-\rho_\lambda)\mu_\lambda \\ +\frac{1}{2}(1-\alpha)^2 \sigma_c^2 + \frac{1}{2} A_1^2 (1-\alpha)^2 \sigma_\lambda^2 \lambda_t \\ +\lambda_t (e^{\varphi_\alpha} - 1) \end{array}\right\}$$

which simplifies to

$$\begin{aligned} v_t - \log C_t &= \left\{\beta\mu_c + \beta A_0 + A_1\beta(1-\rho_\lambda)\mu_\lambda + \frac{1}{2}\beta(1-\alpha)\sigma_c^2\right\} \\ &\quad + \left\{A_1\beta\rho_\lambda + \frac{1}{2}A_1^2\beta(1-\alpha)\sigma_\lambda^2 + \left(\frac{\beta}{1-\alpha}\right)(e^{\varphi_\alpha}-1)\right\}\lambda_t. \end{aligned}$$

By identification with Equation IA.92, we deduce

$$\begin{aligned} A_0 &= \beta\mu_c + \beta A_0 + A_1\beta(1-\rho_\lambda)\mu_\lambda + \frac{1}{2}\beta(1-\alpha)\sigma_c^2 \\ A_1 &= A_1\beta\rho_\lambda + \frac{1}{2}A_1^2\beta(1-\alpha)\sigma_\lambda^2 + \left(\frac{\beta}{1-\alpha}\right)(e^{\varphi_\alpha}-1). \end{aligned}$$

Thus,

$$A_0 = \frac{1}{1-\beta}\left\{\beta\mu_c + A_1\beta(1-\rho_\lambda)\mu_\lambda + \frac{1}{2}\beta(1-\alpha)\sigma_c^2\right\}$$

and

$$0 = 2A_1(\beta\rho_\lambda - 1) + A_1^2\beta(1-\alpha)\sigma_\lambda^2 + 2\left(\frac{\beta}{1-\alpha}\right)(e^{\varphi_\alpha}-1)$$

which implies

$$A_1 = \frac{(1-\beta\rho_\lambda) \pm \sqrt{(\beta\rho_\lambda - 1)^2 - \left\{2\left(\frac{\beta}{1-\alpha}\right)\left(e^{\varphi_\alpha}-1\right)\right\}\left\{\beta\left(1-\alpha\right)\sigma_\lambda^2\right\}}}{\beta\left(1-\alpha\right)\sigma_\lambda^2}.$$

We choose the negative A_1. Note that

$$\upsilon_t - \log C_t = A_0 + A_1\lambda_t.$$

The log-SDF takes the form

$$m_{t+1} = \log\beta - \Delta c_{t+1} + (1-\alpha)\,\upsilon_{t+1} - \log\left(\mathbb{E}_t \exp\left\{(1-\alpha)\,\upsilon_{t+1}\right\}\right)$$

which simplifies to

$$\begin{aligned} m_{t+1} &= \log\beta - \Delta c_{t+1} + (1-\alpha)\,A_0 + (1-\alpha)\,A_1\lambda_{t+1} \\ &\quad + (1-\alpha)\log C_{t+1} - \log\left(\mathbb{E}_t \exp\left\{(1-\alpha)\,\upsilon_{t+1}\right\}\right) \end{aligned}$$

and hence

$$\begin{aligned} m_{t+1} &= \left\{\begin{array}{c} \log\beta - (1-\alpha)\,\mu_c \\ -A_1\left(1-\alpha\right)\left(1-\rho_\lambda\right)\mu_\lambda - \frac{1}{2}\left(1-\alpha\right)^2\sigma_c^2 \end{array}\right\} \\ &\quad -\alpha\Delta c_{t+1} + (1-\alpha)\,A_1\lambda_{t+1} \\ &\quad + \left\{-A_1\left(1-\alpha\right)\rho_\lambda - \frac{1}{2}A_1^2\left(1-\alpha\right)^2\sigma_\lambda^2 - \left(e^{\varphi_\alpha}-1\right)\right\}\lambda_t. \end{aligned}$$

Thus,

$$m_{t+1} = A_0^{\mathrm{s}} + A_1^{\mathrm{s}}\lambda_t + A_2^{\mathrm{s}}\lambda_{t+1} + A_3^{\mathrm{s}}\Delta c_{t+1},$$

where

$$\begin{aligned} A_0^{\mathrm{s}} &= \log\beta - (1-\alpha)\,\mu_c - A_1\left(1-\alpha\right)\left(1-\rho_\lambda\right)\mu_\lambda - \frac{1}{2}\left(1-\alpha\right)^2\sigma_c^2, \\ A_1^{\mathrm{s}} &= -A_1\left(1-\alpha\right)\rho_\lambda - \frac{1}{2}A_1^2\left(1-\alpha\right)^2\sigma_\lambda^2 - \left(e^{\varphi_\alpha}-1\right), \\ A_2^{\mathrm{s}} &= A_1\left(1-\alpha\right), \\ A_3^{\mathrm{s}} &= -\alpha. \end{aligned}$$

The return on the risk-free asset is given by

$$\log R_{f,t\to t+1} = -\log\mathbb{E}_t\left(M_{t\to t+1}\right).$$

Note that

$$\begin{aligned}
& \mathbb{E}_t\left(M_{t\to t+1}\right) \\
= \; & \mathbb{E}_t \exp\left\{A_0^{\mathrm{s}} + A_1^{\mathrm{s}}\lambda_t + A_2^{\mathrm{s}}\lambda_{t+1} + A_3^{\mathrm{s}}\Delta c_{t+1}\right\} \\
= \; & \left(\exp\left\{A_0^{\mathrm{s}} + A_1^{\mathrm{s}}\lambda_t\right\}\right)\mathbb{E}_t \exp\left\{A_2^{\mathrm{s}}\lambda_{t+1} + A_3^{\mathrm{s}}\Delta c_{t+1}\right\} \\
= \; & \left(\exp\left\{\begin{array}{c} A_0^{\mathrm{s}} + A_3^{\mathrm{s}}\mu_c + A_2^{\mathrm{s}}\left(1-\rho_\lambda\right)\mu_\lambda + \frac{1}{2}\left(A_3^{\mathrm{s}}\right)^2\sigma_c^2 \\ +A_1^{\mathrm{s}}\lambda_t + A_2^{\mathrm{s}}\rho_\lambda\lambda_t + \frac{1}{2}\left(A_2^{\mathrm{s}}\right)^2\sigma_\lambda^2\lambda_t \end{array}\right\}\right)\mathbb{E}_t \exp\left\{A_3^{\mathrm{s}}J_{t+1}\right\}.
\end{aligned}$$

Now, note that

$$\mathbb{E}_t\left(\exp\left\{A_3^{\mathrm{s}}J_{t+1}\right\}\right) = \mathbb{E}_t \exp\left\{A_3^{\mathrm{s}}\mu_d N_{t+1} + \frac{N_{t+1}}{2}\left(A_3^{\mathrm{s}}\right)^2\sigma_d^2\right\} = \mathbb{E}_t \exp\left\{\varphi^s N_{t+1}\right\},$$

where

$$\varphi_s = A_3^{\mathrm{s}}\mu_d + \frac{1}{2}\left(A_3^{\mathrm{s}}\right)^2\sigma_d^2.$$

Hence,

$$\mathbb{E}_t\left(\exp\left\{A_3^{\mathrm{s}}J_{t+1}\right\}\right) = \mathbb{E}_t\left\{\exp\left(\lambda_t\left(e^{\varphi_s}-1\right)\right)\right\}.$$

Finally,

$$\mathbb{E}_t\left(M_{t\to t+1}\right) = \exp\left\{\begin{array}{c} A_0^{\mathrm{s}} + A_3^{\mathrm{s}}\mu_c + A_2^{\mathrm{s}}\left(1-\rho_\lambda\right)\mu_\lambda + \frac{1}{2}\left(A_3^{\mathrm{s}}\right)^2\sigma_c^2 \\ +A_1^{\mathrm{s}}\lambda_t + A_2^{\mathrm{s}}\rho_\lambda\lambda_t + \frac{1}{2}\left(A_2^{\mathrm{s}}\right)^2\sigma_\lambda^2\lambda_t \\ +\lambda_t\left(e^{\varphi_s}-1\right) \end{array}\right\}.$$

and

$$\log R_{f,t\to t+1} = A_0^{\mathrm{rf}} + A_1^{\mathrm{rf}}\lambda_t,$$

where

$$\begin{aligned}
A_0^{\mathrm{rf}} &= -\left\{A_0^{\mathrm{s}} + A_3^{\mathrm{s}}\mu_c + A_2^{\mathrm{s}}\left(1-\rho_\lambda\right)\mu_\lambda + \frac{1}{2}\left(A_3^{\mathrm{s}}\right)^2\sigma_c^2\right\}, \\
A_1^{\mathrm{rf}} &= -\left\{A_1^{\mathrm{s}} + A_2^{\mathrm{s}}\rho_\lambda + \frac{1}{2}\left(A_2^{\mathrm{s}}\right)^2\sigma_\lambda^2 + \left(e^{\varphi_s}-1\right)\right\}.
\end{aligned}$$

Following Dew-Becker et al. (2017), we use the Campbell and Shiller (1988) approximation to express the log market return as

$$r_{m,t+1} \approx \kappa_0 + \kappa_1 pd_{t+1} - pd_t + \Delta d_{t+1}$$

where pd_t is the log price-dividend ratio.

We provide a proof of Result IA.13 below.

Proof. Proof of Result IA.13. We conjecture that pd_t is linear in the state variables

$$pd_t = A_{0,m} + A_{1,m}\lambda_t. \tag{IA.93}$$

Thus,

$$\begin{aligned} r_{m,t+1} &\approx \kappa_0 + \kappa_1 \left(A_{0,m} + A_{1,m}\lambda_{t+1}\right) - \left(A_{0,m} + A_{1,m}\lambda_t\right) \\ &\quad + \left(\phi\mu_c + \phi\sigma_c z_{c,t+1} + \phi J_{t+1}\right) \\ &= \kappa_0 + \kappa_1 A_{0,m} + \kappa_1 A_{1,m}\lambda_{t+1} - A_{0,m} - A_{1,m}\lambda_t \\ &\quad + \phi\mu_c + \phi\sigma_c z_{c,t+1} + \phi J_{t+1}. \end{aligned}$$

This expands to

$$\begin{aligned} r_{m,t+1} &= \kappa_0 + \left(\kappa_1 - 1\right) A_{0,m} + \kappa_1 A_{1,m}\left(1 - \rho_\lambda\right)\mu_\lambda + \left(\kappa_1\rho_\lambda - 1\right) A_{1,m}\lambda_t \\ &\quad + \kappa_1 A_{1,m}\sigma_\lambda\sqrt{\lambda_t} z_{\lambda,t+1} + \phi\mu_c + \phi\sigma_c z_{c,t+1} + \phi J_{t+1}. \end{aligned}$$

To identify $A_{0,m}$ and $A_{1,m}$, we use the Euler equation

$$\log\left(\mathbb{E}_t e^{\left(m_{t+1} + r_{m,t+1}\right)}\right) = 0.$$

Note that

$$\begin{aligned} m_{t+1} + r_{m,t+1} &= \left\{\kappa_0 + \left(\kappa_1 - 1\right) A_{0,m} + \kappa_1 A_{1,m}\left(1 - \rho_\lambda\right)\mu_\lambda\right\} + \phi\mu_c + A_0^{\mathrm{s}} \\ &\quad + \left\{\left(\kappa_1\rho_\lambda - 1\right) A_{1,m} + A_1^{\mathrm{s}}\right\}\lambda_t + \kappa_1 A_{1,m}\sigma_\lambda\sqrt{\lambda_t} z_{\lambda,t+1} \\ &\quad + \phi\sigma_c z_{c,t+1} + \phi J_{t+1} + A_2^{\mathrm{s}}\lambda_{t+1} + A_3^{\mathrm{s}}\Delta c_{t+1} \end{aligned}$$

which simplifies to

$$\begin{aligned} m_{t+1} + r_{m,t+1} &= \left\{ \begin{array}{c} \kappa_0 + \left(\kappa_1 - 1\right) A_{0,m} + \kappa_1 A_{1,m}\left(1 - \rho_\lambda\right)\mu_\lambda \\ \\ + A_3^{\mathrm{s}}\mu_c + \phi\mu_c + A_0^{\mathrm{s}} + A_2^{\mathrm{s}}\left(1 - \rho_\lambda\right)\mu_\lambda \end{array} \right\} \\ &\quad + \left\{\left(\kappa_1\rho_\lambda - 1\right) A_{1,m} + A_1^{\mathrm{s}} + A_2^{\mathrm{s}}\rho_\lambda\right\}\lambda_t \\ &\quad + \left(\kappa_1 A_{1,m} + A_2^{\mathrm{s}}\right)\sigma_\lambda\sqrt{\lambda_t} z_{\lambda,t+1} \\ &\quad + \left(\phi\sigma_c + A_3^{\mathrm{s}}\sigma_c\right) z_{c,t+1} + \left(\phi + A_3^{\mathrm{s}}\right) J_{t+1} \end{aligned}$$

Thus

$$\begin{aligned} &\log \mathbb{E}_t e^{\left(m_{t+1} + r_{m,t+1}\right)} \\ &= \left\{ \begin{array}{c} \kappa_0 + \left(\kappa_1 - 1\right) A_{0,m} + \kappa_1 A_{1,m}\left(1 - \rho_\lambda\right)\mu_\lambda \\ \\ + \left(A_3^{\mathrm{s}} + \phi\right)\mu_c + A_0^{\mathrm{s}} + A_2^{\mathrm{s}}\left(1 - \rho_\lambda\right)\mu_\lambda + \frac{1}{2}\left(\phi\sigma_c + A_3^{\mathrm{s}}\sigma_c\right)^2 \end{array} \right\} \\ &\quad + \left\{ \begin{array}{c} \left(\kappa_1\rho_\lambda - 1\right) A_{1,m} + A_1^{\mathrm{s}} + A_2^{\mathrm{s}}\rho_\lambda \\ \\ + \frac{1}{2}\left(\kappa_1 A_{1,m} + A_2^{\mathrm{s}}\right)^2\sigma_\lambda^2 \end{array} \right\}\lambda_t + \log \mathbb{E}_t\left(\exp\left(\left(\phi + A_3^{\mathrm{s}}\right) J_{t+1}\right)\right). \end{aligned}$$

Note that

$$\mathbb{E}_t\left(\exp\left(\left(\phi + A_3^{\mathrm{s}}\right) J_{t+1}\right)\right) = \mathbb{E}_t \exp\left(\varphi_{\phi,s} N_{t+1}\right) = \exp\left(\lambda_t\left(e^{\varphi_{\phi,s}} - 1\right)\right),$$

where

$$\varphi_{\phi,s} = (\phi + A_3^s)\,\mu_d + \frac{1}{2}(\phi + A_3^s)^2\,\sigma_d^2.$$

Therefore,

$$\begin{aligned}
&\log \mathbb{E}_t e^{(m_{t+1}+r_{m,t+1})} \\
&= \left\{ \begin{array}{c} \kappa_0 + (\kappa_1 - 1)\,A_{0,m} + \kappa_1 A_{1,m}\,(1-\rho_\lambda)\,\mu_\lambda \\ +(A_3^s + \phi)\,\mu_c + A_0^s + A_2^s\,(1-\rho_\lambda)\,\mu_\lambda + \frac{1}{2}\,(\phi\sigma_c + A_3^s\sigma_c)^2 \end{array} \right\} \\
&+ \left\{ \begin{array}{c} (\kappa_1\rho_\lambda - 1)\,A_{1,m} + A_1^s + A_2^s\rho_\lambda \\ +\frac{1}{2}\,(\kappa_1 A_{1,m} + A_2^s)^2\,\sigma_\lambda^2 + (e^{\varphi_{\phi,s}} - 1) \end{array} \right\} \lambda_t. \qquad \text{(IA.94)}
\end{aligned}$$

Since, $\log \mathbb{E}_t e^{(m_{t+1}+r_{m,t+1})} = 0$, this implies that each term of Equation IA.94 is zero. As a result, the coefficients from the conjecture in Equation IA.93 are

$$A_{0,m} = \frac{1}{1-\kappa_1}\left\{ \begin{array}{c} \kappa_0 + \kappa_1 A_{1,m}\,(1-\rho_\lambda)\,\mu_\lambda + (A_3^s + \phi)\,\mu_c \\ +A_0^s + A_2^s\,(1-\rho_\lambda)\,\mu_\lambda + \frac{1}{2}\,(\phi\sigma_c + A_3^s\sigma_c)^2 \end{array} \right\}$$

and

$$2\left\{(\kappa_1\rho_\lambda - 1) + \kappa_1 A_2^s\sigma_\lambda^2\right\} A_{1,m} + \kappa_1^2\sigma_\lambda^2 A_{1,m}^2 + 2\left\{\frac{1}{2}\,(A_2^s)^2\,\sigma_\lambda^2 + A_1^s + A_2^s\rho_\lambda + (e^{\varphi_{\phi,s}} - 1)\right\}$$

which simplifies to

$$\mathcal{C} + 2\mathcal{B}.A_{1,m} + \mathcal{A}.A_{1,m}^2 = 0$$

where

$$\begin{aligned}
\mathcal{C} &= 2\left\{A_1^s + A_2^s\rho_\lambda + (e^{\varphi_{\phi,s}} - 1) + \frac{1}{2}\,(A_2^s)^2\,\sigma_\lambda^2\right\} \\
\mathcal{B} &= \left\{(\kappa_1\rho_\lambda - 1) + \kappa_1 A_2^s\sigma_\lambda^2\right\} \\
\mathcal{A} &= \kappa_1^2\sigma_\lambda^2.
\end{aligned}$$

Hence

$$A_{1,m} = \frac{-\mathcal{B} \pm \sqrt{\mathcal{B}^2 - \mathcal{A}.\mathcal{C}}}{\mathcal{A}}.$$

We choose the negative value $A_{1,m}$ as in Dew-Becker et al. (2017). We provide a proof of Result IA.14 below. ■

Proof. Proof of Result IA.14. Let us find the physical moments and truncated moments:

$$\mathbb{E}_t\left(R_{M,t+1}^n\right) = \mathbb{E}_t\left(e^{nr_{m,t+1}}\right).$$

Note that

$$\begin{aligned} nr_{m,t+1} &= n\kappa_0 + n\left(\kappa_1 - 1\right) A_{0,m} + n\kappa_1 A_{1,m}\left(1-\rho_\lambda\right)\mu_\lambda \\ &\quad + n\left(\kappa_1\rho_\lambda - 1\right) A_{1,m}\lambda_t + n\kappa_1 A_{1,m}\sigma_\lambda\sqrt{\lambda_t}z_{\lambda,t+1} \\ &\quad + n\phi\mu_c + n\phi\sigma_c z_{c,t+1} + n\phi J_{t+1}. \end{aligned}$$

Hence

$$\begin{aligned} \mathbb{E}_t\left(R^n_{M,t+1}\right) &= \exp\left\{\begin{array}{c} n\kappa_0 + n\left(\kappa_1 - 1\right) A_{0,m} + n\kappa_1 A_{1,m}\left(1-\rho_\lambda\right)\mu_\lambda \\ +n\phi\mu_c + \frac{1}{2}\left(n\phi\sigma_c\right)^2 \\ + \left\{n\left(\kappa_1\rho_\lambda - 1\right) A_{1,m} + \frac{1}{2}\left(n\kappa_1 A_{1,m}\sigma_\lambda\right)^2\right\}\lambda_t \end{array}\right\} \\ &\quad \times \mathbb{E}_t\left(\exp\left\{n\phi J_{t+1}\right\}\right). \end{aligned}$$

Note that

$$\mathbb{E}_t\left(\exp\left(\left(n\phi\right)J_{t+1}\right)\right) = \mathbb{E}_t\exp\left(\varphi_\phi N_{t+1}\right) = \exp\left(\lambda_t\left(e^{\varphi_\phi} - 1\right)\right),$$

where

$$\varphi_\phi = \left(n\phi\right)\mu_d + \frac{1}{2}\left(n\phi\right)^2\sigma_d^2.$$

Thus,

$$\mathbb{E}_t\left(R^n_{M,t+1}\right) = \exp\left\{\begin{array}{c} n\kappa_0 + n\left(\kappa_1 - 1\right) A_{0,m} + n\kappa_1 A_{1,m}\left(1-\rho_\lambda\right)\mu_\lambda \\ +n\phi\mu_c + \frac{1}{2}\left(n\phi\sigma_c\right)^2 \\ + \left\{n\left(\kappa_1\rho_\lambda - 1\right) A_{1,m} + \frac{1}{2}\left(n\kappa_1 A_{1,m}\sigma_\lambda\right)^2 + \left(e^{\varphi_\phi} - 1\right)\right\}\lambda_t \end{array}\right\}.$$

Now, let us find the truncated moments

$$\begin{aligned} \mathbb{E}_t\left(R^n_{M,t+1}1_{R_{M,t+1}>a}\right) &= \mathbb{E}_t\left(e^{nr_{m,t+1}}1_{nr_{m,t+1}>n\log a}\right) \\ &= \mathbb{E}_t\left(e^{nr_{m,t+1}}1_{nr_{m,t+1}>n\log a}\right) \end{aligned}$$

Note that

$$nr_{m,t+1} = \mathcal{A}_t + Z_{t+1}$$

where

$$\begin{aligned} \mathcal{A}_t &= n\kappa_0 + n\left(\kappa_1 - 1\right) A_{0,m} + n\kappa_1 A_{1,m}\left(1-\rho_\lambda\right)\mu_\lambda \\ &\quad + n\left(\kappa_1\rho_\lambda - 1\right) A_{1,m}\lambda_t + n\phi\mu_c \\ Z_{t+1} &= n\kappa_1 A_{1,m}\sigma_\lambda\sqrt{\lambda_t}z_{\lambda,t+1} + n\phi\sigma_c z_{c,t+1} + n\phi J_{t+1} \end{aligned}$$

■

Proof. Let us compute the risk neutral moments

$$\begin{aligned}\log \mathbb{E}_t^* \left(R_{M,t+1}^n\right) &= \log\left\{\mathbb{E}_t\left(\frac{M_{t+1}}{\mathbb{E}_t M_{t+1}} R_{M,t+1}^n\right)\right\} \\ &= \log R_{f,t+1} + \log\left\{\mathbb{E}_t\left(e^{m_{t+1}+nr_{m,t+1}}\right)\right\}.\end{aligned}$$

Observe that

$$\begin{aligned}m_{t+1}+nr_{m,t+1} &= n\kappa_0 + n\left(\kappa_1-1\right)A_{0,m} + n\kappa_1 A_{1,m}\left(1-\rho_\lambda\right)\mu_\lambda \\ &\quad + n\left(\kappa_1\rho_\lambda - 1\right)A_{1,m}\lambda_t + n\kappa_1 A_{1,m}\sigma_\lambda\sqrt{\lambda_t}z_{\lambda,t+1} \\ &\quad + n\phi\mu_c + n\phi\sigma_c z_{c,t+1} + n\phi J_{t+1} \\ &\quad + A_0^{\mathrm{s}} + A_1^{\mathrm{s}}\lambda_t + A_2^{\mathrm{s}}\lambda_{t+1} + A_3^{\mathrm{s}}c_{t+1},\end{aligned}$$

which simplifies to

$$\begin{aligned}m_{t+1}+nr_{m,t+1} &= \left\{\begin{array}{c} n\kappa_0 + n\left(\kappa_1-1\right)A_{0,m} + n\kappa_1 A_{1,m}\left(1-\rho_\lambda\right)\mu_\lambda \\ \\ +A_0^{\mathrm{s}} + A_2^{\mathrm{s}}\left(1-\rho_\lambda\right)\mu_\lambda + n\phi\mu_c + A_3^{\mathrm{s}}\mu_c \end{array}\right\} \\ &\quad + \left\{n\left(\kappa_1\rho_\lambda-1\right)A_{1,m} + A_1^{\mathrm{s}} + A_2^{\mathrm{s}}\rho_\lambda\right\}\lambda_t \\ &\quad + \left\{n\kappa_1 A_{1,m} + A_2^{\mathrm{s}}\right\}\sigma_\lambda\sqrt{\lambda_t}z_{\lambda,t+1} \\ &\quad + \left(n\phi + A_3^{\mathrm{s}}\right)\sigma_c z_{c,t+1} + \left(n\phi + A_3^{\mathrm{s}}\right)J_{t+1}.\end{aligned}$$

Thus,

$$\mathbb{E}_t^*\left[R_{M,t\to t+1}^n\right] = R_{f,t+1}\exp\left(\begin{array}{c} \left\{\begin{array}{c} n\kappa_0 + n\left(\kappa_1-1\right)A_{0,m} + n\kappa_1 A_{1,m}\left(1-\rho_\lambda\right)\mu_\lambda \\ \\ +A_0^{\mathrm{s}} + A_2^{\mathrm{s}}\left(1-\rho_\lambda\right)\mu_\lambda + n\phi\mu_c + A_3^{\mathrm{s}}\mu_c \end{array}\right\} \\ \\ + \left\{n\left(\kappa_1\rho_\lambda-1\right)A_{1,m} + A_1^{\mathrm{s}} + A_2^{\mathrm{s}}\rho_\lambda\right\}\lambda_t \\ \\ +\frac{1}{2}\left(n\kappa_1 A_{1,m} + A_2^{\mathrm{s}}\right)^2\sigma_\lambda^2\lambda_t \\ \\ +\frac{1}{2}\left(n\phi + A_3^{\mathrm{s}}\right)^2\sigma_c^2 + \lambda_t\left(e^{\varphi_{\phi,s}^*}-1\right) \end{array}\right).$$

Since

$$\mathbb{E}_t\left(\exp\left(\left(n\phi + A_3^{\mathrm{s}}\right)J_{t+1}\right)\right) = \exp\left(\lambda_t\left(e^{\varphi_{\phi,s}^*}-1\right)\right),$$

where

$$\varphi_{\phi,s}^* = \left(n\phi + A_3^{\mathrm{s}}\right)\mu_d + \frac{1}{2}\left(n\phi + A_3^{\mathrm{s}}\right)^2\sigma_d^2.$$

Now, let us compute the truncated risk neutral moment

$$\mathbb{E}_t^*\left(R_{M,t+1}^n 1_{R_{M,t+1}>a}\right) = R_{f,t+1}\mathbb{E}_t\left(e^{m_{t+1}+nr_{m,t+1}}1_{R_{M,t+1}>a}\right).$$

Note that

$$m_{t+1}+nr_{m,t+1} = Z_{t+1}^* + \mathcal{A}_t^*$$

where

$$Z_{t+1}^{*} = \left\{n\kappa_1 A_{1,m} + A_2^{\mathrm{s}}\right\}\sigma_\lambda\sqrt{\lambda_t}z_{\lambda,t+1} + \left(n\phi + A_3^{\mathrm{s}}\right)\sigma_c z_{c,t+1} + \left(n\phi + A_3^{\mathrm{s}}\right)J_{t+1}$$

and

$$\begin{aligned}\mathcal{A}_t^{*} &= \left\{\begin{array}{c} n\kappa_0 + n\left(\kappa_1 - 1\right)A_{0,m} + n.\kappa_1 A_{1,m}\left(1-\rho_\lambda\right)\mu_\lambda \\ \\ +A_0^{\mathrm{s}} + A_2^{\mathrm{s}}\left(1-\rho_\lambda\right)\mu_\lambda + n\phi\mu_c + A_3^{\mathrm{s}}\mu_c \end{array}\right\} \\ &\quad + \left\{n\left(\kappa_1\rho_\lambda - 1\right)A_{1,m} + A_1^{\mathrm{s}} + A_2^{\mathrm{s}}\rho_\lambda\right\}\lambda_t.\end{aligned}$$

Given the state variable λ_t, the truncated risk-neutral moment can be computed at each date. ■

IA.9 Estimating Components in the Risk Quantity and Risk Price Decomposition

In this section, we describe how we estimate all quantities needed for the risk price and risk quantity decomposition described in Proposition 4 both in the data and in the context of the representative agent models. In all cases, we must construct estimates of $\mathbb{P}_t\left[\mathbb{I}_{A_s}\right]$ (the probability of ending up in region A_s) and $\mathbb{E}_t\left[\frac{\mathbb{E}_t[M_{t\to T}]}{M_{t\to T}}\mathbb{I}_{A_s}\right]$. Given estimates of these quantities, we can compute the risk price, $\sigma_{t,M,s}^{*2} \equiv \left(\mathbb{E}_t\left[\frac{\mathbb{E}_t[M_{t\to T}]}{M_{t\to T}}\mathbb{I}_{A_s}\right] - \mathbb{E}_t^{*}\left[\frac{\mathbb{E}_t[M_{t\to T}]}{M_{t\to T}}\mathbb{I}_{A_s}\right]\right) + \mathbb{VAR}_t\left[\mathbb{I}_{A_s}\right]$, since $\mathbb{VAR}_t\left[\mathbb{I}_{A_s}\right] \equiv \mathbb{P}_t\left[\mathbb{I}_{A_s}\right]\left(1-\mathbb{P}_t\left[\mathbb{I}_{A_s}\right]\right)$ and $\mathbb{E}_t^{*}\left[\frac{\mathbb{E}_t[M_{t\to T}]}{M_{t\to T}}\mathbb{I}_{A_s}\right] \equiv \mathbb{P}_t\left[\mathbb{I}_{A_s}\right]$. Given an estimate for $\sigma_{t,M,s}^{*2}$ and our risk premium estimates, $\mathbb{RP}_{t\to T}^{(1)}\left[A_s\right]$, we use Equation 34 to compute the implied risk quantity, $\beta_{t,s}^{*}$.

IA.9.1 Data-Implied Risk Quantities and Prices

First, we can simply use Corollary 1 with $n = 0$ to construct estimates of $\mathbb{P}_t\left[\mathbb{I}_{A_s}\right]$ at different horizons. Next, to compute $\mathbb{E}_t\left[\frac{\mathbb{E}_t[M_{t\to T}]}{M_{t\to T}}\right]$, we can use Equation 19 to express $\frac{\mathbb{E}_t[M_{t\to T}]}{M_{t\to T}}\mathbb{I}_{A_s}$ as

$$\frac{\mathbb{E}_t\left[M_{t\to T}\right]}{M_{t\to T}}\mathbb{I}_{A_s} = \frac{\mathbb{I}_{A_s} + \sum_{k=1}^{\infty}\theta_k\left(x_s\right)\sum_{j=0}^{k}\frac{k!}{j!(k-j)!}\left(-1\right)^j\left(x_s - R_{f,t\to T}\right)^j\left(x_T - R_{f,t\to T}\right)^{k-j}\mathbb{I}_{A_s}}{1 + \sum_{k=1}^{\infty}\theta_k\left(x_s\right)\sum_{j=0}^{k}\frac{k!}{j!(k-j)!}\left(-1\right)^j\left(x_s - R_{f,t\to T}\right)^j\mathbb{E}_t^{*}\left(x_T - R_{f,t\to T}\right)^{k-j}}.$$

Taking expectations under the physical measure on both sides of the above equation yields

$$\mathbb{E}_t\left[\frac{\mathbb{E}_t\left[M_{t\to T}\right]}{M_{t\to T}}\mathbb{I}_{A_s}\right] = \frac{\mathbb{P}_t\left[\mathbb{I}_{A_s}\right] + \sum_{k=1}^{\infty}\theta_k\left(x_s\right)\sum_{j=0}^{k}\frac{k!}{j!(k-j)!}\left(-1\right)^j\left(x_s - R_{f,t\to T}\right)^j\mathbb{E}_t\left[\left(x_T - R_{f,t\to T}\right)^{k-j}\mathbb{I}_{A_s}\right]}{1 + \sum_{k=1}^{\infty}\theta_k\left(x_s\right)\sum_{j=0}^{k}\frac{k!}{j!(k-j)!}\left(-1\right)^j\left(x_s - R_{f,t\to T}\right)^j\mathbb{E}_t^{*}\left(x_T - R_{f,t\to T}\right)^{k-j}} \quad \text{(IA.95)}$$

We use Corollary 1 to estimate the necessary physical moments, $\mathbb{E}_t\left[\left(x_T - R_{f,t\to T}\right)^{k-j}\mathbb{I}_{A_s}\right]$, and truncate the outer summation at $k = 3$ as we do when estimating other physical moments in the paper.

IA.9.2 Model-Implied Risk Quantities and Prices

Our strategy for computing $\mathbb{P}_t\left[\mathbb{I}_{A_s}\right]$ and $\mathbb{E}_t\left[\frac{\mathbb{E}_t[M_{t\to T}]}{M_{t\to T}}\mathbb{I}_{A_s}\right]$ is model-dependent, and we go through each case in turn below. In each case, we make use of information highlighted in Internet Appendix IA.8 regarding each model's setup.

IA.9.2.1 Bansal and Yaron (2004) and Bansal, Kiku, and Yaron (2012)

The log SDF from Internet Appendix IA.8.5.1 is

$$\log M_{t\to t+1} = \theta\log\delta - \frac{\theta}{\psi}\Delta c_{t+1} - (1-\theta)\left(\kappa_0 + \kappa_1 z_{t+1} - z_t + \Delta c_{t+1}\right)$$

and the log market return is

$$\log R_{M,t\to t+1} = \mathbb{A}^{\mathrm{m}}_{0,t} + \mathbb{A}^{\mathrm{m}}_{x,t}\eta_{x,t+1} + \mathbb{A}^{\mathrm{m}}_{\omega}\omega_{t+1} + \mathbb{A}^{\mathrm{m}}_{d,t}\eta_{d,t+1} + \mathbb{A}^{\mathrm{m}}_{c,t}\eta_{c,t+1}$$

with

$$\begin{aligned}
\mathbb{A}^{\mathrm{m}}_{0,t} &= \mathbb{A}^{\mathrm{er}}_0 + \mathbb{A}^{\mathrm{er}}_1 x_t + \mathbb{A}^{\mathrm{er}}_2\sigma_t^2\\
\mathbb{A}^{\mathrm{m}}_{x,t} &= \kappa_{1,m}A_{1,m}\phi_x\sigma_t\\
\mathbb{A}^{\mathrm{m}}_{\omega} &= \kappa_{1,m}A_{2,m}\phi_\sigma\\
\mathbb{A}^{\mathrm{m}}_{d,t} &= \phi_d\sigma_t\\
\mathbb{A}^{\mathrm{m}}_{c,t} &= \phi_{d,c}\sigma_t.
\end{aligned}$$

Thus, and since shocks in this model are normally-distributed,

$$\begin{aligned}
\mathbb{P}_t\left[\mathbb{I}_{A_d}\right] &= \mathbb{P}_t\left[R_{M,t\to t+1} < \underline{x}\right]\\
&= \mathbb{P}_t\left[\log R_{M,t\to t+1} < \log\underline{x}\right]\\
&= \mathbb{P}_t\left[\mathbb{A}^{\mathrm{m}}_{0,t} + \mathbb{A}^{\mathrm{m}}_{x,t}\eta_{x,t+1} + \mathbb{A}^{\mathrm{m}}_{\omega}\omega_{t+1} + \mathbb{A}^{\mathrm{m}}_{d,t}\eta_{d,t+1} + \mathbb{A}^{\mathrm{m}}_{c,t}\eta_{c,t+1} < \log\underline{x}\right]\\
&= \mathbb{P}_t\left[\mathbb{A}^{\mathrm{m}}_{x,t}\eta_{x,t+1} + \mathbb{A}^{\mathrm{m}}_{\omega}\omega_{t+1} + \mathbb{A}^{\mathrm{m}}_{d,t}\eta_{d,t+1} + \mathbb{A}^{\mathrm{m}}_{c,t}\eta_{c,t+1} < \log\underline{x} - \mathbb{A}^{\mathrm{m}}_{0,t}\right]\\
&= \mathbb{P}_t\left[Z_{N(0,1)} < \frac{\log\underline{x} - \mathbb{A}^{\mathrm{m}}_{0,t}}{\sqrt{\left(\mathbb{A}^{\mathrm{m}}_{x}\right)^2 + \left(\mathbb{A}^{\mathrm{m}}_{\omega}\right)^2 + \left(\mathbb{A}^{\mathrm{m}}_{d}\right)^2 + \left(\mathbb{A}^{\mathrm{m}}_{c}\right)^2}}\right].
\end{aligned}$$

Next

$$\begin{aligned}
\mathbb{P}_t\left[\mathbb{I}_{A_u}\right] &= \mathbb{P}_t\left[R_{M,t\to t+1} > \overline{x}\right]\\
&= 1 - \mathbb{P}_t\left[R_{M,t\to t+1} < \overline{x}\right]\\
&= 1 - \mathbb{P}_t\left[Z_{N(0,1)} < \frac{\log\overline{x} - \mathbb{A}^{\mathrm{m}}_{0,t}}{\sqrt{\left(\mathbb{A}^{\mathrm{m}}_{x,t}\right)^2 + \left(\mathbb{A}^{\mathrm{m}}_{\omega}\right)^2 + \left(\mathbb{A}^{\mathrm{m}}_{d,t}\right)^2 + \left(\mathbb{A}^{\mathrm{m}}_{c,t}\right)^2}}\right],
\end{aligned}$$

and

$$\begin{aligned}
\mathbb{P}_t\left[\mathbb{I}_{A_c}\right] &= \mathbb{P}_t\left[\underline{x} < R_{M,t\to t+1} < \overline{x}\right]\\
&= 1 - \left(\mathbb{P}_t\left[R_{M,t\to t+1} < \underline{x}\right] + \mathbb{P}_t\left[R_{M,t\to t+1} > \overline{x}\right]\right).
\end{aligned}$$

Next, we have

$$\begin{aligned}\log \frac{\mathbb{E}_t M_{t\to t+1}}{M_{t\to t+1}} &= \log \frac{1}{R_{f,t\to t+1} M_{t\to t+1}} \\ &= -\log R_{f,t\to t+1} - \log M_{t\to t+1},\end{aligned}$$

where $R_{f,t\to t+1}$ is the risk-free rate implied by the model. We replace $\log R_{f,t\to t+1}$ and $\log M_{t\to t+1}$ by their expressions from Internet Appendix IA.8.5.1 and obtain

$$\log \frac{\mathbb{E}_t M_{t\to t+1}}{M_{t\to t+1}} = -\log R_{f,t\to t+1} - A^{\text{sdf}}_{0,t} - A^{\text{sdf}}_{c,t}\eta_{c,t+1} - A^{\text{sdf}}_{x,t}\eta_{x,t+1} - A^{\text{sdf}}_{\omega}\omega_{t+1}$$

with

$$\begin{aligned}A^{\text{sdf}}_{0,t} &= \theta \log \delta + \left\{-\frac{\theta}{\psi} - (1-\theta)\right\}\mu_c - (1-\theta)\kappa_0 - (1-\theta)\kappa_1 A_0 \\ &\quad - (1-\theta)\kappa_1 A_2 \overline{\sigma}^2 (1-\nu) + (1-\theta) A_0 \\ &\quad + \left\{-\frac{\theta}{\psi} - (1-\theta) - (1-\theta)\kappa_1 A_1 \rho + (1-\theta) A_1\right\} x_t + (1-\kappa_1\nu)(1-\theta) A_2 \sigma_t^2 \\ A^{\text{sdf}}_{c,t} &= \left\{-\frac{\theta}{\psi} - (1-\theta)\right\}\phi_c \sigma_t \\ A^{\text{sdf}}_{x} &= -(1-\theta)\kappa_1 A_1 \phi_x \sigma_t \\ A^{\text{sdf}}_{\omega} &= -(1-\theta)\kappa_1 A_2 \phi_\sigma.\end{aligned}$$

Next, note that

$$\frac{\mathbb{E}_t M_{t\to t+1}}{M_{t\to t+1}} = \exp\left(-\log R_{f,t\to t+1} - A^{\text{sdf}}_{0,t} - A^{\text{sdf}}_{c,t}\eta_{c,t+1} - A^{\text{sdf}}_{x,t}\eta_{x,t+1} - A^{\text{sdf}}_{\omega}\omega_{t+1}\right).$$

Given the state variables we recover at time t, we simulate the multivariate normal $\mathcal{N}(0,1)$ for $(\eta_{x,t+1}, \omega_{t+1}, \eta_{d,t+1}, \eta_{c,t+1})$ one million times and compute $\frac{\mathbb{E}_t M_{t\to t+1}}{M_{t\to t+1}}$ and $R_{M,t\to t+1}$. This us allows us to estimate $\mathbb{E}_t\left[\frac{\mathbb{E}_t[M_{t\to T}]}{M_{t\to T}}\mathbb{I}_{A_s}\right]$ and $\mathbb{P}_t\left[\mathbb{I}_{A_s}\right]$ as the average of the respective simulated data at each date. We can also derive a closed-form expression for $\mathbb{E}_t\left[\frac{\mathbb{E}_t M_{t\to t+1}}{M_{t\to t+1}}\right]$, which we use as a check on the simulations, as:

$$\mathbb{E}_t\left[\frac{\mathbb{E}_t M_{t\to t+1}}{M_{t\to t+1}}\right] = \exp\left(-\log R_{f,t\to t+1} - A^{\text{sdf}}_{0,t} + \frac{1}{2}\left(\left(A^{\text{sdf}}_{c,t}\right)^2 + \left(A^{\text{sdf}}_{x,t}\right)^2 + \left(A^{\text{sdf}}_{\omega}\right)^2\right)\right).$$

IA.9.2.2 Drechsler and Yaron (2011)

We can always express the log inverse SDF as

$$\log \frac{\mathbb{E}_t M_{t\to t+1}}{M_{t\to t+1}} = -\log R_{f,t\to t+1} - \log M_{t\to t+1}.$$

In this model (see Internet Appendix IA.8.5.3), we have

$$\log M_{t\to t+1} = \left\{\theta \log \delta - (1-\theta)\left[\kappa_0 + A_0(\kappa_1 - 1)\right] - (\theta - 1) A' Y_t\right\} - \Lambda' Y_{t+1},$$

$$\log R_{f,t\to t+1} = -\left\{\begin{array}{c} \theta\log\delta + \mathbf{f}\left(-\Lambda\right) \\ -\left(1-\theta\right)\left[\kappa_0 + A_0\left(\kappa_1 - 1\right)\right] \end{array}\right\} - \left(\left(1-\theta\right)A + \mathbf{g}\left(-\Lambda\right)\right)' Y_t,$$

and

$$\log R_{M,t\to t+1} = \left(\kappa_{0,m} + \kappa_{1,m}A_{0,m} - A_{0,m}\right) - A_m' Y_t + \left(\kappa_{1,m}A_m + e_d\right)' Y_{t+1}.$$

Given the state variables we recover at time t, we simulate the multivariate normal N(0,1) for the shocks, z_{t+1}, in this model along with jumps J_{t+1} five million times and compute $\frac{\mathbb{E}_t M_{t\to t+1}}{M_{t\to t+1}}$ and $R_{M,t\to t+1}$. This us allows us to estimate $\mathbb{E}_t\left[\frac{\mathbb{E}_t[M_{t\to T}]}{M_{t\to T}}\mathbb{I}_{A_s}\right]$ and $\mathbb{P}_t\left[\mathbb{I}_{A_s}\right]$ as the average of the respective simulated data at each date. We can also derive a closed-form expression for $\mathbb{E}_t\left[\frac{\mathbb{E}_t M_{t\to t+1}}{M_{t\to t+1}}\right]$, which we use as a check on the simulations, using the expression

$$\frac{\mathbb{E}_t M_{t\to t+1}}{M_{t\to t+1}} = \exp\left\{-\log R_{f,t\to t+1} - \left\{\begin{array}{c} \theta\log\delta - \left(1-\theta\right)\left[\kappa_0 + A_0\left(\kappa_1 - 1\right)\right] \\ -\left(\theta-1\right)A' Y_t \end{array}\right\} + \Lambda' Y_{t+1}\right\}.$$

Taking expectations yields

$$\begin{aligned}\mathbb{E}_t\left[\frac{\mathbb{E}_t M_{t\to t+1}}{M_{t\to t+1}}\right] &= \exp\left\{-\log R_{f,t\to t+1} - \left\{\begin{array}{c} \theta\log\delta - \left(1-\theta\right)\left[\kappa_0 + A_0\left(\kappa_1 - 1\right)\right] \\ -\left(\theta-1\right)A' Y_t \end{array}\right\}\right\} \\ &\quad \times\mathbb{E}_t\left(\exp\Lambda' Y_{t+1}\right)\end{aligned}$$

where

$$\mathbb{E}_t\left[\exp\Lambda' Y_{t+1}\right] = \exp\left(\mathbf{f}\left(\Lambda\right) + \mathbf{g}\left(\Lambda\right)Y_t\right).$$

IA.9.2.3 Habit Formation Models: Bekaert, Engstrom, and Ermolov (2023)

We can always express the log inverse SDF as

$$\log\frac{\mathbb{E}_t M_{t\to t+1}}{M_{t\to t+1}} = -\log R_{f,t\to t+1} - \log M_{t\to t+1}.$$

In this model (see Internet Appendix IA.8.6), we have:

$$\log M_{t\to t+1} = m_0 + m_q q_t + m_n n_t + m_{\omega,p}\omega_{p,t+1} + m_{\omega,n}\omega_{n,t+1} + m_{\omega,q}\omega_{q,t+1},$$

$$\log R_{f,t\to t+1} = f_0 + f_q q_t + f_n n_t + f_p p_t + f_s s_t,$$

and

$$\log R_{M,t\to t+1} = r_0 + r_p p_t + r_n n_t + r_q q_t + r_s s_t + r_{\omega p}\omega_{p,t+1} + r_{\omega n}\omega_{n,t+1} + r_{\omega q}\omega_{q,t+1}.$$

Given the state variables we recover at time t, we simulate the shocks, $(\omega_{p,t+1}, \omega_{n,t+1}, \omega_{q,t+1})$, 50 million times and compute $\frac{\mathbb{E}_t M_{t\to t+1}}{M_{t\to t+1}}$ and $R_{M,t\to t+1}$. This us allows us to estimate $\mathbb{E}_t\left[\frac{\mathbb{E}_t[M_{t\to T}]}{M_{t\to T}}\mathbb{I}_{A_s}\right]$ and $\mathbb{P}_t\left[\mathbb{I}_{A_s}\right]$ as the average of the respective simulated data at each date. We can also derive a

closed-form expression for $\mathbb{E}_t\left[\frac{\mathbb{E}_t M_{t\to t+1}}{M_{t\to t+1}}\right]$, which we use as a check on the simulations, using the expression

$$\begin{aligned}\log\frac{\mathbb{E}_t M_{t\to t+1}}{M_{t\to t+1}} &= -\log R_{f,t\to t+1} - \log M_{t\to t+1}\\ &= -\log R_{f,t\to t+1} - m_0 - m_q q_t - m_n n_t\\ &\quad -m_{\omega,p}\omega_{p,t+1} - m_{\omega,n}\omega_{n,t+1} - m_{\omega,q}\omega_{q,t+1}.\end{aligned}$$

Taking expectations yields

$$\begin{aligned}\mathbb{E}_t\left[\frac{\mathbb{E}_t M_{t\to t+1}}{M_{t\to t+1}}\right] &= \mathbb{E}_t\left[\exp\begin{pmatrix}-\log R_{f,t\to t+1} - m_0 - m_q q_t - m_n n_t\\ -m_{\omega,p}\omega_{p,t+1} - m_{\omega,n}\omega_{n,t+1} - m_{\omega,q}\omega_{q,t+1}\end{pmatrix}\right]\\ &= \exp\begin{pmatrix}-\log R_{f,t\to t+1} - m_0 - m_q q_t - m_n n_t\\ -g\left(-m_{\omega,p}\right)p_t - g\left(-m_{\omega,n}\right)n_t - g\left(-m_{\omega,q}\right)s_t\end{pmatrix}.\end{aligned}$$

IA.9.2.4 Gabaix (2012)

We can always express the log inverse SDF as

$$\log\frac{\mathbb{E}_t M_{t\to t+1}}{M_{t\to t+1}} = -\log R_{f,t\to t+1} - \log M_{t\to t+1}.$$

In this model (see Internet Appendix IA.8.7.1), we have

$$\begin{aligned}\log\frac{\mathbb{E}_t M_{t\to t+1}}{M_{t\to t+1}} &= -\log R_{f,t\to t+1} - \log M_{t+1}\\ &= -\log R_{f,t\to t+1} - (\log\delta - \gamma\Delta c_{t+1})\end{aligned}$$

where

$$\Delta c_{t+1} = \mu_c + \sigma_c\varepsilon_{c,t+1} + J_{c,t+1}.$$

Thus,

$$\begin{aligned}\log\frac{\mathbb{E}_t M_{t\to t+1}}{M_{t\to t+1}} &= -\log R_{f,t\to t+1} - \log\delta + \gamma\Delta c_{t+1}\\ &= -\log R_{f,t\to t+1} - \log\delta + \gamma\left(\mu_c + \sigma_c\varepsilon_{c,t+1} + J_{c,t+1}\right)\\ &= -\log R_{f,t\to t+1} - \log\delta + \gamma\mu_c + \gamma\sigma_c\varepsilon_{c,t+1} + \gamma J_{c,t+1}\end{aligned}$$

The log-risk-free rate is

$$\log R_{f,t+1} = -\log\delta + \gamma\mu_c - \frac{1}{2}\gamma^2\sigma_c^2 - \lambda\left(e^{\varphi_G} - 1\right)$$

and the log-market return is

$$\log R_{M,t\to t+1} = \kappa_0 + \kappa_1 f\left[L_{t+1}\right] - n f\left[L_t\right] + n\Delta d_{t+1}.$$

Given the state variables we recover at time t, we simulate the shocks, $(\varepsilon_{c,t+1}, \varepsilon_{L,t+1}, J_{c,t+1})$, 10 million times and compute $\frac{\mathbb{E}_t M_{t\to t+1}}{M_{t\to t+1}}$ and $R_{M,t\to t+1}$. This us allows us to estimate $\mathbb{E}_t\left[\frac{\mathbb{E}_t[M_{t\to T}]}{M_{t\to T}}\mathbb{I}_{A_s}\right]$ and $\mathbb{P}_t\left[\mathbb{I}_{A_s}\right]$ as the average of the respective simulated data at each date. We can also derive a closed-form expression for $\mathbb{E}_t\left[\frac{\mathbb{E}_t M_{t\to t+1}}{M_{t\to t+1}}\right]$, which we use as a check on the simulations, using the expression

$$\frac{\mathbb{E}_t M_{t\to t+1}}{M_{t\to t+1}} = \exp\left\{-\log R_{f,t\to t+1} - \log\delta + \gamma\mu_c + \gamma\sigma_c\varepsilon_{c,t+1} + \gamma J_{c,t+1}\right\}.$$

Taking expectations yields

$$\begin{aligned}\mathbb{E}_t\left[\frac{\mathbb{E}_t M_{t\to t+1}}{M_{t\to t+1}}\right] &= \left(\exp\left\{-\log R_{f,t\to t+1} - \log\delta + \gamma\mu_c\right\}\right)\mathbb{E}_t\exp\left\{\gamma\sigma_c\varepsilon_{c,t+1} + \gamma J_{c,t+1}\right\}\\ &= \left(\exp\left\{-\log R_{f,t\to t+1} - \log\delta + \gamma\mu_c\right\}\right)\left(\mathbb{E}_t\exp\left\{\gamma\sigma_c\varepsilon_{c,t+1}\right\}\right)\left(\mathbb{E}_t\exp\left\{\gamma J_{c,t+1}\right\}\right)\end{aligned}$$

where

$$\mathbb{E}_t\exp\left\{\gamma J_{c,t+1}\right\} = \exp\left(\lambda\left(e^{\widetilde{\varphi}_G} - 1\right)\right)$$

with

$$\widetilde{\varphi}_G = \gamma\mu_d + \frac{1}{2}\gamma^2\sigma_d^2$$

and

$$\mathbb{E}_t\exp\left\{\gamma\sigma_c\varepsilon_{c,t+1}\right\} = \exp\left(\frac{1}{2}\gamma^2\sigma_c^2\right).$$

IA.9.2.5 Wachter (2013)

We can always express the log inverse SDF as

$$\log\frac{\mathbb{E}_t M_{t\to t+1}}{M_{t\to t+1}} = -\log R_{f,t\to t+1} - \log M_{t\to t+1}.$$

In this model (see Internet Appendix IA.8.7.2), we have

$$\log M_{t\to t+1} = A_0^s + A_1^s\lambda_t + A_2^s\lambda_{t+1} + A_3^s\Delta c_{t+1}.$$

The log-risk-free rate is

$$\log R_{f,t\to t+1} = A_0^{\text{rf}} + A_1^{\text{rf}}\lambda_t$$

and the log-market return is

$$\begin{aligned}\log R_{M,t\to t+1} &= \kappa_0 + (\kappa_1 - 1)A_{0,m} + \kappa_1 A_{1,m}(1-\rho_\lambda)\mu_\lambda + (\kappa_1\rho_\lambda - 1)A_{1,m}\lambda_t\\ &\quad + \kappa_1 A_{1,m}\sigma_\lambda\sqrt{\lambda_t}z_{\lambda,t+1} + \phi\mu_c + \phi\sigma_c z_{c,t+1} + \phi J_{t+1}.\end{aligned}$$

Given the state variables we recover at time t, we simulate the shocks, $(z_{\lambda,t+1}, z_{c,t+1}, J_{t+1})$, 10 million times and compute $\frac{\mathbb{E}_t M_{t\to t+1}}{M_{t\to t+1}}$ and $R_{M,t\to t+1}$. This us allows us to estimate $\mathbb{E}_t\left[\frac{\mathbb{E}_t[M_{t\to T}]}{M_{t\to T}}\mathbb{I}_{A_s}\right]$ and $\mathbb{P}_t\left[\mathbb{I}_{A_s}\right]$ as the average of the respective simulated data at each date. We can also derive a closed-form expression for $\mathbb{E}_t\left[\frac{\mathbb{E}_t M_{t\to t+1}}{M_{t\to t+1}}\right]$, which we use as a check on the simulations, using the

expression

$$\log \frac{\mathbb{E}_t M_{t\to t+1}}{M_{t\to t+1}} = -\log R_{f,t\to t+1} - A_0^s - A_1^s \lambda_t - A_2^s \lambda_{t+1} - A_3^s \Delta c_{t+1}.$$

Taking expectations yields

$$\begin{aligned}
\mathbb{E}_t\left[\frac{\mathbb{E}_t M_{t\to t+1}}{M_{t\to t+1}}\right] &= \mathbb{E}_t \exp\left\{-\log R_{f,t\to t+1} - A_0^s - A_1^s\lambda_t - A_2^s\lambda_{t+1} - A_3^s \Delta c_{t+1}\right\} \\
&= \exp\left\{-\log R_{f,t\to t+1} - A_0^s - A_1^s\lambda_t\right\} \mathbb{E}_t \exp\left\{-A_2^s\lambda_{t+1} - A_3^s \Delta c_{t+1}\right\} \\
&= \exp\left\{-\log R_{f,t\to t+1} - A_0^s - A_1^s\lambda_t\right\} \mathbb{E}_t \exp\left\{\begin{array}{c} -A_2^s\lambda_{t+1} \\ -A_3^s\left(\mu_c + \sigma_c z_{c,t+1} + J_{t+1}\right) \end{array}\right\} \\
&\quad \exp\left\{\begin{array}{c} -\log R_{f,t\to t+1} \\ -A_0^s - A_1^s\lambda_t - A_3^s\mu_c \end{array}\right\} \mathbb{E}_t \exp\left\{\begin{array}{c} -A_2^s\lambda_{t+1} - A_3^s\sigma_c z_{c,t+1} \\ -A_3^s J_{t+1} \end{array}\right\}.
\end{aligned}$$

Recall that

$$\lambda_{t+1} = (1-\rho_\lambda)\mu_\lambda + \rho_\lambda \lambda_t + \sigma_\lambda \sqrt{\lambda_t} z_{\lambda,t+1}.$$

Thus,

$$\begin{aligned}
\mathbb{E}_t\left[\frac{\mathbb{E}_t M_{t\to t+1}}{M_{t\to t+1}}\right] &= \exp\left\{\begin{array}{c} -\log R_{f,t\to t+1} \\ -A_0^s - A_1^s\lambda_t - A_3^s\mu_c \\ -A_2^s\left((1-\rho_\lambda)\mu_\lambda + \rho_\lambda\lambda_t\right) \end{array}\right\} \mathbb{E}_t \exp\left\{\begin{array}{c} -A_2^s\sigma_\lambda\sqrt{\lambda_t} z_{\lambda,t+1} \\ -A_3^s\sigma_c z_{c,t+1} - A_3^s J_{t+1} \end{array}\right\} \\
&= \exp\left\{\begin{array}{c} -\log R_{f,t\to t+1} \\ -A_0^s - A_1^s\lambda_t - A_3^s\mu_c \\ -A_2^s\left((1-\rho_\lambda)\mu_\lambda + \rho_\lambda\lambda_t\right) \end{array}\right\} \exp\left\{\begin{array}{c} +\frac{1}{2}\left(A_2^s\sigma_\lambda\right)^2\lambda_t \\ +\frac{1}{2}\left(A_3^s\sigma_c\right)^2 \end{array}\right\} \mathbb{E}_t \exp\left(-A_3^s J_{t+1}\right) \\
&= \exp\left\{\begin{array}{c} -\log R_{f,t\to t+1} \\ -A_0^s - A_1^s\lambda_t - A_3^s\mu_c \\ -A_2^s\left((1-\rho_\lambda)\mu_\lambda + \rho_\lambda\lambda_t\right) \\ +\frac{1}{2}\left(A_2^s\sigma_\lambda\right)^2\lambda_t + \frac{1}{2}\left(A_3^s\sigma_c\right)^2 \end{array}\right\} \mathbb{E}_t \exp\left(-A_3^s J_{t+1}\right).
\end{aligned}$$

Note that

$$\mathbb{E}_t \exp\left(-A_3^s J_{t+1}\right) = \exp\left(\lambda_t\left(e^{\overline{\varphi}} - 1\right)\right)$$

with

$$\overline{\varphi} = -A_3^s\mu_d + \frac{1}{2}\left(A_3^s\right)^2\sigma_d^2.$$

Hence,

$$\mathbb{E}_t\left\{\frac{\mathbb{E}_t M_{t\to t+1}}{M_{t\to t+1}}\right\} = \exp\left\{\begin{array}{c} -\log R_{f,t\to t+1} \\ -A_0^s - A_1^s\lambda_t - A_3^s\mu_c \\ -A_2^s\left(\left(1-\rho_\lambda\right)\mu_\lambda + \rho_\lambda\lambda_t\right) \\ +\frac{1}{2}\left(A_2^s\sigma_\lambda\right)^2\lambda_t + \frac{1}{2}\left(A_3^s\sigma_c\right)^2 \end{array}\right\}\exp\left(\lambda_t\left(e^{\overline{\varphi}}-1\right)\right).$$

IA.10 Discussion of Differences with Respect to the Decomposition in Beason and Schreindorfer (2022)

Beason and Schreindorfer (2022) present a related decomposition of the *unconditional* equity risk premium that generates different implications for the relative contributions for downside, central, and upside risk premia to the total risk premium compared to our results. Namely, results in Beason and Schreindorfer (2022) imply that their equivalent of the downside, central, and upside risk premia constitute (approximately) 80%, 30%, and -10% of the total equity risk premium, respectively. This empirical result is very different than our baseline results (Table 2, Panel B), which imply the downside and central risk premia contribute similar amounts to the total risk premium (unconditionally) at about 45% each, and the upside risk premium contributes about 10% of the total risk premium unconditionally. To understand these different empirical results, we discuss three differences between our methodology and that in Beason and Schreindorfer (2022). First, Beason and Schreindorfer (2022) use a slightly different definition of the risk premium decomposition than we use herein. Second, their unconditional decomposition makes use of different empirical techniques to estimate the physical and risk-neutral market return densities than we use herein. Third, Jensen's inequality effects could explain some of the discrepancy between our respective decomposition results. We discuss each of these issues in more detail below.

We begin by discussing the relationship between our definition of the equity risk premium decomposition relative to that in Beason and Schreindorfer (2022). Starting with their Equation 4 and redefining their net market returns, R, in that equation to be gross returns (to be consistent with our consistent use of gross market returns), their truncated of risk premium associated with market returns between x_1 and x_2 is given by:

$$\widetilde{\mathbb{RP}}^{(1)}\left[A_{x_{12}}\right] \equiv \int_{x_1}^{x_2} R_M\left(f\left(R_M\right) - f^*\left(R_M\right)\right)dR_M. \tag{IA.96}$$

We use $\widetilde{\mathbb{RP}}^{(1)}\left[A_{x_{12}}\right]$ to designate this risk premium to highlight that this definition is analogous to (but not exactly the same as) our definition of the risk premium, $\mathbb{RP}^{(1)}\left[A_s\right]$, in Equation 29.[65] f and f^* represent the unconditional physical and risk-neutral return densities, respectively. To highlight the differences between the two risk premium definitions, we focus on the downside region for clarity. This corresponds to our case where $A_s = A_d$. The same case is obtained from Equation IA.96 by setting $x_1 = 0$ and $x_2 = \underline{x}$, which is the cutoff for our downside region (0.9). In this case,

[65] We remove the "$t \to T$" subscripts for simplicity since Beason and Schreindorfer (2022) consider only the one-month horizon.

the Beason and Schreindorfer (2022) risk premium definition becomes:

$$\widetilde{\mathbb{RP}}^{(1)}\left[A_d\right] \equiv \int_0^{\underline{x}} R_M\left(f\left(R_M\right) - f^*\left(R_M\right)\right) dR_M. \tag{IA.97}$$

Equivalently, we can express this integral in terms of expectation operators:

$$\widetilde{\mathbb{RP}}^{(1)}\left[A_d\right] \equiv \mathbb{E}\left[R_M \mathbb{I}_{A_d}\right] - \mathbb{E}^*\left[R_M \mathbb{I}_{A_d}\right]$$

where $\mathbb{I}_{A_d}$ is an indicator function for realizations of market returns in region A_d (that is, $R_M \in [0, \underline{x}]$). Using the identity $R_M \equiv R_M - R_f + R_f$, we can express the Beason and Schreindorfer (2022) downside risk premium in terms of a component that is equivalent to the unconditional version of our downside risk premium, $\mathbb{RP}^{(1)}\left[A_d\right]$, plus a component that is equivalent to a contingent claim that pays off one dollar in the event that $R_M \in A_d$:

$$\begin{aligned}
\widetilde{\mathbb{RP}}^{(1)}\left[A_d\right] &\equiv \mathbb{E}\left[\left(R_M - R_f + R_f\right)\mathbb{I}_{A_d}\right] - \mathbb{E}^*\left[\left(R_M - R_f + R_f\right)\mathbb{I}_{A_d}\right] \\
&= \mathbb{E}\left[\left(R_M - R_f\right)\mathbb{I}_{A_d}\right] - \mathbb{E}^*\left[\left(R_M - R_f\right)\mathbb{I}_{A_d}\right] \\
&\quad + \mathbb{E}\left[R_f \mathbb{I}_{A_d}\right] - \mathbb{E}^*\left[R_f \mathbb{I}_{A_d}\right] \\
&\equiv \mathbb{RP}^{(1)}\left[A_d\right] + R_f\left(\mathbb{E}\left[\mathbb{I}_{A_d}\right] - \mathbb{E}^*\left[\mathbb{I}_{A_d}\right]\right).
\end{aligned} \tag{IA.98}$$

Intuitively, this discrepancy exists because Beason and Schreindorfer (2022) define the truncated equity risk premium in terms of market returns in Equation IA.96, whereas we define our truncated risk premia in terms of excess market returns throughout. Note that when integrating Equation IA.96 over the entire return space ($x_1 = 0$, $x_2 \to \infty$), the two definitions are consistent since $\int_0^\infty R_M f^*\left(R_M\right) dR_M = R_f$. However, the two definitions are distinct when the region of interest is a subset of the return space. For completeness, the truncated market risk premia in the central and upside regions in Beason and Schreindorfer (2022) are related to ours as follows:

$$\widetilde{\mathbb{RP}}^{(1)}\left[A_c\right] \equiv \mathbb{RP}^{(1)}\left[A_c\right] + R_f\left(\mathbb{E}\left[\mathbb{I}_{A_c}\right] - \mathbb{E}^*\left[\mathbb{I}_{A_c}\right]\right) \text{ and} \tag{IA.99}$$

$$\widetilde{\mathbb{RP}}^{(1)}\left[A_u\right] \equiv \mathbb{RP}^{(1)}\left[A_u\right] + R_f\left(\mathbb{E}\left[\mathbb{I}_{A_u}\right] - \mathbb{E}^*\left[\mathbb{I}_{A_u}\right]\right) \tag{IA.100}$$

Therefore, the unconditional truncated market risk premia under our definition will be different than those implied by the Beason and Schreindorfer (2022) by terms related to the risk premia on contingent claims of the form $\mathbb{E}\left[\mathbb{I}_{A_s}\right] - \mathbb{E}^*\left[\mathbb{I}_{A_s}\right]$ that pay off one dollar in each respective region of market returns, $s \in \{d, c, u\}$. We call these "Arrow-Debreu risk premia" and define

$$\mathbb{RP}_t^{(0)}\left[A_s\right] \equiv \mathbb{E}_t\left[\mathbb{I}_{A_s}\right] - \mathbb{E}_t^*\left[\mathbb{I}_{A_s}\right].$$

How do we expect these differences highlighted in Equations IA.98-IA.100 to manifest in terms of the measured truncated risk premia? Using our methodology, we can compute the conditional Arrow-Debreu risk premia, $\mathbb{RP}_t^{(0)}\left[A_s\right]$, by setting $n = 0$ in Corollary 1 to estimate $\mathbb{E}\left[\mathbb{I}_A\right]$ and using standard techniques described in Internet Appendix IA.5 to estimate the risk-neutral counterpart. We plot estimated $\mathbb{RP}_t^{(0)}\left[A_s\right]$ in Figure IA.19. The unconditional (over time) average values of $\mathbb{RP}_t^{(0)}\left[A_s\right]$ for $s \in \{d, c, u\}$ are -1.88%, 1.35%, and 0.58% (annualized and in percent), respectively. Our unconditional average values of $\mathbb{RP}_t^{(1)}\left[A_s\right]$ for $s \in \{d, c, u\}$ (reported in Table 2 and Figure 2) are 4.45%, 3.33%, and 0.97%, respectively (annualized and in percent). Therefore, the discrepancy in

the risk premium decomposition definitions could cause large differences in our measured $\mathbb{RP}^{(1)}[A_s]$ compared to $\widetilde{\mathbb{RP}}^{(1)}[A_s]$ implied by Beason and Schreindorfer (2022).

Our unconditional values of $\mathbb{RP}_t^{(0)}[A_s]$ imply the following relationships (all else equal) between our unconditional $\mathbb{RP}^{(1)}[A_s]$ and the $\widetilde{\mathbb{RP}}^{(1)}[A_s]$ values implied in Beason and Schreindorfer (2022):

$$\begin{aligned}
\widetilde{\mathbb{RP}}^{(1)}[A_d] &< \mathbb{RP}^{(1)}[A_d], \\
\widetilde{\mathbb{RP}}^{(1)}[A_c] &> \mathbb{RP}^{(1)}[A_c], \text{ and} \\
\widetilde{\mathbb{RP}}^{(1)}[A_u] &> \mathbb{RP}^{(1)}[A_u].
\end{aligned}$$

Figure 1 in Beason and Schreindorfer (2022) actually imply the opposite relationships between our respective truncated risk premia. Namely, their Figure 1 implies

$$\begin{aligned}
\widetilde{\mathbb{RP}}^{(1)}[A_d] &> \mathbb{RP}^{(1)}[A_d], \\
\widetilde{\mathbb{RP}}^{(1)}[A_c] &< \mathbb{RP}^{(1)}[A_c], \text{ and} \\
\widetilde{\mathbb{RP}}^{(1)}[A_u] &< \mathbb{RP}^{(1)}[A_u].
\end{aligned}$$

Why is this the case? This brings us to the second major difference between our decomposition and that in Beason and Schreindorfer (2022), which is related to how they estimate the physical and risk-neutral densities. In their case, they estimate f using realized historical returns and estimate f^* using an optimization approach over conditional f^* implied by option prices. Their this procedure yields an estimate for $\mathbb{E}[f^*]/\mathbb{E}[f]$ that is not monotonically decreasing in market returns (see Beason and Schreindorfer (2022), Figure 2).[66] The fact that their $\mathbb{E}[f^*]/\mathbb{E}[f]$ is only slightly decreasing in the central region yields an implied central risk premium contribution (approximately 30%) that is lower than that implied by our methodology (approximately 45%). The fact that their $\mathbb{E}[f^*]/\mathbb{E}[f]$ is slightly increasing in the upside region yields an implied upside risk premium that is negative with a contribution to the total risk premium of approximately -10% (compared to our estimate of approximately 10%).

We sidestep the issue of estimating the physical and risk-neutral densities by using our transformation between risk-neutral and physical moments implied by Corollary 1. As can be see in Figure IA.9, our methodology implies conditional SDFs that are (approximately) monotonically decreasing in market returns. The result is that our downside, central, and upside risk premia are all positive so that each has a positive contribution to the overall risk premium. Finally, the implied magnitude of the downside risk premium in Beason and Schreindorfer (2022) is larger than our unconditional value because their $\mathbb{E}[f^*]/\mathbb{E}[f]$ (their Figure 2) is higher than our conditional SDFs in the downside region (see Figure IA.9). This implies that their $\mathbb{E}[f] - \mathbb{E}[f^*]$ is higher than our implied value in this region, yielding a larger downside risk premium.

The third potential contributor to differences between our risk premium contribution measures and those in Beason and Schreindorfer (2022) is related to Jensen's inequality. Beason and Schreindorfer (2022) compute their contributions effectively by integrating over $\mathbb{E}[f] - \mathbb{E}[f^*]$, whereas we first compute conditional contributions and average over these. One way to make our measures more comparable to theirs would be to compute contributions directly from the unconditional average risk premium levels. For instance, using results reported in Table 2, we could compute: $\mathbb{E}\left[\mathbb{RP}_{t\to T}^{(1)}[A_d]\right]/\mathbb{E}\left[\mathbb{RP}_{t\to T}^{(1)}[A]\right] = 4.45/8.72 \approx 51\%$. Since our estimate of the downside risk pre-

[66] Note that the ratio $\mathbb{E}[f^*]/\mathbb{E}[f]$ is not exactly the same as the unconditional SDF, which is given by $\mathbb{E}[f^*/f]$.

mium contribution reported in Table 2 is approximately 46%, this implies that even ignoring the Jensen's inequality terms would not reconcile the large differences between our risk premium contribution estimates and those in Beason and Schreindorfer (2022).

References for Internet Appendix

Bansal, R., D. Kiku, and A. Yaron (2012). "An empirical evaluation of the long-run risks model for asset prices." *Critical Finance Review* 1 (1), pp. 183–221.

Bansal, R. and A. Yaron (2004). "Risks for the long run: A potential resolution of asset pricing puzzles." *Journal of Finance* 59 (4), pp. 1481–1509.

Barone-Adesi, G., N. Fusari, A. Mira, and C. Sala (2020). "Option market trading activity and the estimation of the pricing kernel: A Bayesian approach." *Journal of Econometrics* 216 (2), pp. 430–449.

Bates, D. (2006). "Maximum likelihood estimation of latent affine processes." *Review of Financial Studies* 19 (3), pp. 909–965.

Beason, T. and D. Schreindorfer (2022). "Dissecting the equity premium." *Journal of Political Economy* 130 (8), pp. 2203–2222.

Bekaert, G. and E. Engstrom (2017). "Asset return dynamics under habits and bad environment-good environment fundamentals." *Journal of Political Economy* 125 (3), pp. 713–760.

Bekaert, G., E. Engstrom, and A. Ermolov (2023). "The variance risk premium in equilibrium models." *Review of Finance*. rfad005.

Bollerslev, T., G. Tauchen, and H. Zhou (2009). "Expected stock returns and variance risk premia." *Review of Financial Studies* 22 (11), pp. 4463–4493.

Campbell, J. and J. Cochrane (1999). "By force of habit: A consumption-based explanation of aggregate stock market behavior." *Journal of Political Economy* 107 (2), pp. 205–251.

Campbell, J. and R. Shiller (1988). "Stock prices, earnings, and expected dividends." *Journal of Finance* 43 (3), pp. 661–676.

Carr, P. and D. Madan (2001). "Optimal positioning in derivative securities." *Quantitative Finance* 1, pp. 19–37.

Carr, P. and L. Wu (2009). "Variance risk premia." *Review of Financial Studies* 22 (3), pp. 1311–1341.

Chabi-Yo, F. and J. Loudis (2020). "The conditional expected market return." *Journal of Financial Economics* 137 (3), pp. 752–786.

Dew-Becker, I., S. Giglio, A. Le, and M. Rodriguez (2017). "The price of variance risk." *Journal of Financial Economics* 123 (2), pp. 225–250.

Drechsler, I. and A. Yaron (2011). "What's vol got to do with it." *Review of Financial Studies* 24 (1), pp. 1–45.

Epstein, L. and S. Zin (1989). "Substitution, risk aversion, and the temporal behavior of consumption and asset returns: A theoretical framework." *Econometrica* 57 (4), pp. 937–965.

Gabaix, X. (2012). "Variable rare disasters: An exactly solved framework for ten puzzles in macro-finance." *Quarterly Journal of Economics* 127 (2), pp. 645–700.

Garleanu, N., L. H. Pedersen, and A. M. Poteshman (2009). "Demand-based options pricing." *Review of Financial Studies* 22 (10), pp. 4259–4299.

Gatheral, J. and A. Jacquier (2014). "Arbitrage-free SVI volatility surfaces." *Quantitative Finance* 14 (1), pp. 59–71.

Hastie, T., R. Tibshirani, and J. Friedman (2009). *The Elements of Statistical Learming: Data Mining, Inference, and Prediction*. 2nd ed. New York, NY: Springer.

Jackwerth, J. C. and H. Cuesdeanu (2018). "The pricing kernel puzzle: Survey and outlook." *Annals of Finance* 14, pp. 289–329.

Lien, D.-H. D. (1985). "Moments of truncated bivariate log-normal distributions." *Economic Letters* 19, pp. 243–247.

Linn, M., S. Shive, and T. Shumway (2018). "Pricing kernel monotonicity and conditional information." *Review of Financial Studies* 31 (2), pp. 493–531.

Newey, W. and K. West (1987). "A simple, positive semi-definite, heteroskedasticity and autocorrelation consistent covariance matrix." *Econometrica* 55 (3), pp. 703–708.

Newey, W. and K. West (1994). "Automatic lag selection in covariance matrix estimation." *Review of Economic Studies* 61 (4), pp. 631–653.

Noussair, C. N., S. T. Trautmann, and G. VanDeKuilen (2014). "Higher order risk attitudes, demographics, and financial decisions." *Review of Economic Studies* 81 (1), pp. 325–355.

Rompolis, L. S. and E. Tzavalis (2017). "Retrieving risk neutral moments and expected quadratic variation from option prices." *Review of Quantitative Finance and Accounting* 48, pp. 955–1002.

Rosenberg, J. and R. Engle (2002). "Empirical pricing kernels." *Journal of Financial Economics* 64 (3), pp. 341–372.

Wachter, J. (2013). "Can time-varying risk of rare disasters explain aggregate stock market volatility?" *Journal of Finance* 68 (3), pp. 987–1035.

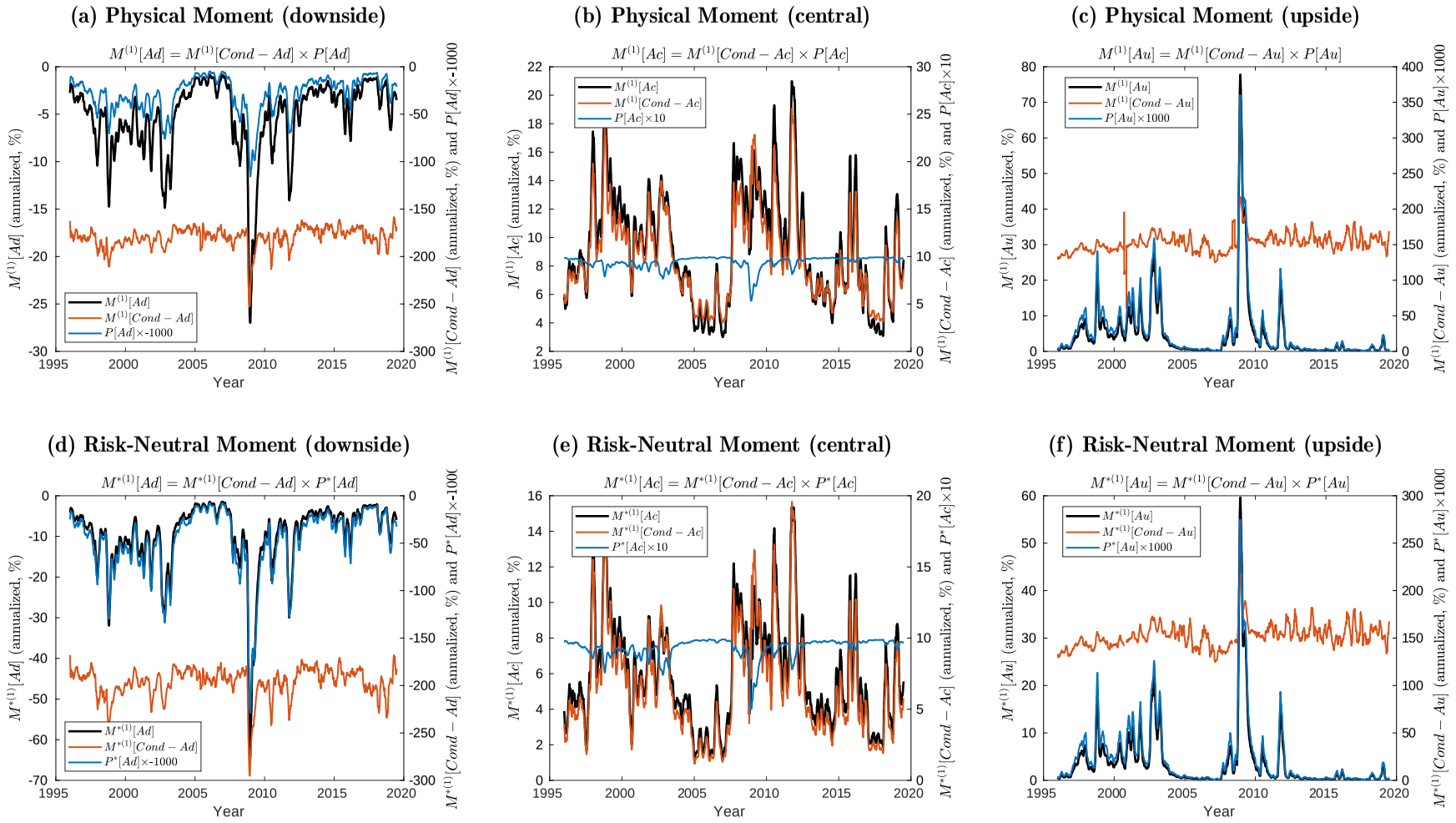

Figure IA.1
Data-Implied Physical and Risk-Neutral First Moment Decompositions

These graphs plot physical and risk-neutral first-moment decompositions using results from the data-implied risk premium decompositions from Section 4.2 based on Proposition 3 using preference parameters reported in Table 1. In particular, they plot the truncated first moments of excess market returns ($\mathbb{M}^{(1)}_{t\to T}[A_s] \equiv \mathbb{E}_t\left[(R_{M,t\to T} - R_{f,t\to T})\,\mathbb{I}_{A_s}\right]$ and $\mathbb{M}^{*(1)}_{t\to T}[A_s] \equiv \mathbb{E}^*_t\left[(R_{M,t\to T} - R_{f,t\to T})\,\mathbb{I}_{A_s}\right]$), the corresponding conditional moments ($\mathbb{M}^{(1)}_{t\to T}[Cond.-A_s] \equiv \mathbb{E}_t\left[(R_{M,t\to T} - R_{f,t\to T})\,|\,\mathbb{I}_{A_s}\right]$ and $\mathbb{M}^{*(1)}_{t\to T}[Cond.-A_s] \equiv \mathbb{E}^*_t\left[(R_{M,t\to T} - R_{f,t\to T})\,|\,\mathbb{I}_{A_s}\right]$), and probabilities ($\mathbb{P}_t[A_s]$ and $\mathbb{P}^*_t[A_s]$). Panels (a)-(c) ((d)-(f)) plot results related to the physical (risk-neutral) moments associated with A_d, A_c, and A_u, respectively. The truncated and conditional moments are reported in annualized percent. The probabilities are scaled according to labels in the plots for easier visualization. All moments are measured with respect to the 30-day horizon and use A_d=$[0, 0.9]$, A_c=$[0.9, 1.1]$, and A_u=$[1.1, +\infty)$. All time series are smoothed by averaging over two months of lagged daily data to reduce the appearance of noise.

(a) Physical Downside Probability ($\mathbb{P}_t\left[\boldsymbol{A_d}\right]$) **(b) Physical Central Probability ($\mathbb{P}_t\left[\boldsymbol{A_c}\right]$)** **(c) Physical Upside Probability ($\mathbb{P}_t\left[\boldsymbol{A_u}\right]$)**

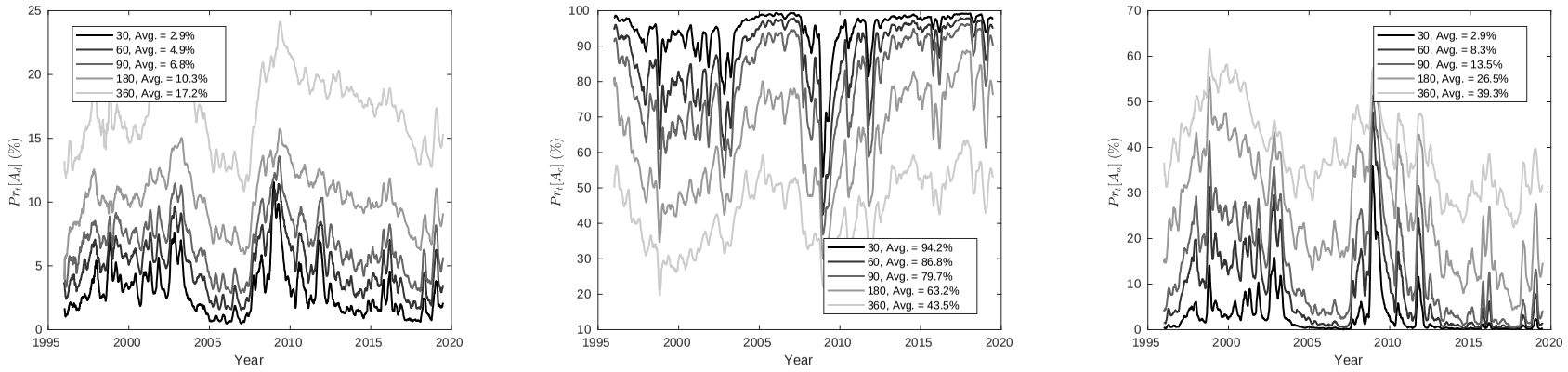

Figure IA.2
Data-Implied Physical Probabilities

These graphs plot physical probabilities, $\mathbb{P}_t\left[A_s\right]$, of entering each region of interest by the end of each horizon of interest (30, 60, 90, 180, and 360 days). Probabilities are computed according to Corollary 1 using preference parameters reported in Table 1. All moments use A_d=$[0, 0.9]$, A_c=$[0.9, 1.1]$, and A_u=$[1.1, +\infty)$. All time series are smoothed by averaging over two months of lagged daily data to reduce the appearance of noise.

(a) Downside Region **(b) Central Region** **(c) Upside Region**

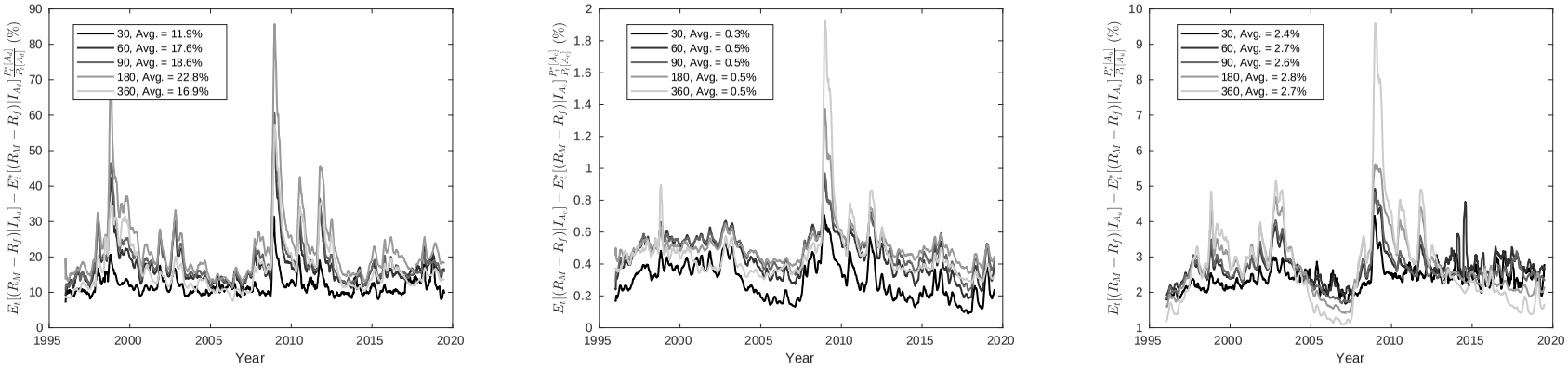

Figure IA.3
Data-Implied Risk Premium Component from the First Term in Equation IA.3

These graphs plot the first term in Equation IA.3 ($\mathbb{E}_t\left[(R_{M,t\to T} - R_{f,t\to T}) \mid \mathbb{I}_{A_s}\right] - \mathbb{E}_t^*\left[(R_{M,t\to T} - R_{f,t\to T}) \mid \mathbb{I}_{A_s}\right] \frac{\mathbb{P}_t^*[A_s]}{\mathbb{P}_t[A_s]}$) for each region of interest and for each horizon we study (30, 60, 90, 180, and 360 days). Physical probabilities are computed according to Corollary 1 using preference parameters reported in Table 1. All moments use A_d=$[0, 0.9]$, A_c=$[0.9, 1.1]$, and A_u=$[1.1, +\infty)$. All time series are smoothed by averaging over two months of lagged daily data to reduce the appearance of noise.

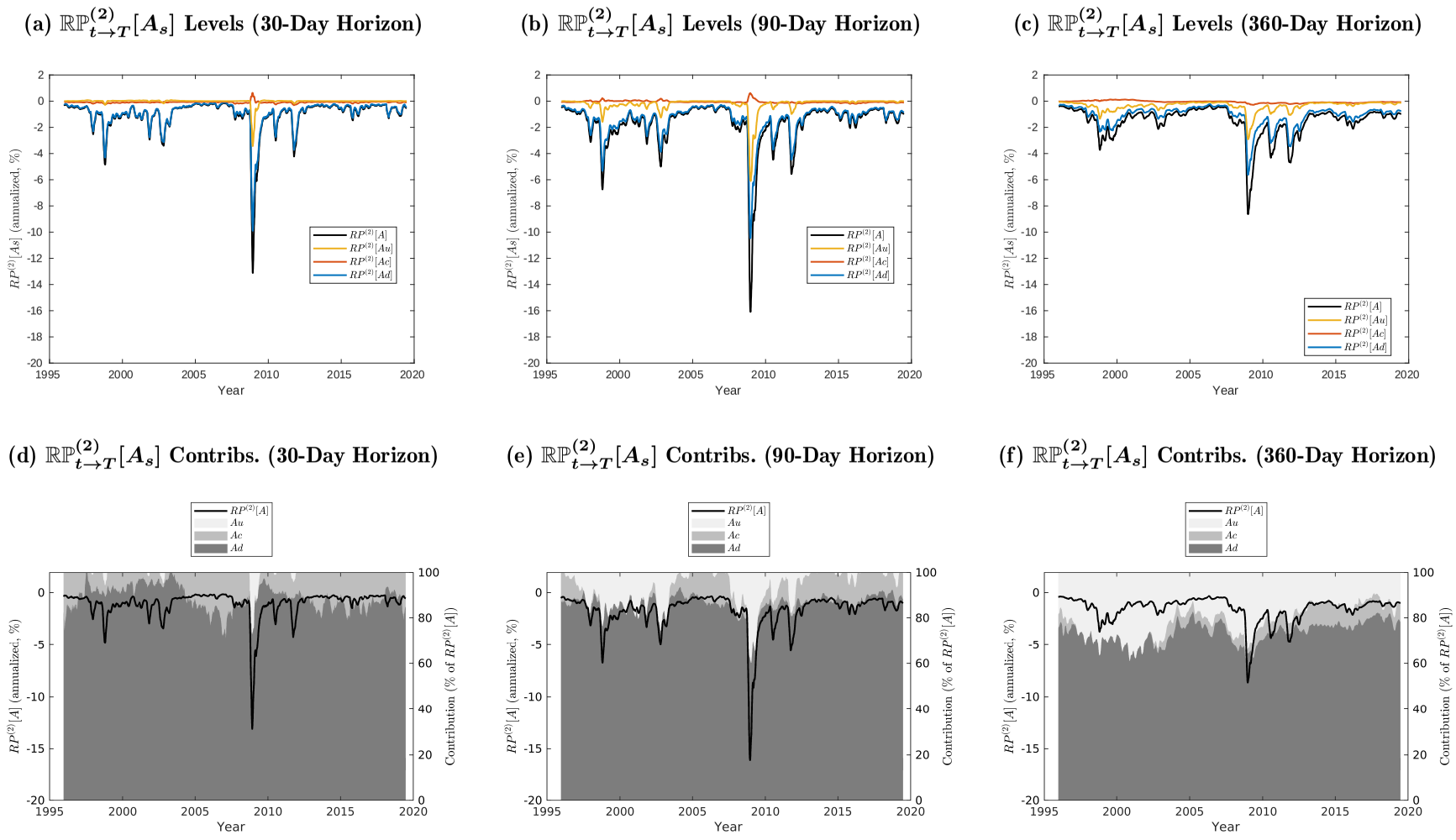

Figure IA.4
Data-Implied Variance Risk Premium Decomposition

These graphs plot the data-implied risk premium decompositions from Section 4.2 based on Proposition 3 with $n = 2$ (i.e., the variance risk premium). The decompositions use preference parameters reported in Table 1. Panels (a)-(c) plot the annualized risk premium levels at each date in percent. Risk premia are annualized by multiplying by each horizon (in units of fractions of a year). Panels (d)-(e) plot each component's contribution to the total risk premium at each date as a fraction of the total risk premium. The dark/medium/light shaded regions represent the downside/central/upside risk premium contributions, respectively, and are measured on the left vertical axes. The decompositions are computed at three horizons (30 days - Panels (a) and (d); 90 days - Panels (b) and (e); and 360 days - Panels (c) and (f)) and use A_d=$[0, 0.9]$, A_c=$[0.9, 1.1]$, and A_u=$[1.1, +\infty)$. All time series are smoothed by averaging over two months of lagged daily data to reduce the appearance of noise.

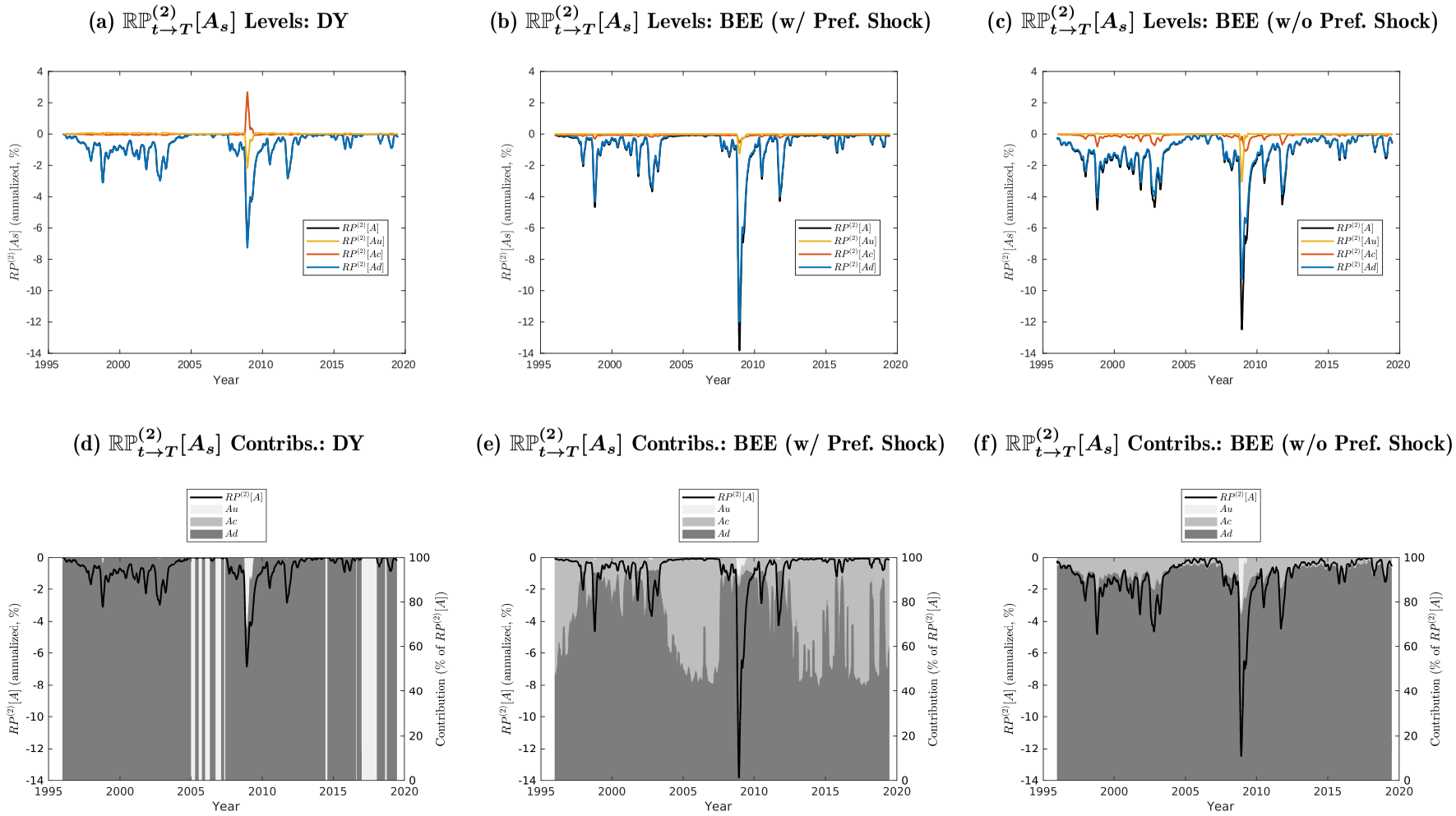

Figure IA.5
Model-Implied Variance Risk Premium Decompositions

These graphs plot model-implied variance risk premium decompositions (i.e., $n = 2$) based on Proposition 3 for the following models: Drechsler and Yaron (2011) (Panels (a)/(d)), Bekaert, Engstrom, and Ermolov (2023) with preference shocks (Panels (b)/(e)), Bekaert, Engstrom, and Ermolov (2023) without preference shocks (Panels (c)/(f)), Gabaix (2012) (Panels (g)/(i)), and Wachter (2013) (Panels (h)/(j)). Panels (a)-(c) and (g)-(h) (see continued figure below) plot the annualized risk premium levels for each model at each date in percent. Risk premia are annualized by multiplying by each horizon (in units of fractions of a year). Panels (d)-(e) and (i)-(j) (see continued figure below) plot each component's contribution to the total risk premium for each model at each date as a fraction of the total risk premium. The dark/medium/light shaded regions represent the downside/central/upside risk premium contributions, respectively. All decompositions use a 30-day horizon to match model calibration frequencies in the original papers (monthly), and set A_d=$[0, 0.9]$, A_c=$[0.9, 1.1]$, and A_u=$[1.1, +\infty)$. All time series are smoothed by averaging over two months of lagged daily data to reduce the appearance of noise.

(g) $\mathbb{RP}^{(2)}_{t\to T}[A_s]$ Levels: Gabaix

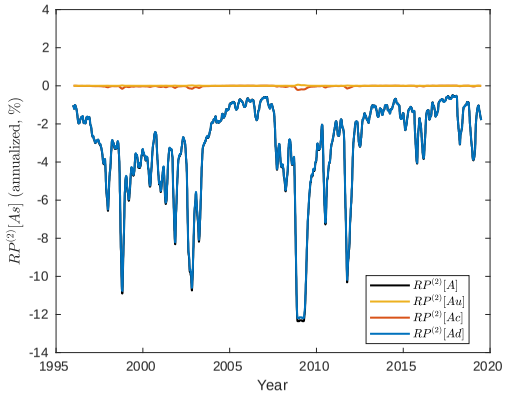

(h) $\mathbb{RP}^{(2)}_{t\to T}[A_s]$ Levels: Wachter

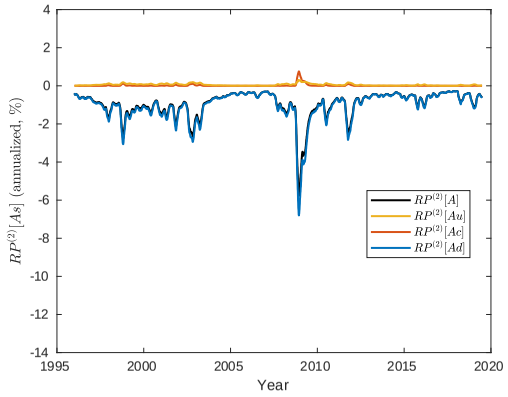

(i) $\mathbb{RP}^{(2)}_{t\to T}[A_s]$ Contribs.: Gabaix

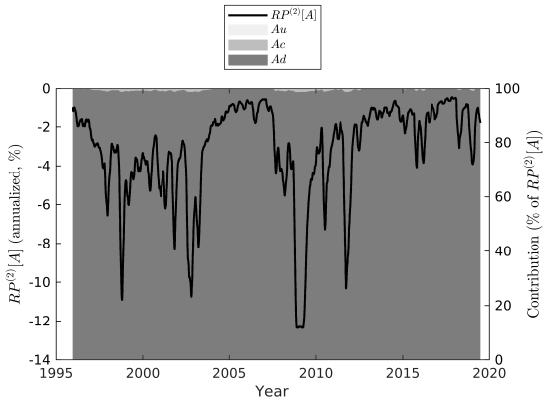

(j) $\mathbb{RP}^{(2)}_{t\to T}[A_s]$ Contribs.: Wachter

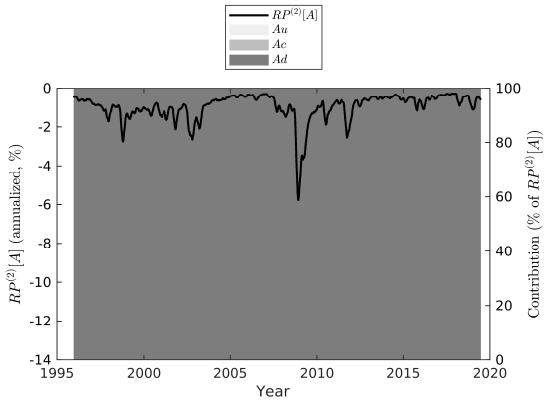

Figure IA.5
Model-Implied Variance Risk Premium Decompositions (continued)

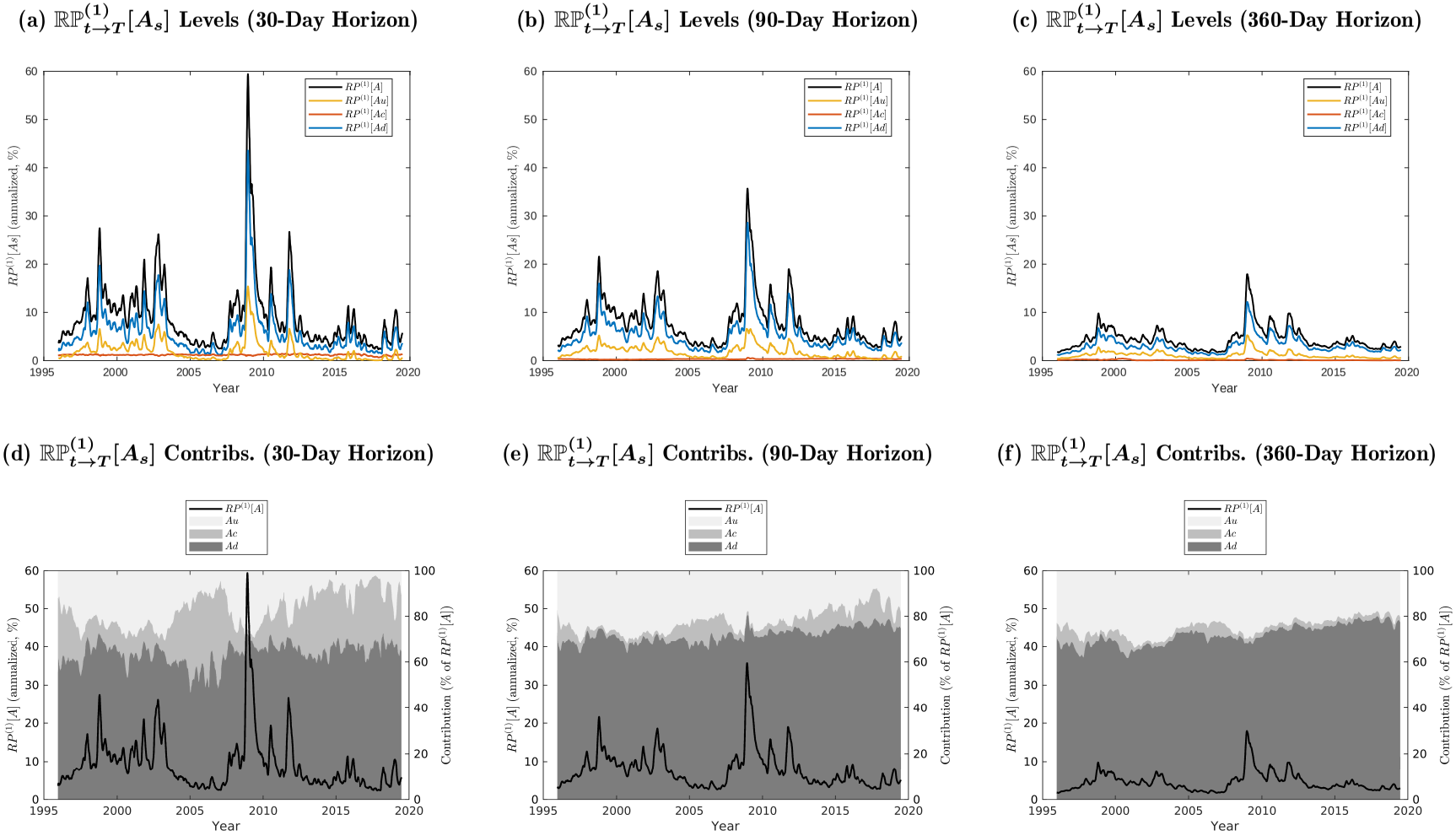

Figure IA.6
Data-Implied Market Risk Premium Decomposition ($\pm 5\%$ Cutoffs)

These graphs plot the data-implied risk premium decompositions from Internet Appendix IA.3.4 based on Proposition 3 with $n = 1$ (i.e., the market risk premium). The decompositions use preference parameters reported in Table IA.6. Panels (a)-(c) plot the annualized risk premium levels at each date in percent. Panels (d)-(e) plot each component's contribution to the total risk premium at each date as a fraction of the total risk premium. The dark/medium/light shaded regions represent the downside/central/upside risk premium contributions, respectively, and are measured on the left vertical axes. The decompositions are computed at three horizons (30 days - Panels (a) and (d); 90 days - Panels (b) and (e); and 360 days - Panels (c) and (f)) and use A_d=$[0, 0.95]$, A_c=$[0.95, 1.05]$, and A_u=$[1.05, +\infty)$. All time series are smoothed by averaging over two months of lagged daily data to reduce the appearance of noise.

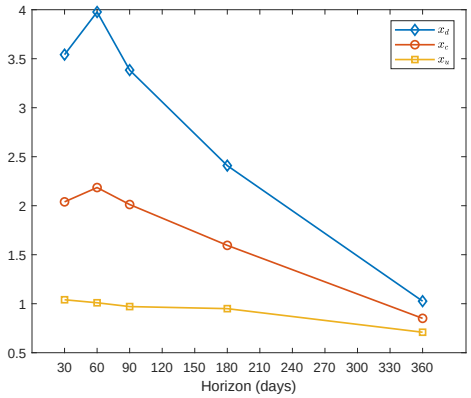

Figure IA.7
Relative Risk Aversion ($1/\tau(x_s)$)

This graph plots estimates of relative risk aversion based on reported values of $\tau(x_s)$ in Table 1. Relative risk aversion is simply $1/\tau(x_s)$ (see Equation 14). Values are plotted for three points in the return space (x_d, x_c, and x_u) corresponding to the regions A_d, A_c, and A_u, respectively, and across five horizons (30, 60, 90, 180, and 360 days).

(a) $\tau(x_s)$ **(b) $\rho(x_s)$** **(c) $\kappa(x_s)$**

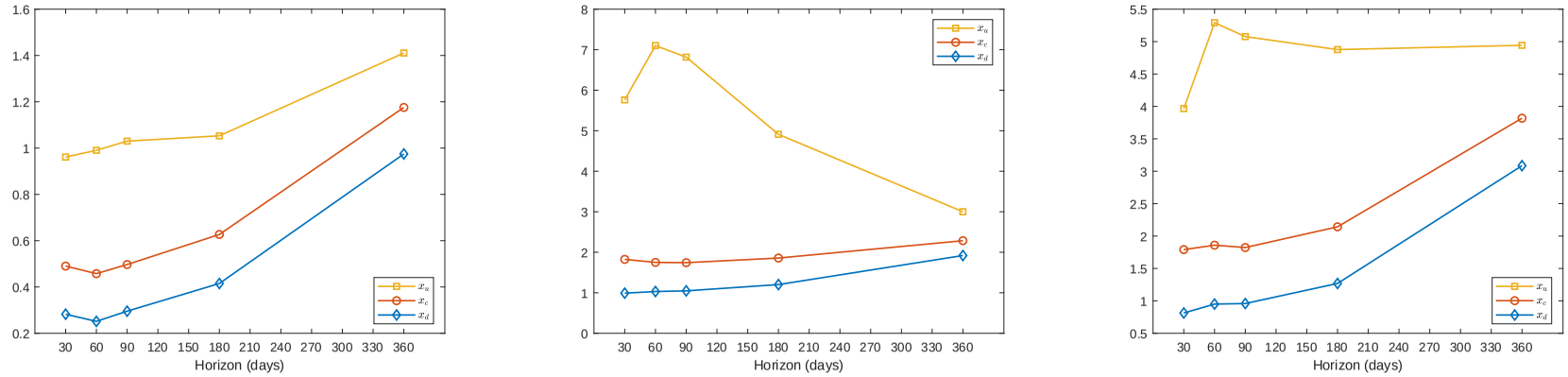

Figure IA.8
Estimated Preference Parameters

These graphs plot estimates of $\tau(x_s)$ (Panel (a)), $\rho(x_s)$ (Panel (b)), and $\kappa(x_s)$ (Panel (c)) based on reported values in Table 1. Values are plotted for three points in the return space (x_d, x_c, and x_u) corresponding to the regions A_d, A_c, and A_u, respectively, and across five horizons (30, 60, 90, 180, and 360 days).

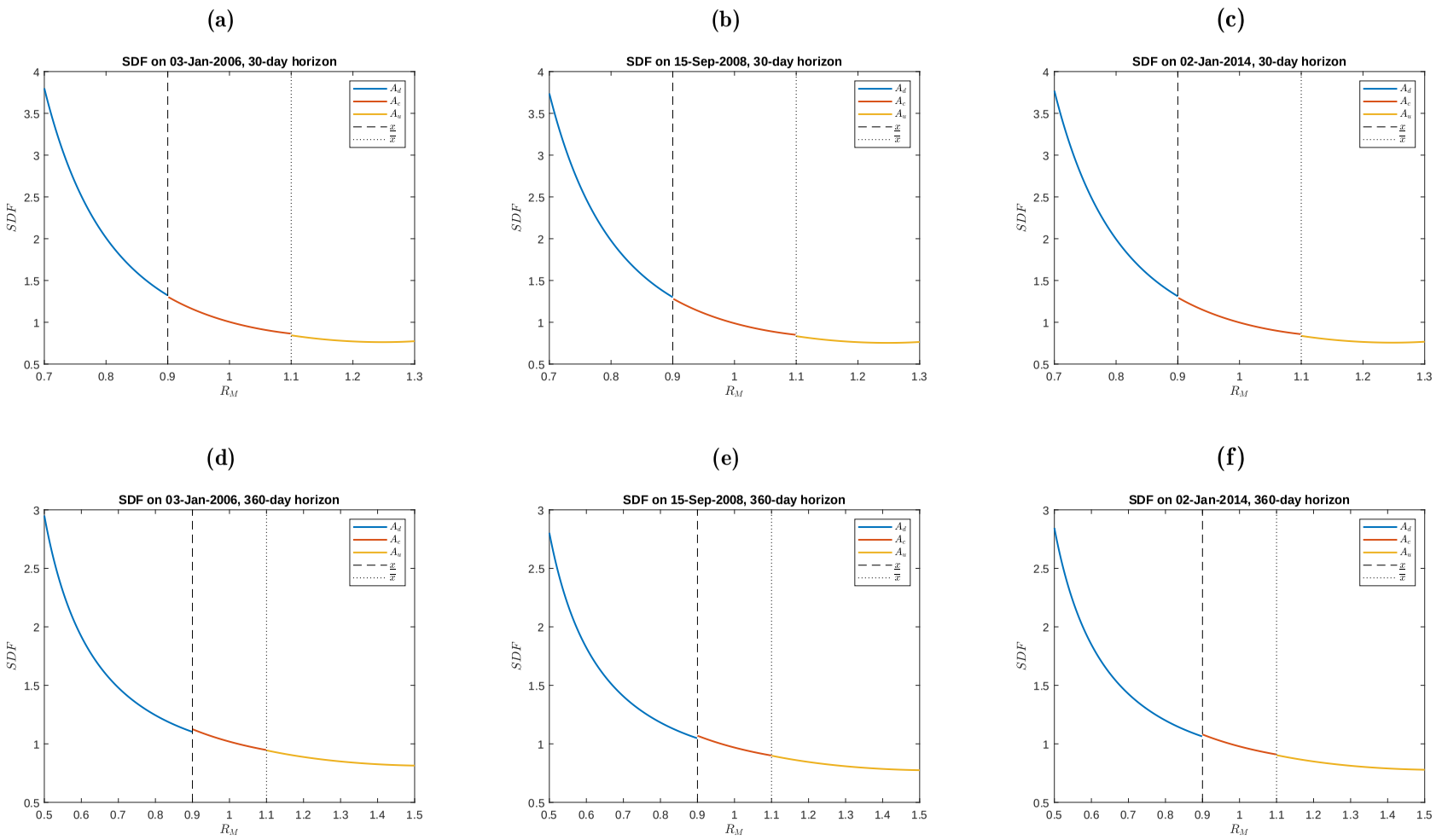

Figure IA.9
Implied SDF at Selected Dates

These graphs plot estimated values of the SDF across three regions of interest (A_d, A_c, and A_u) with region boundaries at $\underline{x} = 0.9$ and $\overline{x} = 1.1$ according to the inverse of the terms in Equation 18 using estimated preference parameters from Table 1. The SDF is estimated at two horizons (30 days - Panels (a), (b), and (c); and 360 days - Panels (d), (e), and (f)), and on three dates (3 January, 2006 - Panels (a) and (d); 15 September, 2008 - Panels (b) and (e); and 2 January, 2014 - Panels (c) and (f)). The plots also make use of $\mathbb{M}^{*(n)}_{t\to T}[A_s]$ estimates from options prices on these dates.

(a) SDF from Rosenberg and Engle (2002)

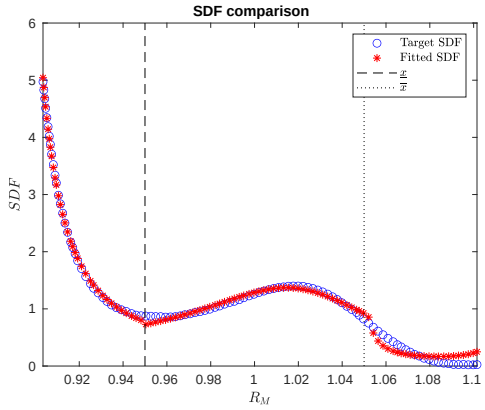

(b) SDF from Beason and Schreindorfer (2022)

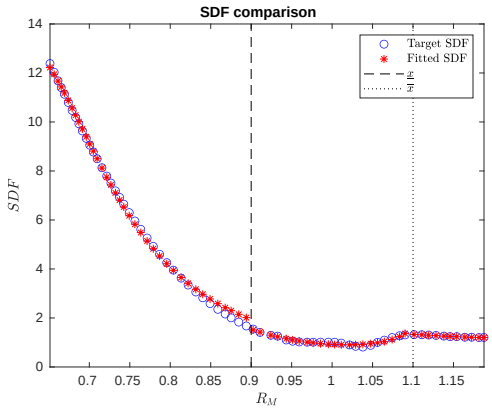

Figure IA.10
Matching Non-Monotonic SDFs

This table plots SDFs implied by Equation 18 using preference parameters reported in Table IA.9, which were optimized to minimize the square differences between SDF values from Rosenberg and Engle (2002) Figure 6 (Panel A) or Beason and Schreindorfer (2022) Figure 2 (Panel B). See Internet Appendix IA.3.7 for more details.

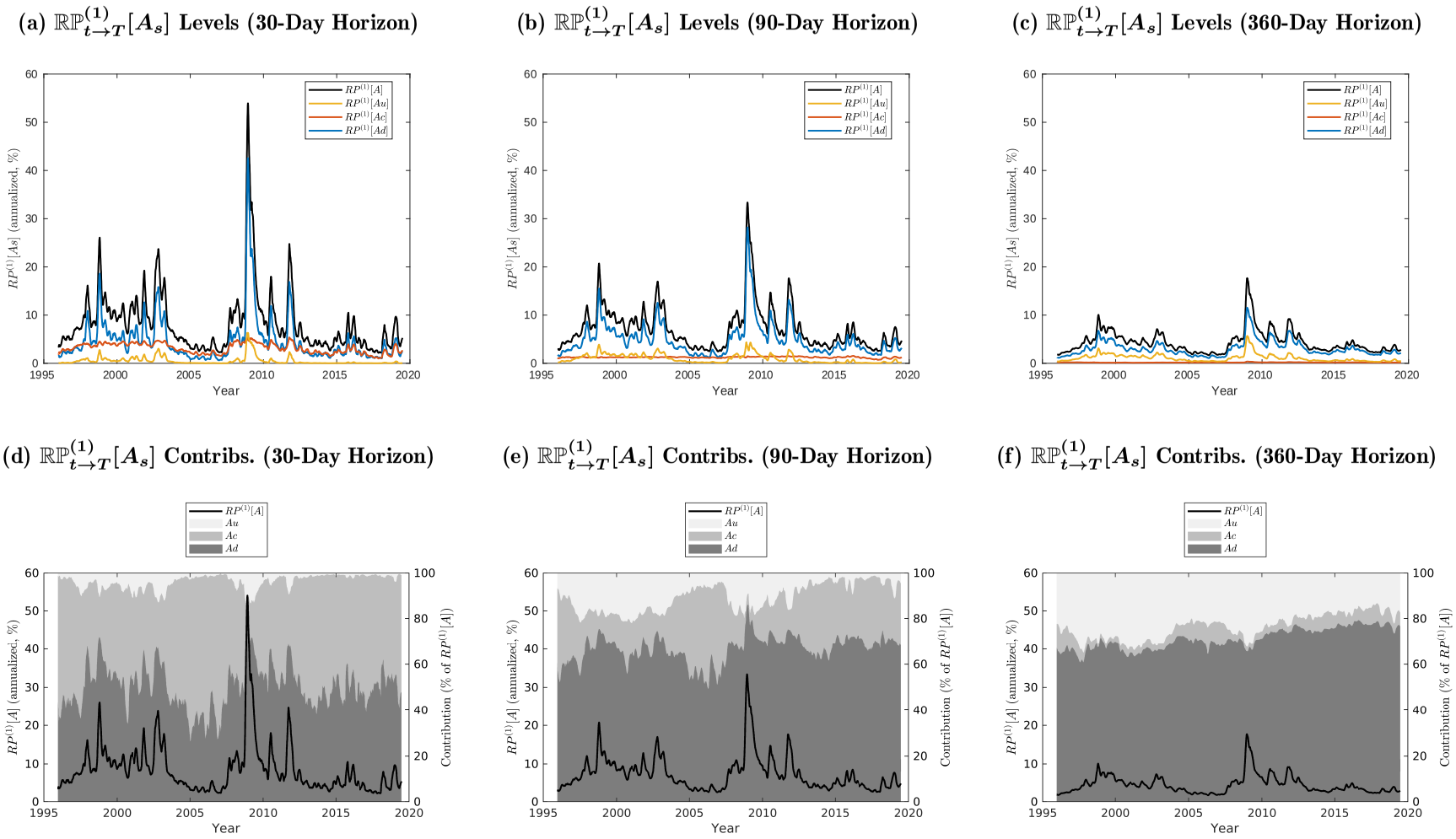

Figure IA.11
Data-Implied Market Risk Premium Decomposition (Corollary 2)

These graphs plot the data-implied risk premium decompositions from Internet Appendix IA.3.8 based on Proposition 3 with $n = 1$ (i.e., the market risk premium) using physical moments constructed according to Corollary 2 (as opposed to our main results in Figure 2, which use physical moments constructed according to Corollary 1 using preference parameters reported in Table 1). These decompositions use preference parameters reported in Table IA.11. Panels (a)-(c) plot the annualized risk premium levels at each date in percent. Panels (d)-(e) plot each component's contribution to the total risk premium at each date as a fraction of the total risk premium. The dark/medium/light shaded regions represent the downside/central/upside risk premium contributions, respectively, and are measured on the left vertical axes. The decompositions are computed at three horizons (30 days - Panels (a) and (d); 90 days - Panels (b) and (e); and 360 days - Panels (c) and (f)) and use A_d=$[0, 0.9]$, A_c=$[0.9, 1.1]$, and A_u=$[1.1, +\infty)$. All time series are smoothed by averaging over two months of lagged daily data to reduce the appearance of noise.

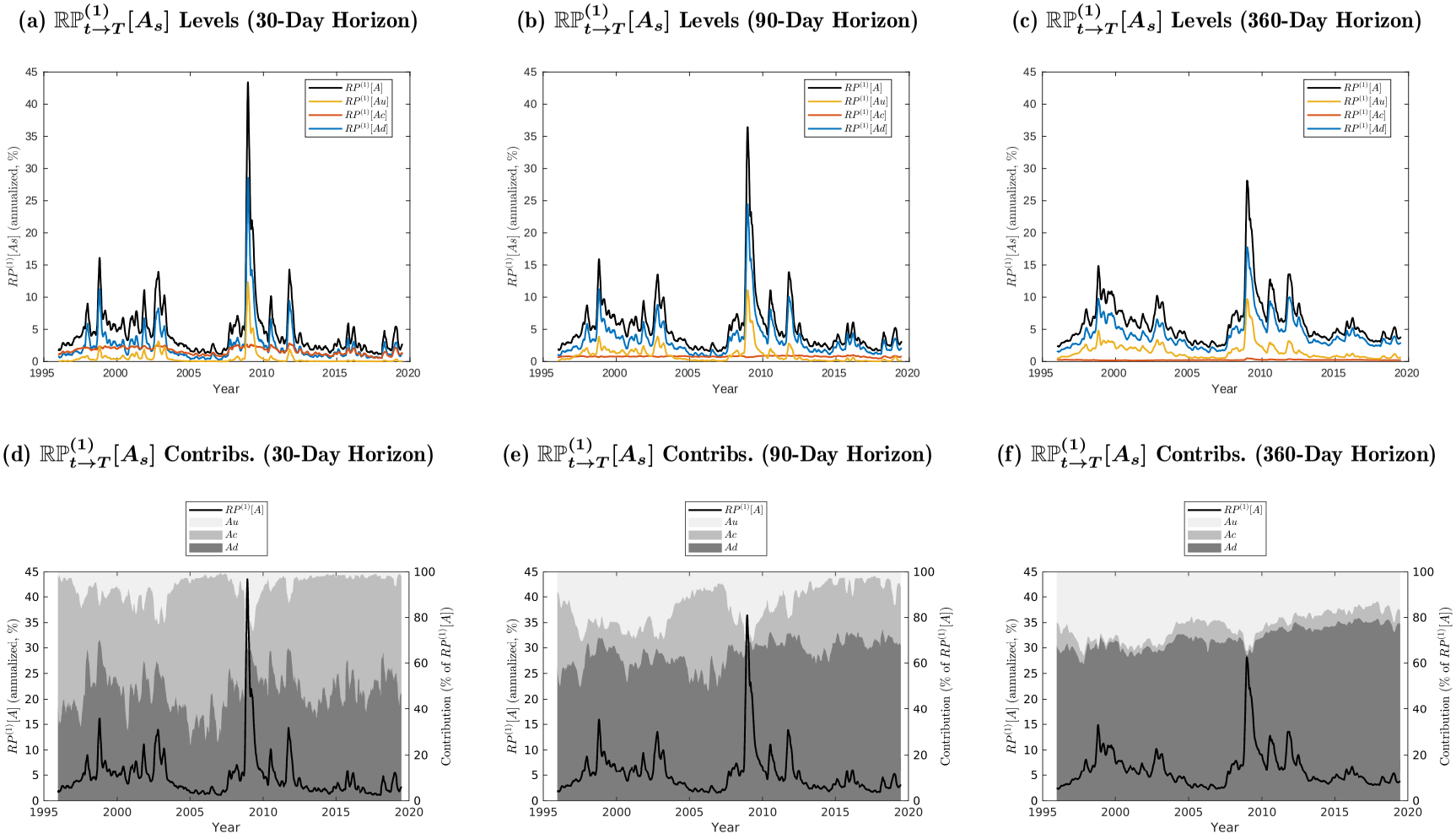

Figure IA.12
Data-Implied Market Risk Premium Decomposition (Restricted Preference Parameters)

These graphs plot the data-implied restricted risk premium decompositions from Section IA.3.9 based on Proposition 3 with $n = 1$ (i.e., the market risk premium). The decompositions set preference parameters to be $\tau = 1$, $\rho = 2$, and $\kappa = 4$ across all regions and horizons. Panels (a)-(c) plot the annualized risk premium levels at each date in percent. Panels (d)-(e) plot each component's contribution to the total risk premium at each date as a fraction of the total risk premium. The dark/medium/light shaded regions represent the downside/central/upside risk premium contributions, respectively. The decompositions are computed at three horizons (30 days - Panels (a) and (d); 90 days - Panels (b) and (e); and 360 days - Panels (c) and (f)) and use A_d=[0, 0.9], A_c=[0.9, 1.1], and A_u=[1.1, $+\infty$). All time series are smoothed by averaging over two months of lagged daily data to reduce the appearance of noise.

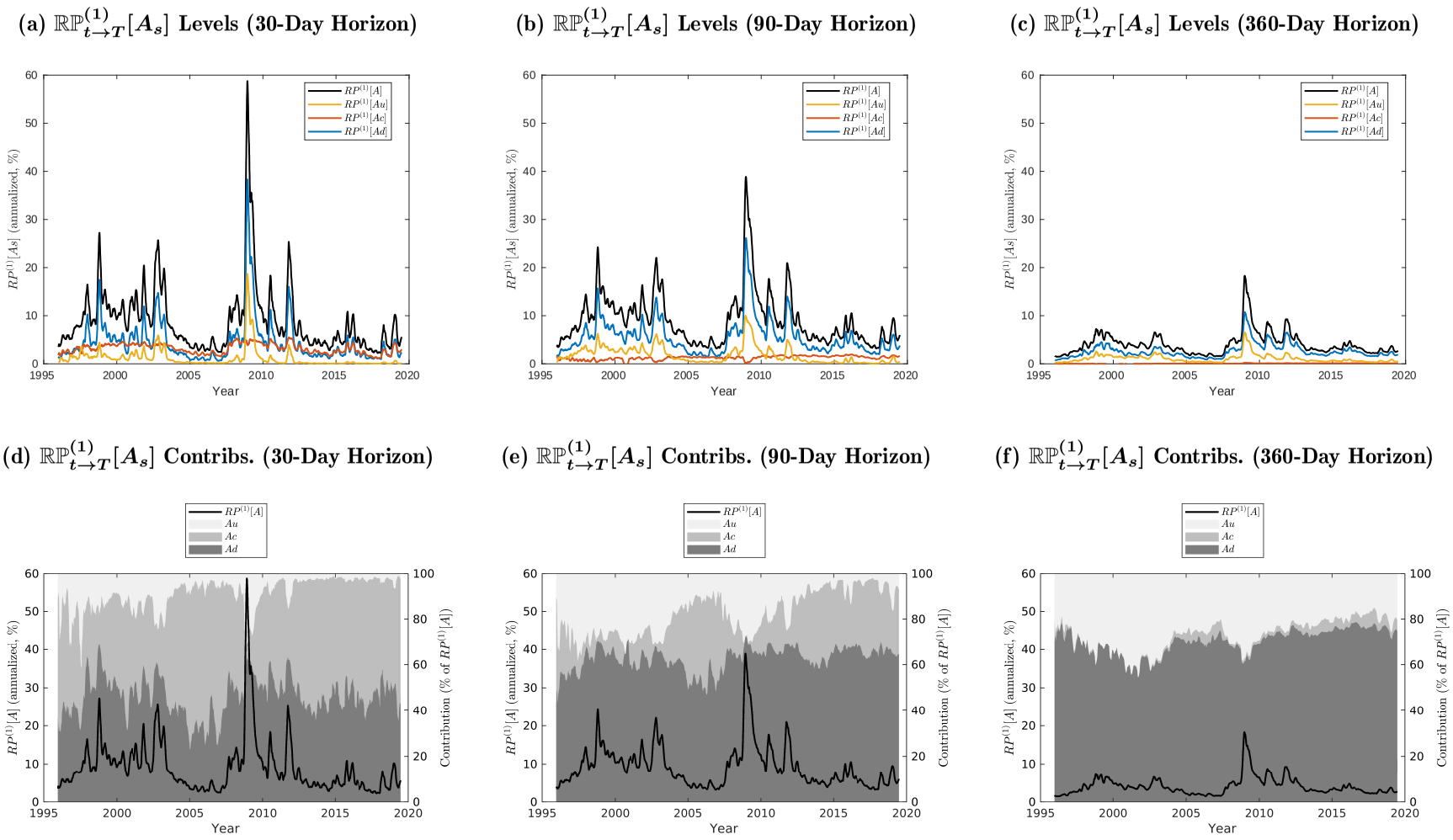

Figure IA.13
Data-Implied Market Risk Premium Decomposition (Observed Prices)

These graphs plot the data-implied risk premium decompositions from Section 4.2 based on Proposition 3 with $n = 1$ (i.e., the market risk premium). The decompositions use risk-neutral moments computed by numerically integrating over observed option prices directly rather than using the implied volatility fitting method. Preference parameters are also re-estimated using these moments. Panels (a)-(c) plot the annualized risk premium levels at each date. Panels (d)-(e) plot each component's contribution to the total risk premium at each date as a fraction of the total risk premium. The dark/medium/light shaded regions represent the downside/central/upside risk premium contributions, respectively, and are measured on the left vertical axes. The decompositions are computed at three horizons (30 days - Panels (a) and (d); 90 days - Panels (b) and (e); and 360 days - Panels (c) and (f)) and use A_d=$[0, 0.9]$, A_c=$[0.9, 1.1]$, and A_u=$[1.1, +\infty)$. All time series are smoothed by averaging over two months of lagged daily data to reduce the appearance of noise.

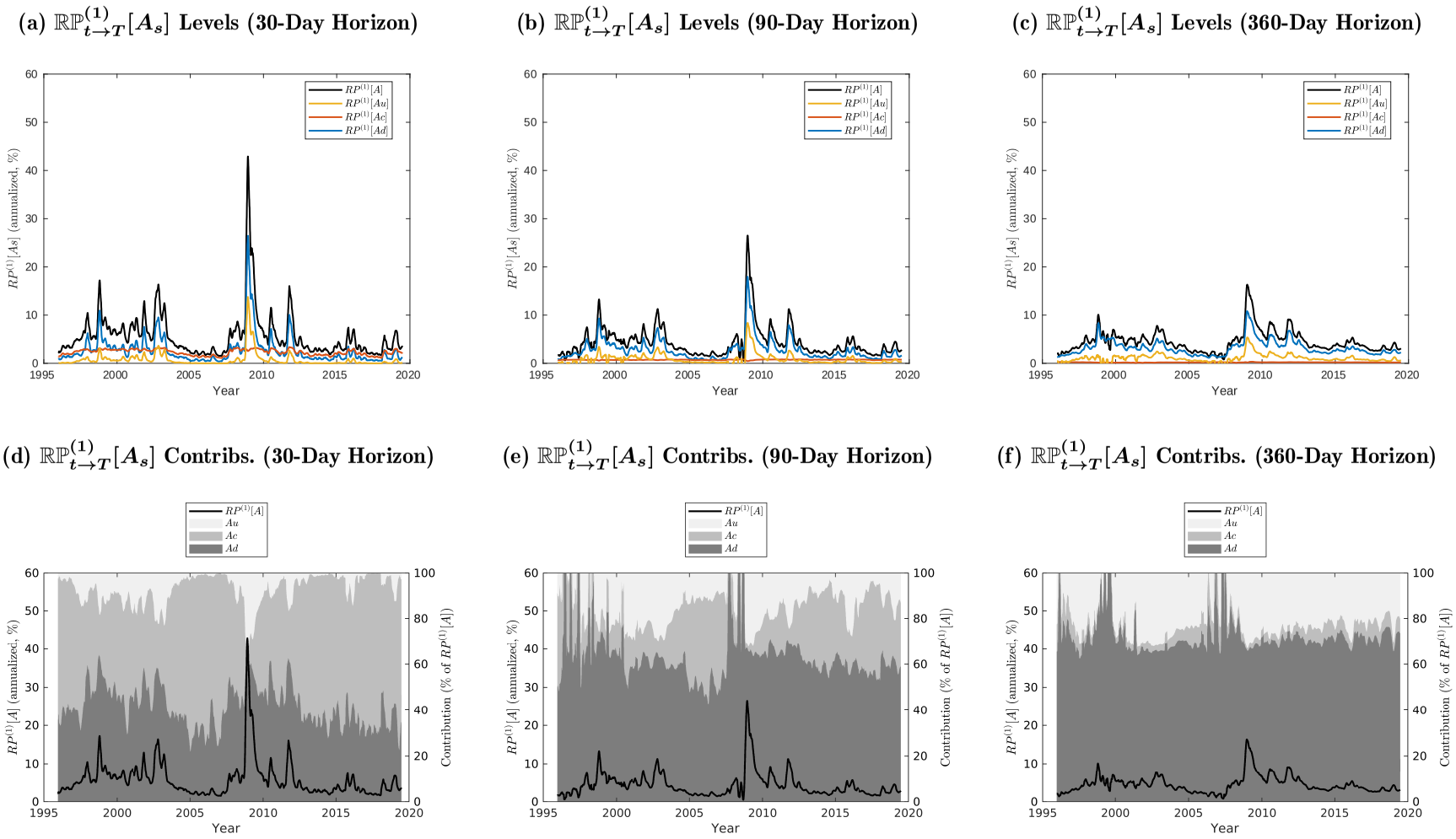

Figure IA.14
Data-Implied Market Risk Premium Decomposition (SVI)

These graphs plot the data-implied risk premium decompositions from Section 4.2 based on Proposition 3 with $n = 1$ (i.e., the market risk premium). The decompositions use risk-neutral moments computed by numerically integrating over option prices computed using SVI-modeled implied volatility (see Internet Appendix IA.3.11) rather than using our baseline implied volatility fitting method described in footnote 10. Preference parameters are also re-estimated using these moments. Panels (a)-(c) plot the annualized risk premium levels at each date. Panels (d)-(e) plot each component's contribution to the total risk premium at each date as a fraction of the total risk premium. The dark/medium/light shaded regions represent the downside/central/upside risk premium contributions, respectively, and are measured on the left vertical axes. The decompositions are computed at three horizons (30 days - Panels (a) and (d); 90 days - Panels (b) and (e); and 360 days - Panels (c) and (f)) and use A_d=$[0, 0.9]$, A_c=$[0.9, 1.1]$, and A_u=$[1.1, +\infty)$. All time series are smoothed by averaging over two months of lagged daily data to reduce the appearance of noise.

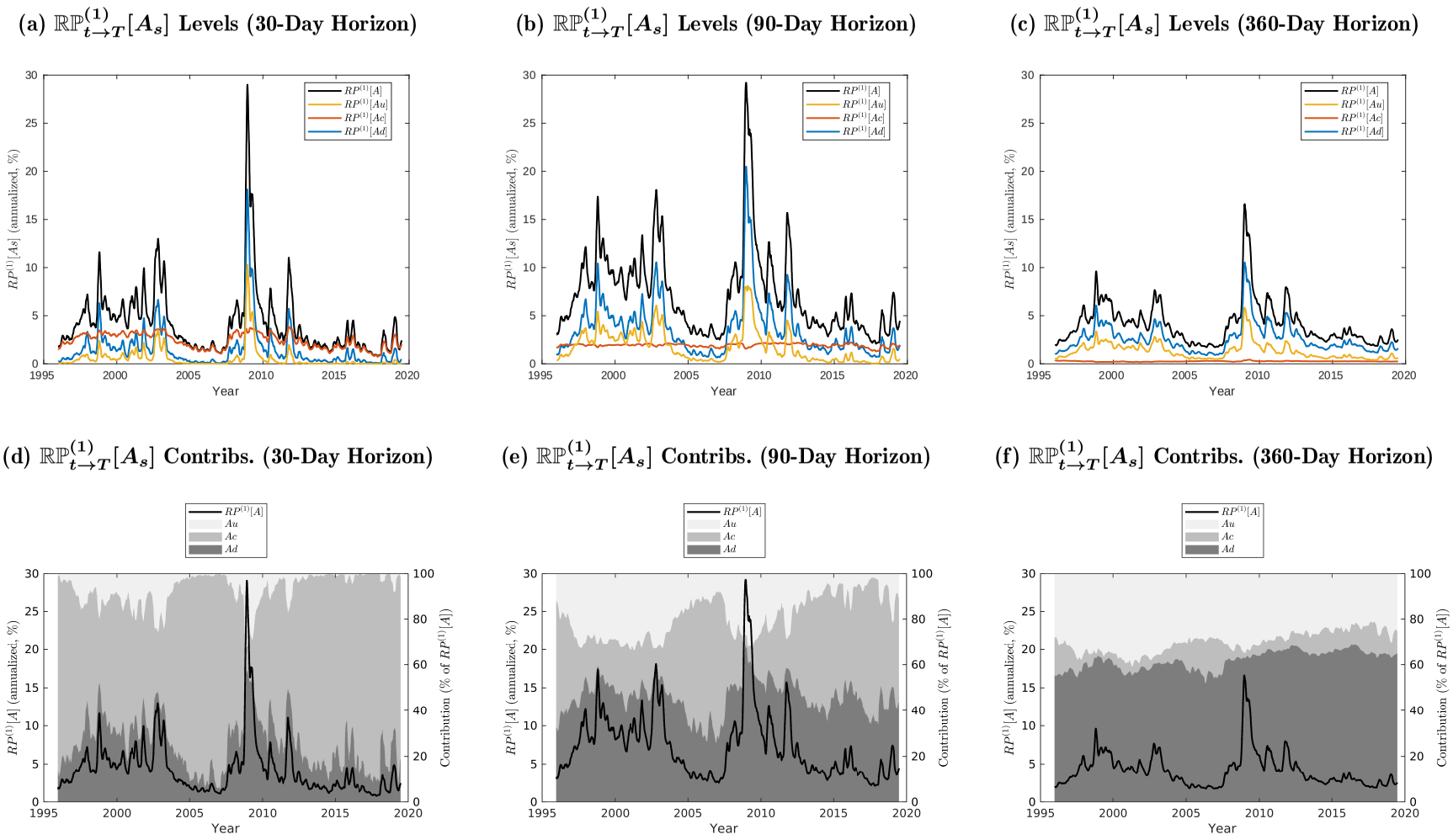

Figure IA.15
Data-Implied Market Risk Premium Decomposition (Overpriced Put Option Adjustment)

These graphs plot the data-implied risk premium decompositions from Section 4.2 based on Proposition 3 with $n = 1$ (i.e., the market risk premium). The decompositions use risk-neutral moments computed using the mispricing adjustment described in Subsection IA.3.12. Preference parameters are also re-estimated using these moments. Panels (a)-(c) plot the annualized risk premium levels at each date. Panels (d)-(e) plot each component's contribution to the total risk premium at each date as a fraction of the total risk premium. The dark/medium/light shaded regions represent the downside/central/upside risk premium contributions, respectively, and are measured on the left vertical axes. The decompositions are computed at three horizons (30 days - Panels (a) and (d); 90 days - Panels (b) and (e); and 360 days - Panels (c) and (f)) and use A_d=$[0, 0.9]$, A_c=$[0.9, 1.1]$, and A_u=$[1.1, +\infty)$. All time series are smoothed by averaging over two months of lagged daily data to reduce the appearance of noise.

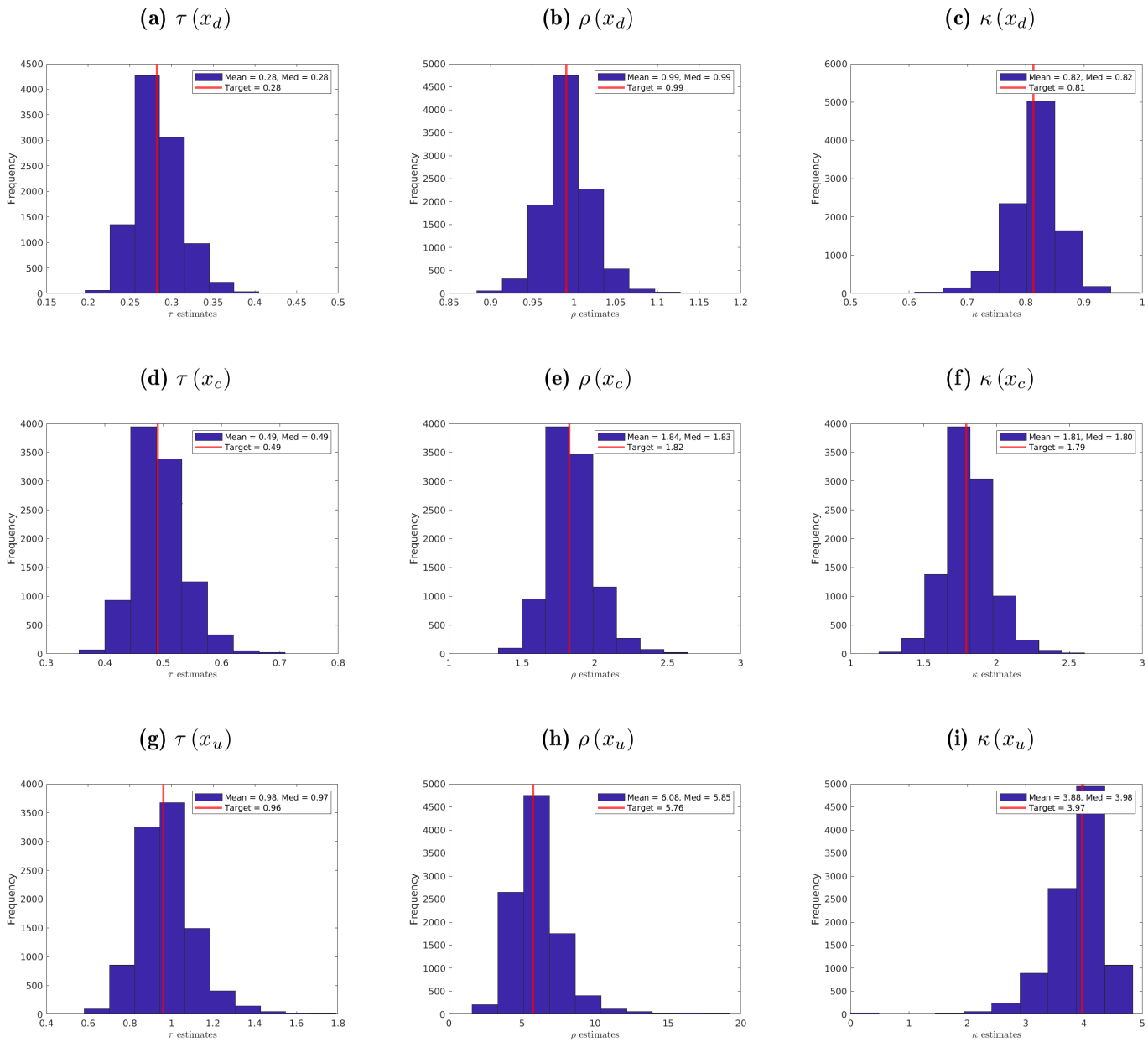

Figure IA.16
Simulated Parameter Estimates Given Noise in LHS Variable (Main Parameter Estimates)

This figure shows simulated parameter distributions (in blue), according to the simulation procedure described in Internet Appendix IA.6.2, along with the target parameter values (red lines). The target parameters are from Table 1 in our main draft.

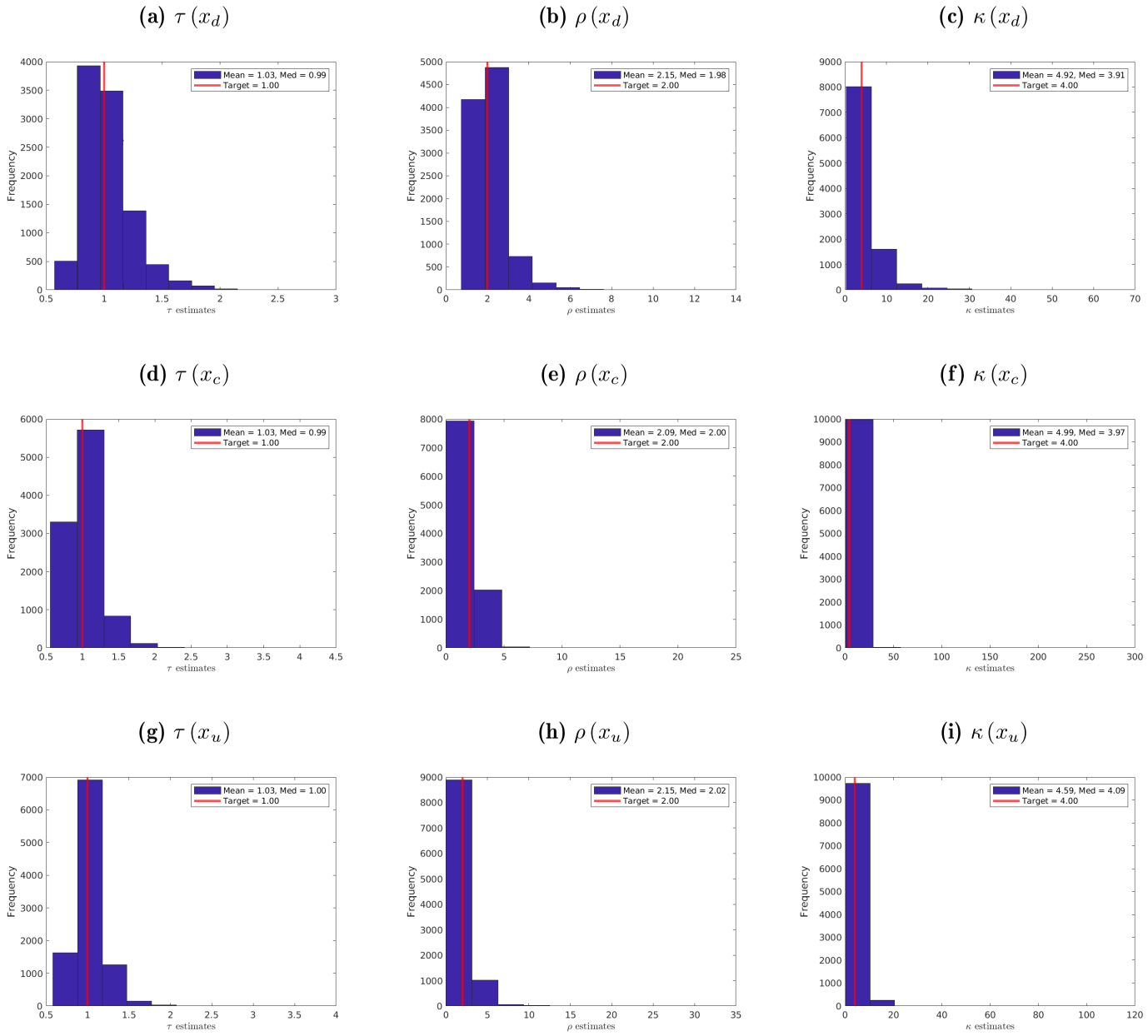

Figure IA.17
Simulated Parameter Estimates Given Noise in LHS Variable (Restricted Parameters)

This figure shows simulated parameter distributions (in blue), according to the simulation procedure described in Internet Appendix IA.6.2, along with the target parameter values (red lines). The target parameters are from our restricted decomposition from Internet Appendix IA.3.9 ("Data-Implied Decomposition Using Restricted Preference Parameters") (i.e., $\tau(x_s) = 1$, $\rho(x_s) = 2$, and $\kappa(x_s) = 4$).

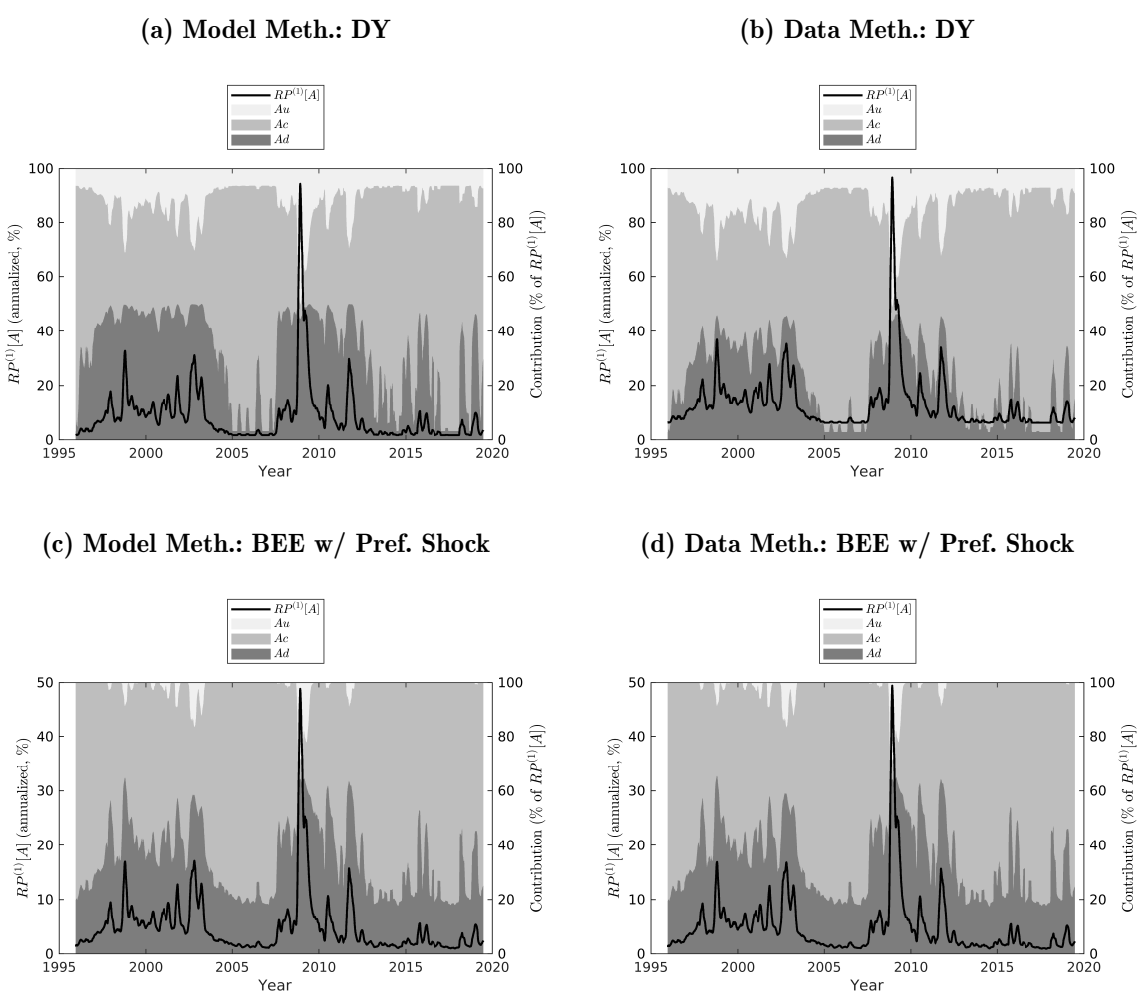

Figure IA.18
Model-Implied and Data-Methodology-Implied Model Market Risk Premium Decompositions

These graphs compare plots of the model-implied market risk premium decompositions to the data-methodology-applied-to-models (DMAM) market risk premium decompositions (see Subsection 5.3 for a description of the latter decompositions). Plots labeled "Model Meth." report original model-implied market risk premium decomposition results. Plots labeled "Data Meth." report DMAM market risk premium decompositions. Panels (a) and (b) report results for the Drechsler and Yaron (2011) ("DY") model. Panels (c)-(f) report results for the Bekaert, Engstrom, and Ermolov (2023) ("BEE") model with and without preference shocks (continued on next page). Panels (g) and (h) report results for the Gabaix (2012) model. Panels (i)-(j) report results for the Wachter (2013) model. Solid black lines represent the total conditional market risk premium and dark/medium/light shaded regions represent the downside/central/upside risk premium contributions, respectively. All decompositions use a 30-day horizon to match model calibration frequencies in the original papers (monthly), and set A_d=[0, 0.9], A_c=[0.9, 1.1], and A_u=[1.1, +∞). All time series are smoothed by averaging over two months of lagged daily data to reduce the appearance of noise.

(e) Model Meth.: BEE w/o Pref. Shock

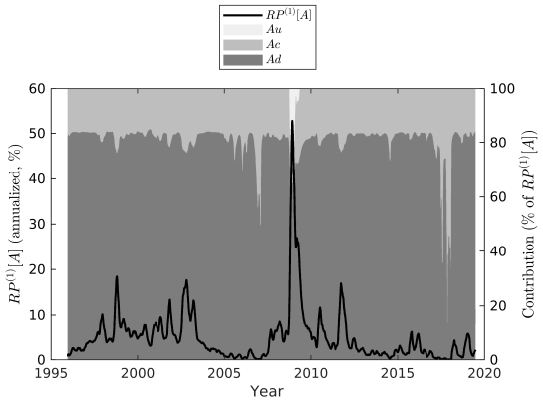

(f) Data Meth.: BEE w/o Pref. Shock

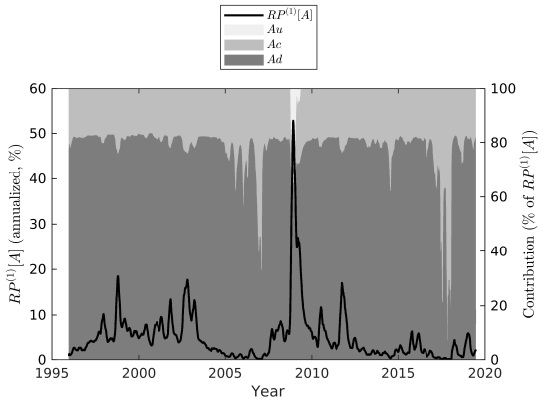

(g) Model Meth.: Gabaix

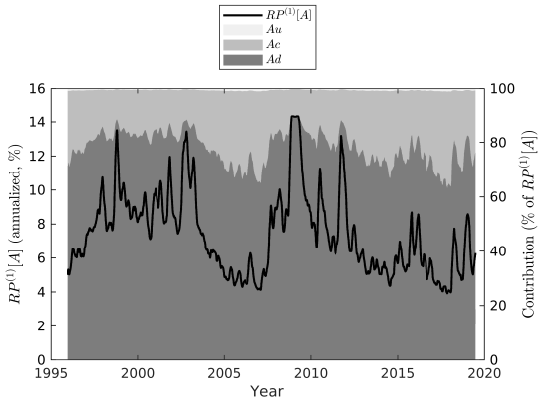

(h) Data Meth.: Gabaix

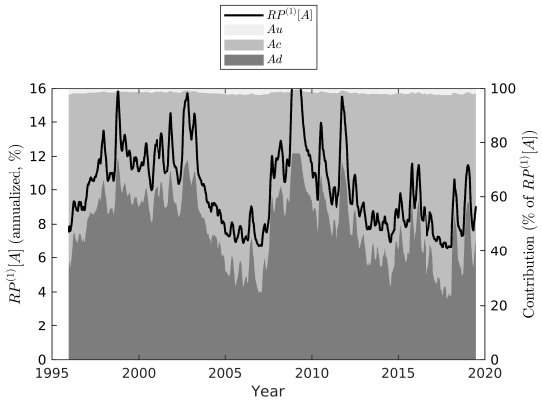

(i) Model Meth.: Wachter

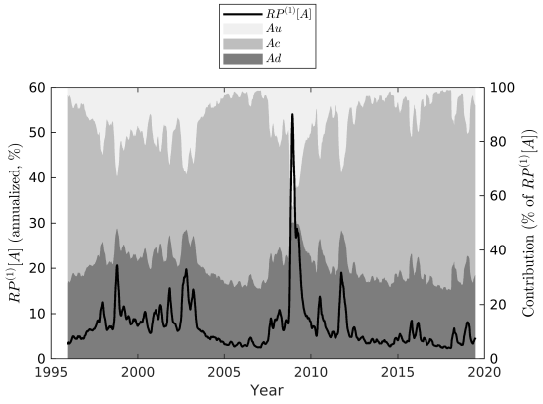

(j) Data Meth.: Wachter

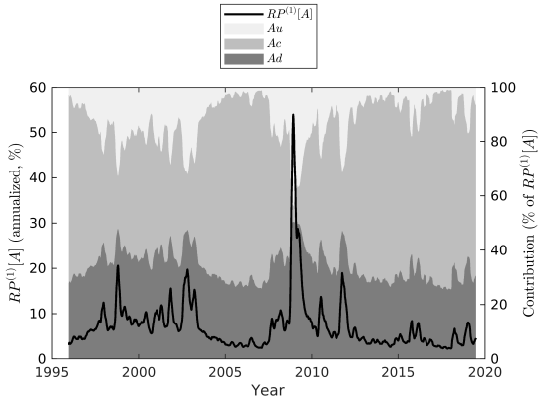

Figure IA.18
Model-Implied and Data-Methodology-Applied-To-Models Market Risk Premium Decompositions (continued)

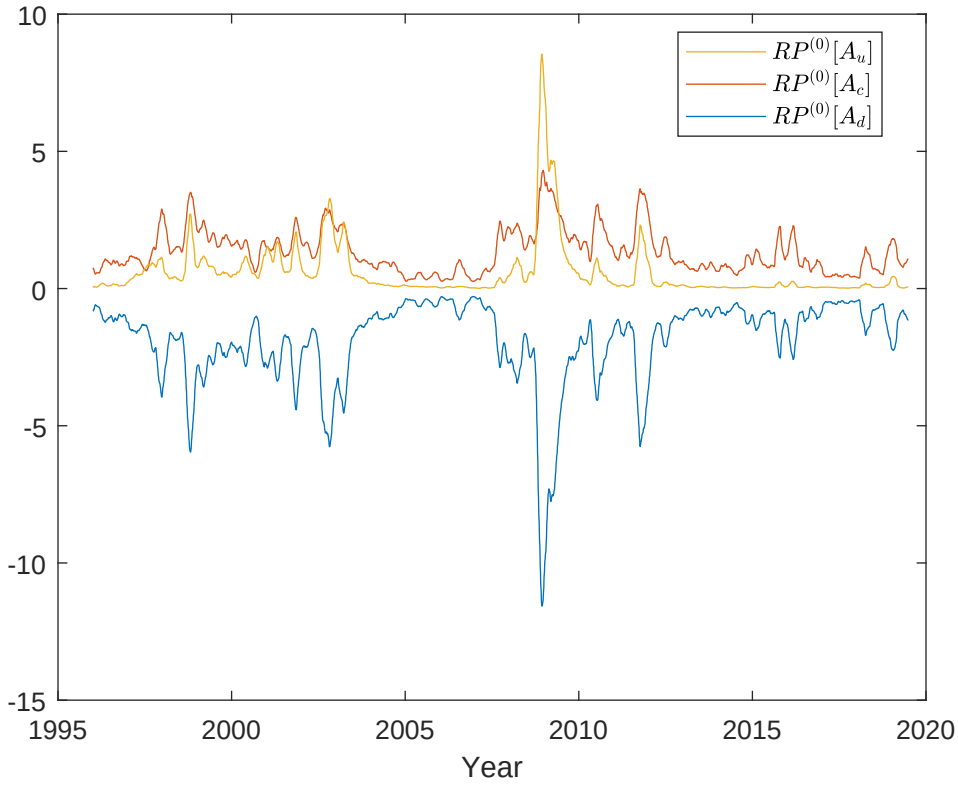

Figure IA.19
Arrow-Debreu Risk Premia

This graph plots the data-implied Arrow-Debreu risk premia of the form $\mathbb{RP}_t^{(0)}[A_s] \equiv \mathbb{E}_t[\mathbb{I}_{A_s}] - \mathbb{E}_t^*[\mathbb{I}_{A_s}]$ estimated using preference parameters reported in Table 1 to estimate $\mathbb{E}_t[\mathbb{I}_{A_s}]$ according to Corollary 1 with $n = 0$ and $\mathbb{E}_t^*[\mathbb{I}_{A_s}]$ according to standard techniques described in Internet Appendix IA.5. These are computed at the 30-day horizon and annualized to be consistent with plots of our market risk premium in Figure 2. The decompositions use A_d=$[0, 0.9]$, A_c=$[0.9, 1.1]$, and A_u=$[1.1, +\infty)$. All time series are smoothed by averaging over two months of lagged daily data to reduce the appearance of noise.

Table IA.1
Data-Implied Variance Risk Premium Decomposition Summary Statistics

This table reports summary statistics for the data-implied risk premium decomposition according to Proposition 3 using preference parameters reported in Table 1 with $n = 2$ (i.e., the variance risk premium). Panel A reports statistics for the risk premium levels (annualized and in percent) and Panel B reports statistics for the contributions of risk premia from each region to the total risk premium (as fractions of the total risk premium, in percent). A_d=[0, 0.9], A_c=[0.9, 1.1], and A_u=[1.1, $+\infty$) and these labels correspond to the downside, central, and upside risk premia, respectively. $A = A_d \cup A_c \cup A_u$ and this label corresponds to the total risk premium. Statistics reported under "Unconditional" use the full estimated time series for each risk premium measure. Statistics reported under "Cond. Means" report the means for each time series conditional on 30-day risk-neutral variance ($\mathbb{M}^{*(2)}_{t\to T}[A]$) falling below its first quartile ("Lo"), between its first and third quartiles ("Mid"), or above its third quartile ("Hi"). These correspond to periods of low, moderate, or high market volatility, respectively. Statistics are reported for risk premium decompositions at 30-, 60-, 90-, 180-, and 360-day horizons, and are based on daily data from January 1996 through June 2019.

		Panel A: $\mathbb{RP}^{(2)}_{t\to T}[A_s]$ (%)					**Panel B:** $\mathbb{RP}^{(2)}_{t\to T}[A_s]/\mathbb{RP}^{(2)}_{t\to T}[A]$ (%)				
		Cond. Means			**Unconditional**		**Cond. Means**			**Unconditional**	
Horizon (days)	**Region**	**Lo**	**Mid**	**Hi**	**Mean**	**St. Dev.**	**Lo**	**Mid**	**Hi**	**Mean**	**St. Dev.**
30	A	-0.29	-0.67	-2.50	-1.03	1.46					
	A_d	-0.25	-0.60	-2.22	-0.92	1.19	83.28	89.15	92.11	88.42	6.94
	A_c	-0.05	-0.09	-0.11	-0.09	0.10	19.19	14.56	7.63	13.99	6.87
	A_u	0.01	0.02	-0.14	-0.02	0.33	-2.47	-3.71	0.26	-2.41	4.54
60	A	-0.51	-1.10	-3.65	-1.59	1.99					
	A_d	-0.44	-0.97	-2.97	-1.34	1.46	87.83	89.79	85.96	88.34	4.05
	A_c	-0.07	-0.10	-0.02	-0.07	0.12	14.06	9.94	2.43	9.09	5.63
	A_u	0.01	-0.01	-0.61	-0.16	0.63	-1.89	0.27	11.62	2.57	6.77
90	A	-0.62	-1.26	-3.72	-1.71	1.91					
	A_d	-0.54	-1.08	-2.88	-1.39	1.32	88.44	87.61	81.84	86.37	4.38
	A_c	-0.07	-0.08	0.03	-0.05	0.10	12.56	7.56	-0.01	6.92	5.98
	A_u	0.01	-0.07	-0.83	-0.24	0.69	-1.00	4.83	18.17	6.71	8.60
180	A	-0.88	-1.63	-4.13	-2.07	2.03					
	A_d	-0.73	-1.31	-3.05	-1.60	1.39	85.57	82.37	76.88	81.80	4.35
	A_c	-0.08	-0.04	0.08	-0.02	0.11	8.99	2.95	-2.30	3.15	5.86
	A_u	-0.04	-0.25	-1.11	-0.41	0.71	5.44	14.68	25.42	15.06	9.04
360	A	-0.81	-1.34	-2.67	-1.54	1.21					
	A_d	-0.62	-0.98	-1.83	-1.10	0.82	78.33	74.97	69.77	74.51	4.61
	A_c	-0.06	-0.05	-0.05	-0.06	0.09	7.09	3.72	0.93	3.87	5.20
	A_u	-0.11	-0.28	-0.77	-0.36	0.39	14.58	21.31	29.30	21.62	7.41

Table IA.2
Representative Agent Model-Implied Variance Risk Premium Decomposition Summary Statistics

This table reports summary statistics for the model-implied risk premium decompositions based on representative agent models described in Section 5 with $n = 2$ (i.e., the variance risk premium). Panel A reports statistics for the risk premium levels (annualized and in percent) and Panel B reports statistics for the contributions of risk premia from each region to the total risk premium (as fractions of the total risk premium, in percent). Results are reported for the following models: Drechsler and Yaron (2011) ("DY"), Bekaert, Engstrom, and Ermolov (2023) ("BEE") with and without preference shocks, Gabaix (2012) ("Gabaix"), and Wachter (2013) ("Wachter"). A_d=[0, 0.9], A_c=[0.9, 1.1], and A_u=[1.1, $+\infty$) and these labels correspond to the downside, central, and upside risk premia, respectively. $A = A_d \cup A_c \cup A_u$ and this label corresponds to the total risk premium. Statistics reported under "Unconditional" use the full estimated time series for each risk premium measure. Statistics reported under "Cond. Means" report the means for each time series conditional on 30-day risk-neutral variance ($\mathbb{M}^{*(2)}_{t\to T}[A]$) falling below its first quartile ("Lo"), between its first and third quartiles ("Mid"), or above its third quartile ("Hi"). These correspond to periods of low, moderate, or high market volatility, respectively. Results are based on state variables extracted from the data under each model using their original calibrations, which are monthly in all cases, and use daily data from January 1996 through June 2019.

			Panel A: $\mathbb{RP}^{(2)}_{t\to T}[A_s]$ **(%)**					**Panel B:** $\mathbb{RP}^{(2)}_{t\to T}[A_s]/\mathbb{RP}^{(2)}_{t\to T}[A]$ **(%)**				
			Cond. Means			**Unconditional**		**Cond. Means**			**Unconditional**	
Class	**Model**	**Region**	**Lo**	**Mid**	**Hi**	**Mean**	**St. Dev.**	**Lo**	**Mid**	**Hi**	**Mean**	**St. Dev.**
LRR	**DY**	A	0.00	-0.42	-1.94	-0.69	0.99					
		A_d	-0.01	-0.44	-1.96	-0.71	1.01	-62.36	100.17	101.62	59.90	209.08
		A_c	0.00	-0.01	0.06	0.01	0.25	4.09	1.83	1.26	2.25	4.87
		A_u	0.01	0.03	-0.03	0.01	0.21	158.28	-2.00	-2.88	37.85	206.57
Habit	**BEE (w/ P.S.)**	A	-0.07	-0.31	-2.46	-0.79	1.62					
		A_d	-0.03	-0.25	-2.27	-0.70	1.46	46.26	70.41	92.51	69.90	19.57
		A_c	-0.04	-0.06	-0.14	-0.07	0.07	53.75	29.65	7.11	30.04	19.68
		A_u	0.00	0.00	-0.05	-0.01	0.12	0.00	-0.06	0.38	0.06	0.96
	BEE (w/o P.S.)	A	-0.17	-0.91	-3.19	-1.30	1.60					
		A_d	-0.16	-0.86	-2.74	-1.15	1.28	86.96	94.28	88.78	91.08	15.13
		A_c	-0.01	-0.06	-0.34	-0.12	0.19	13.04	5.74	10.55	8.77	15.07
		A_u	0.00	0.00	-0.10	-0.02	0.27	0.00	-0.02	0.67	0.16	2.22
Disaster	**Gabaix**	A	-0.87	-2.46	-6.81	-3.15	2.68					
		A_d	-0.87	-2.45	-6.74	-3.13	2.65	101.16	99.67	98.96	99.86	0.92
		A_c	0.01	-0.01	-0.08	-0.03	0.04	-0.90	0.40	1.14	0.26	0.84
		A_u	0.00	0.00	0.01	0.00	0.01	-0.26	-0.06	-0.11	-0.12	0.11
	Wachter	A	-0.38	-0.78	-1.90	-0.96	0.76					
		A_d	-0.39	-0.82	-2.10	-1.03	0.87	102.14	104.70	109.47	105.25	3.07
		A_c	0.00	0.00	0.07	0.02	0.08	-0.44	0.19	-2.11	-0.54	1.67
		A_u	0.01	0.04	0.13	0.06	0.06	-1.70	-4.89	-7.36	-4.71	2.33

Table IA.3
Comparing Data- and Model-Implied Variance Risk Premium Decompositions

This table compares the variance risk premium decomposition results from the data with that from the models. Panel A (Panel B) reports comparisons between the levels (contributions). The left portion of each panel reports the average differences between the data and models (i.e., the averages of $\mathbb{RP}^{(2)}_{t\to T,\,data}[A_s] - \mathbb{RP}^{(2)}_{t\to T,\,model}[A_s]$ for the levels and $\mathbb{RP}^{(2)}_{t\to T,\,data}[A_s]/\mathbb{RP}^{(2)}_{t\to T,\,data}[A] - \mathbb{RP}^{(2)}_{t\to T,\,model}[A_s]/\mathbb{RP}^{(2)}_{t\to T,\,model}[A]$ for the contributions). The right portion of each panel reports the corridor measure for each region. This measure is constructed as the fraction of days on which a model-based value that falls within a certain bandwidth of the corresponding data-based value, where the bandwidth is constant over time. In the case of risk premium levels, the bandwidth is taken to be ±15% of the time series average of the corresponding level measure. In the case of risk premium contributions, the bandwidth is taken to be ±15 percentage points. "Agg." represents aggregations of the corridor measures across each region and is meant to be a measure of overall model fit across the three regions of interest. It is a weighted sum of measures across the three regions where the weights are equal to the average contribution from each region (e.g., weights for measures from regions A_d, A_c, and A_u are 88.42%, 13.99%, and -2.41%, respectively, based on results from Table IA.1, Panel B). The data-implied decomposition measures are based on the data-implied variance risk premium decomposition time series (30-day horizon) summarized in Table IA.1 and the corresponding model-implied variance risk premium decomposition time series based on representative agent models summarized in Table IA.2. Results are reported for the following models: Drechsler and Yaron (2011) ("DY"), Bekaert, Engstrom, and Ermolov (2023) ("BEE") with and without preference shocks, Gabaix (2012) ("Gabaix"), and Wachter (2013) ("Wachter"). A_d=[0, 0.9], A_c=[0.9, 1.1], and A_u=[1.1, +∞) and these labels correspond to the downside, central, and upside risk premia, respectively. $A = A_d \cup A_c \cup A_u$ and this label corresponds to the total risk premium. T-statistics for the mean differences are reported in parentheses and are computed according to Newey and West (1987) with lag values according to Newey and West (1994), with one slight modification. Since we have overlapping data, we multiply the Newey and West (1994)-implied lag value by the number of overlapping days (21) and use this as our lag value. Data is daily and runs from January 1996 through June 2019.

	Panel A: Levels									**Panel B: Contributions**							
	Mean diff. (annualized, %)				**Corridor measure (%)**					**Mean diff. (annualized, %)**			**Corridor measure (%)**				
Model	A	A_d	A_c	A_u	A	A_d	A_c	A_u	**Agg.**	A_d	A_c	A_u	A_d	A_c	A_u	**Agg.**	
DY	-0.34	-0.20	-0.10	-0.03	20.40	25.36	1.01	17.61	22.14	28.52	11.74	-40.26	41.85	72.38	69.03	45.46	
	(-5.69)	(-5.71)	(-4.89)	(-2.51)						(2.03)	(10.71)	(-2.74)					
BEE (w/ P.S.)	-0.25	-0.22	-0.01	-0.01	18.18	15.21	28.01	9.49	17.14	18.52	-16.05	-2.47	45.52	51.05	98.70	45.01	
	(-4.67)	(-3.47)	(-1.03)	(-0.47)						(5.44)	(-4.85)	(-4.88)					
BEE (w/o P.S.)	0.26	0.24	0.03	0.00	38.14	34.56	10.37	9.37	31.78	-2.65	5.22	-2.57	86.16	78.10	99.02	84.73	
	(3.05)	(3.56)	(1.01)	(0.11)						(-1.31)	(2.51)	(-5.52)					
Gabaix	2.12	2.21	-0.06	-0.03	0.63	0.25	1.34	15.92	0.03	-11.44	13.73	-2.29	72.58	61.23	98.00	70.38	
	(6.52)	(6.59)	(-5.75)	(-0.80)						(-8.25)	(10.37)	(-3.79)					
Wachter	-0.07	0.11	-0.10	-0.08	57.00	30.43	0.10	20.69	26.42	-16.83	14.53	2.30	40.12	61.16	97.73	41.68	
	(-0.86)	(2.74)	(-10.27)	(-2.00)						(-18.95)	(13.65)	(2.91)					

Table IA.4
Data-Implied Risk Quantities and Risk Prices by Horizon

This table reports time series averages of level variables from the data-implied risk quantities and risk prices at different horizons (30-, 60-, 90-, 180-, and 360-day) in each region of interest using the decomposition: $\mathbb{RP}^{(1)}_{t\to T}[A_s] \equiv \beta^*_{t,s} \cdot \sigma^{*2}_{t,M,s}$. The risk price can further be decomposed as: $\sigma^{*2}_{t,M,s} \equiv \omega_{t,M,s} + \sigma^2_{t,s}$. Results from the 30-day horizon match results reported for the data-implied decomposition in Table 6. All risk quantity and risk price variables are defined in Proposition 4. The data-implied decomposition measures are based on the data-implied market risk premium decomposition time series summarized in Table 2. A_d=[0, 0.9], A_c=[0.9, 1.1], and A_u=[1.1, $+\infty$) and these labels correspond to the downside, central, and upside risk premia, respectively. $A = A_d \cup A_c \cup A_u$ and this label corresponds to the total risk premium. Data is daily and runs from January 1996 through June 2019.

Panel A: Mean Levels

	$\beta^*_{t,s}$				$\sigma^{*2}_{t,M,s}$ (annualized, %)				$\omega_{t,M,s}$ (annualized, %)			$\sigma^2_{t,s}$ (annualized, %)		
Horizon (days)	A	A_d	A_c	A_u	A	A_d	A_c	A_u	A_d	A_c	A_u	A_d	A_c	A_u
30	0.45	0.20	0.06	0.02	20.29	20.92	83.50	40.12	-12.39	23.34	8.79	33.31	60.16	31.33
60	0.39	0.32	0.04	0.02	25.64	16.45	83.02	55.41	-11.46	21.55	14.21	27.91	61.48	41.19
90	0.42	0.34	0.02	0.02	21.49	15.15	73.75	56.81	-10.18	15.85	14.56	25.33	57.90	42.24
180	0.45	0.39	0.01	0.03	16.43	12.23	51.30	49.26	-6.46	8.39	13.00	18.68	42.91	36.26
360	0.61	0.27	0.01	0.04	7.11	10.88	26.89	29.96	-3.47	2.86	6.65	14.35	24.03	23.32

Table IA.5
Variance Decompositions for Data-Implied Market Risk Premia by Horizon

This table reports data-implied market risk premium variance decomposition results in each region of interest at different horizons (30-, 60-, 90-, 180-, and 360-day). The risk premium in each region ($\mathbb{RP}^{(1)}_{t\to T}[A_s] \equiv \beta^*_{t,s} \cdot \sigma^{*2}_{t,M,s}$) can be approximated using a linear projection onto $\beta^*_{t,s}$ and $\sigma^{*2}_{t,M,s}$ (i.e., $\mathbb{RP}^{(1)}_{t\to T}[A_s] = a + b \cdot \beta^*_{t,s} + c \cdot \sigma^{*2}_{t,M,s} + \varepsilon_{t,s}$). The risk price can be decomposed further as $\sigma^{*2}_{t,M,s} \equiv \omega_{t,M,s} + \sigma^2_{t,s}$, allowing us to express the risk premium as $\mathbb{RP}^{(1)}_{t\to T}[A_s] = a + b \cdot \beta^*_{t,s} + c \cdot \omega_{t,M,s} + c \cdot \sigma^2_{t,s} + \varepsilon_{t,s}$. All variables related to risk prices and quantities are defined in Proposition 4. Each contribution is reported in percent and is computed as described in Equation 39 such that the sum across all contributions explains 100% of the variance of the risk premium of interest. Each risk premium's time series standard deviation is reported in the first column (annualized and in percent). The data-implied decomposition measures are based on the data-implied market risk premium decomposition time series summarized in Table 2. A_d=[0, 0.9], A_c=[0.9, 1.1], and A_u=[1.1, $+\infty$) and these labels correspond to the downside, central, and upside risk premia, respectively. $A = A_d \cup A_c \cup A_u$ and this label corresponds to the total risk premium. Data is daily and runs from January 1996 through June 2019.

Region	Horizon (days)	St. Dev.	$b \cdot \beta^*_{t,s}$	$c \cdot \omega_{t,M,s}$	$c \cdot \sigma^2_{t,s}$	$\varepsilon_{t,s}$
A	**30**	7.50	-1.31	100.95	0.00	0.37
	60	6.99	-0.52	99.58	0.00	0.94
	90	5.60	-2.79	101.42	0.00	1.38
	180	4.15	-5.79	104.70	0.00	1.09
	360	2.48	5.25	94.58	0.00	0.17
A_d	**30**	4.97	21.97	-48.49	110.88	15.64
	60	4.90	58.35	-30.78	66.66	5.78
	90	4.01	66.65	-26.10	54.97	4.48
	180	3.06	64.24	-7.02	37.39	5.39
	360	1.71	68.05	-2.23	26.57	7.61
A_c	**30**	1.18	7.70	11.27	44.89	36.14
	60	0.46	11.64	6.53	33.75	48.09
	90	0.19	-16.56	6.61	24.59	85.36
	180	0.09	123.37	28.72	-62.26	10.17
	360	0.05	87.08	14.46	-2.03	0.49
A_u	**30**	2.15	4.79	24.96	62.01	8.24
	60	2.13	23.92	23.96	45.79	6.33
	90	1.75	48.08	17.21	31.08	3.63
	180	1.22	69.80	13.08	14.46	2.66
	360	0.81	94.93	2.48	0.94	1.65

Table IA.6
Preference Parameter Estimates ($\pm 5\%$ Cutoffs)

This table reports preference parameters estimates for $\tau(x_s)$ (Equation 14), $\rho(x_s)$ (Equation 15), and $\kappa(x_s)$ (Equation 16) with $s \in \{d, c, u\}$ and $x_d = 0.92$, $x_c = 1.00$, and $x_u = 1.08$. These correspond to the three regions of interest in the gross market return space defined by A_d=$[0, 0.95]$, A_c=$[0.95, 1.05]$, and A_u=$[1.05, +\infty)$. $1/\tau(x_s)$ is the relative risk aversion. Parameters are estimated separately for each of five horizons (30, 60, 90, 180, and 360 days). Estimations are done using nonlinear least squares according to the description in Subsection 4.2. Values in brackets represent the 95% confidence intervals obtained from 10,000 block bootstrap simulations. The block length is set to be four years for simulations at all horizons. Parameters are estimated using daily S&P 500 excess market return data (ex dividend) from CRSP and risk-neutral moments computed from daily option prices obtained from Option Metrics. Data is daily and ranges from January 1996 through June 2019.

		Horizon (days)				
Region	**Parameter**	**30**	**60**	**90**	**180**	**360**
A_d	$1/\tau(x_d)$	3.11	2.80	2.41	1.81	0.94
		[1.96, 5.15]	[1.92, 4.31]	[1.52, 4.08]	[1.12, 4.59]	[0.68, 1.97]
	$\tau(x_d)$	0.32	0.36	0.42	0.55	1.07
		[0.19, 0.51]	[0.23, 0.52]	[0.24, 0.66]	[0.22, 0.89]	[0.51, 1.47]
	$\rho(x_d)$	1.28	1.36	1.39	1.56	2.14
		[0.80, 1.64]	[1.06, 1.76]	[0.97, 1.99]	[0.99, 2.36]	[0.97, 2.83]
	$\kappa(x_d)$	1.25	1.42	1.44	1.82	3.53
		[0.60, 1.62]	[1.03, 2.02]	[0.93, 2.41]	[0.97, 3.68]	[1.05, 5.22]
A_c	$1/\tau(x_c)$	2.11	1.93	1.75	1.44	0.86
		[1.41, 4.21]	[1.37, 3.07]	[1.17, 3.09]	[1.01, 3.38]	[0.70, 1.70]
	$\tau(x_c)$	0.47	0.52	0.57	0.70	1.17
		[0.24, 0.71]	[0.33, 0.73]	[0.32, 0.85]	[0.30, 0.99]	[0.59, 1.42]
	$\rho(x_c)$	2.11	2.18	2.14	2.14	2.35
		[0.76, 2.97]	[1.24, 3.16]	[0.97, 3.34]	[0.98, 3.45]	[0.59, 3.74]
	$\kappa(x_c)$	2.18	2.40	2.32	2.57	3.86
		[0.59, 2.83]	[1.30, 3.45]	[0.96, 3.73]	[1.07, 4.43]	[1.11, 5.41]
A_u	$1/\tau(x_u)$	1.29	1.21	1.16	1.10	0.77
		[0.97, 3.91]	[0.95, 2.23]	[0.86, 2.48]	[0.80, 2.61]	[0.65, 1.53]
	$\tau(x_u)$	0.78	0.83	0.86	0.91	1.31
		[0.26, 1.03]	[0.45, 1.05]	[0.40, 1.16]	[0.38, 1.25]	[0.65, 1.53]
	$\rho(x_u)$	5.13	5.14	4.62	3.48	2.80
		[0.69, 6.76]	[1.48, 7.21]	[0.89, 7.32]	[0.72, 7.68]	[0.09, 6.30]
	$\kappa(x_u)$	4.34	4.82	4.35	3.97	4.61
		[0.50, 4.76]	[1.70, 5.68]	[0.90, 6.29]	[1.14, 7.11]	[1.10, 7.43]

Table IA.7
Data-Implied Market Risk Premium Decomposition Summary Statistics ($\pm 5\%$ Cutoffs)

This table reports summary statistics for the data-implied risk premium decomposition according to Proposition 3 using preference parameters reported in Table 1 with $n = 1$ (i.e., the market risk premium). Panel A reports statistics for the risk premium levels (annualized, in percent) and Panel B reports statistics for the contributions of risk premia from each region to the total risk premium (as fractions of the total risk premium, in percent). A_d=$[0, 0.95]$, A_c=$[0.95, 1.05]$, and A_u=$[1.05, +\infty)$ and these labels correspond to the downside, central, and upside risk premia, respectively. $A = A_d \cup A_c \cup A_u$ and this label corresponds to the total risk premium. Statistics reported under "Unconditional" use the full estimated time series for each risk premium measure. Statistics reported under "Cond. Means" report the means for each time series conditional on 30-day risk-neutral variance ($\mathbb{M}^{*(2)}_{t\to T}[A]$) falling below its first quartile ("Lo"), between its first and third quartiles ("Mid"), or above its third quartile ("Hi"). These correspond to periods of low, moderate, or high market volatility, respectively. Statistics are reported for risk premium decompositions at 30-, 60-, 90-, 180-, and 360-day horizons, and are based on daily data from January 1996 through June 2019.

		Panel A: $\mathbb{RP}^{(1)}_{t\to T}[A_s]$ **(%)**					**Panel B:** $\mathbb{RP}^{(1)}_{t\to T}[A_s]/\mathbb{RP}^{(1)}_{t\to T}[A]$ **(%)**				
		Cond. Means			**Unconditional**		**Cond. Means**			**Unconditional**	
Horizon (days)	**Region**	**Lo**	**Mid**	**Hi**	**Mean**	**St. Dev.**	**Lo**	**Mid**	**Hi**	**Mean**	**St. Dev.**
30	A	3.38	7.30	18.65	9.16	7.72					
	A_d	1.99	4.58	12.66	5.95	5.55	59.58	63.23	67.11	63.28	5.58
	A_c	1.07	1.30	1.17	1.21	0.19	32.91	19.52	7.62	19.89	10.37
	A_u	0.26	1.34	4.79	1.93	2.28	7.51	17.26	25.27	16.82	8.23
60	A	3.63	7.29	16.84	8.76	6.41					
	A_d	2.47	5.00	11.99	6.12	4.81	68.98	69.38	70.77	69.63	4.03
	A_c	0.61	0.57	0.48	0.56	0.10	17.65	8.79	3.24	9.62	5.87
	A_u	0.48	1.63	4.28	2.01	1.72	13.37	21.83	25.99	20.75	6.60
90	A	3.58	6.71	14.23	7.81	5.08					
	A_d	2.56	4.73	10.27	5.57	3.85	72.27	71.34	71.94	71.72	3.56
	A_c	0.37	0.32	0.29	0.33	0.07	10.86	5.33	2.20	5.93	3.59
	A_u	0.59	1.58	3.56	1.83	1.30	16.87	23.33	25.87	22.35	5.27
180	A	3.55	6.05	11.52	6.79	3.94					
	A_d	2.61	4.34	8.36	4.91	2.98	74.99	72.97	72.57	73.38	3.29
	A_c	0.15	0.15	0.20	0.16	0.07	4.41	2.65	1.68	2.85	1.28
	A_u	0.71	1.46	2.85	1.62	0.95	20.59	24.38	25.75	23.77	3.73
360	A	2.58	4.07	7.23	4.49	2.50					
	A_d	1.91	2.90	4.99	3.17	1.73	75.12	71.59	68.97	71.82	4.59
	A_c	0.08	0.13	0.19	0.13	0.09	3.45	3.49	2.80	3.30	1.99
	A_u	0.54	1.01	2.02	1.14	0.75	21.43	24.93	28.23	24.88	3.96

Table IA.8

Market Risk Premium Decompositions with Modified Decomposition Preference Parameters (30-day horizon)

This table reports summary statistics for the data-implied risk premium decomposition according to Proposition 3 with $n = 1$ (i.e., the market risk premium) using our original preference parameters reported in Table 1 along with modified versions of these parameters. Panel A reports average risk premium levels (annualized, in percent). Panel B reports statistics for the contributions of risk premia from each region to the total risk premium (as fractions of the total risk premium, in percent). Panel C reports preference parameter values used in each decomposition with the "Modified Parameter" column indicating which parameters were modified from their original values, while holding all other parameter values fixed. For instance, in the rows labeled "$\tau(x_d)$, $\tau(x_c)$, and $\tau(x_u)$," we modify τ parameters in all regions while keeping $\rho's$ and $\kappa's$ at their original values. Columns labeled "Orig." represent results based on original parameter values. For instance, the "Orig." column in Panel A presents original average market risk premium results from Table 2 for a comparison with results when modifying parameters. Columns labeled "Less SD/2" ("Plus SD/2") represent decomposition results based on using preference parameter values that are either one-half of a standard deviation lower (higher) than their original values based on the bootstrap analysis used to generate results reported in Table 1. A_d=$[0, 0.9]$, A_c=$[0.9, 1.1]$, and A_u=$[1.1, +\infty)$ and these labels correspond to the downside, central, and upside risk premia, respectively. $A = A_d \cup A_c \cup A_u$ and this label corresponds to the total risk premium. All results are for risk premium decompositions at the 30-day horizon, and are based on daily data from January 1996 through June 2019.

		Panel A: $\mathbb{RP}^{(1)}_{t\to T}[A_s]$ (%)			**Panel B:** $\frac{\mathbb{RP}^{(1)}_{t\to T}[A_s]}{\mathbb{RP}^{(1)}_{t\to T}[A]}$ (%)			**Panel C:** Parameter values		
Modified Parameters	**Region**	**Less SD/2**	**Orig.**	**Plus SD/2**	**Less SD/2**	**Orig.**	**Plus SD/2**	**Less SD/2**	**Orig.**	**Plus SD/2**
$\tau(x_d)$, $\tau(x_c)$, **and** $\tau(x_u)$	A	9.92	8.72	7.67						
	A_d	4.79	4.45	4.09	43.17	45.67	47.38	0.23	0.28	0.34
	A_c	4.00	3.33	2.85	49.59	47.84	46.65	0.41	0.49	0.57
	A_u	1.22	0.97	0.79	7.24	6.48	5.97	0.82	0.96	1.11
$\rho(x_d)$, $\rho(x_c)$, **and** $\rho(x_u)$	A	9.21	8.72	8.15						
	A_d	4.82	4.45	4.03	47.49	45.67	43.54	0.93	0.99	1.05
	A_c	3.34	3.33	3.32	46.70	47.84	49.20	1.55	1.82	2.91
	A_u	0.91	0.97	1.03	5.81	6.48	7.26	4.78	5.76	6.75
$\kappa(x_d)$, $\kappa(x_c)$, **and** $\kappa(x_u)$	A	8.09	8.72	9.32						
	A_d	4.17	4.45	4.71	44.70	45.67	46.54	0.72	0.81	0.91
	A_c	3.31	3.33	3.35	48.71	47.84	47.06	1.54	1.79	2.05
	A_u	0.94	0.97	0.99	6.59	6.48	6.40	3.35	3.97	4.58

Table IA.9
Preference Parameters for Matching Non-Monotonic SDFs

This table reports preference parameters $\tau(x_s)$ (Equation 14), $\rho(x_s)$ (Equation 15), and $\kappa(x_s)$ (Equation 16) with $s \in \{d, c, u\}$ optimized to minimize the square differences between the parameter-based SDF in Equation 18 and those from either Rosenberg and Engle (2002) (Figure 6) or Beason and Schreindorfer (2022) (Figure 2). These parameters are used to generate the plots in Figure IA.10. See Internet Appendix IA.3.7 for more details.

		SDF to Match	
		Rosenberg and Engle (2002)	**Beason and Schreindorfer (2022)**
Region	**Parameter**	**Figure 6**	**Figure 2**
A_u	$\tau(x_d)$	0.03	0.16
	$\rho(x_d)$	0.89	0.62
	$\kappa(x_d)$	0.73	0.28
A_u	$\tau(x_c)$	-0.13	0.55
	$\rho(x_c)$	-2.77	13.48
	$\kappa(x_c)$	-9.92	-6.84
A_u	$\tau(x_u)$	0.13	0.67
	$\rho(x_u)$	17.99	4.64
	$\kappa(x_u)$	21.57	-44.56

Table IA.10
Preference Parameter Estimates (Corollary 2)

This table reports preference parameters estimates for a single set of τ, ρ, and κ based on Corollary 2. We assume these are constant over time rather than a function of $R_{f,t\to T}$ for parsimony. $1/\tau$ is the relative risk aversion. Parameters are estimated separately for each of five horizons (30, 60, 90, 180, and 360 days). Estimations are done using nonlinear least squares according to the description in Subsection 4.2 (but adapted to apply to Corollary 2 rather than Corollary 1 as in our main results). Values in brackets represent the 95% confidence intervals obtained from 10,000 block bootstrap simulations. The block length is set to be four years for simulations at all horizons. Parameters are estimated using daily S&P 500 excess market return data (ex dividend) from CRSP and risk-neutral moments computed from daily option prices obtained from Option Metrics. Data is daily and ranges from January 1996 through June 2019.

	Horizon (days)				
Parameter	**30**	**60**	**90**	**180**	**360**
$\boldsymbol{1/\tau}$	1.87	1.67	1.53	1.30	0.79
	[1.36, 4.20]	[1.23, 2.98]	[1.08, 2.96]	[0.96, 2.92]	[0.64, 1.23]
$\boldsymbol{\tau}$	0.54	0.60	0.65	0.77	1.27
	[0.24, 0.73]	[0.34, 0.81]	[0.34, 0.93]	[0.34, 1.04]	[0.81, 1.56]
$\boldsymbol{\rho}$	2.62	2.69	2.57	2.42	2.28
	[0.74, 3.78]	[1.24, 4.03]	[0.92, 4.18]	[0.78, 4.33]	[0.00, 4.62]
$\boldsymbol{\kappa}$	2.74	2.98	2.79	2.96	4.17
	[0.57, 3.64]	[1.30, 4.33]	[0.94, 4.53]	[1.09, 5.29]	[1.38, 6.29]

Table IA.11

Data-Implied Market Risk Premium Decomposition Summary Statistics (Corollary 2)

This table reports summary statistics for the data-implied risk premium decomposition according to Proposition 3 using the single set of preference parameters reported in Table IA.10 with $n = 1$ (i.e., the market risk premium) to construct physical moments according to Corollary 2. Panel A reports statistics for the risk premium levels (annualized, in percent) and Panel B reports statistics for the contributions of risk premia from each region to the total risk premium (as fractions of the total risk premium, in percent). A_d=[0, 0.9], A_c=[0.9, 1.1], and A_u=[1.1, $+\infty$) and these labels correspond to the downside, central, and upside risk premia, respectively. $A = A_d \cup A_c \cup A_u$ and this label corresponds to the total risk premium. Statistics reported under "Unconditional" use the full estimated time series for each risk premium measure. Statistics reported under "Cond. Means" report the means for each time series conditional on 30-day risk-neutral variance ($\mathbb{M}^{*(2)}_{t\to T}[A]$) falling below its first quartile ("Lo"), between its first and third quartiles ("Mid"), or above its third quartile ("Hi"). These correspond to periods of low, moderate, or high market volatility, respectively. Statistics are reported for risk premium decompositions at 30-, 60-, 90-, 180-, and 360-day horizons, and are based on daily data from January 1996 through June 2019.

		Panel A: $\mathbb{RP}^{(1)}_{t\to T}[A_s]$ **(%)**					**Panel B:** $\mathbb{RP}^{(1)}_{t\to T}[A_s]/\mathbb{RP}^{(1)}_{t\to T}[A]$ **(%)**				
		Cond. Means			**Unconditional**		**Cond. Means**			**Unconditional**	
Horizon (days)	**Region**	**Lo**	**Mid**	**Hi**	**Mean**	**St. Dev.**	**Lo**	**Mid**	**Hi**	**Mean**	**St. Dev.**
30	A	3.08	6.66	17.06	8.36	7.04					
	A_d	1.26	3.25	10.93	4.67	5.34	40.69	48.01	61.36	49.52	10.62
	A_c	1.77	3.16	4.47	3.14	1.13	58.09	49.03	30.45	46.65	12.85
	A_u	0.04	0.22	1.56	0.51	0.93	1.22	2.95	8.20	3.83	3.53
60	A	3.26	6.58	15.27	7.92	5.83					
	A_d	1.80	4.06	10.88	5.20	4.70	54.77	61.37	69.64	61.79	8.17
	A_c	1.38	1.97	2.22	1.88	0.39	43.16	31.66	16.76	30.81	11.30
	A_u	0.07	0.51	2.07	0.79	0.98	2.08	6.98	13.60	7.41	5.48
90	A	3.29	6.20	13.20	7.23	4.73					
	A_d	2.05	4.12	9.59	4.97	3.80	61.95	66.22	71.53	66.48	6.39
	A_c	1.09	1.31	1.31	1.25	0.16	33.95	22.71	11.22	22.65	9.54
	A_u	0.13	0.74	2.21	0.95	0.94	4.10	11.07	17.24	10.87	6.40
180	A	3.39	5.83	11.17	6.56	3.81					
	A_d	2.41	4.16	8.23	4.74	2.99	70.94	71.50	73.21	71.79	4.49
	A_c	0.59	0.57	0.54	0.57	0.08	18.07	10.81	5.32	11.25	5.42
	A_u	0.36	1.06	2.31	1.20	0.86	10.99	17.69	21.47	16.96	5.80
360	A	2.46	3.95	7.11	4.37	2.44					
	A_d	1.81	2.81	4.85	3.07	1.64	73.70	71.25	68.56	71.19	4.72
	A_c	0.18	0.18	0.19	0.18	0.04	7.77	5.00	2.79	5.14	2.37
	A_u	0.44	0.94	2.03	1.09	0.80	18.53	23.75	28.66	23.67	5.54

Table IA.12
Restricted Data-Implied Market Risk Premium Decomposition Summary Statistics

This table reports summary statistics for the restricted data-implied risk premium decomposition according to Proposition 3 with $n = 1$ (i.e., the market risk premium). The decompositions set preference parameters to be $\tau = 1$, $\rho = 2$, and $\kappa = 4$ across all regions and horizons. Panel A reports statistics for the risk premium levels (annualized, in percent) and Panel B reports statistics for the contributions of risk premia from each region to the total risk premium (as fractions of the total risk premium, in percent). A_d=[0, 0.9], A_c=[0.9, 1.1], and A_u=[1.1, $+\infty$) and these labels correspond to the downside, central, and upside risk premia, respectively. $A = A_d \cup A_c \cup A_u$ and this label corresponds to the total risk premium. Statistics reported under "Unconditional" use the full estimated time series for each risk premium measure. Statistics reported under "Cond. Means" report the means for each time series conditional on 30-day risk-neutral variance ($\mathbb{M}^{*(2)}_{t\to T}[A]$) falling below its first quartile ("Lo"), between its first and third quartiles ("Mid"), or above its third quartile ("Hi"). These correspond to periods of low, moderate, or high market volatility, respectively. Statistics are reported for risk premium decompositions at 30-, 60-, 90-, 180-, and 360-day horizons, and are based on daily data from January 1996 through June 2019.

		Panel A: $\mathbb{RP}^{(1)}_{t\to T}[A_s]$ **(%)**					**Panel B:** $\mathbb{RP}^{(1)}_{t\to T}[A_s]/\mathbb{RP}^{(1)}_{t\to T}[A]$ **(%)**				
		Cond. Means			**Unconditional**		**Cond. Means**			**Unconditional**	
Horizon (days)	**Region**	**Lo**	**Mid**	**Hi**	**Mean**	**St. Dev.**	**Lo**	**Mid**	**Hi**	**Mean**	**St. Dev.**
30	A	1.61	3.53	10.19	4.72	4.96					
	A_d	0.64	1.65	6.05	2.50	3.30	39.75	45.91	57.16	47.18	10.09
	A_c	0.93	1.68	2.36	1.66	0.60	58.20	49.26	29.12	46.46	13.74
	A_u	0.03	0.19	1.71	0.53	1.36	2.05	4.83	13.71	6.35	6.07
60	A	1.91	3.94	10.33	5.03	4.69					
	A_d	1.03	2.32	6.71	3.09	3.22	53.32	58.51	64.17	58.63	7.81
	A_c	0.81	1.16	1.25	1.09	0.22	43.42	31.38	15.18	30.34	12.16
	A_u	0.06	0.44	2.31	0.81	1.41	3.26	10.11	20.65	11.03	8.20
90	A	2.16	4.23	10.31	5.24	4.45					
	A_d	1.34	2.72	6.88	3.41	3.06	61.23	64.12	66.53	64.00	6.36
	A_c	0.70	0.83	0.79	0.79	0.10	33.25	21.46	9.46	21.40	10.01
	A_u	0.12	0.65	2.58	1.00	1.41	5.52	14.43	24.01	14.60	8.78
180	A	2.70	4.84	10.30	5.67	4.07					
	A_d	1.91	3.36	7.03	3.92	2.77	70.41	69.71	68.61	69.61	5.20
	A_c	0.44	0.42	0.37	0.41	0.06	17.05	9.74	4.23	10.19	5.43
	A_u	0.33	1.02	2.83	1.30	1.34	12.55	20.55	27.16	20.20	7.50
360	A	3.35	5.50	10.34	6.17	3.79					
	A_d	2.49	3.91	6.97	4.32	2.49	74.17	71.38	68.01	71.24	5.09
	A_c	0.24	0.24	0.25	0.24	0.06	7.51	4.80	2.62	4.93	2.31
	A_u	0.60	1.32	3.05	1.57	1.31	18.32	23.81	29.37	23.83	6.00

Table IA.13
Forecasting Regressions Using Restricted Data-Implied Risk Premia

This table reports excess market return forecasting regression results based on the specification in Equation 33 using risk premia from the restricted decomposition described in Subsection IA.3.9. In the case of the truncated moment regressions, we use moments estimated using ±5% cutoffs rather than ±10% cutoffs due to data availability (i.e., the limited number of observations when market returns are above (below) 10% (−10%)). See Internet Appendix IA.3.4 for more details regarding the ±5% decomposition. Results under "Full Sample" use data from January 1996 through June 2019. Results under "Ex Crisis" use the same time period but exclude data from August 2008 through January 2009 (i.e., data from the height of the 2008 Financial Crisis). Results are reported for 30-, 90-, and 360-day forecast horizons. Excess market returns are measured as ex-dividend returns on the S&P 500 index obtained from CRSP less the risk-free rate obtained from Kenneth French's website. Data is daily, and excess returns at each horizon are computed by compounding daily returns to the horizon of interest and subtracting the compounded risk-free rate. T-statistics are reported in parentheses and are computed according to Newey and West (1987) with lag values according to Newey and West (1994), with one slight modification. Since we have overlapping data, we multiply the Newey and West (1994)-implied lag value by the number of trading days in each horizon and use this as our lag value.

Regression: $(R_{M,t\to T} - R_{f,t\to T}) \cdot I_{A_s} = a_T + b_T \mathbb{M}^{(1)}[A_s] + \varepsilon_{t\to T}$

	Full Sample												**Ex Crisis**											
Horizon (days)	**30**				**90**				**360**				**30**				**90**				**360**			
	I	***II***	***III***	***IV***	***I***	***II***	***III***	***IV***	***I***	***II***	***III***	***IV***	***I***	***II***	***III***	***IV***	***I***	***II***	***III***	***IV***	***I***	***II***	***III***	***IV***
a_T	4.17	1.04	-2.39	0.68	2.94	4.72	-1.92	2.45	0.63	12.71	-0.60	4.15	-4.34	-2.30	-2.19	-2.68	-4.79	-1.26	-1.89	-1.87	1.75	10.35	-0.62	4.56
$t(a_T = 0)$	(1.02)	(0.35)	(-1.10)	(0.31)	(0.71)	(0.93)	(-2.97)	(0.85)	(0.13)	(2.37)	(-2.95)	(0.99)	(-1.16)	(-1.12)	(-0.97)	(-1.70)	(-1.16)	(-0.46)	(-2.90)	(-0.64)	(0.36)	(1.49)	(-3.14)	(0.88)
$\mathbb{M}^{(1)}_{t\to T}$	0.39				0.51				0.85				2.86				2.58				1.01			
$t\,(b_T = 0)$	(0.40)				(0.59)				(2.03)				(4.09)				(4.13)				(1.67)			
$t\,(b_T = 1)$	(-0.63)				(-0.57)				(-0.36)				(2.66)				(2.53)				(0.02)			
$\mathbb{M}^{(1)}_{t\to T}[A_d]$		0.84				1.22				4.51				0.50				0.42				3.49		
$t\,(b_T = 0)$		(3.03)				(1.85)				(2.48)				(3.05)				(1.36)				(1.59)		
$t\,(b_T = 1)$		(-0.58)				(0.34)				(1.93)				(-3.08)				(-1.88)				(1.13)		
$\mathbb{M}^{(1)}_{t\to T}[A_c]$			1.43				1.27				0.34				1.43				1.28				0.36	
$t\,(b_T = 0)$			(4.01)				(4.21)				(3.42)				(3.90)				(4.21)				(3.74)	
$t\,(b_T = 1)$			(1.20)				(0.90)				(-6.53)				(1.17)				(0.92)				(-6.63)	
$\mathbb{M}^{(1)}_{t\to T}[A_u]$				0.80				0.73				0.72				1.15				1.16				0.73
$t\,(b_T = 0)$				(3.68)				(2.67)				(1.63)				(7.44)				(4.21)				(1.18)
$t\,(b_T = 1)$				(-0.93)				(-0.98)				(-0.65)				(0.98)				(0.58)				(-0.43)
R^2 (%)	0.10	3.47	1.79	10.76	0.53	3.58	5.13	8.19	3.65	11.50	2.69	5.70	3.29	1.34	1.80	15.44	9.13	0.64	5.22	15.09	4.82	9.34	2.79	4.80

Table IA.14
Data-Implied Market Risk Premium Decomposition Summary Statistics (Observed Prices)

This table reports summary statistics for the data-implied risk premium decomposition according to Proposition 3 with $n = 1$ (i.e., the market risk premium). The decompositions use risk-neutral moments computed by numerically integration over observed option prices directly (see Internet Appendix IA.3.10) rather than using our implied volatility fitting method described in footnote 10. Preference parameters are also re-estimated using these moments. Panel A reports statistics for the risk premium levels (annualized, in percent) and Panel B reports statistics for the contributions of risk premia from each region to the total risk premium (as fractions of the total risk premium, in percent). A_d=[0, 0.9], A_c=[0.9, 1.1], and A_u=[1.1, $+\infty$) and these labels correspond to the downside, central, and upside risk premia, respectively. $A = A_d \cup A_c \cup A_u$ and this label corresponds to the total risk premium. Statistics reported under "Unconditional" use the full estimated time series for each risk premium measure. Statistics reported under "Cond. Means" report the means for each time series conditional on 30-day risk-neutral variance ($\mathbb{M}^{*(2)}_{t\to T}[A]$) falling below its first quartile ("Lo"), between its first and third quartiles ("Mid"), or above its third quartile ("Hi"). These correspond to periods of low, moderate, or high market volatility, respectively. Statistics are reported for risk premium decompositions at 30-, 60-, 90-, 180-, and 360-day horizons, and are based on daily data from January 1996 through June 2019.

		Panel A: $\mathbb{RP}^{(1)}_{t\to T}[A_s]$ **(%)**					**Panel B:** $\mathbb{RP}^{(1)}_{t\to T}[A_s]/\mathbb{RP}^{(1)}_{t\to T}[A]$ **(%)**				
		Cond. Means			**Unconditional**		**Cond. Means**			**Unconditional**	
Horizon (days)	**Region**	**Lo**	**Mid**	**Hi**	**Mean**	**St. Dev.**	**Lo**	**Mid**	**Hi**	**Mean**	**St. Dev.**
30	A	3.28	7.10	18.22	8.93	7.59					
	A_d	1.22	3.17	10.36	4.48	4.93	37.53	44.53	55.80	45.60	9.76
	A_c	1.88	3.21	4.42	3.18	1.14	58.26	47.47	29.09	45.57	13.89
	A_u	0.13	0.60	3.22	1.14	2.22	4.21	8.00	15.11	8.83	8.22
60	A	4.07	8.18	18.57	9.75	6.96					
	A_d	2.03	4.52	11.43	5.63	4.69	50.96	57.04	63.24	57.07	7.59
	A_c	1.67	2.20	2.05	2.03	0.59	43.13	29.59	13.59	28.97	13.00
	A_u	0.23	1.12	4.34	1.70	2.19	5.91	13.37	23.17	13.96	10.09
90	A	4.25	7.94	16.45	9.14	5.73					
	A_d	2.41	4.75	10.30	5.55	3.81	58.64	62.78	66.00	62.55	6.02
	A_c	1.34	1.38	0.92	1.25	0.49	33.43	19.57	7.10	19.92	11.74
	A_u	0.31	1.39	4.20	1.83	1.84	7.93	17.65	26.90	17.53	10.29
180	A	4.10	6.99	13.15	7.81	4.41					
	A_d	2.67	4.52	8.58	5.07	3.04	68.96	69.54	69.44	69.37	4.27
	A_c	0.62	0.41	0.19	0.40	0.26	16.46	7.07	1.56	8.04	6.72
	A_u	0.55	1.55	3.46	1.78	1.30	14.58	23.39	29.00	22.59	7.68
360	A	2.34	3.69	6.63	4.09	2.44					
	A_d	1.60	2.41	4.04	2.62	1.52	73.77	71.37	65.35	70.47	5.76
	A_c	0.11	0.06	0.06	0.07	0.07	5.13	1.97	0.72	2.44	2.43
	A_u	0.45	0.91	2.07	1.08	0.88	21.10	26.66	33.93	27.09	7.22

Table IA.15

Data-Implied Market Risk Premium Decomposition Summary Statistics (SVI)

This table reports summary statistics for the data-implied risk premium decomposition according to Proposition 3 with $n = 1$ (i.e., the market risk premium). The decompositions use risk-neutral moments computed by numerically integration over option prices computed using SVI-modeled implied volatility (see Internet Appendix IA.3.11) rather than using our baseline implied volatility fitting method described in footnote 10. Preference parameters are also re-estimated using these moments. Panel A reports statistics for the risk premium levels (annualized, in percent) and Panel B reports statistics for the contributions of risk premia from each region to the total risk premium (as fractions of the total risk premium, in percent). A_d=[0, 0.9], A_c=[0.9, 1.1], and A_u=[1.1, $+\infty$) and these labels correspond to the downside, central, and upside risk premia, respectively. $A = A_d \cup A_c \cup A_u$ and this label corresponds to the total risk premium. Statistics reported under "Unconditional" use the full estimated time series for each risk premium measure. Statistics reported under "Cond. Means" report the means for each time series conditional on 30-day risk-neutral variance ($\mathbb{M}^{*(2)}_{t\to T}[A]$) falling below its first quartile ("Lo"), between its first and third quartiles ("Mid"), or above its third quartile ("Hi"). These correspond to periods of low, moderate, or high market volatility, respectively. Statistics are reported for risk premium decompositions at 30-, 60-, 90-, 180-, and 360-day horizons, and are based on daily data from January 1996 through June 2019.

		Panel A: $\mathbb{RP}^{(1)}_{t\to T}[A_s]$ **(%)**					**Panel B:** $\mathbb{RP}^{(1)}_{t\to T}[A_s]/\mathbb{RP}^{(1)}_{t\to T}[A]$ **(%)**				
		Cond. Means			**Unconditional**		**Cond. Means**			**Unconditional**	
Horizon (days)	**Region**	**Lo**	**Mid**	**Hi**	**Mean**	**St. Dev.**	**Lo**	**Mid**	**Hi**	**Mean**	**St. Dev.**
30	A	2.19	4.47	11.72	5.71	5.15					
	A_d	0.68	1.85	6.47	2.71	3.26	30.72	40.13	52.94	40.98	10.05
	A_c	1.49	2.35	3.03	2.30	0.64	68.44	54.26	31.13	52.03	15.73
	A_u	0.02	0.29	2.23	0.71	1.58	0.84	5.61	15.93	7.00	7.06
60	A	1.98	3.88	9.62	4.84	4.07					
	A_d	0.91	2.17	6.11	2.84	2.76	45.26	55.52	62.91	54.80	27.29
	A_c	0.96	1.20	1.23	1.15	0.15	49.92	33.28	15.80	33.07	18.92
	A_u	0.08	0.48	2.28	0.83	1.37	4.82	11.20	21.29	12.13	39.81
90	A	1.97	3.47	8.35	4.31	3.52					
	A_d	1.06	2.26	5.59	2.79	2.35	53.96	61.38	54.40	57.78	205.78
	A_c	0.70	0.76	0.70	0.73	0.06	37.16	22.34	7.29	22.29	71.65
	A_u	0.18	0.42	2.07	0.77	1.49	8.87	16.28	38.30	19.93	274.22
180	A	2.49	4.20	8.62	4.88	3.25					
	A_d	1.57	2.84	5.88	3.28	2.25	63.49	64.70	69.00	65.47	81.29
	A_c	0.41	0.38	0.33	0.38	0.05	17.45	9.47	4.54	10.23	18.76
	A_u	0.47	0.94	2.42	1.19	1.16	19.06	25.83	26.46	24.30	99.08
360	A	2.66	4.13	7.12	4.51	2.42					
	A_d	1.91	2.97	5.08	3.23	1.63	77.65	69.71	78.75	73.95	178.74
	A_c	0.21	0.20	0.19	0.20	0.04	9.94	5.05	3.03	5.77	30.51
	A_u	0.52	0.93	1.83	1.05	1.05	12.41	25.25	18.22	20.28	204.75

Table IA.16
Data-Implied Market Risk Premium Decomposition Summary Statistics (Mispricing Adjustment)

This table reports summary statistics for the data-implied risk premium decomposition according to Proposition 3 with $n = 1$ (i.e., the market risk premium). The decompositions use risk-neutral moments computed using the mispricing adjustment described in Subsection IA.3.12. Preference parameters are also re-estimated using these moments. Panel A reports statistics for the risk premium levels (annualized, in percent) and Panel B reports statistics for the contributions of risk premia from each region to the total risk premium (as fractions of the total risk premium, in percent). A_d=$[0, 0.9]$, A_c=$[0.9, 1.1]$, and A_u=$[1.1, +\infty)$ and these labels correspond to the downside, central, and upside risk premia, respectively. $A = A_d \cup A_c \cup A_u$ and this label corresponds to the total risk premium. Statistics reported under "Unconditional" use the full estimated time series for each risk premium measure. Statistics reported under "Cond. Means" report the means for each time series conditional on 30-day risk-neutral variance ($\mathbb{M}^{*(2)}_{t\to T}[A]$) falling below its first quartile ("Lo"), between its first and third quartiles ("Mid"), or above its third quartile ("Hi"). These correspond to periods of low, moderate, or high market volatility, respectively. Statistics are reported for risk premium decompositions at 30-, 60-, 90-, 180-, and 360-day horizons, and are based on daily data from January 1996 through June 2019.

		Panel A: $\mathbb{RP}^{(1)}_{t\to T}[A_s]$ **(%)**					**Panel B:** $\mathbb{RP}^{(1)}_{t\to T}[A_s]/\mathbb{RP}^{(1)}_{t\to T}[A]$ **(%)**				
		Cond. Means			**Unconditional**		**Cond. Means**			**Unconditional**	
Horizon (days)	**Region**	**Lo**	**Mid**	**Hi**	**Mean**	**St. Dev.**	**Lo**	**Mid**	**Hi**	**Mean**	**St. Dev.**
30	A	1.43	3.37	8.80	4.24	3.77					
	A_d	0.17	0.87	4.05	1.49	2.28	10.79	23.13	40.19	24.31	12.31
	A_c	1.32	2.44	3.39	2.40	0.84	88.82	72.08	43.38	69.09	19.00
	A_u	0.01	0.20	1.82	0.56	1.25	0.39	4.79	16.43	6.60	7.35
60	A	2.80	6.03	13.77	7.16	5.20					
	A_d	0.71	2.35	7.28	3.17	3.38	25.91	38.28	49.58	38.01	10.11
	A_c	1.87	2.64	2.85	2.50	0.45	70.90	47.73	23.52	47.47	19.00
	A_u	0.09	0.94	3.94	1.48	1.91	3.19	13.99	26.91	14.52	10.10
90	A	3.19	6.38	13.20	7.29	4.59					
	A_d	1.16	2.97	7.39	3.63	3.03	36.34	45.87	53.82	45.48	8.09
	A_c	1.72	2.04	1.94	1.93	0.19	56.13	34.78	16.36	35.51	16.07
	A_u	0.24	1.34	4.02	1.73	1.71	7.53	19.35	29.83	19.01	9.72
180	A	3.27	5.92	11.38	6.62	3.88					
	A_d	1.73	3.37	6.94	3.85	2.60	52.86	56.70	59.83	56.52	5.22
	A_c	0.92	0.88	0.77	0.87	0.08	29.33	16.49	7.57	17.47	9.05
	A_u	0.58	1.64	3.68	1.88	1.40	17.81	26.82	32.59	26.01	7.01
360	A	2.25	3.75	6.84	4.15	2.33					
	A_d	1.39	2.32	4.25	2.57	1.51	61.94	61.98	61.49	61.85	4.10
	A_c	0.27	0.26	0.25	0.26	0.04	12.67	7.71	3.99	8.02	3.97
	A_u	0.56	1.15	2.35	1.30	0.87	25.39	30.31	34.51	30.13	4.85

Table IA.17
Utility-Implied Market Risk Premium Decomposition Average Values

This table reports average values for components of risk premium decomposition according to Proposition 3 assuming the representative investor has a specific utility function, and uses results from Section IA.4. Panel A reports average values for the risk premium levels (annualized) and Panel B reports average contributions of risk premia from each region to the total risk premium (as fractions of the total risk premium). A_d=[0, 0.9], A_c=[0.9, 1.1], and A_u=[1.1, $+\infty$) and these labels correspond to the downside, central, and upside risk premia, respectively. $A = A_d \cup A_c \cup A_u$ and this label corresponds to the total risk premium. Statistics are reported for risk premium decompositions at 30-, 60-, 90-, 180-, and 360-day horizons, and are based on daily data from January 1996 through June 2019.

		Preference Assumption									
		Log	**CRRA**			**CARA**			**HARA**		
Horizon (days)	**Region**		$\alpha = 3$	$\alpha = 5$	$\alpha = 7$	$\alpha = 3$	$\alpha = 5$	$\alpha = 7$	$RRA = 1$	$RRA = 1.1$	$RRA = 1.2$
		Panel A: Average Market Risk Premium Levels ($\mathbb{RP}^{(1)}_{t\to T}[A_s]$)									
30	A	4.13	11.19	17.30	22.86	11.03	17.38	23.38	4.13	4.54	4.95
	A_d	1.93	4.59	6.27	7.37	4.31	6.00	7.15	1.95	2.15	2.34
	A_c	1.63	4.73	7.65	10.35	4.71	7.63	10.31	1.60	1.77	1.93
	A_u	0.56	1.85	3.34	5.10	2.00	3.72	5.87	0.57	0.63	0.69
60	A	4.24	11.03	16.63	21.58	10.89	16.91	22.64	4.20	4.62	5.04
	A_d	2.32	5.34	7.16	8.29	5.01	6.89	8.09	2.31	2.54	2.77
	A_c	1.05	2.97	4.68	6.14	2.93	4.62	6.05	1.02	1.13	1.23
	A_u	0.84	2.66	4.71	7.05	2.89	5.32	8.38	0.84	0.93	1.01
90	A	4.28	10.85	16.14	20.79	10.78	16.68	22.52	4.23	4.65	5.07
	A_d	2.50	5.58	7.35	8.40	5.24	7.09	8.23	2.47	2.72	2.97
	A_c	0.74	2.01	3.09	3.93	1.97	3.02	3.81	0.70	0.77	0.84
	A_u	1.01	3.19	5.60	8.34	3.51	6.47	10.34	1.03	1.13	1.23
180	A	4.36	10.37	15.00	19.10	10.51	16.19	22.22	4.25	4.67	5.09
	A_d	2.70	5.62	7.11	7.90	5.30	6.93	7.81	2.64	2.90	3.17
	A_c	0.36	0.85	1.17	1.31	0.80	1.07	1.16	0.32	0.35	0.39
	A_u	1.27	3.83	6.62	9.76	4.33	8.08	13.12	1.26	1.38	1.51
360	A	4.47	9.83	13.96	17.90	10.48	16.66	24.29	4.24	4.66	5.08
	A_d	2.82	5.32	6.42	6.92	5.08	6.35	6.92	2.68	2.94	3.21
	A_c	0.16	0.25	0.19	0.03	0.18	0.06	-0.16	0.14	0.15	0.17
	A_u	1.46	4.19	7.25	10.85	5.15	10.16	17.44	1.39	1.53	1.67

Table IA.17
Utility-Implied Market Risk Premium Decomposition Average Values (continued)

Horizon (days)	Region	Preference Assumption: Log	CRRA $\alpha=3$	CRRA $\alpha=5$	CRRA $\alpha=7$	CARA $\alpha=3$	CARA $\alpha=5$	CARA $\alpha=7$	HARA $RRA=1$	HARA $RRA=1.1$	HARA $RRA=1.2$
Panel B: Average Market Risk Premium Contributions ($\mathbb{RP}^{(1)}_{t\to T}[A_s]/\mathbb{RP}^{(1)}_{t\to T}[A]$, in Percent)											
30	A_d	41.83	37.05	32.99	29.61	35.38	31.66	28.47	42.41	42.34	42.29
	A_c	50.44	53.53	55.92	57.48	54.35	56.24	57.39	49.67	49.75	49.81
	A_u	7.74	9.43	11.10	12.92	10.27	12.10	14.14	7.92	7.91	7.90
60	A_d	52.64	46.98	42.18	38.07	44.92	40.41	36.39	52.90	52.87	52.85
	A_c	33.83	36.42	38.27	39.26	37.00	38.29	38.81	33.22	33.28	33.32
	A_u	13.53	16.60	19.55	22.67	18.09	21.29	24.80	13.88	13.85	13.83
90	A_d	57.73	51.50	46.20	41.61	49.16	44.03	39.35	58.01	57.98	57.95
	A_c	24.18	25.86	27.11	27.49	26.12	26.82	26.70	23.03	23.14	23.23
	A_u	18.09	22.64	26.69	30.90	24.72	29.15	33.96	18.95	18.88	18.82
180	A_d	63.05	55.88	49.72	44.25	52.90	46.48	40.35	63.23	63.20	63.18
	A_c	11.41	11.60	11.51	10.75	11.28	10.74	9.58	10.33	10.43	10.51
	A_u	25.54	32.51	38.77	44.99	35.81	42.79	50.07	26.44	26.37	26.31
360	A_d	64.80	56.67	49.37	42.62	52.29	43.49	34.81	64.82	64.81	64.80
	A_c	4.75	3.74	2.47	1.06	2.93	1.43	0.01	4.27	4.32	4.35
	A_u	30.45	39.59	48.16	56.32	44.77	55.07	65.18	30.91	30.87	30.84

Table IA.18
Data- versus Model-Implied State Variable Processes

This table reports summary statistics for state variable processes extracted from the data (according to the methodology in Section 5) and based on model simulations. Panels A and B reports results for the Bansal and Yaron (2004) and Bansal, Kiku, and Yaron (2012) models, respectively. Panel C reports results for the Bollerslev, Tauchen, and Zhou (2009) model. Panel D reports results for the Drechsler and Yaron (2011) model. Panels E and F report results for the Bekaert, Engstrom, and Ermolov (2023) models with and without preference shocks, respectively. Panel G reports results for the Gabaix (2012) model. Panel H reports results for the Wachter (2013) model. Models are simulated at the monthly frequency for 100 million periods and used to compute the "Simulation-implied" statistics. State variables extracted from the data are available at the daily frequency. To be consistent with model simulations, we compute 21 sets of each data-implied statistic from non-overlapping daily data sampled every 21 days (since there approximately 21 trading days in each calendar month). The "Data-implied" statistics are averages across each statistic from these 21 sets. 95% confidence intervals on the simulated statistics are computed to correspond to confidence intervals we expect to see under the model null given a random sample of 282 months (which corresponds to the number of months we observe in our data from January 1996 through June 2019). They are based on randomly sampling 10,000 sets of 282 months of data from the full 100 million simulated months for each model. The confidence intervals answer the question: "With 95% confidence, would we expect to observe our data-implied statistics under the model null?" "SV1" and "SV2" under the Correlation heading correspond with the first and second state variables from each model ordered according to their appearance in the first column.

Variable	Source	Mean	St. Dev.	Autocorr.	Corr.	
					SV1	SV2
Panel A: Bansal and Yaron (2004)						
x_t	**Data-implied**	-2.1E-6	2.6E-3	0.91		
	Simulation-implied	9.7E-6	1.4E-3	0.96		
	[95% CI]	[-1.7E-3, 1.8E-3]	[8.2E-4, 2.2E-3]	[0.92, 0.99]		
σ_t^2	**Data-implied**	6.1E-5	8.4E-5	0.80	0.56	
	Simulation-implied	6.1E-5	1.1E-5	0.97	0.00	
	[95% CI]	[4.3E-5, 7.8E-5]	[6.0E-6, 1.8E-5]	[0.93, 0.99]	[-0.64, 0.65]	
Panel B: Bansal, Kiku, and Yaron (2012)						
x_t	**Data-implied**	-3.3E-5	5.5E-3	0.85		
	Simulation-implied	8.3E-6	1.2E-3	0.96		
	[95% CI]	[-1.4E-3, 1.5E-3]	[4.3E-4, 2.3E-3]	[0.91, 0.99]		
σ_t^2	**Data-implied**	7.3E-5	6.5E-5	0.80	0.81	
	Simulation-implied	7.3E-5	1.6E-5	0.98	0.00	
	[95% CI]	[1.2E-5, 1.7E-4]	[7.5E-6, 3.2E-5]	[0.93, 1.00]	[-0.67, 0.68]	
Panel C: Bollerslev, Tauchen, and Zhou (2009)						
$\sigma_{g,t}^2$	**Data-implied**	-4.6E-5	8.3E-3	0.78		
	Simulation-implied	4.6E-6	4.4E-3	0.96		
	[95% CI]	[-5.4E-3, 5.4E-3]	[2.5E-3, 7.6E-3]	[0.91, 0.99]		
q_t	**Data-implied**	1.4E-6	2.8E-5	0.97	-0.73	
	Simulation-implied	1.3E-6	1.7E-6	0.76	0.00	
	[95% CI]	[7.9E-7, 2.0E-6]	[9.8E-7, 2.8E-6]	[0.60, 0.88]	[-0.34, 0.34]	

Table IA.18
Data- versus Model-Implied State Variable Processes (continued)

Variable	Source	Mean	St. Dev.	Autocorr.	Corr.	
					SV1	SV2
Panel D: Drechsler and Yaron (2011)						
x_t	**Data-implied**	5.6E-6	2.7E-3	0.80		
	Simulation-implied	-2.3E-6	1.1E-3	0.96		
	[95% CI]	[-1.4E-3, 1.3E-3]	[4.8E-4, 2.2E-3]	[0.90, 0.99]		
$\overline{\sigma}_t^2$	**Data-implied**	1.20	1.50	0.90	0.79	
	Simulation-implied	1.05	0.42	0.97	0.00	
	[95% CI]	[0.51, 1.69]	[0.26, 0.68]	[0.92, 0.99]	[-0.61, 0.63]	
σ_t^2	**Data-implied**	1.11	1.80	0.79	1.00	0.79
	Simulation-implied	1.07	1.77	0.81	0.00	0.21
	[95% CI]	[0.35, 2.45]	[0.42, 4.55]	[0.67, 0.93]	[-0.46, 0.45]	[-0.18, 0.54]
Panel E: Bekaert, Engstrom, and Ermolov (2023) (with Preference Shocks)						
n_t	**Data-implied**	2.12	1.62	0.81		
	Simulation-implied	2.14	1.19	0.97		
	[95% CI]	[0.38, 6.77]	[0.26, 3.19]	[0.93, 0.99]		
q_t	**Data-implied**	1.00	0.15	0.92	0.54	
	Simulation-implied	1.00	0.15	0.97	0.88	
	[95% CI]	[0.77, 1.51]	[0.04, 0.38]	[0.93, 0.99]	[0.23, 1.00]	
s_t	**Data-implied**	5.4E-3	1.4E-2	0.75	0.83	0.70
	Simulation-implied	3.7E-3	2.8E-3	0.55	0.00	0.08
	[95% CI]	[3.3E-3, 5.1E-3]	[4.3E-5, 1.1E-2]	[0.51, 0.73]	[-0.17, 0.24]	[-0.13, 0.33]
Panel F: Bekaert, Engstrom, and Ermolov (2023) (without Preference Shocks)						
n_t	**Data-implied**	0.08	0.11	0.79		
	Simulation-implied	0.08	0.05	0.97		
	[95% CI]	[0.02, 0.25]	[0.01, 0.14]	[0.93, 0.99]		
q_t	**Data-implied**	1.00	0.18	0.90	0.77	
	Simulation-implied	1.00	0.13	0.97	0.98	
	[95% CI]	[0.87, 1.38]	[0.02, 0.39]	[0.92, 0.99]	[0.85, 1.00]	
Panel G: Gabaix (2012)						
L_t	**Data-implied**	0.70	0.59	0.80		
	Simulation-implied	0.69	0.16	0.97		
	[95% CI]	[0.45, 1.01]	[0.08, 0.29]	[0.93, 0.99]		
Panel H: Wachter (2013)						
λ_t	**Data-implied**	3.0E-3	2.8E-3	0.80		
	Simulation-implied	2.9E-3	1.5E-3	0.97		
	[95% CI]	[6.5E-4, 8.1E-3]	[4.6E-4, 3.6E-3]	[0.93, 0.99]		

Table IA.19
Representative Agent Model-Implied Risk Premium Decomposition Summary Statistics Compared to Decompositions Evaluated at Unconditional Average State Variable Values

This table compares model-implied risk premium decomposition results using our extracted state variables to those computed at unconditional model state variable values for each model. Panel 1A (2A) reports average risk premium levels for the market (variance) risk premium decompositions. Panel 1B (2B) reports risk premium contributions to the market (variance) risk premium based on the average values from Panel 1A (2A). Columns labeled "Extracted" correspond to the original model-implied decomposition results using extracted state variables (the "Extracted" column in Panel 1A (2A) corresponds to results in Table 4 (Table IA.2)). Columns labeled "Uncond." correspond to average risk premium values from decompositions evaluated at the unconditional state variable values from each model (i.e., they do not depend on our state variable extraction methodology). Results are reported for the following models: Bansal and Yaron (2004) ("BY"), Bansal, Kiku, and Yaron (2012) ("BKY"), Drechsler and Yaron (2011) ("DY"), Bekaert, Engstrom, and Ermolov (2023) ("BEE") with and without preference shocks, Gabaix (2012) ("Gabaix"), and Wachter (2013) ("Wachter"). A_d=[0, 0.9], A_c=[0.9, 1.1], and A_u=[1.1, $+\infty$) and these labels correspond to the downside, central, and upside risk premia, respectively. $A = A_d \cup A_c \cup A_u$ and this label corresponds to the total risk premium. Extracted state variable results use data from January 1996 through June 2019 (as in Tables 4 and IA.2).

			Panel 1A: $\mathbb{RP}^{(1)}_{t\to T}[\boldsymbol{A_s}]$ (%)		**Panel 1B:** $\frac{\mathbb{RP}^{(1)}_{t\to T}[\boldsymbol{A_s}]}{\mathbb{RP}^{(1)}_{t\to T}[\boldsymbol{A}]}$ (%)		**Panel 2A:** $\mathbb{RP}^{(2)}_{t\to T}[\boldsymbol{A_s}]$ (%)		**Panel 2B:** $\frac{\mathbb{RP}^{(2)}_{t\to T}[\boldsymbol{A_s}]}{\mathbb{RP}^{(2)}_{t\to T}[\boldsymbol{A}]}$ (%)	
Class	**Model**	**Region**	**Extracted**	**Uncond.**	**Extracted**	**Uncond.**	**Extracted**	**Uncond.**	**Extracted**	**Uncond.**
LRR	**BY**	$\boldsymbol{A}$	5.66	5.63						
		$\boldsymbol{A_d}$	0.28	0.06	4.86	1.01				
		$\boldsymbol{A_c}$	4.62	5.36	81.64	95.33				
		$\boldsymbol{A_u}$	0.76	0.21	13.49	3.67				
	BKY	$\boldsymbol{A}$	6.75	5.24						
		$\boldsymbol{A_d}$	0.32	0.08	4.67	1.54				
		$\boldsymbol{A_c}$	5.61	4.90	83.16	93.64				
		$\boldsymbol{A_u}$	0.82	0.25	12.17	4.81				
	DY	$\boldsymbol{A}$	8.51	7.80			-0.69	-0.67		
		$\boldsymbol{A_d}$	3.69	3.47	43.38	44.45	-0.71	-0.70	102.83	104.18
		$\boldsymbol{A_c}$	3.06	3.49	36.00	44.77	0.01	-0.02	-1.51	2.86
		$\boldsymbol{A_u}$	1.76	0.84	20.62	10.78	0.01	0.05	-1.46	-7.04

Table IA.19
Representative Agent Model-Implied Risk Premium Decomposition Summary Statistics Compared to Decompositions Evaluated at Unconditional Average State Variable Values (continued)

			Panel 1A: $\mathbb{RP}^{(1)}_{t\to T}[\boldsymbol{A_s}]$ (%)		Panel 1B: $\frac{\overline{\mathbb{RP}^{(1)}_{t\to T}[\boldsymbol{A_s}]}}{\mathbb{RP}^{(1)}_{t\to T}[\boldsymbol{A}]}$ (%)		Panel 2A: $\mathbb{RP}^{(2)}_{t\to T}[\boldsymbol{A_s}]$ (%)		Panel 2B: $\frac{\overline{\mathbb{RP}^{(2)}_{t\to T}[\boldsymbol{A_s}]}}{\mathbb{RP}^{(2)}_{t\to T}[\boldsymbol{A}]}$ (%)	
Class	**Model**	**Region**	**Extracted**	**Uncond.**	**Extracted**	**Uncond.**	**Extracted**	**Uncond.**	**Extracted**	**Uncond.**
Habit	**BEE (w/ Pref. Shocks)**	$\boldsymbol{A}$	4.85	4.49			-0.79	-0.62		
		$\boldsymbol{A_d}$	2.23	1.86	46.08	41.41	-0.70	-0.55	88.85	88.86
		$\boldsymbol{A_c}$	2.32	2.63	47.81	58.59	-0.07	-0.07	9.41	11.21
		$\boldsymbol{A_u}$	0.30	0.00	6.10	0.00	-0.01	0.00	1.72	-0.07
	BEE (w/o Pref. Shocks)	$\boldsymbol{A}$	4.86	4.81			-1.30	-1.31		
		$\boldsymbol{A_d}$	3.84	3.99	79.15	83.08	-1.15	-1.22	89.16	93.08
		$\boldsymbol{A_c}$	0.88	0.81	18.03	16.92	-0.12	-0.09	8.96	6.96
		$\boldsymbol{A_u}$	0.14	0.00	2.82	0.00	-0.02	0.00	1.86	-0.04
Disaster	**Gabaix**	$\boldsymbol{A}$	7.42	8.12			-3.15	-3.34		
		$\boldsymbol{A_d}$	5.93	6.63	80.00	81.63	-3.13	-3.32	99.29	99.33
		$\boldsymbol{A_c}$	1.44	1.45	19.43	17.83	-0.03	-0.02	0.82	0.71
		$\boldsymbol{A_u}$	0.04	0.04	0.57	0.54	0.00	0.00	-0.11	-0.05
	Wachter	$\boldsymbol{A}$	7.20	7.18			-0.96	-0.99		
		$\boldsymbol{A_d}$	2.76	2.57	38.36	35.78	-1.03	-1.05	107.49	106.20
		$\boldsymbol{A_c}$	3.10	3.60	43.02	50.09	0.02	0.00	-1.68	0.25
		$\boldsymbol{A_u}$	1.34	1.01	18.62	14.13	0.06	0.06	-5.84	-6.45

Table IA.20
Representative Agent Model Market Risk Premium Decomposition Summary Statistics Using Data-Implied Decomposition Methodology Applied to Model Data

This table compares original model-implied market risk premium decomposition results from Table 4 to DMAM market risk premium decompositions (see Subsection 5.3 for a description of the latter decompositions). Panel A (B) reports statistics related to risk premium levels (contributions). Columns labeled "Model Meth." present results using our original model-implied decomposition methodology reported in Table 4, which are repeated here for comparison. Columns labeled "Data Meth." refer to the DMAM decompositions. For each methodology, we report time series averages ("Mean" columns), standard deviation ("StDev" columns), and the correlation between the original model-implied time series and the DMAM time series. Results are reported for the following models: Drechsler and Yaron (2011) ("DY"), Bekaert, Engstrom, and Ermolov (2023) ("BEE") with and without preference shocks, Gabaix (2012) ("Gabaix"), and Wachter (2013) ("Wachter"). A_d=[0, 0.9], A_c=[0.9, 1.1], and A_u=[1.1, $+\infty$) and these labels correspond to the downside, central, and upside risk premia, respectively. $A = A_d \cup A_c \cup A_u$ and this label corresponds to the total risk premium. Extracted state variable results use data from January 1996 through June 2019 (as in Tables 4 and IA.2).

			Panel A: $\mathbb{RP}^{(1)}_{t\to T}[A_s]$ (%)					**Panel B:** $\frac{\mathbb{RP}^{(1)}_{t\to T}[A_s]}{\mathbb{RP}^{(1)}_{t\to T}[A]}$ (%)				
			Model Meth.		**Data Meth.**			**Model Meth.**		**Data Meth.**		
Class	**Model**	**Region**	**Mean**	**StDev**	**Mean**	**StDev**	**Corr**	**Mean**	**StDev**	**Mean**	**StDev**	**Corr**
LRR	**DY**	A	8.51	11.23	12.97	11.03	1.00					
		A_d	3.69	5.50	3.98	5.61	1.00	30.58	18.44	21.99	15.14	0.96
		A_c	3.06	1.46	6.40	0.71	0.92	58.00	23.54	64.33	22.15	0.98
		A_u	1.76	4.91	2.59	5.28	1.00	11.42	7.25	13.68	7.87	0.99
Habit	**BEE (w/ Pref. Shocks)**	A	4.85	5.84	4.70	5.86	1.00					
		A_d	2.23	3.80	2.19	3.83	1.00	33.42	13.94	33.45	14.35	1.00
		A_c	2.32	1.12	2.21	1.08	1.00	65.28	16.79	65.24	17.16	1.00
		A_u	0.30	1.47	0.30	1.49	1.00	1.31	4.43	1.31	4.44	1.00
	BEE (w/o Pref. Shocks)	A	4.86	6.36	4.91	6.36	1.00					
		A_d	3.84	4.48	3.85	4.49	1.00	78.85	14.31	76.36	15.04	0.98
		A_c	0.88	1.09	0.93	1.08	1.00	20.86	14.31	23.36	15.09	0.98
		A_u	0.14	1.40	0.14	1.40	1.00	0.29	2.65	0.29	2.66	1.00
Disaster	**Gabaix**	A	7.42	2.50	10.17	2.51	1.00					
		A_d	5.93	2.47	5.31	2.74	1.00	77.94	6.52	48.91	13.81	0.99
		A_c	1.44	0.04	4.70	0.23	-0.98	21.42	6.31	49.47	13.35	0.99
		A_u	0.04	0.00	0.15	0.02	0.91	0.64	0.20	1.62	0.46	0.99
	Wachter	A	7.20	6.24	7.13	6.24	1.00					
		A_d	2.76	3.21	2.73	3.21	1.00	33.89	6.18	33.72	6.11	1.00
		A_c	3.10	0.72	3.08	0.75	1.00	54.48	15.33	54.72	15.24	1.00
		A_u	1.34	2.67	1.33	2.66	1.00	11.63	9.17	11.56	9.15	1.00

Table IA.21

Bollerslev, Tauchen, and Zhou (2009)**-Implied Market Risk Premium Decomposition Summary Statistics**

This table reports summary statistics for the model-implied risk premium decompositions based on Bollerslev, Tauchen, and Zhou (2009) ("BTZ") described in Section IA.8.5.2 with $n = 1$ (i.e., the market risk premium). This table is analogous to Table 4 in the main draft, but just focused on the BTZ model. Panel A reports statistics for the risk premium levels (annualized, in percent) and Panel B reports statistics for the contributions of risk premia from each region to the total risk premium (as fractions of the total risk premium, in percent). A_d=[0, 0.9], A_c=[0.9, 1.1], and A_u=[1.1, $+\infty$) and these labels correspond to the downside, central, and upside risk premia, respectively. $A = A_d \cup A_c \cup A_u$ and this label corresponds to the total risk premium. Statistics reported under "Unconditional" use the full estimated time series for each risk premium measure. Statistics reported under "Cond. Means" report the means for each time series conditional on 30-day risk-neutral variance ($\mathbb{M}^{*(2)}_{t\to T}[A]$) falling below its first quartile ("Lo"), between its first and third quartiles ("Mid"), or above its third quartile ("Hi"). These correspond to periods of low, moderate, or high market volatility, respectively. Results are based on state variables extracted from the data under each model using their original calibrations, which are monthly in all cases, and use daily data from January 1996 through June 2019.

			Panel A: $\mathbb{RP}^{(1)}_{t\to T}[A_s]$ **(%)**					**Panel B:** $\mathbb{RP}^{(1)}_{t\to T}[A_s]/\mathbb{RP}^{(1)}_{t\to T}[A]$ **(%)**				
			Cond. Means			**Unconditional**		**Cond. Means**			**Unconditional**	
Class	**Model**	**Region**	**Lo**	**Mid**	**Hi**	**Mean**	**St. Dev.**	**Lo**	**Mid**	**Hi**	**Mean**	**St. Dev.**
LRR	**BTZ**	A	-8.52	-4.50	60.38	10.71	144.62					
		A_d	-0.02	-26.63	-38.18	-22.87	69.72	0.02	10.28	20.17	10.19	26.50
		A_c	-9.46	11.56	24.22	9.47	68.05	99.14	83.05	53.16	79.60	31.33
		A_u	0.96	10.58	74.34	24.11	65.91	0.84	6.67	26.67	10.21	21.55

Table IA.22

Average Conditional Differences Between Data- and Model-Implied Decompositions: Bollerslev, Tauchen, and Zhou (2009)

This table reports summary statistics for the conditional differences between our main data-implied market risk premium decomposition time series (30-day horizon) summarized in Table 2 and the corresponding model-implied market risk premium decomposition time series based on the Bollerslev, Tauchen, and Zhou (2009) model reported in Table IA.21. This table is analogous to Table 5 in the main draft, but just focused on the BTZ model. Panel A reports statistics for the annualized level differences (i.e., $\mathbb{RP}^{(1)}_{t\to T,\,data}[A_s] - \mathbb{RP}^{(1)}_{t\to T,\,model}[A_s]$) and Panel B reports statistics for the contribution differences (i.e., $\mathbb{RP}^{(1)}_{t\to T,\,data}[A_s]/\mathbb{RP}^{(1)}_{t\to T,\,data}[A] - \mathbb{RP}^{(1)}_{t\to T,\,model}[A_s]/\mathbb{RP}^{(1)}_{t\to T,\,model}[A]$). A_d=$[0, 0.9]$, A_c=$[0.9, 1.1]$, and A_u=$[1.1, +\infty)$ and these labels correspond to the downside, central, and upside risk premia, respectively. $A = A_d \cup A_c \cup A_u$ and this label corresponds to the total risk premium. T-statistics are reported in parentheses and are computed according to Newey and West (1987) with lag values according to Newey and West (1994), with one slight modification. Since we have overlapping data, we multiply the Newey and West (1994)-implied lag value by the number of overlapping days (21) and use this as our lag value. Data is daily and runs from January 1996 through June 2019.

		Panel A: $\mathbb{RP}^{(1)}_{t\to T}[A_s]$ **differences (%)**				**Panel B:** $\mathbb{RP}^{(1)}_{t\to T}[A_s]/\mathbb{RP}^{(1)}_{t\to T}[A]$ **differences (%)**		
Class	**Model**	A	A_d	A_c	A_u	A_d	A_c	A_u
LRR	**BTZ**	-2.00	27.32	-6.14	-23.14	35.48	-31.75	-3.73
		(-0.05)	(1.59)	(-0.38)	(-1.66)	(5.49)	(-5.44)	(-0.81)